Studying Centrosome Formation and the Consequences of Centrosome Loss in *Drosophila melanogaster*

Janina Baumbach

Lincoln College

Doctor of Philosophy

2014

Declaration

I hereby declare that this dissertation is the result of my own work and includes nothing, which is the outcome of work done in collaboration except where specifically indicated in the text. This dissertation is not substantially the same as any that I have submitted for a degree or diploma or any other qualification at any other university. I further state that no part of my dissertation has already been, or is concurrently being, submitted for any such degree, diploma or other qualification.

Janina Baumbach

October 2013

Part of the data presented in this thesis have been published:

Baumbach, J., Levesque, M. P., and Raff, J.W. 2012. Centrosome loss or amplification does not dramatically perturb global gene expression in *Drosophila*. Biology Open 1:983-993

Acknowledgements

I would like to start by thanking Jordan for being an excellent supervisor and for giving me the opportunity to work in his lab. He has been immensely supportive and encouraging throughout my DPhil and his enthusiasm for science has been truly inspiring.

Next, I would like to thank all past and present members of the Raff lab for making the lab a great place to work. Thank you Alan, Anna, Cat, Emilie, Hélio, Jenny, Matt, Metta, Nadine, Paul, Richard, Saroj, Violet and Zsofi for all your help, advice and inspiring discussions about science throughout the past 4 years, for all the fun we had at tea breaks, lab retreats, lab dinners and in the pub on Friday nights. I am particularly grateful to Alan and Paul for teaching me a lot about science, it has been great to collaborate with you.

The Sir William Dunn School of Pathology has been a nice place to work at. I would especially like to thank the Admin staff, the Media kitchen and the Proteomics facility for all of their help. I am extremely grateful to the Dunn School and the E.P. Abraham Research Fund for funding my DPhil studies.

I am very grateful to Francis Barr and Ricardo Nunes Bastos for their valuable advice on how to perform the TiO_2 phosphopeptide enrichment. I would like to thank Mitch Levesque for his huge help with performing the microarray experiments and his advice on microarray data analysis.

Thanks to Claudia for helping me to keep up the spirits with lots of runs and fun dinners. Thank you Anna, Ulrike, Luiseach, Magda for being great housemates!

Thank you, Chris, for being by my side during the past years and helping me to stay focused throughout my DPhil.

Finally, my biggest thanks goes to my family. Danke Mama und Papa, dass ihr mich immer unterstützt habt und mich darin bestärkt habt, das zu tun was mir Spass macht. Danke Elisa, dass du auch immer für mich da warst und eine tolle Schwester bist! Danke, Oma, dafür dass du wir oft im Palmengarten und im Senckenbergmuseum in Frankfurt waren als ich ein Kind war. Dadurch hast du mein Interesse an der Natur und der Biologie sehr unterstützt.

This thesis is for my family.

Abstract

Studying Centrosome Formation and the Consequences of Centrosome Loss in *Drosophila melanogaster*

Janina Baumbach, Lincoln College
Doctor of Philosophy
2014

Centrioles are conserved microtubule-based structures that are required for the formation of two important cellular organelles, centrosomes and cilia. Centrosomes form the poles of the mitotic spindle and consist of a pair of centrioles surrounded by a matrix of pericentriolar material (PCM) that has the ability to nucleate and organise microtubules. Centrosome defects are implicated into a variety of human diseases including cancer, microcephaly, and ciliopathies. Therefore it is of great interest to understand the mechanisms that lead to centrosome formation and the consequences that centrosome defects have in cells.

I have analysed the roles of several centrosomal proteins in centrosome assembly in *Drosophila.* My results indicate that Sak/PLK4 is only required for the initial step of centriole duplication, but has no further role in recruitment of PCM. I show that two proteins important for PCM recruitment, Asterless (Asl) and Spd-2, are preferentially phosphorylated when they are integrated into the centrosome and I identified these phosphorylation sites using a phosphoproteomic screen. A phosphorylation site in Asl is specifically phosphorylated in mitosis, and the phosphorylation state of Spd-2 regulates its maintenance at the centrosome, suggesting that phosphorylation of PCM proteins is an important mechanism to ensure PCM assembly specifically at the centrosome and in mitosis.

I have performed a global transcriptional analysis of flies lacking centrosomes or having extra centrosomes to investigate the effects of centrosomal defects on a cellular level. Surprisingly, my results indicate that centrosome defects *per se* do not dramatically alter cellular physiology. Finally, I demonstrate that in the absence of centrioles acentrosomal microtubule-organising centres (aMTOCs) are formed in an Asl- and Cnn-dependent fashion, and I show that these aMTOCs can contribute to spindle focusing in acentrosomal cells.

Abbreviations

3D-SIM	3 dimensional structured illumination microscopy
AmpR	ampicillin resistance
aMTOC	acentrosomal microtubule organising centre
Ana	Anastral
Asl	Asterless
ASPM	Abnormal spindle-like microcephaly-associated protein
α-tub	α-tubulin
ATP	adenosine triphosphate
BIRC5	baculoviral inhibitor of apoptosis repeat-containing 5
Brca	Breast cancer
BS^3	bis sulfosuccinimidyl suberate
BSA	bovine serum albumin
CDCA8	cell division cycle associated 8
Cdk	Cyclin-dependent kinase
CDK5RAP2	Cdk5 regulatory subunit associated protein 1
CDS	coding DNA sequence
CENPJ	Centromere protein J
Cep	Centrosomal protein
CG	Celera genomic
Chk	Checkpoint kinase
ch-TOG	colonic and hepatic tumor over-expressed gene
c-nap1	Centrosomal Nek2-associated protein 1
Cnn	Centrosomin
CP	centriolar protein
CPAP	Centrosomal P4.1-associated protein
CPC	chromosomal passenger complex
CT	cycle threshold
DAVID	database for annotation, visualization and integrated discovery
Dhc	Dynein heavy chain
DNA	deoxyribonucleic acid
DPLP	*Drosophila* pericentrin-like protein
DRE	downstream regulatory element
DSas	*Drosophila* Spindle Assembly Abnormal Protein
DTACC	*Drosophila* transforming acidic coiled-coil protein
DTT	dithiothreitol
EDTA	ethylene diamine tetraacetic acid
EF	elongation factor
eGFP	enhanced green fluorescent protein
EGTA	ethylene glycol tetraacetic acid
ELISA	enzyme-linked immunosorbent assay
EM	electron microscopy
EMS	ethyl methanesulfonate
ET	electron tomography
FACS	fluorescence-activated cell sorting
FBXW	F-box/WT repeat-containing protein
FDR	false discovery rate
FRAP	fluorescent recovery after photobleaching

GA	glycolic acid
GAP	GTPase activating protein
GCP	γ-tubulin complex component
GCRMA	guanosine cytidine robust multiarray analysis
GDP	guanosine diphosphate
GO	gene ontology
Grip	Gamma-tubulin ring protein
GTP	guanosine triphosphate
γ-tub	γ-tubulin
γ-TuRCs	γ-tubulin ring complexes
γ-TuSC	γ-tubulin small complex
h	hours
HAUS	human augmin complex
HRP	horseradish peroxidase
HSET	kinesin-like protein 2
HURP	hepatoma upregulated protein
IF	immuno fluorescence
IFT	intraflagellar transport
INCENP	inner centromere protein
IP	immuno precipitation
KanR	kanamycin resistance
KD	kinase dead
kDa	kilo Dalton
K-fibre	kinetochore fibre
K-PIPES	potassium piperazine 2-ethanesulfonic acid
l	liter
LC-MS/MS	liquid chromatography-tandem mass spectrometry
limma	linear models for microarray
M	molar
Mad	Mitotic arrest deficient
MAP	microtubule associated protein
MBP	maltose binding protein
MCAK	Mitotic centromere-associated kinesin
MCPH	autosomal recessive primary microcephaly
MCRS1	Microspherule protein 1
µg	micrograms
MI	mitotic index
min	minutes
ml	milliliter
mM	millimolar
Mps	Monopolar spindles
mRNA	messenger ribonucleic acid
Msps	mini spindles
Mst	Misato
MT	microtubule
MTOC	microtubule organising centre
Ncd	non-claret disjunctional
NDE	nudE neurodevelopment protein
NEBD	nuclear envelope breakdown
NEDD1	Neural precursor cell expressed, developmentally down-regulated 1
Nek2	NIMA (never in mitosis gene a)-related kinase 2

NudE	nuclear distribution E
NuMA	nuclear mitotic apparatus protein
ORF	open reading frame
OrR	OregonR
P	probability
PACT	Pericentrin-AKAP450 centrosome targeting domain
PB	polo box
PBD	polo box domain
PBS	phosphate buffered saline
PBT	phosphate buffered saline + tween
PCM	pericentriolar material
PCR	polymerase chain reaction
PDGFR	platelet-derived growth factor receptor
PLK	Polo like kinase
PMSF	phenylmethylsulfonyl fluoride
PP	protein phosphatase
qPCR	quantitative polymerase chain reaction
Ran	Ras (rat sarcoma)-related nuclear protein
RCC1	Regulator of chromosome condensation 1
RNAi	RNA interference
s	seconds
S2 cells	Schneider 2 cells
Sak	Snk/Plk-akin kinase
SakOE	Sak overexpression
SAPs	Sas-6/Ana2 Particles
SB	laemmli sample buffer
SCF	Skp/Cullin/F-box containing complex
SDS-PAGE	sodium dodecyl sulfate polyacrylamide gel electrophoresis
Shh	Sonic hedgehog
SIL	SCL (stem cell leukemia gene coding)-interrupting locus protein
STIL	SCL/TAL1 interrupting locus
Spd	Spindle defective protein
SUMO	small ubiquitin-like modifier
TBS	Tris-buffered saline
TBST	Tris-buffered saline + tween
TPX2	targeting protein for Xklp2
UAS	upstream activation sequence
Ubq	Ubiquitin
Unc	Uncoordinated
w	*white*
Wac	WW domain-containing adapter protein with coiled-coil
WB	Western blotting
WDR	WD repeat domain
Wnt	Wingless-related integration site
WT	wild type
XMAP215	*Xenopus* microtubule associated protein 215kDa
yw	*yellow white*
ZeoR	Zeocin resistance
ZYG	Zygotic defective
♀	female
♂	male

Contents

List of Figures and Tables

1 Introduction

1.1 Centrioles, centrosomes and cilia

1.1.1 The structure of the centriole

Centrioles are conserved eukaryotic organelles that have many important cellular functions. They serve as basal bodies to template nucleation of cilia and flagella, and organise pericentriolar material (PCM) to form the centrosome. Most eukaryotic organisms have centrioles, including almost all animal cells, but higher plants and yeasts lack centrioles, although it is widely believed that they descended from a common ancestor that once contained centrioles (Carvalho-Santos et al., 2010; Hodges et al., 2010; Marshall, 2009).

The major structural element of centrioles are microtubules (MTs), which are polarised structures assembled of heterodimeric subunits consisting of α- and β-tubulin (Fan et al., 1996). These heterodimers associate head-to-tail to form protofilaments. MTs are then formed through lateral association of usually 13 protofilaments to build long hollow tubes with a 25nm diameter. MTs grow by addition of GTP-bound heterodimers to the plus end (ending with a β-tubulin) (Mitchison, 1993), which form a stable GTP-cap promoting MT growth (Figure 1.1A). After a short time the GTP bound to β-tubulin is hydrolysed to GDP, rendering the MT structure less stable. If GTP is hydrolysed before new dimers are added, MTs can rapidly disassemble (MT shrinkage) (Figure 1.1A). MTs alternate between these two states, a phenomenon called dynamic instability (Mitchison and Kirschner, 1984), allowing for rapid rearrangement of the MT cytoskeleton. In cells, MTs are often nucleated from γ-tubulin ring complexes (γ-

TuRCs) consisting of γ-tubulin and several other proteins, which together act as scaffolds for α/β-dimers to polymerise (Figure 1.1B) (Gunawardane et al., 2000; Kollman et al., 2011; Kollman et al., 2010; Moritz et al., 1995; Oegema et al., 1999; Zheng et al., 1995).

Centrioles are cylindrical structures typically ~500nm long and ~250nm in diameter, and consist of 9 microtubule (MT) triplets, doublets or singlets, depending on the organism and cell type. In *Drosophila* embryos centrioles are only ~200nm long and are composed of MT singlets or doublets (Callaini et al., 1997; Moritz et al., 1995), while they are composed of triplets and can reach a length of up to 2.6μm in *Drosophila* primary spermatocytes (Gonzalez et al., 1998). Only the innermost MT protofilament in a centriole doublet or triplet is built from a complete ring of 13 protofilaments, as the outer B and C tubules are incomplete (Figure 1.1 C) (Linck and Stephens, 2007; Tilney et al., 1973). In contrast to the dynamic MTs of the cytoskeleton, MTs in the centriole are stabilised, presumably through posttranslational modifications of the tubulin heterodimers, such as polyglutamylation (Bobinnec et al., 1998b; Eddé et al., 1990), detyrosination (Gundersen and Bulinski, 1986) and acetylation (Piperno and Fuller, 1985). In vertebrate cells mature centrioles carry distal and sub-distal appendages (Vorobjev and Chentsov Yu, 1982), which have been implicated in MT anchoring (Bornens, 2001) and ciliogenesis (Ishikawa et al., 2005; Joo et al., 2013; Sillibourne et al., 2013; Tanos et al., 2013). Interestingly, *Drosophila* centrioles do not appear to have equivalent appendage structures, even in primary spermatocytes (Gonzalez et al., 1998).

In many organisms including *Chlamydomonas, Paramecium*, mammals, and *Drosophila* (Anderson and Brenner, 1971; Callaini et al. 1997, Cavalier-Smith, 1974; Dippell, 1968) a central cartwheel structure is found at the centre of the centriole (Figure

1.1D,F). The cartwheel consists of a central hub of ~22nm diameter from which 9 radial spokes emanate towards the 9 microtubule triplets (Gönczy, 2012), and is important to establish the 9-fold symmetry of the centriolar MTs (Section 1.2.2). In some species (such as *Drosophila*) the cartwheel structure is usually found permanently in the centriole and extends throughout the centriole length, but in others (such as most vertebrates) it is lost in mature centrioles and is found only at the proximal end of the daughter centrioles (Alvey, 1985). In *C. elegans* centrioles do not contain a cartwheel structure, but rather a long central tube around which nine A tubules are assembled (Pelletier et al., 2006a).

Several studies have attempted to identify the centriole proteome. Many candidate centriole and basal body proteins have been found by proteomic screens involving centrioles/basal bodies isolated from *Chlamydomonas* and *Tetrahymena* (Keller et al., 2005; Kilburn et al., 2007). Genomic approaches have also proved to be very useful in finding new genes involved in cilia/basal body biogenesis by comparing the proteome of ciliated and nonciliated organisms (Avidor-Reiss et al., 2004; Li et al., 2004). Transcriptomic approaches further contributed to finding new candidate centriole and cilia proteins, for example by comparing the transcriptome of multiciliated mouse cells with the general mouse transcriptome (Hoh et al., 2012) and by analysing the transcriptome of *Chlamydomonas* undergoing ciliogenesis (Albee et al., 2013).

A B

Figure 1.1.A and 1.1.B originally presented here cannot be made freely available via ORA due to copyright reasons. The images were sourced at “Alberts et al. 2008, Molecular Biology of the Cell, Fifth Edition.

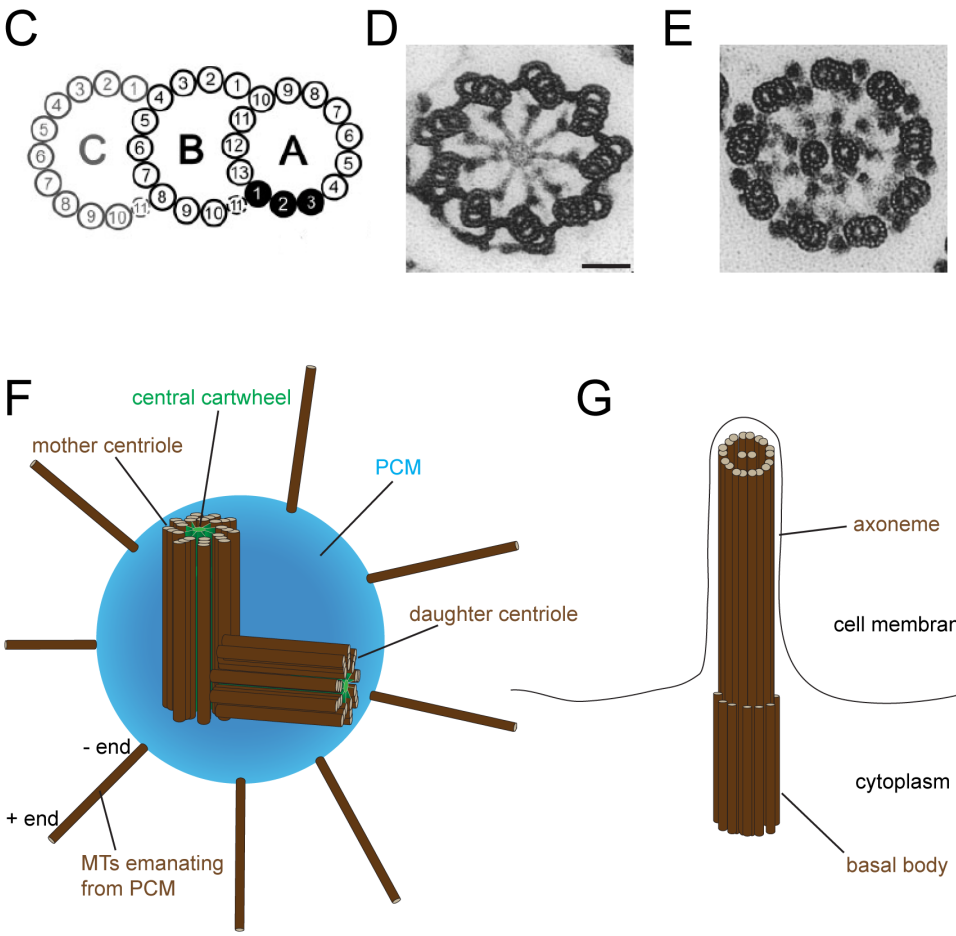

Figure 1.1: The structure of centrioles, centrosomes, cilia and flagella.
Figure legends see next page.

Figure 1.1: The structure of centrioles, cilia and flagella. (A) Microtubules (MTs) consist of protofilaments which are formed by heterodimers of α-tubulin (light green) and β-tubulin (dark green). MTs grow by addition of GTP-bound heterodimers (red) to the plus end. After a short time GTP hydrolysis takes place making the MT less stable. The GTP-bound cap protects from degradation and promotes MT growth. If GTP-hydrolysis takes place before adding on new dimers the MT rapidly dissassembles. These two states of growth and shrinkage of MTs alternate (dynamic instability). **(B)** MTs are nucleated from γ-tubulin ring complexes (γ-TuRCs) consisting of γ-tubulin and several other proteins. **(C)** Schematic of MT triplet of a centriole showing its A, B and C tubule. The A tubule consists of a ring of 13 protofilaments, to which the outer incomplete B and C tubules are attached. It is not clear if the 11th component is a genuine protofilament and is shown in a dotted line. **(D)** Electron microscopy cross section of a centriole consisting of 9 MT triplets and a central cartwheel with 9 spokes emanating to the MT triplets. **(E)** Electron microscopy cross-section of a flagellar axoneme **(F)** Schematic showing a pair of centrioles within the centrosome. Mother and daughter centrioles are arranged perpendicularly to each other and surrounded by a matrix of protein called pericentriolar material (PCM). Proteins of the PCM nucleate and organise microtubules (MTs), and the minus ends of MTs are anchored at protein complexes in the PCM. **(G)** Centrioles form the basal body of cilia and flagella. They template formation of a MT-based structure, the axoneme. The axoneme is formed of 9 MT doublets and can have two central MTs as shown here (9 + 2), or is without these (9 + 0). (A,B) are modified from “Molecular Biology of the Cell” fifth edition Alberts et al. 2008; (C-E) are taken from Linck and Stephens, 2007. Scale bar 50nm.

1.1.2 The centrosome

Centrosomes consist of a pair of centrioles arranged in a perpendicular fashion, surrounded by an amorphous electron dense protein matrix, the PCM (Figure 1.1F) (Chrétien et al., 1997; Ibrahim et al., 2009; Paintrand et al., 1992; Vorobjev and Chentsov, 1982). The pair of centrioles consists of one older mother centriole and a younger daughter centriole. The PCM contains many proteins involved in nucleating, organising and stabilising MTs, allowing the centrosome to function as the major MT organising centre (MTOC) in many animal cells (Bornens, 2001; Doxsey et al., 2005). Further important functions of the centrosome comprise mitotic spindle assembly, cell motility and cell polarity, maintenance of cell shape and intracellular transport (Bettencourt-Dias and Glover, 2007; Bornens, 2012; Nigg and Raff, 2009; Rieder et al., 2001).

The most prominent function of centrosomes is the formation of the poles of the mitotic spindle. In most vertebrate cells the amount of PCM organised by the pair of centrioles remains constantly low during interphase and increases drastically during prophase (Khodjakov and Rieder, 1999) to facilitate efficient mitotic spindle assembly. In some cell types, centrosomes also organise MT arrays in interphase, for example in mammalian monocytes and fibroblasts (Rieder et al., 2001). The position of the interphase centrosome has been shown to be important for orientation of the leading edge in migrating cells (Gomes and Gundersen, 2006).

Similarly, in most *Drosophila* somatic cells centrosomes do not appear to have a major role in MT nucleation in interphase, as centrioles organise little PCM and nucleate few, if any, MTs in interphase (Martinez-Campos et al., 2004; Rogers et al., 2008). There is

one system, however, where centrosomes have been shown to have a function outside mitosis in *Drosophila*. In asymmetrically dividing *Drosophila* neural stem cells (neuroblasts) the daughter centriole retains PCM during interphase (Conduit and Raff, 2010; Januschke et al., 2011) and organises a MT aster that helps establish/maintain the orientation of asymmetric cell division (Januschke and Gonzalez, 2010). Interestingly, localisation of the protein centrobin to the daughter centriole is sufficient to drive PCM organisation by the daughter centriole in interphase neuroblasts (Januschke et al., 2013).

Centrosomes have been suggested to act as "coordination centres" within the cell to which many proteins can localise in high concentrations. For example, many cell cycle regulators and checkpoint proteins are concentrated at centrosomes (Doxsey et al., 2005). Cdk1/Cyclin B is first activated at centrosomes during the entry into mitosis (Jackman et al., 2003) and Cyclin B is first destroyed at centrosomes during the exit from mitosis in fly embryos (Huang and Raff, 1999; Wakefield et al., 2000). It has also been shown that the localisation of Cdk2/Cyclin E to centrosomes is required for the proper initiation of S-Phase (Ferguson and Maller, 2010), Aurora A and Polo/Plk1, which are important regulators of mitosis, also prominently localise to centrosomes (Barr and Gergely, 2007; Glover, 2005).

Several proteins involved in DNA damage repair and stress response also localise to centrosomes. The centrosomal localisation of Chk1 has been suggested to regulate activation of centrosomal Cdk1/Cyclin B (Krämer et al., 2004; Sorino et al., 2013) and DNA damage leads to increased Chk2 localisation to centrosomes in *Drosophila* embryos (Takada et al., 2003). BRCA1 and p53 have been shown to localise to centrosomes in mitosis (Hsu and White, 1998; Tritarelli et al., 2004). Regarding the important functions of centrosomes it is not surprising that centrosome defects are

correlated with several human disorders, most notably cancer, microcephaly and dwarfism (Bettencourt-Dias et al., 2011; Nigg and Raff, 2009; Zyss and Gergely, 2009). It is intriguing that many of these disorders have also been linked to defective DNA damage repair (Section 1.2.1).

1.1.3 Cilia and flagella

Besides their role at the centrosome, centrioles are also required for the formation of cilia and flagella. It is thought that all species that form centrioles also form cilia at some stage of their life cycle (Marshall, 2009) and while centrioles can be dispensable for mitosis in many systems (Azimzadeh et al., 2012; Basto et al., 2006; Khodjakov et al., 2000; Mahoney et al., 2006) (Section 1.2.5), they are strictly required for the formation of cilia and flagella (Dawe et al., 2006). When a centriole migrates to the cell cortex to form a cilium or flagellum, it becomes known as a basal body.

Cilia and flagella are structurally similar and their names are often used interchangeably. They consist of an axoneme that extends directly from the centriole MTs and is surrounded by a ciliary membrane (Figure 1.1G). The axoneme consists of 9 doublet MTs, which directly grow out of the MT triplets of the basal body. Motile cilia have an additional MT pair in the middle of the axoneme (Figure 1.1E) (9 + 2 arrangement), while nonmotile or primary cilia lack the central pair (9 + 0 arrangement) (Singla, 2006). Motile cilia also have dynein arms which allow the MT doublets to slide relative to each other by ATP-dependent conformational changes of dynein heavy chains, enabling the cilia to beat (Fliegauf et al., 2007). The term nonmotile cilia is potentially misleading, however, as at least some 9 + 0 cilia can exhibit some motility (Nonaka et al., 1998).

Ciliogenesis usually occurs in quiescent cells (G0) or during G1 phase of the cell cycle in proliferating cells. As basal bodies migrate to the cell surface and dock onto the actin-rich cortex, they associate with membrane vesicles during a process called ciliary vesicle docking (Ishikawa and Marshall, 2011; Sorokin, 1962). Many proteins of the distal and subdistal appendages of centrioles have been shown to be important for this process (Ishikawa et al., 2005; Joo et al., 2013; Sillibourne et al., 2013; Tanos et al., 2013). After fusion of the ciliary vesicle with the plasma membrane, the basal body nucleates MTs, which grow out to form the axoneme. This requires the selective transport of ciliary proteins to the tip of the cilium by intraflagellar transport (IFT) (Ishikawa and Marshall, 2011). Mammalian epithelial cells can often be multiciliated and in this case centrioles are amplified prior to ciliogenesis, which can lead to production of 200-300 centrioles per cell (Dawe et al., 2006).

Cilia and flagella can have various functions (Satir and Christensen, 2008). For example, motile cilia in multiciliated cells in the mammalian respiratory tract clear out debris (Afzelius, 1976), and also have chemosensory functions (such as the bitter taste sensation), which can be positively coupled with the beat frequency (Shah et al., 2009). Primary cilia are present on most vertebrate cells and sense mechanical and chemical signals. For example, primary cilia in renal epithelial cells measure the flow of the surrounding fluid (Nauli et al., 2003). Primary cilia are important during mammalian development, for example they perform a twirling motion on the embryonic node which creates a leftward flow essential for the development of the left/right axis of the embryo (Nonaka et al., 1998). Furthermore, cilia function has been implicated in several signalling pathways in vertebrates, such as the Sonic hedgehog (Shh), Wnt, PDGFR and Notch signalling pathways (Berbari et al., 2009; Eggenschwiler and Anderson, 2007; Ezratty et al., 2011). Remarkably, it appears that cilia are essential for all Shh signalling

in vertebrates, and mice with mutations in IFT machinery proteins have developmental defects related to compromised Shh signalling (Corbit et al., 2005; Huangfu et al., 2003).

Given these diverse roles for cilia in mammals, it is not surprising that ciliary defects are implicated with a growing group of diseases in humans called ciliopathies (Badano et al., 2006). These include abnormalities in left/right asymmetry (situs inversus) (Nonaka et al., 1998), polycystic kidney disease, retinitis pigmentosa, and other ciliopathic genetic disorders such as Meckel-Gruber and Bardet-Biedl syndrome (Badano et al., 2006; Eley et al., 2005; Nigg and Raff, 2009).

In *Drosophila* cilia are only found in the male germline in form of the sperm flagellum, and on type I sensory neurons of the peripheral nervous system, which innervate mechano- and chemosensory bristles. Furthermore, Hedgehog signalling is not connected with cilia in *Drosophila* (Roy, 2012).

1.2 Centriole duplication

1.2.1 The importance of controlling centrosome numbers and centrosome integrity

Centriole duplication is tightly correlated with cell cycle progression: it happens once, and only once, per cell cycle. Given the key functions of centrosomes (Section 1.1.2) it is vitally important that centriole duplication and centrosome formation is tightly regulated. Failure of centriole duplication would lead to cells without centrioles. Centrosomes nucleate the majority of mitotic spindle MTs and although most cells can

still divide without centrioles by using alternative spindle assembly pathways (Section 1.4), centrioles are essential for development in many embryonic systems such as *Xenopus, Drosophila* and *C. elegans* (Kirkham et al., 2003; Klotz et al., 1990; Leidel and Gönczy, 2003; Stevens et al., 2007).

Moreover, defects in centrosome integrity can have devastating effects in at least some vertebrate cells. Mutations in several centrosomal genes have been implicated in the neurodevelopmental disorder autosomal recessive primary microcephaly (MCPH) which causes a small brain size in patients (Woods et al., 2005). These include mutations in CENPJ/CPAP/HsSAS-4, CEP215/CDK5RAP2, ASPM, STIL/SIL, MCPH1, WDR62, NDE1, CEP135, CEP63, CDK6 and CEP152/Asl (Alkuraya et al., 2012; Bakircioglu et al., 2012; Bond et al., 2005; Dauber et al., 2012; Guernsey et al., 2010; Gul et al., 2006; Hussain et al., 2012; Hussain et al., 2013; Jackson et al., 2002; Kumar et al., 2009; Shen, 2005; Sir et al., 2011; Yu et al., 2010). The small brain size has been suggested to be caused by misregulation of symmetric and asymmetric cell divisions during neural development (Woods et al., 2005). Mutations in the centriolar/centrosomal proteins Pericentrin, CEP152/Asl and CENPJ/CPAP/HsSAS-4 can also cause other phenotypes in humans, such as primordial dwarfism and Seckel syndrome (Al-Dosari et al., 2010; Griffith et al., 2008; Kalay et al., 2010; Rauch et al., 2008), pathologies often associated with defective DNA damage signalling, leading to increased genomic instability. A mouse model with a hypomorphic mutation in CENPJ recapitulates many of the clinical features of Seckel syndrome, and also leads to large scale genomic instability, increased cell death and mitotic failure, which presumably contributes to the dwarfism associated with Seckel syndrome (McIntyre et al., 2012).

When centrioles duplicate more than once per cell cycle this leads to centrosome amplification, and can have similarly deleterious effects. Centrosome amplification is a common feature of many tumours (Chng and Fonseca, 2009; Guo et al., 2007; Jung et al., 2007; Kawamura et al., 2003; Kayser et al., 2005; Nakajima et al., 2004; Pihan et al., 1998; Pihan et al., 2001). Moreover, it could be shown that centrosome defects appear in the earliest identifiable steps in human cancer (Lingle et al., 2002; Pihan et al., 2003), which suggests that they might promote tumourigenesis rather than arising as a byproduct of oncogenic transformation. Centrosome amplification usually correlates with the grade of chromosomal instability and can be used as a measurement of the aggressiveness of a tumour (Zyss and Gergely, 2009). As early as 1914 it had been suggested that aneuploidy caused by missegregation of genetic material is responsible for tumour formation and that changes in centrosome number could be responsible for this effect by assembling multipolar spindles (Boveri, 2008; Boveri, 1914).

Although there is plenty of observational evidence, there still is little experimental proof to support the model that centrosome amplification causes genomic instability and as a result cancer (Zyss and Gergely, 2009). The first causative relationship between centrosome amplification and tumourigenesis has been demonstrated in *Drosophila*, where transplantation of tissue with amplified centrosomes into the abdomen of an adult fly can lead to overgrowth of the respective tissue (Basto et al., 2008). These tumours share many traits with human tumours, for example they become immortal, metastatic and highly aneuploid (Basto et al., 2008).

It has long been assumed that amplified centrosomes would promote tumourigenesis by forming multipolar spindles, which would lead to aneuploid daughter cells (Boveri 1914; Boveri 2008). Recently it has been shown that the mechanism by which

supernumerary centrosomes can cause chromosomal instability is a bit more complex (Ganem et al., 2009; Silkworth et al., 2009). Although cells with supernumerary centrosomes often initially form a multipolar spindle, these very rarely result in multipolar anaphases and almost all cells ultimately divide in a bipolar manner (Basto et al., 2008; Kwon et al., 2008). In the few cases where multipolar division actually occurs the daughter cells either undergo mitotic cell death or cell cycle arrest (Ganem et al., 2009). Bipolar cell division is achieved through clustering and partial inactivation of extra centrosomes (Basto et al., 2008; Godinho et al., 2009; Kwon et al., 2008; Quintyne et al., 2005). Essential for efficient clustering of extra centrosome is the minus end-directed motor HSET/Ncd (Basto et al., 2008; Kwon et al., 2008). Furthermore, the interaction between cell adhesion and the actin and MT cytoskeleton plays a role in suppressing multipolar mitoses in cells with extra centrosomes (Kwon et al., 2008).

Thus, it appears that many cells with extra centrosomes, including cancer cells possess powerful mechanisms that suppress multipolar mitoses and thereby avoid the constant generation of highly aneuploid cells, which would not be viable. During the clustering of the initially multipolar spindles, however, some individual centromeres can attach to multiple centrosomes. When centrosome clustering takes place these centromeres can end up being attached to both spindle poles - a so called merotelic attachment (Ganem et al., 2009; Silkworth et al., 2009). As merotelic attachments are not recognized by the spindle assembly checkpoint (Cimini, 2008), mitosis proceeds and the chromosomes appear as lagging chromosomes in anaphase potentially generating chromosome missegregation (Ganem et al., 2009; Silkworth et al., 2009). The resulting chromosomal instability is considered by many to be a driving force for tumourigenesis (Gordon et al., 2012; Holland and Cleveland, 2012a; Thompson et al., 2010). Furthermore, merotelic attachments can lead to the formation of micronuclei, which have been suggested to

further promote tumourigenesis as they can lead to impaired DNA replication and so to new mutations that drive tumourigenesis (Crasta et al., 2012; Hammond et al., 2013; Holland and Cleveland, 2012b). Interestingly, driving centrosome amplification specifically in the developing mouse central nervous system leads to microcephaly in these mice as a high proportion of neural stem cells fail to cluster supernumerary centrosomes, leading to aneuploidy and increased cell death (Marthiens et al., 2013).

1.2.2 The centriole duplication cycle

Centrioles are duplicated and segregated to the daughter cells in each cell division cycle. Centriole duplication is tightly correlated with the cell cycle and can be subdivided into several steps (Figure 1.2A). At the end of mitosis the pair of centrioles disengage, losing their tight orthogonal arrangement, a process which is required for licensing centriole duplication (Tsou and Stearns, 2006). After disengagement the centrioles are still connected by flexible cohesion fibres and this centriole cohesion has been shown to be dependent on the proteins Rootletin, Nek2 and C-Nap1 (Bahe, 2005; Faragher, 2003; Fry et al., 1998). Thus, each daughter cell inherits one pair of disengaged centrioles at the end of mitosis. Disengagement allows formation of a procentriole orthogonally to each mother centriole in S-phase. Electron microscopy studies have shown that the earliest structure observed during this process in *Chlamydomonas, Paramecium* and rhesus monkey cells is an amorphous disc. Next, a cartwheel structure consisting of a central hub and 9 radial spokes appears, and subsequently around this cartwheel the A-tubules form, followed by the B- and C-tubules (Anderson and Brenner, 1971; Cavalier-Smith, 1974; Dippell, 1968). The tubules elongate until the procentrioles have matured into fully-grown centrioles. In G2, as the cells prepare to enter mitosis, the two pairs of centrioles start to accumulate PCM and separate. This dramatic increase in PCM

recruitment is called centrosome maturation and enables centrosomes to nucleate more MTs for efficient spindle assembly during mitosis.

Although centrioles are remarkably complex structures, two genome-wide RNAi screens in *Drosophila* tissue culture cells identified only a relatively small set of ~18 genes that reduce centrosome numbers when knocked down (Dobbelaere et al., 2008; Goshima et al., 2007). *In vivo,* only 6 of these 18 genes appear to encode proteins that are absolutely essential for centriole duplication: Asl, Sak, Ana2, DSas-6, DSas-4 and Ana1, and the mutation of any one of these genes leads to the formation of flies that lack centrioles (Basto et al., 2006; Bettencourt-Dias et al., 2005; Blachon et al., 2009; Blachon et al., 2008; Peel et al., 2007; Rodrigues-Martins et al., 2007a) (this result for *ana2* mutants is an unpublished result from our lab). Moreover, the overexpression of any of the first 5 proteins, but not of Ana1, can lead to centrosome amplification in at least some *Drosophila* tissues (Basto et al., 2008; Peel et al., 2007; Stevens et al., 2010a).

Asl (CEP152 in humans) appears to be essential for centriole duplication in flies, humans and zebrafish (Blachon et al., 2008; Cizmecioglu et al., 2010; Hatch et al., 2010; Sir et al., 2011; Sonnen et al., 2013) but there is no obvious homologue of Asl in worms. Asl/CEP152 acts in centriole duplication by its ability to act as a scaffold and bind to Sak/Plk4 and DSas-4/CPAP (Dzhindzhev et al., 2010a) and recruit Sak/Plk4 to the centriole (Cizmecioglu et al., 2010; Dzhindzhev et al., 2010a; Hatch et al., 2010; Sonnen et al., 2013). Asl also has an important role in PCM recruitment (Bonaccorsi et al., 1998; Conduit et al., 2010; Dzhindzhev et al., 2010b; Lawo et al., 2012; Varmark et al., 2007) (Section 1.3.1).

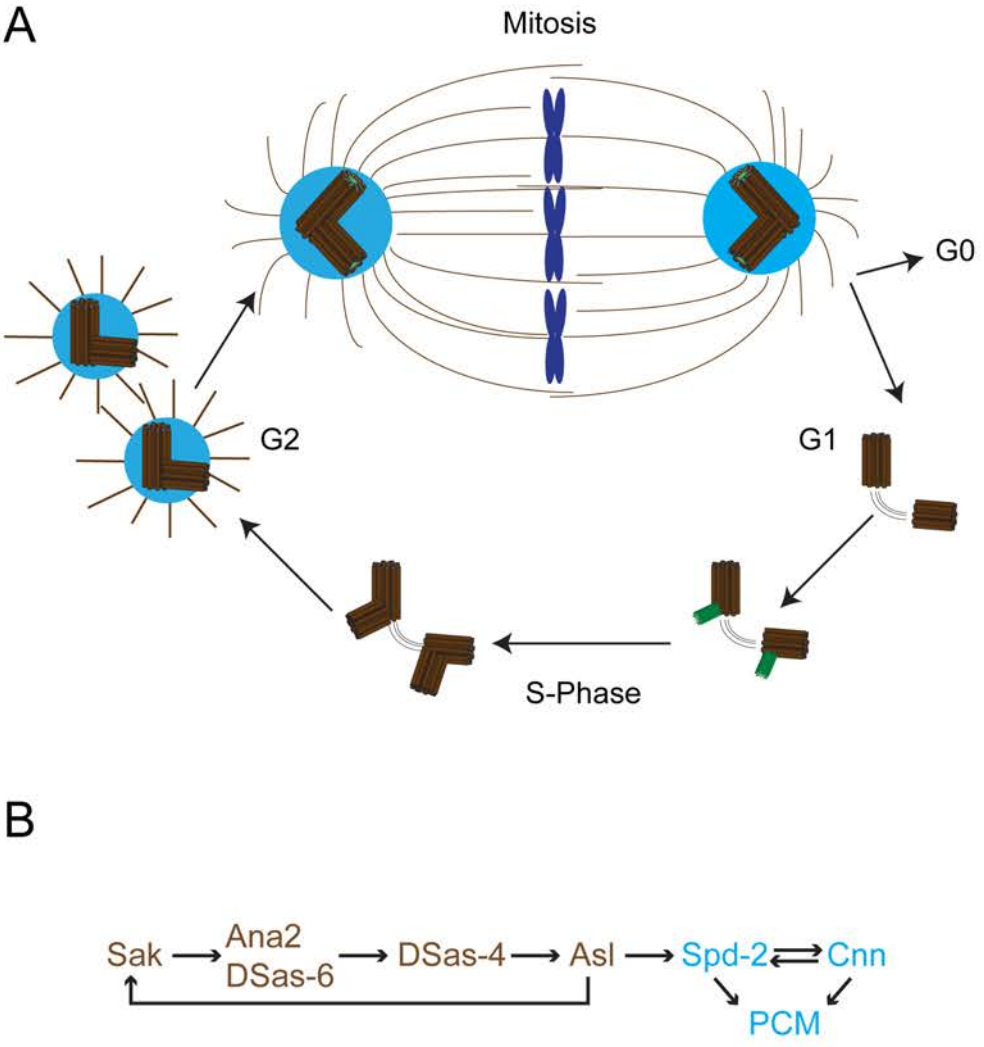

Figure 1.2: The centriole duplication cycle and centrosome assembly pathway. (A) The pair of centrioles (brown) is at the core of the centrosome and is surrounded by PCM (blue). In mitosis two centrosomes form the two poles of the mitotic spindle. At the end of mitosis the cells can either become quiescent (and centrioles can become basal bodies for ciliogenesis then), or they enter G1 phase. The pair of centrioles disengages, which allows formation of a small structure at the proximal end of each mother called a cartwheel structure (green) at the beginning of S-Phase. During S-Phase the centriolar MTs assemble around the cartwheel. In G2 as the cells prepare for mitosis the two pairs of centrioles separate and start to recruit PCM (blue) and nucleate MTs, enabling efficient spindle assembly in mitosis. **(B)** The molecular pathway of centrosome formation in *Drosophila.* Note that centriolar proteins are indicated in brown, and PCM proteins are indicated in blue. Asl has a special role, as it is required for centriole duplication by recruiting Sak to the mother centriole, and also for PCM recruitment by recruiting Spd2 to the centriole in mitosis.

Sak (Plk4 in mammalian cells, its functional counterpart in *C. elegans* is ZYG-1) is essential for centriole duplication in flies, human cells and worms (Bettencourt-Dias et al., 2005; Habedanck et al., 2005; O'Connell et al., 2001). It has been shown in *C. elegans* that ZYG1 recruits SAS-6 to the mother centriole by a direct interaction that is independent of the kinase activity of ZYG-1; during a second step, ZYG1 then phosphorylates an unknown protein (that almost certainly is not SAS-6), which is required for the stable assembly of SAS-6 into the centriole structure (Lettman et al., 2013). ZYG1 is also needed for the recruitment of the *C. elegans* homologue of Ana2, SAS5, to the centriole (Delattre et al., 2004), and there is strong evidence that Sak also loads DSas-6 and Ana2 onto the centriole in *Drosophila* (Stevens et al., 2010b).

Homologues of SAS-6 have been shown to be required for centriole duplication in *Drosophila* (Peel et al., 2007; Rodrigues-Martins et al., 2007a), *Chlamydomonas* (Nakazawa et al., 2007), *Tetrahymena* (Culver et al., 2009), *D. rerio* (Yabe et al., 2007) and human cells (Leidel et al., 2005; Strnad et al., 2007). SAS-6 is a component of the cartwheel and is required to establish the robust 9-fold symmetry of the centriole (Culver et al., 2009; Nakazawa et al., 2007; Rodrigues-Martins et al., 2007a; Stevens et al., 2010b). How this might be achieved has recently been elucidated by X-ray crystallography and EM, which reveal how SAS-6 forms homodimers through a C-terminal coiled-coil domain, and these homodimers can interact through their N-terminal domains to form oligomers (Kitagawa et al., 2011; Van Breugel et al., 2011). The structures of the SAS-6 homologues of *D. rerio* and *C. reinhardtii* suggest that several of these homodimers can assemble into cartwheel-like structure consisting of a central ring from which the coiled-coil domains of SAS-6 emanate as radial spokes (Kitagawa et al., 2011; Van Breugel et al., 2011). There is some evidence that a nine-fold symmetric ring is the most stable oligomeric structure for SAS-6, potentially

explaining why centrioles are always 9-fold symmetric (Kitagawa et al., 2011; Van Breugel et al., 2011). However, the N-terminal head group interaction is relatively weak, and it is unclear whether it would be sufficiently strong to enforce the strict 9-fold symmetry of the centriole (Cottee et al., 2011).

Although the X-Ray structures did not indicate whether the SAS-6 cartwheel-like structures were organised as a stack or as a spiral inside centrioles *in vivo* (Cottee et al., 2011), recent studies of the *Trichonympha* cartwheel by cryoelectron tomography have shown that the cartwheel consists of a stack with multiple segments. Each segment consists of two central rings that are joined by their spokes towards the periphery of the cartwheel (Guichard et al., 2012; Guichard et al., 2013). These stacked segments are asymmetric at the periphery (where the coiled coil regions of SAS-6 are closest to the centriolar MTs) giving the carthwheel a polarity along the proximal-distal axis (Guichard et al., 2012; Guichard et al., 2013). Intriguingly, the *C. elegans* SAS-6 coiled-coil dimer can assemble into a spiral structure with 9-fold symmetry (Hilbert et al., 2013), indicating that the architecture of the central tube in *C. elegans* centrioles may be quite different from the cartwheel structure found in *Danio rerio, Trichonympha* and *Chlamydomonas reinhardtii*.

It is likely, that further proteins are needed for the robust oligomerisation of the cartwheel stack (Cottee et al., 2011; Guichard et al., 2013), and likely candidates are CEP135, DSAS-4/CPAP and Ana2/STIL. CEP135 has been implicated in the structural integrity of the cartwheel in flies, human cells and *Chlamydomonas* (Hiraki et al., 2007; Lin et al., 2013; Roque et al., 2013) presumably by linking the cartwheel to the outer MTs. Ana2/STIL/SAS5 is required for centriole duplication in flies, human cells and worms (Arquint et al., 2012; Delattre et al., 2004; Stevens et al., 2010a; Tang et al.,

2011; Vulprecht et al., 2012). It has been shown in flies and worms that DSas-6/SAS-6 and Ana2/SAS-5 are recruited to the procentriole in a complex, and this recruitment is dependent on Sak/ZYG-1 (Delattre et al., 2006; Pelletier et al., 2006a; Stevens et al., 2010b). SAS-6 and SAS-5 together form the central tube in *C. elegans*, and recruit SAS-4 (Delattre et al., 2006; Pelletier et al., 2006b). DSas-4/SAS-4/CPAP is required for centriole duplication in mammalian cells, *Drosophila, C. elegans* and *Paramecium* (Basto et al., 2006; Gogendeau et al., 2011; Kleylein-Sohn et al., 2007; Leidel and Gönczy, 2003). In *C. elegans* the addition of the centriolar MTs is dependent on SAS-4 (Delattre et al., 2006; Pelletier et al., 2006b), but its molecular role in *Drosophila* has yet to be identified. In mammalian cells CPAP recruits tubulin dimers to the growing procentriole and is required for the elongation of centrioles, and overexpression of CPAP leads to abnormally long centrioles (Kohlmaier et al., 2009; Schmidt et al., 2009; Tang et al., 2009). In human cells, flies, worms and zebrafish Ana2/STIL/SAS-5 and DSas-4/CPAP/SAS-4 interact (Cottee et al., 2013; Tang et al., 2011; Vulprecht et al., 2012), and this interaction is essential for centriole assembly (Cottee et al., 2013).

Taken together, the five proteins Asl, Sak, DSas-6, Ana2 and DSas-4 represent the core centriole duplication factors in *Drosophila* (Stevens et al., 2010a). A combination of the existing literature in flies and other species and unpublished data from our lab suggests that they act in a putative pathway where Asl recruits Sak to the centriole (Dzhindzhev et al., 2010b), which then in turn is required to load on a complex of Ana2 and DSas-6 (Stevens et al., 2010b) and phosphorylate an unknown target critical for cartwheel formation (Lettman et al., 2013). Next, DSas-4 is recruited to the centriole, which finally loads on Asl on the newly formed centriole (both unpublished results from our lab) (Figure 1.2B). Asl also initiates PCM recruitment in flies, as it is important for recruitment of the PCM proteins Spd-2 and Cnn to the centriole (Section 1.3.1 and

Section 3.1) (Bonaccorsi et al., 1998; Conduit et al., 2010; Dzhindzhev et al., 2010a; Varmark et al., 2007). Although Ana1 is required for centriole duplication in *Drosophila* (Blachon et al., 2009), I do not include it as a core duplication factor here as its overexpression does not lead to centrosome amplification and its molecular role is still unclear.

In other organisms, there are several additional proteins that are also implicated in centriole duplication. For example, in *C. elegans* Spd-2 is essential for centriole duplication by recruiting the Sak/PLK4 functional homologue Zyg1 to the mother centriole (Kemp et al., 2004; O'Connell et al., 2000; Pelletier et al., 2004). In contrast, in flies Spd-2 is only required for PCM recruitment (Conduit et al., 2010; Dix and Raff, 2007; Giansanti et al., 2008). Recent data suggest that in human cells the homologues of Spd-2 (CEP192) and Asl (CEP152) act redundantly in centriole duplication by recruiting Sak/PLK4 to the centriole (Sonnen et al., 2013). Furthermore, in human cells there are several additional duplication factors, for example CEP63 is involved in centriole duplication in human and mouse cells by forming a complex together with CEP152 which has been shown to be important for efficient SAS-6 recruitment (Brown et al., 2013; Sir et al., 2011). There is no *Drosophila* homologue known for CEP63.

1.2.3 *De novo* centriole formation

Centriole duplication does not necessarily have to be templated by a mother centriole. In some organisms *de novo* formation of centrioles has been observed, for example in the early mouse embryo (Gueth-Hallonet et al., 1993) and in parthenogenic Hymenopteran insects (Riparbelli et al., 1998; Riparbelli et al., 2005; Tram and Sullivan, 2000). Planarians have also been shown to live without centrioles in all of their cells, but they

can form centrioles *de novo* in cells that will become multiciliated (Azimzadeh et al., 2012). Centriole ablation in human cultured cells and in *Chlamydomonas* often leads to *de novo* formation of new centrioles, and this process seems to require the same proteins as canonical centriole duplication (Khodjakov, 2002; La Terra, 2005; Marshall et al., 2001). In *Drosophila*, the individual overexpression any one of the five canonical core duplication proteins can lead to the *de novo* formation of centriole-like structures (Dzhindzhev et al., 2010b; Peel et al., 2007; Rodrigues-Martins et al., 2007c; Stevens et al., 2010a) and in the case of Sak and Asl these structures appear to contain *bona fide* centrioles (Dzhindzhev et al., 2010b; Rodrigues-Martins et al., 2007c).

1.2.4 Mechanisms controlling centriole numbers

As discussed in Section 1.2.1, having too many or no centrosomes can have deleterious effects on cells and organisms. Therefore there are several mechanisms in the cell to ensure that each daughter cell inherits exactly one pair of centrioles after each cell division, and that only one procentriole is formed next to each mother centriole during centriole duplication.

Centriole duplication begins near the G1-S boundary and lasts until G2 (Doxsey et al., 2005), and only during this time are conditions in the cell permissive for centriole duplication. It has been shown in *Xenopus* egg extracts and mammalian cells that the activity of Cyclin-dependent kinase 2 (Cdk2) in complex with cyclin E is required for centriole duplication (Hinchcliffe, 1999; Matsumoto et al., 1999). So far two centriolar Cdk2 targets have been found, nucleophosmin and CP110 (Chen et al., 2002; Okuda et al., 2000); Nucleophosmin in particular appears to be a good candidate to control centriole duplication as Nucleophosmin phosphorylated by Cdk2 gets removed from the

centrosome in S-Phase, allowing duplication to take place (Okuda et al., 2000). Interestingly, however, Nucleophosmin has not been identified in several genome-wide RNAi screens that have identified factors required for centriole duplication (Dobbelaere et al., 2008; Goshima et al., 2007). Cdk2 also appears to control centriole duplication in mice by stabilising Mps1p kinase, which promotes centriole duplication in S phase (Fisk and Winey, 2001). Mps1 has a well-conserved role in spindle checkpoint function (Musacchio and Salmon, 2007), but, as with Nucleophospmin, its role in centriole duplication remains somewhat controversial (Stucke et al., 2002).

Plk2 is activated at the G1-S phase transition and has also been shown to function in centriole duplication (Warnke et al., 2004). In human cell culture, Plk2 phosphorylates CPAP and this phosphorylation is critical for procentriole formation (Chang et al., 2010). Furthermore, Plk2 phosphorylation of F-box/WE repeat-containing protein 7 (Fbxw7) induces destabilisation of Fbxw7, and Fbxw7 is a regulator of ubiquitin-mediated degradation of cyclin E, which promotes centriole duplication in complex with Cdk2 (Cizmecioglu et al., 2012).

Prolonged S phase alone, however, is usually not sufficient to enable cells to undergo repeated cycles of centriole duplication (Fisk and Winey, 2001), indicating that there are further mechanisms that license centriole duplication. It is known that at the end of mitosis the pair of centrioles disengages by losing the tight orthogonal arrangement, and this process is required to enable centrioles to duplicate (Tsou and Stearns, 2006). It has been shown that centriole disengagement is dependent on Separase in *Xenopus* egg extract and human cells (Tsou and Stearns, 2006; Tsou et al., 2009b), and, in analogy to cleavage of cohesin around the chromatids in mitosis (Uhlmann et al., 1999), there is some evidence that Separase is responsible for cleavage of Cohesin at the centrioles in

human cells, although how this might enable centriole disengagement is unclear (Schöckel et al., 2011). In *Drosophila*, however, cleavage of Cohesin does not appear to be sufficient for centriole disengagement (Oliveira and Nasmyth, 2013). It has recently been shown that Plk1 also has an important role in promoting centriole disengagement, and this may even be more important than the role of Separase (Tsou et al., 2009a).

Another major regulatory mechanism of centriole duplication appears to be the tight regulation of the levels of several key centriole duplication factors. The levels of Sak/Plk4 in the cell are very low and are tightly regulated; this is accomplished, at least in part, by trans-autophosphorylation of Sak/Plk4. The SCF (Skp/Cullin/F-box) E3 ligase recognises autophosphorylated Sak/Plk4 and targets it for degradation by the proteasome (Cunha-Ferreira et al., 2009; Guderian et al., 2010; Rogers et al., 2009; Sillibourne et al., 2010) (discussed in more detail in Section 4.1). The tight regulation of Sak/Plk4 levels have been shown to be crucial, as overexpression leads to centriole overduplication (Kleylein-Sohn et al., 2007; Peel et al., 2007). Furthermore, in human cultured cells, levels of SAS-6 are correlated with the cell cycle and this is important to restrict procentriole formation (Strnad et al., 2007). It has been shown that the SCF E3 ligase together with Fbxw5 as substrate-targeting unit targets SAS-6 for destruction (Puklowski et al., 2011).

1.2.5 Flies with abnormal centrosome numbers

Flies with mutations in genes for any of the core centriole duplication proteins lack centrioles (Basto et al., 2006; Bettencourt-Dias et al., 2005; Blachon et al., 2008; Blachon et al., 2009; Peel et al., 2007; Rodrigues-Martins et al., 2007a). These flies can duplicate centrioles during embryonic stages due to the maternal contribution of mRNA

and protein into the embryo, but subsequently lose their centrioles during larval stages. Given the important functions of centrioles and centrosomes, it was very surprising when it was first shown that these flies can develop with near normal timing and eclose in near normal ratios to form morphologically normal adults (Basto et al., 2006). Somatic cell divisions took longer in these flies, but cells divided normally in a bipolar fashion by employing alternative pathways of spindle assembly (Section 1.4). There was only a small, but significant, increase in chromosome segregation errors. The adult flies that eclosed died, however, as they could not walk or feed due to the lack of primary cilia (caused by the lack of centrioles/basal bodies) in certain sensory neurons, which are essential for proprio-, mechano- and chemoreception (Basto et al., 2006).

Although many cell types appeared to be relatively unperturbed by the lack of centrioles/centrosomes in flies, one cell type that seemed to be more sensitive to centrosome defects was the neural precursor cells in the larval central nervous system. These large stem-cell-like cells are called neuroblasts and normally divide asymmetrically to generate one self-renewing neuroblast and one smaller ganglion mother cell, which can then divide a few more times before differentiating into a neuron or glial cell (Doe, 2008; Knoblich, 2010). It is believed that centrosomes are important for asymmetrical divisions like this, because astral MTs emanating from the centrosomes contact the cell cortex to position the mitotic spindle according to various cortical cues (Betschinger and Knoblich, 2004; Gönczy, 2002). In cells lacking centrosomes, these neuroblasts divided symmetrically in 15% of the cases, or failed in cytokinesis in further 15% of cells (Basto et al., 2006). In contrast, female germ line stem cells, which also divide asymmetrically, are not perturbed by the lack of centrosomes (Stevens et al., 2007).

Although mutants that lose their centrioles during larval stages can develop to adulthood (Basto et al., 2006; Bettencourt-Dias et al., 2005; Blachon et al., 2008; Blachon et al., 2009; Peel et al., 2007; Rodrigues-Martins et al., 2007a), centrioles are essential for some stages of development, as embryos lacking the centriole duplication factor DSas-4 or DSas-6 arrest very early in development with very few nuclei that are almost always in a mitotic state (Stevens et al., 2007). Embryogenesis starts with 13 rapid cycles of nuclear division in a common cytoplasm, and is known to be particularly sensitive to centrosome defects (Gergely et al., 2000; Megraw et al., 1999). Nevertheless, it is unclear why embryos lacking centrosomes (apart from the centrosome brought in with the fertilising sperm) arrest in mitosis after only a few rounds of division. One possibility is that in flies the destruction of Cyclin B at the end of mitosis starts at centrosomes (Huang and Raff, 1999), and if these detach from the spindle in the embryo, Cyclin B is not properly destroyed leading to a mitotic arrest very similar to that seen in the *DSas-4* and *DSas-6* mutant embryos (Wakefield et al., 2000). Perhaps spindles lacking centrosomes cannot degrade Cyclin B in these embryos, leading to the mitotic arrest.

Flies that overexpress the core duplication factor Sak driven by the ubiquitin promoter (*SakOE* flies) can also develop normally and eclose as morphologically normal adults (Basto et al., 2008). These flies are viable and fertile and can be kept as stocks in the lab, although a significant fraction of the eggs laid by *SakOE* females die during very early embryonic development for reasons that are not clear (and are not clearly related to the presence of extra centrosomes) (Peel et al., 2007). Cell divisions in *SakOE* larval brains and imaginal discs were slowed down, as cells with multiple centrosomes often formed multipolar spindles in prophase which activated the spindle assembly checkpoint (Yang et al., 2008). The spindle assembly checkpoint stalls mitosis until

multiple centrosomes have become clustered into two poles, a process which is dependent on the kinesin Ncd/HSET (Basto et al., 2008; Kwon et al., 2008). Accordingly, Mad2 (a component of the spindle assembly checkpoint) and Ncd, which are not normally essential in flies, were essential in flies that have too many centrosomes (Basto et al., 2008). Furthermore, similarly to flies lacking centrosomes, the asymmetric neuroblast divisions were perturbed in developing *SakOE* brains with ~10% of neuroblasts dividing in a symmetrical manner (Basto et al., 2008).

Intriguingly, brain tissue of flies that either lack centrosomes or have amplified centrosomes are prone to forming tumours in abdominal transplantation assays (Basto et al., 2008; Castellanos et al., 2008). The reason for this is unclear, but it is believed that tumour formation is in some way related to the failure in asymmetric neuroblast divisions (Castellanos et al., 2008; Gonzalez, 2007). When neuroblasts divide symmetrically rather than asymmetrically cell fate determinants that regulate self renewal can end up in both daughter cells, giving rise to two neuroblast-like daughters which both have the potential to self-renew (Lee et al., 2006; Wang et al., 2006). This can lead to an expansion of the neuroblast pool (Basto et al., 2008) and overgrowth of the respective tissue (Gonzalez, 2007). It is still unclear, however, how malignant transformation of these tissues is driven – as tumours formed by brain tissue lacking centrosomes and having extra centrosomes develop many cancerous traits such as being highly aneuploid, metastatic and immortal (Basto et al., 2008; Castellanos et al., 2008). Perhaps the low levels of aneuploidy generated by centrosome loss or amplification are important for this transformation.

1.3 Pericentriolar Material (PCM)

The PCM surrounding the centriole pair in centrosomes is the major source of MT nucleation in most cells. It has been described as a complex lattice structure consisting of protein aggregates (Dictenberg et al., 1998). Recently, super-resolution microscopy has demonstrated that the interphase PCM is organised into spatial subdomains. In centrosomes of both human and *Drosophila* cells different PCM proteins were organised in a toroidal pattern with progressively larger, overlapping diameters (Fu and Glover, 2012; Lawo et al., 2012; Mennella et al., 2012; Sonnen et al., 2012). The Asl/CEP152 and Spd-2/CEP192 rings were localised closer to the centriole, while the γ–tubulin and Cnn/CDK5RAP2 toroids were in the outer region of the PCM. Interestingly in both *Drosophila* and human cells, Pericentrin and DPLP (*Drosophila* pericentrin like protein) were organised in the shape of fibrils that emanated from the centriole and spanned the width of the interphase PCM, with the C-terminal domain binding to the centriole and the N-terminal domain extending out into the periphery (Lawo et al., 2012; Mennella et al., 2012). In fly cells, DPLP seems to be essential for organising the interphase PCM (Mennella et al., 2012), although it seems that the centrosomes in many *Drosophila* cell types often organise very little PCM during interphase (Martinez-Campos et al., 2004; Rogers et al., 2008). The organisation of the PCM during mitosis (when the PCM is much larger) was also investigated in some of these studies, and, although less clearly organised than the interphase PCM, there were hints that the mitotic PCM is also organised into subdomains (Fu and Glover, 2012; Lawo et al., 2012; Mennella et al., 2012; Sonnen et al., 2012).

PCM proteins, such as Asl, Spd-2, Cnn and DPLP tend to be large proteins with many predicted coiled-coil domains (Santos et al., 2013), enabling them to function as

scaffolds for the recruitment of other proteins. It is known, for example, that Cnn can directly recruit γ-tubulin, DTACC and Msps to centrosomes in *Drosophila* (Zhang and Megraw, 2007), proteins that either nucleate or stabilise MTs. γ-tubulin is a part of the γ-TuRC, a protein complex that directly nucleate MTs by enabling α/β dimers to polymerise (Gunawardane et al., 2000; Kollman et al., 2010; Kollman et al., 2011; Moritz et al., 1995; Oegema et al., 1999; Zheng et al., 1995). TACC proteins cooperate with Msps/XMAP215/ch-TOG to directly regulate MT dynamics and stabilise centrosomal MTs (Barros et al., 2005; Gergely et al., 2003; Kinoshita et al., 2002; Lee et al., 2001).

The PCM allows the centrosome to function as a "coordination centre" where many proteins implicated in cell cycle regulation, DNA damage repair and stress response can come together at high concentrations (Section 1.1.2) (Doxsey et al., 2005; Hsu and White, 1998; Jackman et al., 2003; Krämer et al., 2004; Sorino et al., 2013; Tritarelli et al., 2004). Several proteomic screens have attempted to identify a complete inventory of centrosomal proteins over the last years and these studies have suggested that several hundred proteins may localise to the PCM (Andersen et al., 2003; Habermann and Lange, 2012; Jakobsen et al., 2011; Müller et al., 2010; Reinders et al., 2006). Although several of the protein-protein interactions involved in the formation of several subcomplexes of centrosomal proteins have been identified, we have very little understanding of how the many hundreds of proteins in the PCM are organised to form a functional structure. Furthermore, many centrosomal proteins undergo posttranslational modifications such as phosphorylation (Habermann et al., 2012), SUMOylation (Cheng et al., 2006; Klein and Nigg, 2009) and ubiquitylation (Li et al., 2013; Puklowski et al., 2011) and further studies are needed to elucidate how these modifications might regulate centrosome assembly and function.

1.3.1 PCM recruitment

The amount of PCM organised by the pair of centrioles increases dramatically at the onset of mitosis. For example, in rat kangaroo kidney epithelial cells, the amount of γ-tubulin increases 3-5 fold in late prophase (Khodjakov and Rieder, 1999) and the increase in the amount of PCM coincides with an increase in the size of centrosomal asters (Palazzo et al., 2000).

Fluorescent recovery after photobleaching (FRAP) experiments of several PCM proteins have shown that the PCM is a highly dynamic structure, and that its components rapidly exchange between the centrosome and cytoplasm with half maximal recovery times often in the order of seconds or minutes (Conduit et al., 2010; Kishi et al., 2009; Mahen et al., 2011; Stenoien et al., 2003). Interestingly, while most proteins recover evenly throughout the PCM, some proteins including Cnn and Spd-2 first recover in the centre of the centrosome and subsequently spread out through the PCM, indicating that their binding sites are located close to the surface of the centriole (Conduit et al., 2010; and unpublished observations).

Several proteins have been implicated in centrosome maturation, these include DSas-4/CPAP (Cho et al., 2006; Gopalakrishnan et al., 2012; Gopalakrishnan et al., 2011), DPLP/Pericentrin (Fu and Glover, 2012; Lawo et al., 2012; Martinez-Campos et al., 2004; Mennella et al., 2012; Sonnen et al., 2012; Zimmerman et al., 2004), Asl/CEP152 (Bonaccorsi et al., 1998; Dzhindzhev et al., 2010b; Lawo et al., 2012; Varmark et al., 2007), Spd-2/CEP192 (Decker et al., 2011; Dix and Raff, 2007; Giansanti et al., 2008; Gomez-Ferreria et al., 2007; Joukov et al., 2010; Pelletier et al., 2004; Zhu et al., 2008b), Cnn/CEP215/CDK5RAP2 (Barr et al., 2010; Choi et al., 2010; Conduit et al.,

2010; Lucas and Raff, 2007; Megraw et al., 1999), Dgp71WD/NEDD1 (Haren, 2006; Haren et al., 2009a; Lüders et al., 2005; Manning et al., 2010), γ-tubulin (Hannak, 2002; Sunkel 1995) and the kinases Polo/Plk1 and Aurora A (Berdnik and Knoblich, 2002; Blagden and Glover, 2003; Hannak, 2001; Hirota et al., 2003; Lane and Nigg, 1996; Lee and Rhee, 2011; Mahen and Venkitaraman, 2012; Sunkel and Glover, 2005). It has been challenging to define a molecular pathway of PCM assembly, partly because different proteins seem to have quite different impact on PCM assembly in different systems and even in different cell types. For example in mammalian cells, PCM recruitment is dependent on Pericentrin and RNAi of Pericentrin in human cultured cells leads to dramatic reduction of the centrosomal levels of CEP215/CDK5RAP2, CEP192 and γ-tubulin (Gomez-Ferreria et al., 2007; Haren et al., 2009b; Lee and Rhee, 2011; Zhu et al., 2008a). In cultured *Drosophila* cells DPLP appears to play a major part in recruiting interphase PCM, and a less major part in recruiting PCM to mitotic centrosomes. Depletion of Pericentrin leads to complete loss of interphase PCM and a significant reduction of Cnn, Spd-2 and γ-tubulin staining in the mitotic PCM matrix (Dobbelaere et al., 2008; Mennella et al., 2012). In contrast, in *Drosophila* cells *in vivo* DPLP has been shown to only have a relatively minor role in mitotic PCM recruitment. Disruption of DPLP function in embryos by injection of antibodies directed against DPLP only has only a minor effect on the rate of Cnn recruitment and the amount of Cnn in the PCM (Conduit et al., 2010); and *Drosophila dplp* mutants only have reduced levels of γ-tubulin in mitotic brain cells (Martinez-Campos et al., 2004). Recent published and unpublished data from our lab have demonstrated that in *Drosophila* the proteins Asl, Spd-2 and Cnn appear to be particularly important for PCM recruitment to mitotic centrosomes (Conduit et al., 2010; Conduit et al., manuscript in preparation) (this is discussed in more detail in the Introduction to Chapter 3, Section 3.1).

The mitotic kinases Polo/Plk1 and Aurora A are thought to be important regulators of mitotic PCM recruitment (Blagden and Glover, 2003). As they have multiple roles in mitosis, it can be challenging to analyse their specific roles in PCM recruitment (Barr and Gergely, 2007; Glover, 2005). In *Drosophila* cultured cells Polo appears to regulate PCM recruitment, and Cnn is phosphorylated specifically in mitosis in a Polo dependent manner (Dobbelaere et al., 2008). Aurora A is required for recruitment of γ-tubulin to the PCM in *C. elegans* and human cells (Hannak, 2001; Hirota et al., 2003), but in *Drosophila* its role is less clear. It has been shown to be required for the recruitment of Cnn and γ-tubulin to mitotic centrosomes in asymmetrically dividing sensory organ precursor cells (Berdnik and Knoblich, 2002; Hutterer et al., 2006), but it seems to have a more minor role in *Drosophila* brain cells or in cultured *Drosophila* cells (Dobbelaere et al., 2008; Giet et al., 2002; Goshima et al., 2007). It has however been shown that Aurora A regulates PCM function, as Aurora A dependent phosphorylation of DTACC is important for the stabilisation of MTs by D-TACC-Msps/XMAP215 complexes in *Drosophila* embryos (Barros et al., 2005).

Little is known yet about the regulation of PCM recruitment by dephosphorylation, but the Protein phosphatase 2A (PP2A) was found to be required for efficient mitotic PCM recruitment in a genome wide RNAi screen in cultured *Drosophila* cells (Dobbelaere et al., 2008). Protein phosphatase 4 (PP4) has been shown to localise to the mitotic centrosome in *C. elegans*, and loss of PP4 affected centrosomal γ-tubulin and Plk1 localisation (Sumiyoshi et al., 2002).

Although generally centrioles are required for efficient PCM assembly (Basto et al., 2006; Bobinnec et al., 1998a), it should be noted that some PCM can still be organised on some spindle poles that lack centrioles. This is, for example, the case in cultured

Drosophila cells that lack centrioles (Debec et al., 1995; Moutinho-Pereira et al., 2009) and I show that it is also the case in some *Drosophila* cells that lack centrioles *in vivo* (Chapter 6). Moreover, Pericentrin and γ-tubulin on the acentrosomal poles of mouse meiotic spindles in oocytes even appear to adapt the same unique lattice structure that is typical for PCM (Dictenberg et al., 1998).

1.4 Mechanisms of spindle assembly

In mitosis, the replicated chromosomes must be equally divided between the two daughter cells, a process that is performed by a complex cytoskeletal machine, the mitotic spindle. Spindle formation starts in prophase and culminates in metaphase, when the chromosomes become aligned at the spindle equator with each of the two sister chromatids connected to one of the two opposing poles. There are three classes of MTs in the mitotic spindle: astral MTs, which radiate away from the centrosomes and can interact with the cell cortex to position the spindle inside the cell; kinetochore MTs, which form bundles of 20-40 parallel MTs (Rieder, 1981) called K-fibres and tether the kinetochore of a chromosome to a spindle pole; and polar MTs, which overlap at the equator of the spindle and are crosslinked by plus end directed motor proteins that push the two halves of the spindle apart (Figure 1.3A) (Alberts et al., 2008). It is now widely believed that several MT nucleation pathways act in the cell to ensure efficient bipolar spindle assembly.

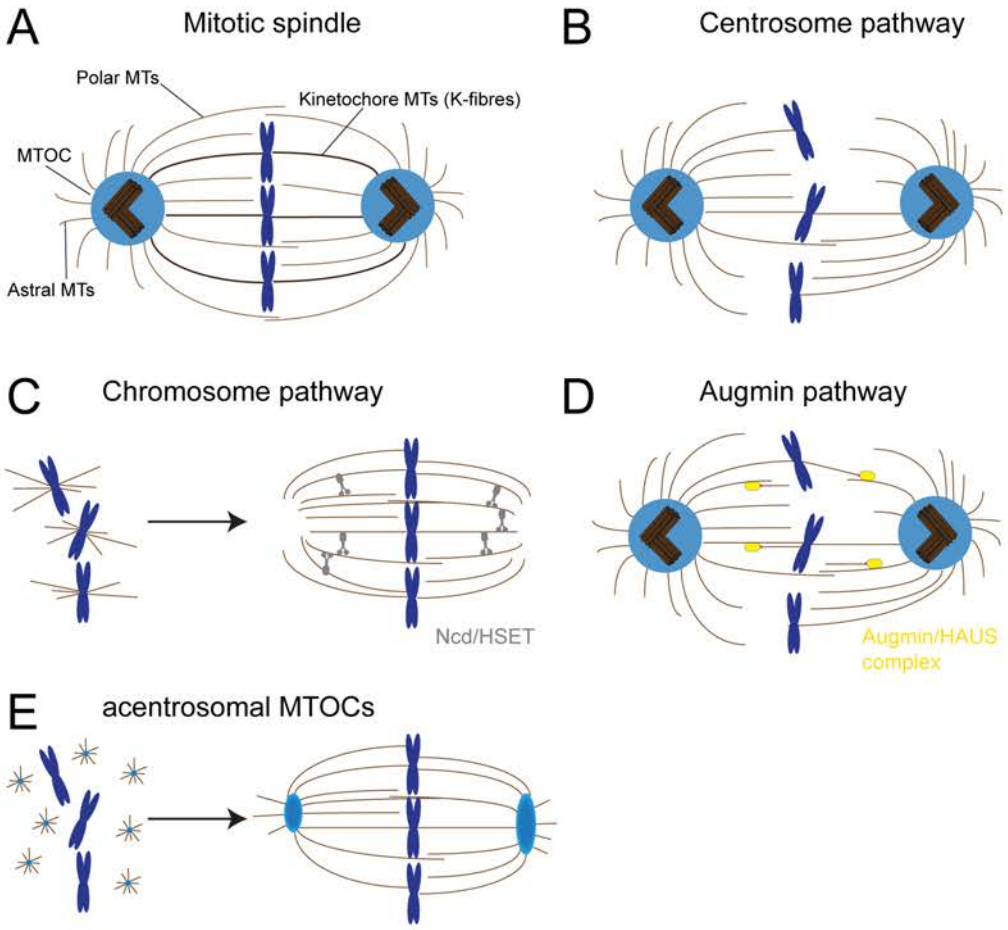

Figure 1.3: Mechanisms of mitotic spindle assembly. (A) The key components of the mitotic spindle. Polar MTs are shown in brown and compose the antiparallel spindle MTs. The kinetochore MT bundles (K-fibres) that connect kinetochores with the centrosomes are indicated in black here. The astral MTs extend away from the spindle poles. **(B)** Search and Capture model for spindle assembly: The MTs nucleated by the centrosomes are highly dynamic and explore the cytoplasm by growing and shrinking until they are captured by a kinetochore. **(C)** MTs can be nucleated and stabilised in the vicinity of the chromosomes by the Ran-GTP driven pathway and the CPC-dependent pathway. The plus ends of chromatin induced MTs are captured by the kinetochores and continue to grow from there. In the absence of centrosomes K-fibres need to be clustered into a bipolar spindle by minus end directed motors such as Ncd/HSET. **(D)** The conserved Augmin/HAUS complex nucleates additional MTs within the spindle by recruiting γ-TuRCs to existing spindle MTs. **(E)** In centrosome-free mouse oocytes the meiotic spindle is organised by multiple aMTOCs that functionally replace centrosomes.

1.4.1 Centrosomal spindle assembly

MT nucleation by the centrosome is performed by γ-tubulin, which forms the γ-tubulin small complex (γ-TuSC) together with γ-tubulin complex components (GCP) 2 and 3. Several γ-TuSCs together with additional GCPs form the γ-tubulin ring complex (γ-TuRC), which templates MT polymerisation (Kollman et al., 2011). As cells prepare for mitosis, the MT cytoskeleton becomes more dynamic, leading to the disassembly of the interphase MT network (Belmont et al., 1990). Concomitantly, the centrosomes organise more PCM and their MT nucleation capacity increases dramatically (Section 1.3.1). Based on this, the "search and capture" model for spindle assembly was proposed (Kirschner and Mitchison, 1986). This model suggested that the dynamic MTs nucleated by the centrosomes grow and shrink and thereby explore the cytoplasm until they become captured by a kinetochore, which would ultimately lead to the assembly of a bipolar spindle (Kirschner and Mitchison, 1986) (Figure 1.3B). Recent studies have suggested additional mechanisms normally cooperate with the search and capture mechanism to ensure proper spindle formation (Magidson et al., 2011; Wollman et al., 2005).

Higher plants lack centrioles (Schmit, 2002), and female meiosis in many species occurs without centrioles (Dumont and Desai, 2012). Furthermore, mitosis can occur in the absence of centrioles in cells or organisms that normally would have centrioles (Basto et al., 2006; Khodjakov et al., 2000; Mahoney et al., 2006). This demonstrates the existence of alternative pathways that are sufficient for spindle assembly. Nevertheless, in fly cells that normally have centrioles, bipolar spindle formation takes longer and is less accurate in the absence of centrosomes (Basto et al., 2006).

1.4.2 Chromosomal spindle assembly pathway

Early experiments in which purified DNA and centrosomes were injected into *Xenopus* eggs showed that both were able to induce MT assembly (Karsenti et al., 1984), which was the first demonstration that chromatin played a role in MT formation. This was confirmed and extended by the incubation of DNA covered beads in *Xenopus* egg extracts, which induced the MT-motor protein dependent formation of a bipolar spindle around the beads in the absence of any centrosomes or kinetochores (Heald et al., 1996; Walczak et al., 1998). Studies over the past decade have shown that there are two distinct pathways for chromosomal MT assembly, one is dependent on GTP-bound Ran and one is triggered by the chromosomal passenger complex (CPC).

The GTP-bound form of Ran GTPase is generated by the chromosome-associated Ran-GTP exchange factor RCC1 whereas its GTPase activating protein RanGAP is cytoplasmic, which leads to a gradient of Ran-GTP surrounding the chromosomes (Kalab, 2002; Kalab and Heald, 2008). Ran-GTP binds to nuclear transport receptors of the importin β superfamily, which leads to transport of several MT-associated proteins into the nucleus that then trigger MT assembly and stability around the chromatin, such as for example TPX2, Aurora A, NuMA, HURP, Aurora B, Msps/XMAP215 (Ciciarello et al., 2007; Kalab and Heald, 2008; Meunier and Vernos, 2012). Ran-GTP has also been shown to regulate MCRS1, a protein that binds to K-fibre minus ends and protects these from depolymerisation (Meunier and Vernos, 2011).

MTs can assemble around chromatin also in the absence of a Ran-GTP gradient, and this process is dependent on the CPC (Kelly et al., 2007; Maresca et al., 2009). The CPC comprises the proteins INCENP, Survivin/BIRC5, borealin/CDCA8 and Aurora B

kinase and can promote spindle assembly partly by suppressing the MT destabilizing factor MCAK (Bolton et al., 2002; Sampath et al., 2004). There is evidence that the CPC detects the coincident presence of chromosomes and emerging MTs to promote MT assembly and thus confines spindle assembly to around the centromeres (Tseng et al., 2010). It is assumed that the Ran-GTP and CPC-dependent pathways work together by promoting MT nucleation near the chromatin and stabilisation of these MTs preferentially near the kinetochore (Maresca et al., 2009; Tulu et al., 2006). The plus ends of these chromatin induced MTs are captured by the kinetochores and continue to grow from there, leading to the formation of K-fibres (Khodjakov, 2003; Maiato et al., 2004).

Centrosomes are not essential for large parts of *Drosophila* development, as the chromosomal pathway of MT nucleation and the augmin pathway (see below) appear to be sufficient to drive bipolar spindle assembly in a manner that is efficient enough to cope with the demands of a developing fly (Basto et al., 2006). In contrast, the chromosomal pathway appears to be essential for cell division in flies as in *misato (mst)* mutants, where kinetochore-driven MT growth is inhibited, bipolar spindle assembly is disrupted, and the mutation results in larval lethality (Mottier-Pavie et al., 2011). Importantly, in the absence of centrosomes minus end directed motor proteins such as Ncd/HSET are essential to focus MT minus-ends into two spindle poles independently of centrosomes (Figure 1.3C) (Walczak et al., 1998).

1.4.3 The augmin pathway

The conserved Augmin/HAUS complex can nucleate additional MTs within the spindle by recruiting γ-TuRCs to existing spindle MTs and has been identified in *Drosophila*,

human cells and *Xenopus* egg extracts (Goshima et al., 2008a; Lawo et al., 2009; Mahoney et al., 2006; Petry et al., 2013b; Wainman et al., 2009) (Figure 1.3D). This multiprotein complex consists of at least nine subunits and binds to spindle MTs where it nucleates a new MT that branches off the side of the existing MT, thereby leading to amplification of the total number of MTs in the spindle (Goshima et al., 2008b; Kamasaki et al., 2013; Meireles et al., 2009; Petry et al., 2013a; Ueharaa et al., 2009; Wainman et al., 2009; Zhu et al., 2009). Interestingly, the new MT is nearly parallel to the MT it branches off from, indicating that the augmin complex also promotes polarisation of the MT array (Kamasaki et al., 2013; Petry et al., 2013a). The absence of the augmin complex in cultured *Drosophila* cells leads to reduced K-fibre formation, spindle bipolarity defects and chromosome misalignment (Goshima et al., 2008b), while disruption of the HAUS complex in human cells has been shown to lead to centrosome fragmentation, destabilisation of K-fibres and defective chromosome segregation (Lawo et al., 2009; Ueharaa et al., 2009). In the absence of centrosomes MT amplification by the augmin complex is required, together with the chromosomal pathway, to build a bipolar spindle (Wainman et al., 2009).

1.4.4 Other pathways of MT nucleation for spindle assembly

In some cases spindle MTs can be nucleated from secondary MTOCs that are independent of centrosomes, chromosomes and the augmin/HAUS complex. For example, in centrosome-free mouse oocytes and early mouse embryos the spindle is organised by multiple acentrosomal MTOCs (aMTOCs) to which γ-tubulin and Pericentrin have been shown to localise (Courtois et al., 2012; Schuh and Ellenberg, 2007; Gueth-Hallonet et al.; 1993 Łuksza et al., 2013; Palacios et al., 1993) (Figure 1.3E). γ-tubulin enriched aMTOCs that are able to mediate *de novo* MT formation have

also been described in acentriolar *Drosophila* cultured cells (Moutinho-Pereira et al., 2009) (Section 6.1). These aMTOCs also exist in acentriolar *Drosophila* mutants *in vivo* and in Chapter 6 I present a detailed analysis of the contribution of aMTOCs to spindle assembly in *Drosophila*. There is also evidence that in *Drosophila* spermatocytes the fenestrated nuclear envelope can nucleate MT bundles independently of chromosomes and centrosomes and so contribute to spindle assembly (Rebollo et al., 2004).

1.4.5 The interplay of spindle assembly pathways

The current view of spindle assembly is that the three major MT nucleation pathways, i.e. the centrosomal, chromosomal and augmin-mediated pathways, cooperate to drive efficient assembly of the mitotic spindle (Meunier and Vernos, 2012; O'Connell and Khodjakov, 2007). Although in many cell types centrosomes appear to be the dominant source of spindle MTs, it is clear that all three pathways make important contributions. Chromatin and centromeres provide an environment that promotes MT assembly through the Ran-GTP and the CPC pathways (Section 1.4.2). In mammalian and *Drosophila* cultured cells the plus ends of these chromatin-induced MTs are captured by the kinetochores and continue to grow from there in a MT bundle (Khodjakov, 2003; Maiato et al., 2004). This leads to the formation of K-fibres with minus ends that are pushed away from the kinetochores, and these then either get directly captured by the MTs emanating from the centrosomes, or are transported poleward along astral microtubules by dynein motors, leading to the integration of the K-fibres into the bipolar spindle (Khodjakov, 2003; Maiato et al., 2004). The augmin complex finally is required for spindle MT amplification, which strengthens the mitotic spindle (Meunier and Vernos, 2012; O'Connell and Khodjakov, 2007). Thus, the traditional "search and capture" mechanism by which MTs nucleated by the centrosomes form a bipolar spindle

by capturing kinetochores has been extended to incorporate all three pathways of MT assembly.

1.5 Thesis Outline

During my DPhil studies I have analysed several different aspects of centrosome function and spindle assembly using the model system *Drosophila melanogaster.* The first half of my thesis focuses on the mechanisms of centrosome formation. In Chapter 3 I describe my analysis of phosphorylation of certain PCM proteins and in Chapter 4 I address the role of Sak kinase in the centrosome formation pathway. The second half of my thesis elucidates the consequences of centrosome loss in *Drosophila.* In Chapter 5 I present a genome wide transcriptional analysis of flies without centrosomes and flies having extra centrosomes, and in Chapter 6 I will describe my detailed analysis of the contribution of aMTOCs to spindle formation in the absence of centrosomes in *Drosophila.*

2 Material and Methods

2.1 Fly husbandry

2.1.1 Fly handling

Flies were kept at 18°C or 25°C on *Drosophila* culture medium (5.5% glucose, 5% yeast extract, 3.5% wheat flour, 1% penicillin/streptomycin, 0.75% agar, 0.4% propionic acid, 0.25% nipagen) in plastic vials or bottles. UAS/Gal4 crosses were also kept at 25°C. Embryos were collected on cranberry juice plates (25% cranberry juice, 2.5% sucrose, 2.1% agar) supplemented with fresh yeast. Standard fly handling techniques were used (Roberts, 1986).

2.1.2 *Drosophila* stocks

For wild type controls, w^{67} or OregonR were used. Balancer chromosomes and markers used are described in Lindsley and Zimm, 1992, all other stocks used in this thesis are listed in Tables 2.1 - 2.3.

Table 2.1. *Transposon insertions, deletion mutants and deficiencies and EMS alleles.*

Fly stock	Description/notes	Origin/Reference
P{GawB}Sak^{NP6647}	P-Element insertion in *sak* gene that could not be excised	Bloomington Stock Center
P{GSV1}GS3043	P-Element insertion in 5'UTR of *cdk12* gene that was excised to cause *sak*^{Aa74} mutant	Bloomington Stock Center
sak$^{Df(3L)Pc23}$	*sak* deficiency	Bloomington Stock Center
sak^{Aa74}	deletion of promoter and part of the *sak* gene	this thesis
sak^{c06612}	PBac{PB}SAKc06612 piggyBac insertion in *sak* gene causing hypomorphic mutation	(Bettencourt-Dias et al., 2005)
DSas-4^{s2214}	P{lacW}l(2)s2214 P-element insertion in *DSas-4* gene causing null mutation	(Basto et al., 2006)
DSas-6^{co2901}	PBac{PB}Sas-^{6co2901} piggyBac	(Peel et al., 2007)

	insertion in *DSas-6* gene causing null mutation	
ana2	EMS allele	(Wang et al., 2011a)
asl^{B46}	deletion of promoter and part of *asl* gene causing null allele	Zsofia Novak, Raff Lab, unpublished
spd-2^{z35711}	EMS null allele	(Giansanti et al., 2008)
spd-2$^{Df(3L)st-j7}$	*spd-2* deficiency	Bloomington Stock Center
spd-2^{G20143}	P{EP}G20143 P-element insertion in *spd-2* gene	(Dix and Raff, 2007)
cnn^{f04547}	piggyBac insertion in *cnn* gene causing null allele	(Lucas and Raff, 2007)
cnn^{HK21}	EMS induced null allele	(Megraw et al., 1999; Vaizel-Ohayon and Schejter, 1999)
ncd^{1}	spontaneous mutation	(Endow et al., 1994) Sturtevant, 1929)
dhc64C$^{6-10}$	EMS hypomorphic allele	(Gepner et al., 1996)
mst^{LB20}	EMS induced null allele	(Mottier-Pavie et al., 2011)
wac^{Delta12}	deletion of most of the *wac* gene causing null allele	(Meireles et al., 2009)

2.1.3 Transgenic lines

Transgenic fly strains were generated by injection of a transformation vector containing the transgene of interest (Section 2.2.5) into *yw* flies. Injection and selection of transgenic flies was performed by BestGene Inc. (Chino Hills, California) or the University of Cambridge Genetics Fly Facility. The transformation vector contains a *white*$^{+}$ marker, and flies carrying the transgene are recognisable by their orange eye colour. I mapped the location of the transgene insertion to determine the chromosome carrying the insertion using standard crossing schemes. The transgenic lines that I generated for this thesis are listed in Table 2.2, and the transgenic lines that were used from other sources are listed in Table 2.3.

Table 2.2. *Transgenic lines generated for this thesis.*

Name	**Notes**
Ubq-Asl^{S372A,T373A}-GFP	used insertion 10122-1-1M on X (BestGene)
Ubq-Asl^{T373E}-GFP	used insertion 10122-2-1M on X (BestGene)
Ubq-Spd-2^{Pmutant}-GFP	used insertion 10339-2-1M on II (BestGene)
UASp-GFP-Sak^{KD}	used insertion #6 on II (Cambridge Genetics)

Table 2.3. *Transgenic lines from other sources used in this thesis.*

Name	Source	Notes
Ubq-GFP-Sak	(Peel et al., 2007)	on II
Ubq-GFP-Cnn	(Conduit et al., 2010)	on II
Ubq-Spd-2-GFP	(Dix and Raff, 2007)	on II
Ncd–γ-tubulin37C-GFP	(Hallen et al., 2008)	on III
Ubq-Jupiter-mCherry	StJohnston lab, unpublished	on III
Ubq-GFP-PACT	(Martinez-Campos et al., 2004)	on III
Act5C-Gal4	Bloomington	on II
Ubq-Asl-GFP	(Stevens et al., 2010a)	on X

2.1.4 Generation of *sak* null mutant sak^{Aa74}

In order to generate a *sak* null mutant I carried out a P-element excision and screened for imprecise excisions. I used the P-element insertion P[$ry^{+}\Delta 2$-3] which encodes a source of transposase that causes mobilisation of other P-elements but itself remains stably in the genome (Robertson et al., 1988). I crossed the P[$ry^{+}\Delta 2$-3] chromosome over the chromosome carrying the P-element insertion P{GSV1}GS3043. I could screen the progeny of these flies for the absence of red eye colour, as P-elements carry the mini-*white* gene conferring red eye colour, and flies with white eyes would have lost the P-element insertion. I crossed all male progeny (~1000 males) individually to 2-3 females containing a balancer chromosome and after fertilisation I used the males to make a single fly DNA preparation. I then screened all males for a deletion inside the *sak* gene by PCR, and excisions were confirmed by sequencing (Section 4.3). The progeny of the males in which a deletion could be detected was set up as a stock.

2.1.5 Assessing whether adult flies are uncoordinated

To assess whether homozygous sak^{Aa74} mutants were uncoordinated pupae needed to be picked out of the vials prior to eclosion, so that they could not get stuck in the food.

Pupae were transferred into small petri dishes onto a piece of damp filter paper (Whatman). Once flies had eclosed they were observed under a dissection microscope to analyse whether they were unable to walk and whether they were holding their wings up, indicating the uncoordination (unc) phenotype.

2.1.6 Treatment of *sak*^{Aa74} mutant flies to obtain mature egg chambers

After eclosion the egg chambers of female flies are still immature, but stage 14 oocytes were required, which take several days to mature (Section 4.5 and 4.6). *sak*^{Aa74} mutants cannot feed or walk, therefore pupae had to be picked into petri dishes as described in Section 2.1.5, and were manually fed with sugar solution for 1-4 days before dissecting ovaries.

2.1.7 Assessing pupation rate of flies

Flies were allowed to lay eggs in vials for 12 hours, the number of flies was adjusted so that ~100 eggs would be laid during that time. Flies were flipped to new vials for a few days after 12 h each, to obtain a large number of vials with laid eggs. The vials were kept at 25°C and the pupation rate was assessed by counting the number of adults that pupated in each vial per day.

2.2 Molecular Biology

2.2.1 PCR

All general polymerase chain reactions (PCRs) were carried out with JumpStart REDTaq ReadyMix PCR Reaction Mix (Sigma) by mixing 5µl JumpStart Mix with 0.5µl forward primer (8µM), 0.5µl reverse primer (8µM), 0.5µl DNA and 3.5µl water using the following PCR protocol:

1. 94°C for 2 min
2. 94°C for 30 s
3. 60°C for 30 s
4. 72°C for x min (1 min/1000 bp); repeat steps 2-4 for 29 times
5. 72°C for 10 min

PCRs for cloning were carried out with Phusion High-Fidelity PCR Master Mix (NEB) by mixing 25µl Master Mix, 2.5µl forward primer (8µM), 2.5µl reverse primer (8µM), 1µl template and 19µl water using the following PCR protocol:

1. 98°C for 30 s
2. 98°C for 10 s
3. 60°C for 10 s
4. 72°C for x min (30 s/1000 bp); repeat steps 2-4 for 29 times
5. 72°C for 10 min

All primers made for this thesis are listed in Table 4.

Table 2.4. *Primer list.*

Name		**Sequence**	**Binding region/Notes**
P8L	for	GCGAAAGTTCCAGGAAGTGG	inside 5'UTR *cdk12* gene, detects deletion in sak^{Aa74}
P8R	rev	TTGAAGTTCCGTTGGGTTGG	inside *sak* coding sequence, detects deletion in sak^{Aa74}
P9L	for	AGTTGTGCAAACTCACCACG	inside ncd gene, detects deletion in ncd^{1}
P9R	rev	GTCCAGGTGCAACACATACG	inside ncd gene, detects deletion in ncd^{1}
M1F	for	CCAAGGGCACAAACATCGCTTTTGAGCC TGCGGAG	*spd-2* S121A
M1R	rev	CTCCGCAGGCTCAAAAGCGATGTTTGTG CCCTTGG	*spd-2* S121A
M2F	for	CCAGAAAGTAACGTGGCTCTGGATTCGG TTGGCGAG	*spd-2* T329A
M2R	rev	CTCGCCAACCGAATCCAGAGCCACGTTA CTTTCTGG	*spd-2* T329A
M3F	for	CGAGATCCTAAGTCTCGCCGCGATCGAC AAGGCGC	*spd-2* S397A
M3R	rev	GCGCCTTGTCGATCGCGGCGAGACTTAG GATCTCG	*spd-2* S397A
M4F	for	CGCGCAAGCCGCTCGCTCCGCTGGCGGA CCATC	*spd-2* S484A

M4R	rev	GATGGTCCGCCAGCGGAGCGAGCGGCTTGCGCG	*spd-2* S484A
M5F	for	GCCAGTGAACAAGAAGAGGGTTGCGATCGCTACAATGGG	*spd-2* S569A
M5R	rev	CCCATTGTAGCGATCGCAACCCTCTTCTTGTTCACTGGC	*spd-2* S569A
M6F	for	CTGGCCAAAAATCTAGCGCCCCTGGCCGCGCCAAGAAGCTGTCTC	*spd-2* S614A, S617A, S618A
M6R	rev	GAGACAGCTTCTTGGCGCGGCCAGGGGCGCTAGATTTTTGGCCAG	*spd-2* S614A, S617, S618A
M7F	for	GGAAGACGTGGGTTGGGAGCCGCCGCTGTTGCAGTGCCACGTAG	*spd-2* T672A, S673A and S674A
M7R	rev	CTACGTGGCACTGCAACAGCGGCGGCTCCCAACCCACGTCTTCC	*spd-2* T672A, S673A and S674A
M8F	for	TCGCGCCTTGTTGGTGCCGCACCGCTGAATCC	*asl* S372A,T373A
M8R	rev	GGATTCAGCGGTGCGGCACCAACAAGGCGCGA	*asl* S372A,T373A
M9F	for	TCGCGCCTTGTTGGTAGCGAACCGCTGAATCC	*asl* T373E
M9R	rev	GGATTCAGCGGTTCGCTACCAACAAGGCGCGA	*asl* T373E
M10F	for	CCAGGATGTGGCCATAATGATGATCGATAAAAAACTAATCC	*sak* K43M
M10R	rev	GGATTAGTTTTTATCGATCATCATTATGGCCACATCCTGG	*sak* K43M
Spd-2_G-F	for	GCAGGCTTCATGGACAGTAGCAGTGGAAGC	for amplification of *spd-2* cDNA for BP reaction
Spd-2_G-R	rev	AGCTGGGTCAAATTTAAAACTAATCGGGACACTGATGC	for amplification of *spd-2* cDNA for BP reaction
AttB1_F	for	GGGGACAAGTTTGTACAAAAAAGCAGGCTTC	Gateway secondary primers
AttB2_R	rev	GGGGACCACTTTGTACAAGAAAGCTGGGTC	Gateway secondary primers
I1F	for	AATTCAGCCACCATGGACAGTAGCAGTGGAAGC	For InFusion Cloning *spd-2* CDS in pRNA
I1R	rev	TGCTCACCATGCTAGCAAATTTAAAACTAATCGGGACACTG	For InFusion Cloning *spd-2* CDS in pRNA
C1F	for	CGATCGCCATGGGAAACACGCCAGGTATAAGCC	to amplify *asl* CDS, contains NcoI site
C1R	rev	TTAAGCGCTAGCGCTGTGACCATTGCCTTTGGG	To amplify *asl* CDS, contains NheI site

2.2.2 Site-directed mutagenesis

Site-directed mutagenesis was performed on pDONR-asl, pDONR-sak and pDONR-Spd-2 vectors using the Quikchange II Kit or Quikchange Multi Site-Directed

Mutagenesis Kit (Agilent) according to manufacturer's instructions. The mutagenesis primers used are listed in Table 2.4.

2.2.3 Sequencing

DNA sequencing was performed by SourceBioscience using Sanger Sequencing, sequencing data were analysed in MacVector.

2.2.4 Cloning

2.2.4.1 Plasmid construction for transgenic fly lines

I received the *spd-2* cDNA in a pOT2 vector (clone LD24702) from Geneservice Ltd. I amplified the coding region of *spd-2* from this vector with *att* sites at either end for Gateway cloning (Life Technologies) (primers are listed in Table 2.4). The PCR fragments were purified with the QIAquick PCR product purification kit (Qiagen) and inserted into the Gateway pDONR Zeo vector creating the vector pDONR-Spd-2. The inserts were verified by sequencing. I received the pDONR-asl vector (Raff lab vector stock, made by Jeroen Dobbelaere) and pDONR-sak vector (kindly provided by Renata Basto) and therefore did not have to make them myself. The pDONR vectors could then be recombined with Ubiquitin (Ubq) and UAS (upstream activation sequence) Destination vectors (Peel et al., 2007) with the coding sequences placed in frame with the eGFP at the C- or N-terminus. All constructs made are listed in Table 2.5. The Ubq promoter drives relatively high expression in all tissues (Lee et al., 1988), and when centriole duplication proteins are driven by this promoter it leads to overexpression as normally these proteins are expressed at very low levels (Peel et al., 2007). Flies with UAS driven transgenes must be crossed to flies expressing Gal4 drivers, and lead to

high level expression in specific tissues depending on the expression pattern of the driver (Brand and Perrimon, 1993).

Table 2.5. *List of constructs made.*

Construct	Description
pRNA-asl^{WT}-EGFP	pRNA with T3 RNA Pol promoter; AmpR
pRNA-asl^{S372A,T373A}-EGFP	pRNA with T3 RNA Pol promoter; AmpR
pRNA-asl^{T373E}-EGFP	pRNA with T3 RNA Pol promoter; AmpR
pRNA-Spd-2^{WT}-EGFP	pRNA with T3 RNA Pol promoter; AmpR
pRNA-Spd-2^{Pmutant}-EGFP	pRNA with T3 RNA Pol promoter; AmpR
pDONR-Spd-2	Gateway Entry vector; ZeoR
pUbq-asl^{S372A,T373A}-EGFP	Gateway Expression vector; KanR
pUbq-asl^{T373E}-EGFP	Gateway Expression vector; KanR
pUbq-Spd-2^{Pmutant}-EGFP	Gateway Expression vector; KanR
pUAS$_P$-sak^{KD}-GFP	Gateway Expression vector; AmpR

2.2.4.2 Plasmid construction for in vitro transcription

For *in vitro* transcriptions the open reading frames (ORF) of *asl* and *spd-2* needed to be cloned into the pRNA-EGFP vector (Oliveira and Nasmyth, 2013) to create the vectors pRNA-asl-EGFP and pRNA-Spd-2-EGFP. The pRNA vector contains a T3 RNA Pol promoter sequence for *in vitro* transcription. The *asl* ORF was amplified from the pDONR-asl vector using primers C1F and C1R (Table 4), the PCR fragments were digested with NheI and NcoI and were ligated into the digested pRNA-EGFP vector. Spd-2 could not be digested in the same way and hence I used the In-Fusion Cloning Kit (Clontech).

2.2.5 Single fly DNA preparation

One anesthetised fly was put in a well of a 96 well plate and mashed using a pipette tip filled with 50µl squishing buffer (10mM Tris HCl pH8, 1mM EDTA pH8, 25mM NaCl, 200µm/ml proteinase K) and the buffer was expelled on the mashed fly. After all flies

had been mashed, the 96 well plate was incubated at 55°C for 30 min and then boiled for 10 min at 95°C and afterwards could be stored at -20°C for several days until use.

2.2.6 *In vitro* transcription

For *in vitro* transcription the pRNA vectors were linearised by AscI restriction digest and then ethanol precipitated. Capped mRNAs were synthesised using the mMessage mMachine T3 Kit (Ambion) and purified with RNeasy columns (Qiagen). RNA was eluted in RNAse free water and used for injections at a concentration of 1μg/μl.

2.3 Proteomics

2.3.1 Protein electrophoresis and western blotting

Samples for western blot analysis were prepared by boiling larval brains with 2x Laemmli sample buffer (SB; contains 0.12M Tris.HCl pH 6.8, 4% SDS, 10% 2-β-mercaptoethanol, 20% glycerol, 0.04% bromophenol blue) for 10 min. Protein samples were separated on a 3-8% precast NuPAGE (Invitrogen) polyacrylamide gel using Novex Tris-Glycine SDS Running Buffer (Life Technologies) and transferred to a nitrocellulose or Hypobond-P membrane (Amersham Biosciences) overnight at 50mA in western transfer buffer (25% methanol, 0.29% glycine, 0.58% Tris, 0.04% SDS). The next morning, the membranes were blocked in milk solution (PBS with 0.1% Tween-20, 5% milk powder) for 1 h at room temperature with gentle agitation, and then incubated with the primary antibody (1-2μg/ml in milk solution) for 2 h. The membranes were briefly washed for 3 times in TBST (TBS + 0.1% Tween-20) and incubated with the appropriate horseradish peroxidase (HRP) coupled secondary antibody (Amersham) (diluted 1/1000 in milk solution) for 1 h. Then, the membranes were washed 3 x 15 min

in TBST with gentle agitation, and finally incubated in chemiluminescent substrate (ECL Western Blot detection reagent, GE Healthcare or Amersham) according to manufacturer's instructions and exposed to X-ray film.

2.3.2 Centrosome isolation

Extract of early *Drosophila* embryos (0-4 h) was made by homogenising 1.5-2g of frozen embryos in a glass homogeniser in Buffer 1 (80mM K-PIPES pH 6.8, 1mM $MgCl_2$, 1mM EGTA, 1mM GTP, 100mM KCl, 14% sucrose) with added protease inhibitor cocktail (1mM benzamidine-HCl, 0.5mM phenanthroline, 10μg/ml aprotinin, 10μg/ml leupeptin, 3μg/ml pepstatinA) and 1mM PMSF, 1mM DTT, and phosphatase inhibitor cocktail 2 and 3, diluted according to manufacturer's instructions (Sigma). The homogenisate was passed through miracloth (Merck) and spun down to remove solids and lipids. Then, centrosomes were isolated from extracts using a modified version of the centrosome isolation protocol of Moritz and Alberts (Moritz et al., 1995) by layering 20ml of embryo extract containing 50% sucrose onto a 1.5ml layer of 70% sucrose. The tubes were spun in a Beckman SW 41 Ti Rotor at 27,000 rpm. This caused the centrosomes to accumulate in the 70% sucrose layer at the bottom of the vial while cytoplasmic proteins remain in the 50% sucrose layer. Following ultracentrifugation, 2.5ml of the supernatant was taken from the top of the tube (cytoplasmic fractions) and 1.2ml were collected from the 70% sucrose layer by piercing a hole into the bottom of the tube (centrosome fractions). Aliquots of the collected fractions were tested by western blotting and the rest were snap frozen in liquid nitrogen.

2.3.3 Phosphatase treatment

For the phosphatase treatment 10μl of the centrosomal fraction was incubated with 10μl of Alkaline Phosphatase (Roche) in a 100μl reaction containing protease inhibitors for

4.5 h at 37°C. To test the specificity of the Phosphatase treatment, the same reaction was carried out in the presence of Phosphatase inhibitor cocktails 2 and 3 (Sigma).

2.3.4 Immunoprecipitations

For immunoprecipitaton of centrosomes from the centrosomal fractions 40µg of anti-Cnn antibody were coupled to 800µl protein A conjugated magnetic Dynabeads (Life Technologies). For immunoprecipitation of cytoplasmic proteins from the cytoplasmic fractions 48µg anti-Spd-2 antibody or 128µg anti-Asl antibody (all antibodies derived from rabbit), respectively, were coupled to 800µl Dynabeads. The ideal amount of antibody for the large-scale immunoprecipitation had been determined in small-scale trial experiments beforehand (data not shown). The dynabead/antibody suspensions were incubated at 4°C overnight, rotating. On the next day, beads were washed with BS^3 conjugation buffer (20mM sodium phosphate, 0.15M NaCl pH 7-9) and then the antibodies were crosslinked to the beads by adding BS^3 crosslinker (Thermo Fisher Scientific) in BS^3 conjugation buffer and rotating for 30 min. The reaction was quenched by adding 1M Tris-HCl pH 7.5 and rotating for further 15 min. Beads were washed 3x with PBT and could then be stored at 4°C until use. For immunoprecipitations, centrosomal and cytoplasmic fractions were diluted 1:1 with dilution buffer (PBS with 0.2% BSA, protease inhibitor cocktail, 1mM PMSF, 20µg/ml DNAse I and Phosphatase inhibitor cocktail 2 and 3), added to the antibody-crosslinked beads and rotated at 4°C for 2 h. Beads were then washed 3x with wash buffer (PBS with 0.003% Triton X-100, protease inhibitor cocktail, 1mM PMSF, 20µg/ml DNAse I and Phosphatase inhibitor cocktail 2 and 3). The beads could then be boiled with 1xSB and separated on a polyacrylamide gel, and the bands containing the proteins of interest for the mass spectrometry analysis were cut out and stored at -20°C.

2.3.5 Sample preparation for mass spectrometry

2.3.5.1 In-gel tryptic digest

The gel pieces were first washed with Solution B (100mM ammonium bicarbonate in 50% acetonitrile) for 1-2 h and then washed in 100% acetonitrile for 10 min, before they were dehydrated in a vacuum concentrator (SpeedVac). 10mM DTT was added for 30 min at 37°C and then discarded, then the gel pieces were washed in 25mM ammonium bicarbonate several times, followed by washing in acetonitrile. Gel pieces were treated with 55mM iodoacetamide for 1 h in the dark, and subsequently washed in Solution B for several times and then in acetonitrile. Pieces were dried in a vacuum concentrator and incubated over night with Promega Sequencing Grade Modified Trypsin (reconstituted and diluted according to manufacturer's instructions). On the next day 1µl of formic acid was added to stop the digest. Then the supernatant containing the peptides was transferred to a new tube. The gel pieces were incubated with extraction buffer (0.001% formic acid in 50% acetonitrile) for 30 min to extract remaining peptides, and the supernatant was then pooled with the existing supernatant. Samples were dehydrated using a vacuum concentrator.

2.3.5.2 Enrichment for phosphopeptides

Enrichment for phosphopeptides was performed according to the protocol used by Prof. Francis Barr's group, Department of Biochemistry, University of Oxford (personal communication). Dried samples containing tryptic peptides were dissolved in GA solution (80mg/ml glycolic acid in 80% acetonitrile and 2% trifluoroacetic acid). The micro-columns were prepared by plugging the bottom of a GelLoader tip (Eppendorf) with a piece of C8-silica matrix (Varian GmbH) and loading 5µl TiO_2 (Hichrom Ltd.)

slurry to the tip and spinning it down. The micro-column was adjusted by washing with 0.6% NH_4OH solution followed by washing with GA solution; the centrifugation speed was adjusted so that the solutions passed through the columns relatively slowly. The dissolved peptides were then loaded on the prepared micro-columns and spun slowly to give phosphopeptides time to bind to the TiO_2. Columns were washed with GA solution followed by 80% acetonitrile + 0.2% trifluoroacetic acid followed by 20% acetonitrile. The bound phosphopeptides were eluted with 0.6% NH_4OH followed with 60% acetonitrile into a new LoBind Eppendorf tube, centrifugation speeds were adjusted to low speeds as phosphopeptides elute very slowly. Samples were then dried in a vacuum concentrator and dissolved in 5% formic acid for mass spectrometry analysis.

2.3.6 Mass spectrometry

Liquid chromatography-tandem mass spectrometry (LC-MS/MS) analysis was performed by the Proteomics Facility of the Sir William Dunn School of Pathology using a LTQ Orbitrap Mass Spectrometer (Thermo Scientific) coupled to a UltiMate 3000 Nano LC system (Thermo Scientific).

2.4 Transcriptomics

2.4.1 RNA preparation

Total RNA was prepared from brains and imaginal discs of 10 third instar larvae per sample. RNA isolation was performed using TRIzol (Life Technologies) according to manufacturer's instructions, followed by chloroform extraction and isopropanol precipitation. The pellet was washed with Ethanol and air dried. Integrity of the purified RNA was assessed on the Agilent Bioanalyzer 2100 (Agilent) for microarray

experiments, or by assessing integrity on an Agarose gel for qPCR experiments. Concentration was determined using a Nanodrop ND-1000 Spectrophotometer (Nanodrop Technologies).

2.4.2 Microarray analysis

For each strain three independent samples were analysed. Per sample 500ng RNA was processed to labelled cRNA using the Affymetrix 3' IVT Express kit according to the manufacturer's instructions and hybridised to Affymetrix *Drosophila* 2.0 GeneChips for 16 h at 45°C. On the next day gene chips were washed and stained with streptavidin-phycoerythrin using the Affymetrix Fluidics Station 450 and scanned on an Affymetrix GeneChip 3000 scanner (all Affymetrix).

2.4.3 Quantitative PCR (qPCR)

For each sample 1μg RNA was treated with DNAseI (Invitrogen Life Technologies) and used for reverse transcription with the Transcriptor High Fidelity cDNA Synthesis Kit (Roche Diagnostics Ltd.) using oligo(dT) primer. The cDNA was diluted 1:2 and 1μl diluted cDNA was then used for qPCR analysis using the SensiMix SYBR No-ROX Kit (Bioline Reagents Ltd) in a MJ Research PTC-200 thermal cycler with a Chromo4 detector (both Biorad). I designed genespecific primers for qPCR analysis using PerlPrimer (Marshall, 2004) (Table 2.6). I designed a primer pair amplifying the 3' region and one amplifying the 5' region of the RNA to be able to assess whether the whole gene was genuinely up- or down-regulated. Amplicons were between 100 and maximal 300 bp long. Expression of the tested genes was measured in triplicates and gene expression levels for each individual sample were normalised to the expression of EF1α. Relative gene expression was determined and expressed as $2^{-DeltaCT}$ (ΔCT =

($CT_{gene} - CT_{EF1alpha}$) x 1000) (Livak and Schmittgen, 2001). At least 2 independent samples were measured per gene and the average and standard error were determined.

Table 2.6. *Primers for qPCR.*

Gene[a]	Sequence 5'-3'	direction
B52-RF	CTACGGCTTTGTGGAATTCGA	forward
B52-RF	CCACAATCAGTCGGTACTCAG	reverse
Brf-RA 3′	AGTTCGGCTCAGTTGTTGGC	forward
Brf-RA 3′	GATGAGCTCCAAGAAACCGC	reverse
Brf-RA 5′	CTACGGCAAGTTTCAGGTGG	forward
Brf-RA 5′	CGATGAGGAGATGGGAGGTG	reverse
CG11357-RA 3′	AGATCGCGTAACAGTGGACG	forward
CG11357-RA 3′	TTCCTGCCATTTCTGTTCCC	reverse
CG11357-RA 5′	TTCATATCGTTCCAAATGGCGG	forward
CG11357-RA 5′	GTGATCTTACTGCCCGTTTCC	reverse
CG11999-RA 3′	CTATGGCAGACCCATCTCCG	forward
CG11999-RA 3′	CGTGCGTTGAGCTCTTCTCC	reverse
CG11999-RA 5′	GCAACGCTGATTTCAACCG	forward
CG11999-RA 5′	CCCTGGAAATGCTGCCTACC	reverse
CG14687-RA 3′	GGAATCAGCATCGTCCTTGC	forward
CG14687-RA 3′	GCCACCGAGAATGGTGGTAA	reverse
CG31157-RB 3′	TACCCATCCGTTCGTTTTCG	forward
CG31157-RB 3′	ACTTGGCACTGGACACATGG	reverse
CG31157-RB 5′	AAGATTCCCTGGGCTAGACTG	forward
CG31157-RB 5′	CGTTGGCCATTGTTATCACAC	reverse
CG31287-RA 3′	TGTACTTGGATATGCTGGCGG	forward
CG31287-RA 3′	GGCAAATTTGTTCCTGTTCC	reverse
CG31287-RA 5′	GAGATTAACCTTATACAGGCGGAG	forward
CG31287-RA 5′	CTTGGTTACCAAATTTACGGAAGG	reverse
CG32055-RA 3′	CAACAATCGTCTCACTTTCTTGCCG	forward
CG32055-RA 3′	TGACAACGCAGAGGGGTTTCCG	reverse
CG32055-RA 5′	CTTCTGTCCGGAGTGTTCGG	forward
CG32055-RA 5′	TGGAGAGACCAGGCAGTTCC	reverse
CG32795-RA 3′	AGGAGATGAAGAATAGCGCCA	forward
CG32795-RA 3′	CGCACTGATTCGTTTAAGTTTCC	reverse
CG32795-RA 5′	CTCTGCGACAGTTCAAAGGG	forward
CG32795-RA 5′	GAATCGAGACATTTACATCGCC	reverse
CG7900-RA 5′	TTAGCATTGAGACGGACACCT	forward
CG7900-RA 5′	CATTCAAAGAACCCTCGCCA	reverse
CG8245-RA 3′	GGTTTGTGGAGGAATCAATTTCTG	forward
CG8245-RA 3′	CATACTGACGATACCTGAATACCC	reverse
CG8245-RA 5′	TCGATATCAGCTTCGCACCC	forward
CG8245-RA 5′	TCGCCATCATGGTCCTTAGC	reverse
CG9279-RB 3′	GACTTTCGCCGCTTTAGAACCATTG	forward
CG9279-RB 3′	CCAGCAGCACCCATTTCCAGATG	reverse
CG9279-RB 5′	GGCAGCATTTACTTCAAGTGTC	forward
CG9279-RB 5′	CCTCTGGTTATCCTGCTCCT	reverse

DSas-4-RA 5′	AACTACCGTGACGAGATCGAG	forward
DSas-4-RA 5′	GCGGAAGGTAACACTTTGGG	reverse
EF1Alpha RA	ATTCGAGACCATAGTGTAATCATCC	forward
EF1Alpha RA	CAATGATGGTCACGTAGTACTTGG	reverse
GNBP2-RB 3′	TATGGGGAGCTGTACGACGG	forward
GNBP2-RB 3′	GTGCTGCCAAAATGAGAGGG	reverse
GNBP2-RB 5′	GTGTCCATACCAGATGAGCCT	forward
GNBP2-RB 5′	GAGACCCAACTTCCGTTCAC	reverse
Hsc70-2-RA 3′	CCATTTCCAACGACAAGGGCAG	forward
Hsc70-2-RA 3′	CGCTGGCACTCTTTCAGGTGACTC	reverse
Hsc70-2-RA 5′	GACTTGGGCACCACCTACTC	forward
Hsc70-2-RA 5′	CATGGCCACCTGGTTCTTGG	reverse
intergenic region between Hsc70-2 and CG31157	CATTTGGCGGAGCTGTAAGG	forward
intergenic region between Hsc70-2 and CG31157	CTCTTGACCAAATGGAGCCG	reverse
path-RA 3′	AAGTTACATTGAATTGCCCCG	forward
path-RA 3′	GACAGATAATTCTGCGGCTCG	reverse
path-RA 5′	CCAACAACCGATAATGAAACTCTC	forward
path-RA 5′	AGTTCTGTAGTACAACTTGTGTCC	reverse
Sak-RA 5′	GAATAGCTACTGAGCTCTCCCA	forward
Sak-RA 5′	CTGAATGTTTGGTATCTGACCGAC	reverse
Sas-6-RA 5′	GAAGCATGAACGCAAGTTGG	forward
Sas-6-RA 5′	TATGTTGGCCTTCTCTTTGTTTCC	reverse
wallenda-RA 3′	AAAACCCAACAAACGCTCCC	forward
wallenda-RA 3′	TGATCGAACGGCCACTTACC	reverse
wallenda-RA 5′	CGGAACTCCAAGAAGAGCAG	forward
wallenda-RA 5′	GTCAATAAAGCGGTTGTTTGCTC	reverse

[a]Genename with information about the transcript that was used for primer design and the region of the gene the primers bind to.

2.5 *Drosophila* cell biology

2.5.1 Fixation and immunostaining of adult ovaries

Ovaries from 5-10 females were dissected in PBS and then fixed for 20 min in 4% formaldehyde in PBT. After washing with PBT and blocking with PBT + 10% BSA the ovaries were incubated overnight with the primary antibody in PBT + 1% BSA. The next day the ovaries were washed in PBT + 1% BSA several times and then incubated with the secondary antibody in PBT + 1% BSA for 2-4 h. After washing in PBT several

times the ovaries were mounted in mounting medium (85% glycerol and 2.5% n-propylgallate).

2.5.2 Fixation and immunostaining of pupal testes

Pupal testes were fixed and stained for super-resolution microscopy. Testes were dissected and fixed in 10% formaldehyde in PBT for 30 min. They were washed in PBS several times and then squashed between a coverslip thickness 1.5 (Marienfeld) as "slide" and thinner coverslip thickness 1 (VWR), and immediately put into liquid nitrogen. After the coverslips were taken out of the liquid nitrogen the thinner coverslip was removed and the thicker coverslip with the testes was incubated in ice cold ethanol for 15 min at -20°C. The slides were washed in PBS and then incubated in a wet chamber with a drop of the primary antibody and GFP-booster (Chromotek) on top over night at 4°C. On the next day the coverslips were washed several times in PBS and then incubated with the secondary antibody for 3 h at 25°C. After several washes in PBS the coverslips were stained in Hoechst33258 for 10 min and afterwards mounted with ProLong Antifade (Life Technologies).

2.5.3 Fixation and immunostaining of larval brains

Brains from third instar larvae were dissected in PBS and fixed for 20 min in 4% formaldehyde in PBS. Fixed brains were transferred to a drop of 45% acetic acid for 15 s and then to a drop of 60% acetic acid on a coverslip where they were incubated for 3 min. The brains were then squashed between the coverslip and a glass slide between two pieces of Whatman paper by tapping the slide with a pencil tip. Then the slides were immediately put into liquid nitrogen. After all slides had been prepared they were taken out of the liquid nitrogen, the coverslip was removed with a razor blade, and the slides were incubated in ice cold methanol for 5 min at -20°C. Samples were rehydrated

in PBT for 1h and then incubated with primary antibodies under a mounted coverslip in a moist chamber overnight at 4°C. On the next day the slides were washed in PBT and incubated with the secondary antibodies for three hours. Next, the slides were washed in PBT, stained for 10 min in Hoechst33258 (Life Technologies) and then mounted in mounting medium.

2.5.4 Fixation of pupal antenna

Pupae were picked after their eyes had just turned orange, and dissected in a PBS drop. Antenna were removed and fixed in a drop of 4% formaldehyde in PBT for 2 h. Then the antenna were washed several times in PBS and mounted in a drop of mounting medium. The third antennal segment was observed on an Olympus FV1000 confocal microscope.

2.5.5 Brain preparation for live analysis

Brains were dissected from third instar larvae in PBS and the attached imaginal discs were removed. The brain was transferred to a drop of PBS on a clean coverslip and covered with a slide, which flattened the brain. The coverslip was sealed with a drop of Voltalef oil (VWR) to stop evaporation of the PBS and brains were analysed on the Perkin Elmer ERS Spinning Disk confocal system, confocal sections were collected every 30-60 s.

2.5.6 Embryo preparation for live analysis

Flies were allowed to lay eggs on a cranberry juice plates with a drop of yeast for 1.5 h and then the eggs were collected, manually dechorionated and aligned on a glass bottom dish with glue. They were observed on the Perkin Elmer ERS Spinning Disk confocal system for several nuclear cycles and confocal sections were taken every 30 s.

2.5.7 Microinjection of embryos with mRNA

Flies were allowed to lay eggs on an apple juice plate with a drop of yeast for 30-45 min. The eggs were then dechorionated by rolling them on a piece of sticky tape, and then aligned on a glass bottom dish with glue (sticky tape dissolved in heptane). The eggs were then slightly dehydrated for 5 min at 25°C, and afterwards covered with a layer of Voltalef oil (VWR). The mRNA was then injected with finely drawn glass needles. After 1 h the translated protein could be observed on the Perkin Elmer ERS Spinning Disk confocal system and confocal sections were collected every 15-20 s.

2.5.8 Antibodies used in this thesis

The antibodies used in this thesis are listed below. The appropriate Alexa 488-, Alexa 568- and Alexa 647-conjugated secondary antibodies were obtained from Molecular Probes and used diluted 1:1000.

Table 2.7. *Antibodies used in this thesis (IF = immunofluorescence, WB = western blotting, IP = immunoprecipitation).*

Protein	Number	Species	Source	Dilution	Notes
Asl	11	rabbit	Raff lab	1:1000	IF testes, IP, WB
Asl	197	rat	Raff lab	1:500	IF brains
Cnn	55	guinea pig	Raff lab	1:500	IF brains
Cnn	37	rabbit	Raff lab	1:1000	IP, WB
Spd-2	57	rabbit	Raff lab	1:500	IF brains, IP, WB
γ-tubulin	142	mouse	Sigma	1:1000	IF brains
α-tubulin DM1 α	141	mouse	Sigma	1:1000	IF brains; monoclonal
DPLP	86	rabbit	Raff lab	1:500	IF brains
DTACC	134	rabbit	Raff lab	1:500	IF brains
Msps	110	rabbit	Raff lab	1:500	IF brains
Aurora A	72	rabbit	Raff lab	1:500	IF brains
Dgp71WD	295267	rabbit	(Vérollet et al., 2006)	1:500	IF brains
Phospho-Asl T373	259 specP	rabbit	Eurogentec	1:100	IF brains
Histone H3 Phospho S10	179	rabbit	Upstate Biotechnology	1:500	IF brains

2.6 Microscopy and image analysis

2.6.1 Microscopes used for the analysis of embryos, brains and testes

Fixed preparations were examined either on a Zeiss Axioskop 2 microscope (Carl Zeiss, Ltd.,) with a CoolSNAP HQ camera (Photometrics), using a 63x/1.25 NA objective (Carl Zeiss, Ltd.) with Immersol oil (Carl Zeiss) using MetaMorph Software (Molecular Devices), or on a Olympus FV1000 confocal microscope using a 60x oil lens with Olympus Fluoview software (Olympus). Live brains and embryos were imaged using a 63x oil lens on a Perkin Elmer ERS Spinning Disk confocal system mounted in an inverted microscope (Axiovert 200M; Carl Zeiss MicroImaging Inc.) with a charge-coupled device camera (Orca ER; Hamamatsu) with Ultraview ERS software (Perkin Elmer). All pictures and time series were analysed using Fiji (Schindelin et al., 2012). Image stacks for super-resolution microscopy were acquired using a Deltavision OMX V3 microscope (Applied Precision) with a 60x/1.42 Oil UPlanSApo oil objective (Olympus) and processed using SoftWorx software (Applied Precision).

2.6.2 Assessing fluorescence intensity of embryonic centrosomes

Embryos in nuclear cycles 10-13 were imaged using the Perkin Elmer ERS Spinning Disk confocal system and confocal sections were collected every 15-20 s. Sections were reconstructed in 3D using Fiji and the fluorescence of individual centrosomes was quantified in each time point using the maximum intensity setting. Data were then analysed in Microsoft Excel.

2.6.3 Analysis of mitotic index

Larval brains were stained with Hoechst and anti-Phospho-Histone H3 to visualise mitotic nuclei. 10 fields of each brain (total 8 brains) were imaged. The total number of

nuclei and the number of mitotic nuclei per image were counted using CellProfiler software (Carpenter et al., 2006), a total of at least 16200 cells per genotype was counted. The mitotic index was calculated as MI = mitotic nuclei/total nuclei * 100. The data were normalised by setting the wild type mitotic index to 1.

2.6.4 Quantification of centrosomes in larval brains

Larval brains were stained with antibodies against Asl and Cnn and imaged on a Zeiss Axioskop 2 microscope. Neuroblasts and ganglion mother cells were scored in prophase in order to ensure that centrosomes were duplicated but extra centrosomes would not be clustered at the spindle poles. Mitotic cells were identified using DNA morphology and dots were scored as centrosomes only if they co-stained for Cnn and Asl.

2.6.5 Quantification of aMTOCs and spindle phenotypes in larval brains

Larval brains were stained with antibodies against α-tubulin to visualise spindle, Cnn to visualise aMTOCs and Phospho-Histone H3 and were imaged on a Zeiss Axioskop 2 microscope. Only mitotic cells identified by Phospho-Histone H3 staining were scored, and all phenotypes were always quantified blind, without knowing which genotype was being counted.

2.6.6 Image manipulation and presentation

Images in this thesis were processed in Fiji (Schindelin et al., 2012) using standard methods. Control and experimental images were adjusted using the same procedures to use the full range of pixel intensities. All images are maximum intensity projections.

2.7 Bioinformatics

2.7.1 Microarray data analysis

I performed quality control of microarray expression data using the Bioconductor package AffyPLM (Gautier et al., 2004). The probe intensities from Affymetrix image files (".CEL" files) were normalised using quantile normalisation (Bolstad et al., 2003), and expression signals of all genes (probesets) were calculated using GCRMA (Guanosine Cytidine robust multiarray analysis) (Wu and Irizarry, 2007). Differentially expressed genes between WT and Experimental samples were identified using the Bioconductor package limma (Smyth, 2005). I then obtained lists of genes that displayed at least 1.5-fold change in expression and a Benjamini-Hochberg FDR-corrected P-value of ≤ 0.05 (Benjamini and Hochberg, 2005). Raw data can be accessed in Gene Expression Omnibus (www.ncbi.nlm.nih.gov/geo/; accession number GSE35240).

2.7.2 Gene ontology enrichment

I analysed the list of differentially expressed genes of *sakOE* compared to w^{67} for enrichment of Gene Ontology (GO) terms using DAVID, a program that weighs the enrichment of a specific GO term in a given dataset relative to the frequency of that term on the Affymetrix *Drosophila* 2.0 chip (Huang et al., 2009; Huang et al., 2008). I looked for enrichment in the GO FAT set, which attempts to filter the broadest terms so that they do not overshadow the more specific terms.

2.7.3 Protein sequence alignments

Alignments of protein sequences were performed with Clustal W (Larkin et al., 2007) using the default settings.

2.7.4 Mass spectrometry data analysis

The tandem mass spectrometry (LC-MS/MS) data were searched against the FlyBase sequence database (http://flybase.bio.indiana.edu/) using Mascot software (Matrix Science). The following settings were used for the searches: Enzyme: Trypsin; fixed modification: carbamidomethylation; variable modifications: methionine oxidation, glutamine/asparagine deamidation; serine/threonine/tyrosine phosphorylation; error tolerance for the precursor ions, 20 ppm; mass error tolerance for the fragment ions, 0.6 Da; number of missed cleavage sites, 3. The MS/MS spectra for identified phosphopeptides were manually inspected in Mascot.

3 Phosphorylation of centrosomal proteins

3.1 Introduction

At the beginning of mitosis the amount of PCM organised by the centrioles increases dramatically, which results in an increase in microtubule-organising activity and therefore promotes efficient mitotic spindle assembly. This process is called 'centrosome maturation' (Section 1.3.1). In *Drosophila*, the centriolar protein Asl has been strongly implicated in PCM recruitment (Bonaccorsi et al., 1998; Conduit et al., 2010; Dzhindzhev et al., 2010b; Varmark et al., 2007). Asl is localised on the surface of the centrioles throughout the cell cycle (Fu and Glover, 2012; Lawo et al., 2012; Mennella et al., 2012; Sonnen et al., 2012), but it does not appear to play a major part in recruiting the PCM to interphase centrioles (Mennella et al., 2012). In fly cells, the centrioles tend to organise only very small amounts of PCM in interphase (Martinez-Campos et al., 2004; Rogers et al., 2008) and the centriolar protein DPLP seems to be particularly important for organising the interphase PCM (Mennella et al., 2012). As cells enter mitosis, however, Asl appears to initiate the recruitment of the PCM proteins Spd-2 and Cnn to the centrioles. Once recruited Spd-2 and Cnn appear to be released from their centriolar-binding sites and they then move slowly away from the centrioles forming "scaffold-like" structures on which many, if not all, other PCM proteins ultimately assemble (Conduit et al., manuscript in preparation). In this way, Spd-2 and Cnn appear to be the key players of mitotic PCM recruitment in *Drosophila*: in the absence of either protein centrosomes can still partially mature, but the loss of both proteins leads to a complete failure in mitotic PCM recruitment (Conduit et al., manuscript in preparation).

How is the initiation of mitotic PCM recruitment regulated? An obvious possibility is that this process is regulated by prostranslational modifications such as phosphorylation. Many cell cycle events are regulated by phosphorylation, and indeed it is known that phosphorylation plays a central role in mitotic PCM recruitment. Early experiments with *Xenopus* egg extract showed that PCM maturation depends on the activity of kinases, as maturation was completely blocked by the addition of kinase inhibitors (Ohta et al., 1993) and Cdc2 kinase activity was shown to promote MT nucleation activity of centrosomes in mitosis (Verde et al., 1990). The kinases Polo/Plk1 and Aurora A have been implicated in centrosome maturation in a variety of different organisms (Berdnik and Knoblich, 2002; Hannak, 2001; Hirota et al., 2003; Lane and Nigg, 1996; Lee and Rhee, 2011; Sunkel and Glover, 1988). Furthermore, phosphorylation of Cnn in *Drosophila* is dependent on Polo (Dobbelaere et al., 2008) and it has been suggested that phosphorylation of Cnn, Spd-2 and Asl might increase the strength of interaction between these proteins and thus lead to increased structural integrity of the PCM and centrosome maturation (Conduit and Raff, 2010).

Several phosphoproteomic screens have identified phosphorylation sites in several centrosomal proteins in *Drosophila* (Bodenmiller et al., 2007; Habermann et al., 2012; Zhai et al., 2008). These studies have not yet, however, lead to identification of sites that have been shown to be functionally relevant for centrosome function. In this chapter I describe a phosphoproteomic screen designed to identify phosphorylation sites in all three of major proteins that appear to regulate the onset of centrosome maturation in *Drosophila*—Asl, DSpd-2 and Cnn. This screen has successfully identified sites that appear to be specifically phosphorylated at centrosomes during mitosis, and I describe my initial attempts to analyse the biological functions of some of these sites by examining flies expressing phosphorylation-resistant point-mutants of these proteins.

Several of these experiments were performed in collaboration with Paul Conduit, a post-doctoral fellow in the laboratory.

3.2 Proteins of the pericentriolar material are phosphorylated when they are at the centrosome

If the functions of Asl, Spd-2 and Cnn in PCM recruitment are regulated by phosphorylation we reasoned that these proteins might be phosphorylated only when incorporated into the centrosome, but not when they were in the cytoplasm. In order to compare centrosomal with cytoplasmic pools of Asl, Spd-2 and Cnn, we isolated centrosomes from *Drosophila* embryo extracts (Moritz and Alberts, 1999). After ultracentrifugation of a partially clarified extract through a sucrose-step gradient, the relatively heavy centrosomes are enriched in the 70% sucrose fraction at the bottom of the centrifuge tube, while the lighter cytoplasmic components remain in the supernatant (Figure 3.1A).

A western blot analysis of this experiment revealed that the centrosomal fractions were devoid of cytoplasmic proteins (as judged by the actin control) and that the centrosomal fractions of Cnn, Spd-2 and Asl all exhibited a clear mobility shift compared to the cytoplasmic fractions (Figure 3.1B). This shift was due to phosphorylation because it disappeared when centrosomal fractions were treated with phosphatases, but not when phosphatase inhibitors were also included. Interestingly, the shift was very distinct for Cnn as essentially all of the Cnn in the centrosomal fraction was shifted, but this was not the case for Spd-2 where there appeared to be 2 different pools of Spd-2 present at the centrosome – one which was phosphorylated and one which was not. In the case of

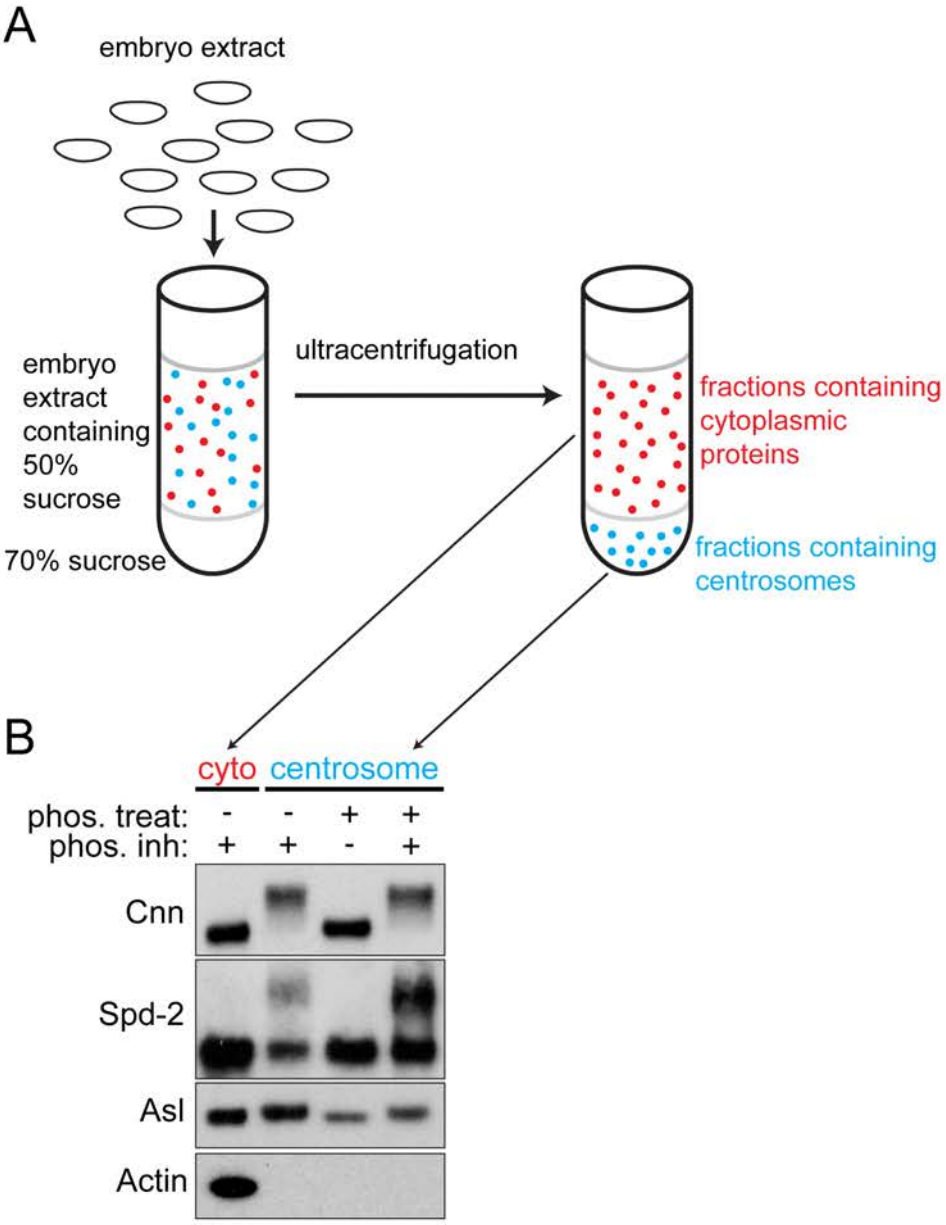

Figure 3.1: PCM proteins are phosphorylated when they are at the centrosome, but not when they are in the cytoplasm. (A) Centrosomes are isolated by layering early Drosophila embryo extract containing centrosomes (blue) and cytoplasmic proteins (red) onto a sucrose gradient. After ultracentrifugation the centrosomes are in the bottom of the vial, whereas cytoplasmic proteins remain in the supernatant. **(B)** Cytoplasmic fractions (1st lane) of Cnn, Spd-2 and Asl are compared with centrosomal fractions (2nd lane) of these proteins. Actin is only found in the cytoplasmic fractions. Note the shift in the gel in the centrosomal fractions. This shift disappears, when the fractions are treated with phosphatases (3rd lane). When adding phosphatase inhibitors, the shift is there again (4th lane). (phos.treat. = phosphatase treatment; phos.inh. = phosphatase inhibitors added)

Asl, the mobility shift was much subtler than for the two other proteins, but it seemed that the entire centrosomal fraction was shifted. This analysis strongly suggests that all three proteins are phosphorylated at the centrosome, and not in the cytoplasm.

We set out to identify phosphorylation sites in Asl, Spd-2 and Cnn. Paul Conduit focused on the analysis of Cnn and has now successfully identified several phosphorylation sites that seem to be important for proper recruitment of Cnn to mitotic centrosomes (P. Conduit, personal communication). I focused on identifying phosphorylation sites in Asl and Spd-2. In the following sections I describe my analysis of Asl and Spd-2.

3.3 Identification of phosphorylation sites in centrosomal proteins

In order to identify sites in Asl and Spd-2 that were phosphorylated specifically at centrosomes, I isolated centrosomes from embryo extracts as described above and then subjected the centrosomal fractions to a further round of affinity-purification with an antibody against Cnn. It should be noted that the embryos used to make the embryo extracts are not synchronised regarding their developmental and cell cycle stage, and the centrosomes isolated therefore come from embryos in all different stages of the cell cycle. In trial experiments, I tested several antibodies for their efficacy in this centrosome affinity-purification step and found that the Cnn antibodies gave the highest yield of highly enriched centrosomes, probably because these are excellent antibodies. To purify cytoplasmic fractions for comparison to the centrosomal fractions I took the cytoplasmic fractions of the embryo extracts (that had been depleted of centrosomes by

ultracentrifugation) and affinity-purified the cytoplasmic Asl and Spd-2 with antibodies directed against these proteins.

These three samples (centrosomal sample, cytoplasmic Asl and cytoplasmic Spd-2) were separated by SDS-PAGE, and I cut out the region of the gel containing the centrosomal and the cytoplasmic Asl and Spd-2 bands. I then performed in-gel tryptic digest, and enriched the samples for phosphopeptides using TiO_2 columns. The samples were analysed by LC-MS/MS in the Proteomics Facility of the Sir William Dunn School of Pathology to identify phosphorylation sites in Asl and Spd-2. In addition we also ran the samples without prior enrichment for phosphopeptides. The LC-MS/MS data were searched against the FlyBase protein sequence database using Mascot software (Section 2.7.4). The Mascot Ion Score of 29, corresponding to a probability of P=0.05, was used as the guideline for considering a peptide as identified. Lower scoring peptides were also considered if they were found consistenly throughout different repetitions of the experiment. I compared phosphopeptides found in centrosomal (Supplementary Table 1) and cytoplasmic (Supplementary Table 2) pools of the proteins, and could identify one Asl phosphorylation site and seven Spd-2 phosphorylation sites, that were phosphorylated consistently and with high confidence when the proteins were localised to the centrosome, but not when they were in the cytoplasm (Table 3.1). All of the Spd-2 sites had been identified in previous phosphoproteomic screens as well (as indicated in Table 3.1) (Habermann et al., 2012; Zhai et al., 2008), although these screens did not differentiate between sites phosphorylated at the centrosome or in the cytoplasm. The Asl site I found had not been reported before.

Table 3.1. *Highscoring Asl and Spd-2 sites phosphorylated at the centrosome but not in the cytoplasm. Phosphorylated residues are marked in red.*

Protein	Peptide sequence	peptide score[1]	position	References
Asl	LVGSTPLNPLDR	25	T373	novel site
Spd2	GTNISFEPAEITGR	53.03	S121	Habermann et al., 2012
Spd2	TNQPLLEPESNVTLDSVGEK	65.26	T329	Zhai et al., 2007
Spd2	RPPSSSEILSLSAIDK	38.85	S397	Zhai et al., 2007
Spd2	KPLSPLADHPQITISR	34.55	S484	Habermann et al., 2012 Zhai et al., 2007
Spd2	RVSIATMGLIPR	29.93	S569	Zhai et al., 2007
Spd2	NLSPLSSPR	42.33	S614	Habermann et al., 2012 Zhai et al., 2007
Spd2	GLGTSSVAVPR	64.8	S673	Habermann et al., 2012 Zhai et al., 2007

[1]*Mascot Ion Score is −10log(P), with P being the probability that the observed match is a random event. Individual ion scores >29 indicate identity or extensive homology ($p<0.05$).*

3.4 Asl is phosphorylated on T373 when it is at the centriole

In Asl I could identify one phosphorylation site on Threonine 373, which was phosphorylated at the centrosome but not in the cytoplasm (Figure 3.2A). I tested whether the site lies in a conserved region of the protein, and aligned the Asl protein sequence across different *Drosophila* and mosquito species (only small regions of Asl are conserved enough to be accurately aligned across a broader spectrum of species, and these putative phosphorylation sites are not within one of these regions). The alignment showed that T373 was conserved across all the species examined (Figure 3.2B).

Interestingly, T373 is located within a potential Cdk1 phosphorylation motif (Songyang et al., 1994). Cdk1 is a key regulator of mitotic entry, and, when bound to mitotic cyclins such as Cyclin A or B, it can phosphorylate specific T or S residues that lie within a so-called polo-box domain binding motif (Cheng et al., 2003; Elia et al., 2003a; Elia et al., 2003b). Binding of the Polo/Plk1 polo-box domain (PBD, comprising polo-box 1 and polo-box 2 and the linker sequence between) to these phosphorylated protein sequences regulates the subcellular localisation of Polo/Plk1 in mitosis. For example, the PBD is required to localise Polo/Plk1 to the centrosomes in mitosis (Elia et al., 2003a). The sequence of the PBD binding motif, S-(pT/pS)-P, resembles the T373 site found in Asl (Figure 3.2A). This suggests the possibility that T373 might get phosphorylated by Cdk1 in mitosis, which then leads to subsequent binding of Polo/Plk1 to Asl, potentially allowing the subsequent phosphorylation of centrosomal targets - such as Cnn (Dobbelaere, 2008) - by Polo/Plk1.

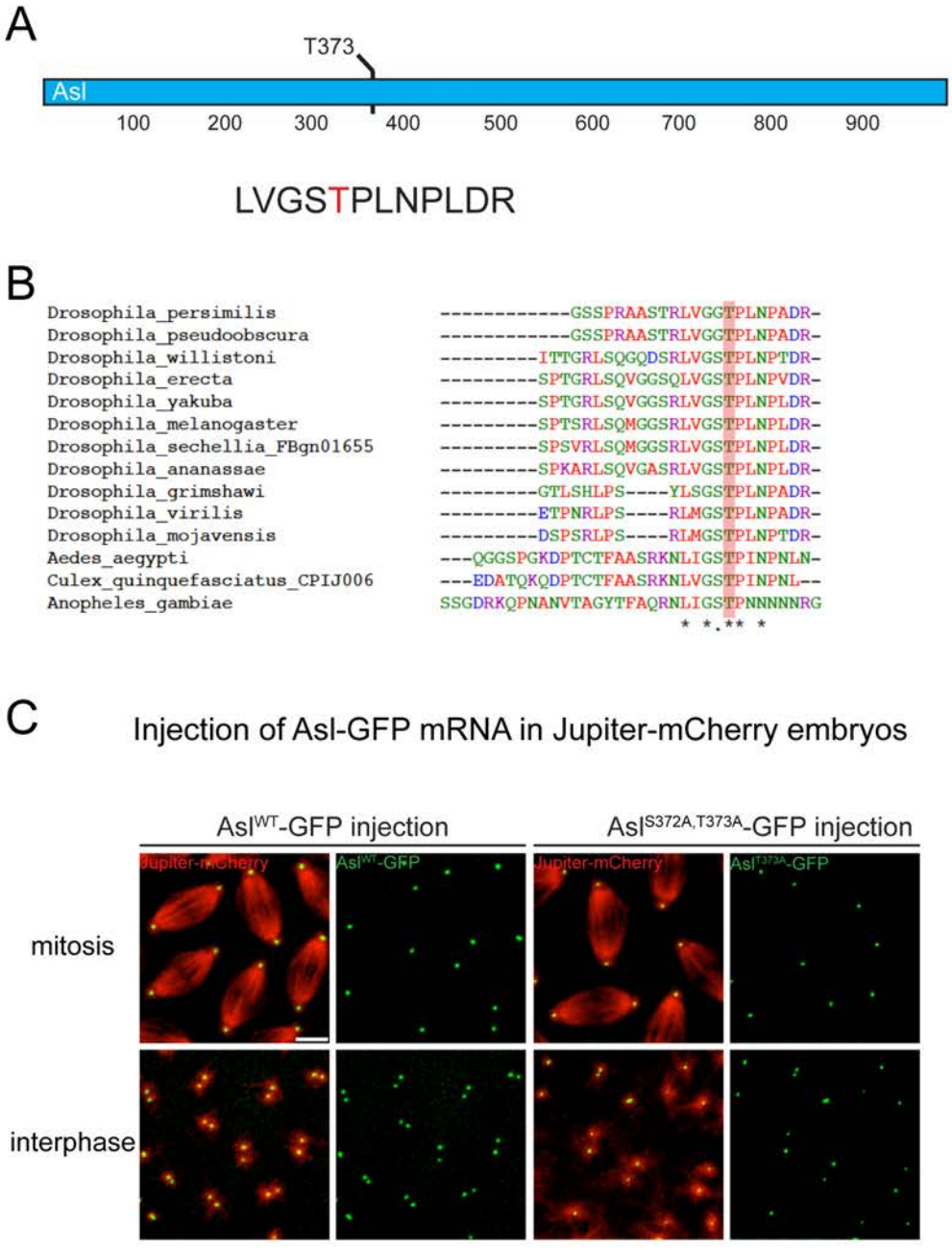

Figure 3.2: Asl is phosphorylated on the conserved site T373 when it is at the centrosome, but phosphorylation is not required to localise it to the centrosome. **(A)** Phosphorylation site T373 in Asl is phosphorylated when Asl is at the centrosome. The site resembles a Cdk1 phosphorylation motif (Songyang, 1994) and a PBD binding motif (Elia, 2003). **(B)** ClustalW alignment of Asl homologues shows that T373 is well conserved across *Drosophila* species and Mosquitoes. **(C)** Asl^{WT}-GFP and Asl^{S372A,T373A}-GFP mRNA were injected into Jupiter-mCherry (red) expressing embryos. Both the WT and phosphomutant forms of the Asl-GFP protein (green) localise to centrosomes after translation, indicating that phosphorylation is not needed for localisation to centrosomes (n=15 embryos) Scale bar is 5μm.

3.5 Asl phosphorylation on T373 is not required for localisation of Asl to the centrosome

My mass spectrometry data indicate that Asl is phosphorylated on T373 only when it is at the centrosome, so I wanted to test whether T373 phosphorylation is required to localise Asl to the centrosome. I made an Asl-GFP construct in which Threonine 373 was exchanged for an Alanine. I decided to mutate the adjacent Serine 372 as well, because mutation of a phosphosite can result in compensating phosphorylation of neighbouring residues that can mask the phenotype of the phospho-mutation (Edwards, 1999). The resulting construct $Asl^{S372A,T373A}$-GFP was cloned into a vector containing a T3 RNA polymerase promoter, and capped Asl-GFP mRNA was transcribed *in vitro*. I then injected $Asl^{S372A,T373A}$-GFP and Asl^{WT}-GFP mRNA into early (0-45 min old) *Drosophila* embryos expressing Jupiter-mCherry (allowing me to visualise MTs). After ~ 1 h the mRNA had been translated in the embryos, and localisation of the GFP-tagged protein could be observed by live-cell imaging. Both the WT control and the Asl phospho-mutant localised to centrosomes in a similar manner (Figure 3.2C). I conclude that phosphorylation of S372 and T373 is not required for localisation of Asl to the centrosome, at least in the presence of WT Asl protein.

3.6 Asl is phosphorylated on Threonine 373 specifically in mitosis

Next, we obtained a phosphospecific Asl antibody that only binds to Asl when it is phosphorylated at T373 from Eurogentec. This antibody was raised in rabbits against a phosphopeptide from this region of Asl. Sera from these rabbits were depleted of

antibodies that recognise non-phosphorylated Asl by passing the sera over a column of non-phosphorylated peptide until there was no more immunoreactivity detectable against the non-phosphorylated peptide in ELISA assays. Antibodies were then purified from these depleted sera with a column containing the phosphopeptide.

I stained *Drosophila* brain cells with this phosphospecific Asl antibody (anti P-Asl) and with an antibody recognising all forms of Asl. I also stained cells for Phospho-Histone H3 to mark mitotic cells. Remarkably, the staining showed that while the general Asl antibody recognised Asl in all cells (as it is localised to centrosomes throughout the cell cycle), the phosphospecific antibody stained Asl only in mitotic cells (Figure 3.3A). Importantly, this is consistent with the observation that phosphorylation on T373 is not needed to localise Asl to the centriole – rather, Asl is localised at the centriole throughout the cell cycle, but only in mitosis it becomes phosphorylated.

Interestingly, Asl phosphorylation on T373 coincides with recruitment of Spd-2 and Cnn in mitotic cells (Figure 3.3B). Asl is thought to initiate the recruitment of Spd-2 and Cnn to the centrosome in mitosis (Conduit et al., manuscript in preparation). My finding suggests that phosphorylation on T373 in mitosis (possibly by Cdk1) might "activate" Asl, so that it leads to the efficient recruitment of Spd-2 and Cnn and so to centrosome maturation. In order to test this hypothesis, I made transgenic flies expressing phosphomutant and phospho-mimicking forms of Asl.

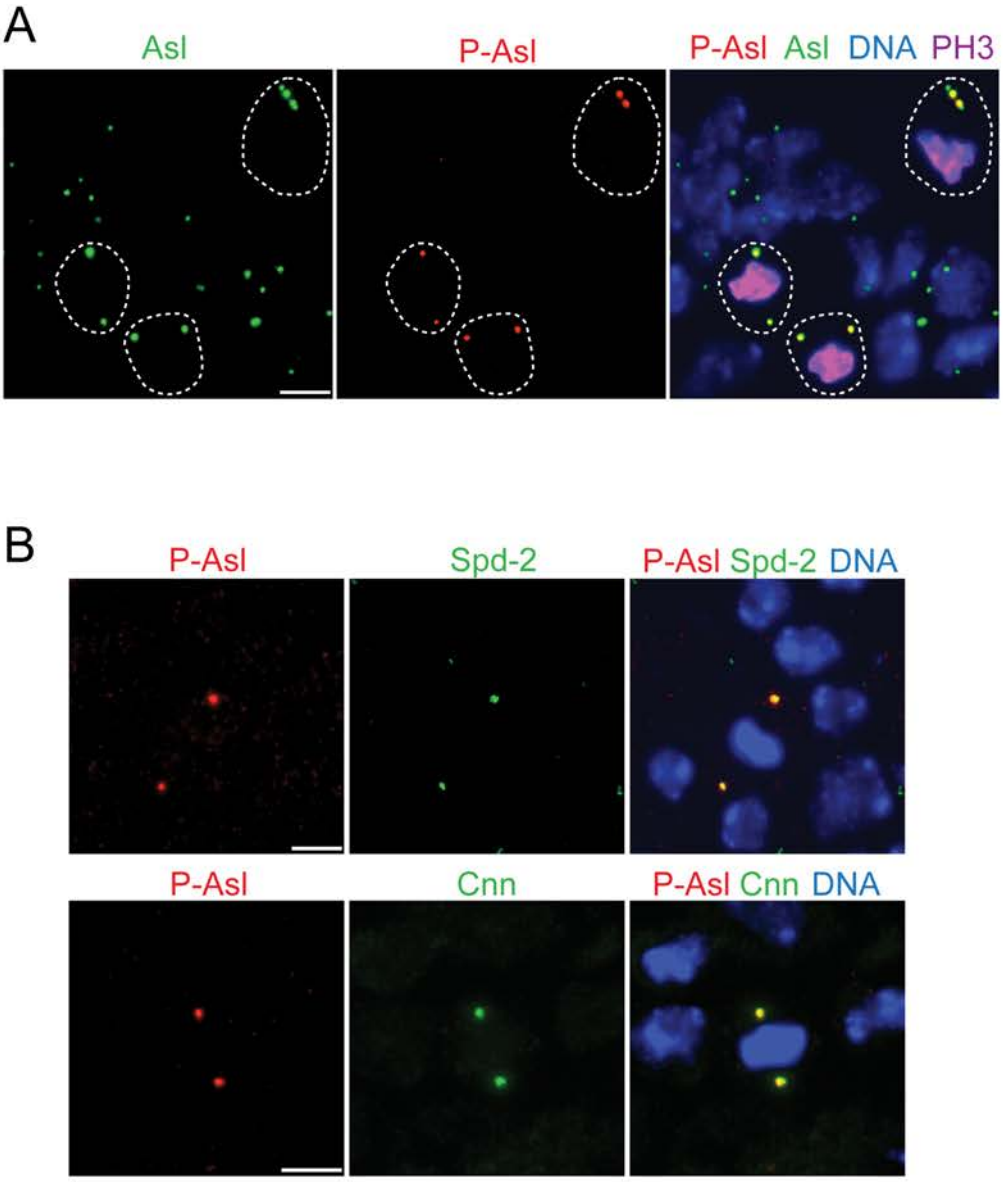

Figure 3.3: Asl is phosphorylated on T373 specifically in mitosis. (A) 3rd instar larval brains stained with anti-Asl (green), anti-P-Asl phosphorylated at T373 (red) and anti-Phospho-Histone H3 to mark mitotic cells. DNA is in blue. Asl is only phosphorylated in mitotic cells (framed in white). **(B)** Phosphorylation of Asl T373 coincides with recruitment of Spd-2 and Cnn to mitotic centrosomes. Larval brains stained with anti-P-Asl (red) and anti-Spd-2 or anti-Cnn (green). DNA is in blue. Scale bars are 5μm.

3.7 Asl T373 phospho-mutants and phospho-mimicking flies do not have any obvious mitotic phenotypes in early embryos

I generated transgenic flies expressing a non-phosphorylatable form of Asl tagged with GFP ($Asl^{S372A,T373A}$-GFP) and a form where T373 was exchanged for a Glutamate to mimic constitutive phosphorylation (Asl^{T373E}-GFP) driven by the ubiquitin promoter. I then crossed these transgenic inserts into an *asl* null mutant background and confirmed the expression of the transgenic inserts by western blot analysis (Figure 3.4A). Flies surviving on these mutated forms of Asl-GFP were viable and fertile, and I could keep them as homozygous stocks in the lab, suggesting that there are no major defects caused by loss of Asl T373 phosphorylation or by mimicking constitutive phosphorylation.

I used these stocks to test the specificity of the Asl T373 phosphospecific antibody by staining brain cells of *Asl-GFP, asl;* $Asl^{S372A,T373A}$*-GFP, asl* and Asl^{T373E}*-GFP, asl* larvae with it. The phosphospecific antibody stains mitotic centrosomes in *Asl-GFP, asl,* but not in *asl;* $Asl^{S372A,T373A}$*-GFP, asl* and Asl^{T373E}*-GFP* confirming that it is specific to Asl phosphorylated on T373 (Figure 3.4B).

Next, I started to analyse whether the Asl phospho-mutant or –mimetic flies showed any mitotic abnormalities. I decided to film early embryos, as functional centrosomes are essential for mitosis in embryos and one can observe many centrosomes as they rapidly proceed in synchrony through the cell cycle. Furthermore, major defects in PCM recruitment lead to a failure of embryonic development (Dix and Raff, 2007; Lucas and Raff, 2007; Varmark et al., 2007). I could, however, not detect any obvious mitotic

abnormalities in any of the stocks (Figure 3.5A). Thus, disappointingly, it appears that phosphorylation on Asl T373 is not essential for proper embryonic development, and it only has a minor, if any, role in PCM recruitment in embryos.

3.8 Asl T373 phospho-mutant and phospho-mimetic flies do not have obvious impairments in PCM recruitment

I wondered whether Asl T373 phospho-mutants might have a more subtle defect in PCM recruitment. I decided to examine the centrosomal recruitment of several PCM components in larval brain cells. I looked at Spd-2 and Cnn, as these proteins are thought to be directly recruited by Asl, and also at γ-tubulin, which is recruited downstream of Spd-2 and Cnn (Conduit et al., manuscript in preparation). All three PCM proteins appeared to be recruited normally to centrosomes in larval brain cells (Figure 3.5B). These data suggest that phosphorylation of Asl T373 does not play a major part in regulating PCM recruitment. I furthermore tested whether Asl phospho-mimetic flies might show any abnormal PCM recruitment in interphase, but no recruitment of Spd-2 could be detected to interphase centrosomes (Figure 3.5C). In comparison, *asl* mutant cells without an Asl-GFP transgene completely lack centrioles and PCM in third instar larval brains (Figure 3.5D).

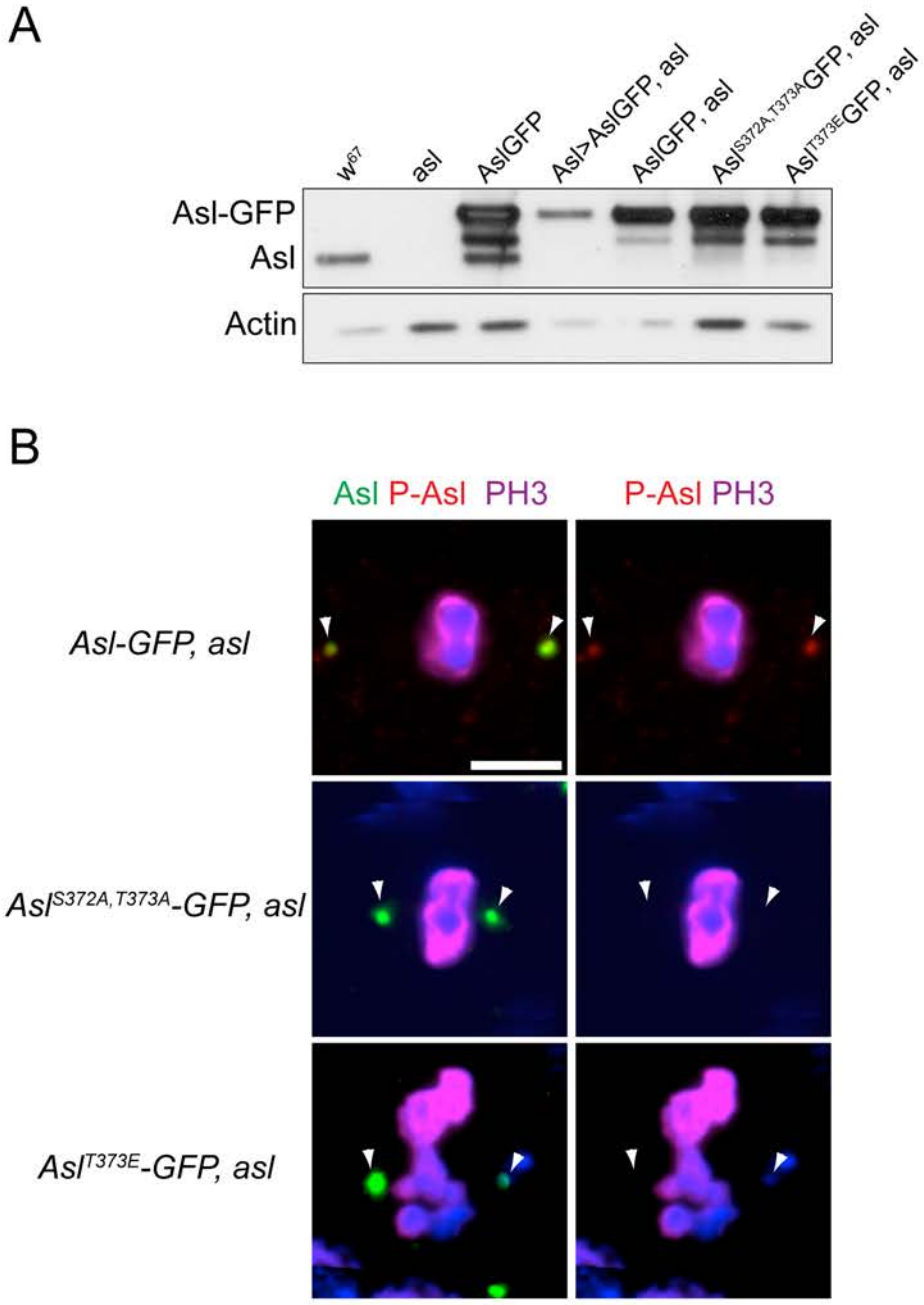

Figure 3.4: Making Asl phospho-mutant and phospho-mimetic fly strains. (A) Expression of *AslGFP, AslGFP*^{S372A,T373A} and *AslGFP*^{T373E} in the *asl* mutant background were confirmed by western blot analysis of larval brain extracts. Actin was stained as loading control. In strains where Asl-GFP is over expressed, a slightly lower band appears which is presumably a degradation product. **(B)** Larval brains were stained with anti-Asl (green), anti-P-Asl (red) and anti-Phospho-Histone H3 (pink). The anti-P-Asl staining disappears in *Asl*^{S372A,T373A}*-GFP, asl* and *Asl*^{T373E}*-GFP, asl* flies, indicating that the antibody indeed is specific for Asl phosphorylated on T373 (centrosomes marked by arrow heads). DNA is in blue, scale bar is 5μm.

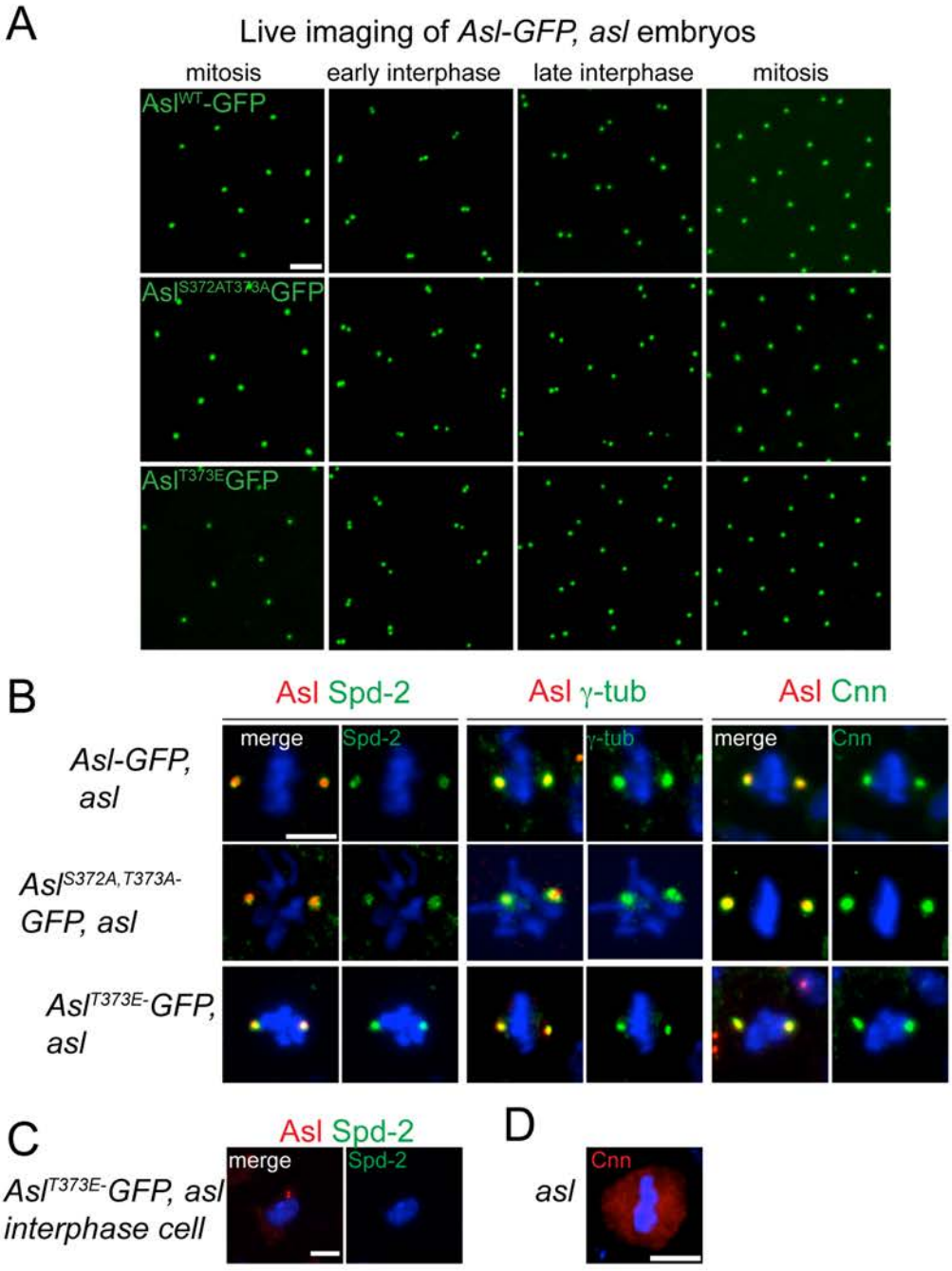

Figure 3.5: *Asl*^{S372A,T373A}*-GFP, asl* and *Asl*^{T373E}*-GFP,asl* embryos proceed normally through mitosis and PCM recruitment in larval brains is not impaired. (A) Asl-GFP, Asl^{S372A,T373A}-GFP or Asl^{T373E}-GFP (in green) in the asl mutant background was filmed in early embryos. There were no obvious defects in mitotic progression in any of the strains (n=20 embryos per genotype). **(B)** Mitotic larval brain cells stained with anti-Spd-2, anti-γ–tub or anti-Cnn (green) and anti-Asl (red). Note that all Asl-GFP constructs rescue the acentriolar *asl* mutant phenotype. Recruitment of Spd-2, γ-tub and Cnn to centrosomes did not appear impaired. DNA is in blue. **(C)** *Asl*^{T373E}*-GFP,asl* cells do not recruit PCM in interphase cells (Asl in red, Spd-2 in green, DNA in blue). **(D)** Shows a mitotic *asl* mutant cell lacking centrioles and PCM for comparison, as shown by the lack of Cnn staining. All scale bars are 5μm.

3.9 Spd-2 from centrosomal fractions is phosphorylated at many sites

My phosphoproteomic analysis identified several high confidence phosphorylation sites in Spd-2 in purified centrosome samples. Multisite phosphorylation in proteins is very common and can have many different functions (Cohen, 2000), and at least one centrosomal protein needs to be phosphorylated at several residues simultaneously in order to activate their function, the γ-TuRC interacting protein Nedd1 needs to be phosphorylated on 4 different residues simultaneously to activate it to bind to γ-tubulin in mammalian cells (Gomez-Ferreria et al., 2012). Therefore I decided to mutate several sites together and test whether the resulting construct would show a phenotype. I mutated the seven sites that were consistently phosphorylated across several experiments and/or had high Mascot ion scores (Table 3.1). In the peptide NLSPLSSPR S614 was phosphorylated with high confidence (Table 3.1), in addition I also mutated S617 although it was only found to be phosphorylated with lower probability (Supplementary Table 1). Furthermore, I also mutated directly adjacent Serines or Threonines in all phosphopeptides to avoid phosphorylation of these neighbouring residues, which could mask the phenotype of the phospho-mutations (Edwards, 1999), leading to a total of 11 mutated residues. All of these sites were phosphorylated only at the centrosome (apart from S614, which I found to be phosphorylated in the cytoplasm as well in a later repetition of the experiment). In total I mutated S121, T329, S397, S484, S569, S614, S617, S618, T672, S673 and S674 (Figure 3.6A). The resulting construct will hereafter be called Spd-2^{Pmutant}-GFP.

A

Residues mutated in Spd-2^{Pmutant}-GFP

MDSSSGSQGNGSFMDQNSLGILNMDNLKVFGDLSSFSKSGRRSGTGRDSPAVHERLREER 60
LRALETLEKPRPSRSSQAKSTALQMRLSTNISELVTDDTIDLNSSSSFALVTPATKGTNI 120
SFEPAEITGRSTLCQAGKQRRREKPSLSVA EILKSSFVEKARLLERKLQDASQAEASYHL 180
SRGSSSSLSDSFNCSRSLPRTADMSELSLNGGGGFSFGSASLAAEGQDESFAPAELMQSK 240
LVLGEISWAQ EFTAMPTATLSTQALKKIAAPTSEIETSVSNSVLAGDPDFSLGNYFQTRS 300
ENIWNIVSNSSPNRSRTNQPLLEPESNVTLDSVGEKTPQPDNKTYTKTDA ITGSNLGRNL 360
MRKMQQDRIETALKSRNGLAAKETKRPPSSSEILSLSAIDKALRDIDLNSDTSTVEVVNH 420
LWEHGRGNNYDDGENKENQSSNSHAERTSCGSNKLTDTMSFTDSVLNSTDFRHLQQSISR 480
KPLSPLADHPQITISRADTDPVETEAEADIDEWPSTPVKEPSRRVRRTKISPRAASPSSS 540
DGVRPLTCTEDENDEEDEDKTPVNKKRVSIATMGLIPRKASSLSSTRLDGCDVAVASSTE 600
RDFGISPNLAKNLSPLSSPRSCLSSPLLDSTTSSDRRQLMSGAARKANSSPAGSEASSTS 660
GFTASGRRGLGTSSVAVPRSISRCSNSSEFSHRDGKLLPLKVTHTTLCWGSTKLRTDVRK 720
SMQVKNTADKRLVIRLGIQGPGFQLVGTDSSTITLQAMECRSVVINFCPTVCGAAIGALS 780
FYAPPGAHNSNQPGLEIPLYGYGGSASITINGLLKGPVGASFLTIGDVCELSAGPLSANL 840
KFHNKGPLTAFVGISVDSTVLMKLRLSEAFEVRPSRLILPPNSERCVQILFRPNREDLKN 900
ILKKTAQVLTLANMRIFCGDEPNRQRMRSLVQRMSSRQREKLTSPMLDSIWGEFPDEQPV 960
RNIGQLNEPPEFILDLVTVVRIIDVALTLNRDFDESSESS LMFLPEADETVLFRTICVAN 1020
SPTPTQSHLLEPVDELLEADTTTLTPVEQNWCVQPGLLEFGVGCSPLATLSVTNSFCSRQ 1080
LIEVTCNVPDLVRISPSECYVSPDGGHAEIDVRLLRSPRQDLLEREPLIVVSMENERISV 1140
PISFKF

B

Injection of Spd-2-GFP mRNA in Jupiter-mCherry embryos

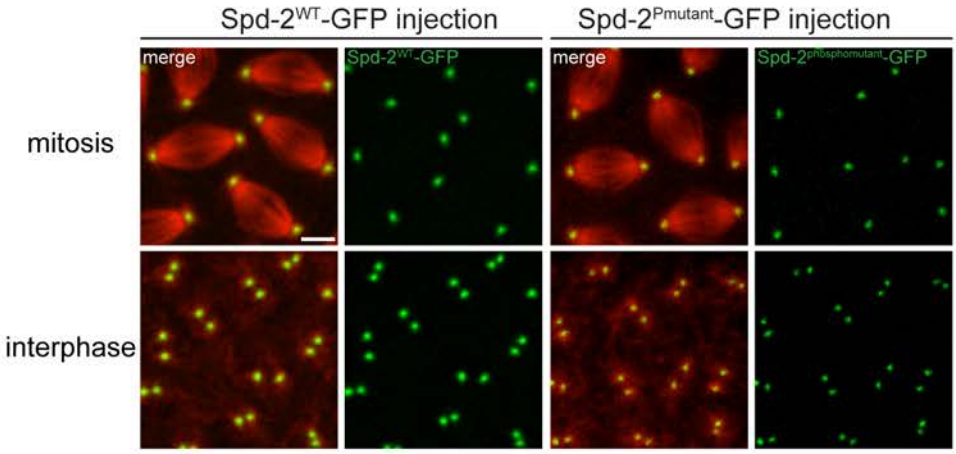

Figure 3.6: Phosphorylation of Spd-2 on 11 different sites is not needed for localisation of Spd-2 to the centrosome. (A) Amino acid sequence of Spd-2, the S and T residues that are mutated in Spd-2^{Pmutant}-GFP are marked in red, and the phosphopeptides found in the LC-MS/MS analysis are marked in blue. **(B)** mRNA injection of Spd-2^{WT}-GFP and Spd-2^{Pmutant}-GFP into early *Drosophila* embryos shows that the translated Spd-2^{Pmutant}-GFP protein (green) does localise to centrosomes (n=15 embryos). Jupiter-mCherry is in red. Scale bar is 5μm.

3.10 Phosphorylation of 11 Spd-2 phosphosites is not required for localisation of Spd-2 to the centrosome

I first wanted to test whether phosphorylation of Spd-2 on these 11 residues was required for localisation of Spd-2 to the centrosome. I tested this, by injecting mRNA of a Spd-2-GFP construct, in which these 11 Serine or Threonine sites were exchanged for Alanines, into early Jupiter-mCherry embryos. I filmed localisation of translated Spd-$2^{Pmutant}$-GFP and could see that it localised to centrosomes in a very similar manner to a WT DSpd-2-GFP protein (Figure 3.6B). The fluorescent signal of Spd-$2^{Pmutant}$-GFP is actually a bit lower; however at this point no conclusions can be drawn from this as the amounts of mRNA injected into the embryos varies a lot due to experimental constraints.

Therefore this result suggests that the phosphorylation at one or more of these sites is not required for localisation of Spd-2 to the centrosome, at least when endogenous Spd-2 is present (as is the case in these embryos).

3.11 Mutation of 11 Spd-2 phosphosites affects turnover of Spd-2 at the centrosome

In order to test the behaviour of Spd-$2^{Pmutant}$ in the absence of endogenous WT Spd-2, I made transgenic flies expressing Spd-$2^{Pmutant}$-GFP and crossed these into the *spd-2* mutant background. As a control, I also generated similar strains expressing a WT Spd-2-GFP protein. I tested the resulting strains by western blot analysis (Figure 3.7A). Both the *Spd-2-GFP, spd-2 and t*he *Spd-$2^{Pmutant}$-GFP, spd-2* strains were viable and fertile

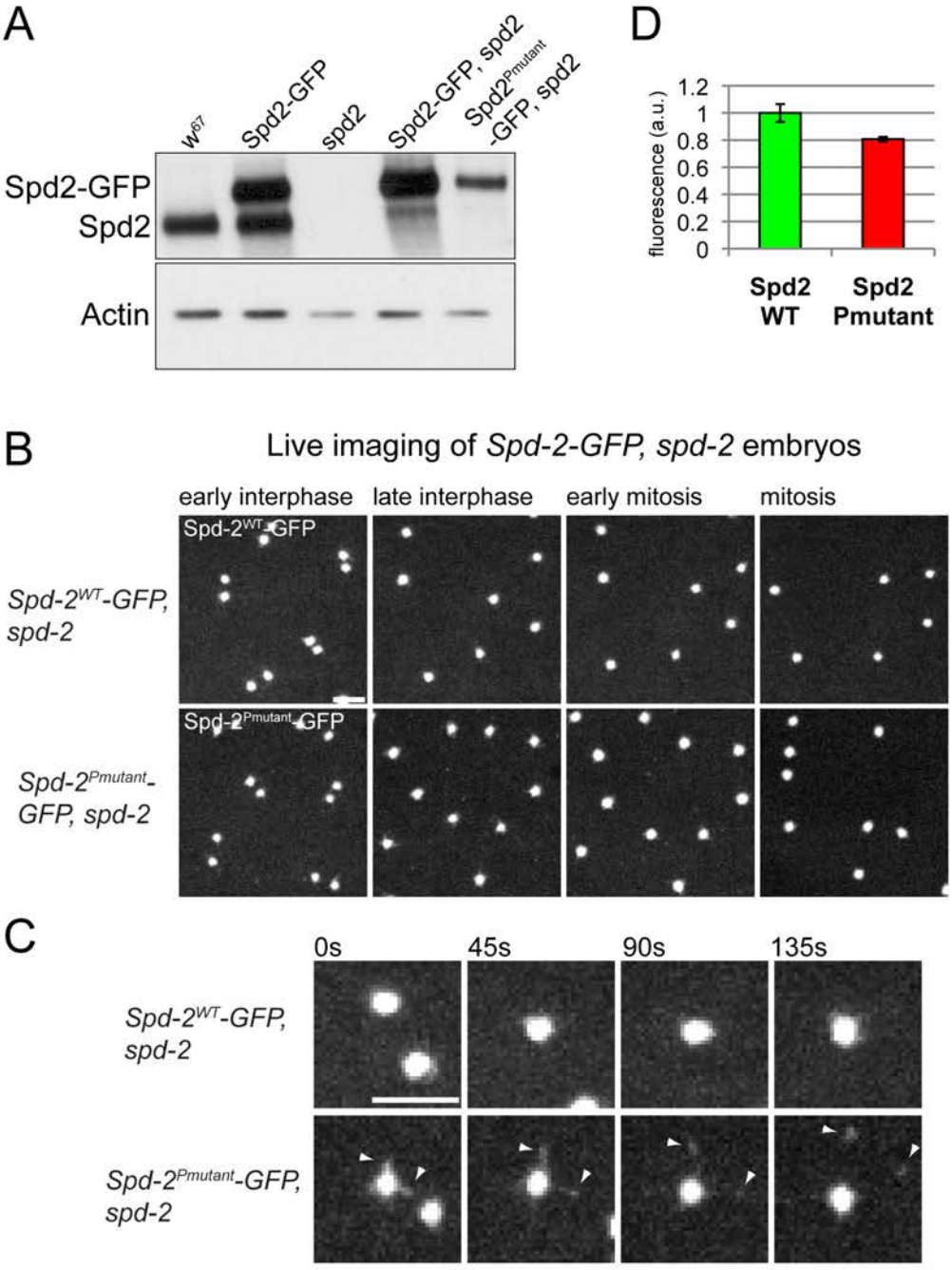

Figure 3.7: Mutation of 11 Spd-2 phosphosites affects turnover of Spd-2 at the centrosome. (A) Western blot analysis of *Spd-2-GFP, spd-2*, *Spd-2^{WT}-GFP, spd-2* and *Spd-2^{Pmutant}-GFP, spd-2* larval brain extracts. **(B)** Spd-2^{WT}-GFP and Spd-2^{Pmutant}-GFP were filmed in the *spd-2* mutant background in early embryos. Note that both constructs rescue the *spd2* mutant, which would not develop at all due to failure in pronuclear fusion. **(C)** Closeup of centrosomes. Note that in *Spd-2^{Pmutant}-GFP, spd-2* embryos flares of Spd-2^{Pmutant}-GFP are ejected from the centrosomes (see arrowheads). **(D)** Fluorescent intensities of Spd-2^{WT}-GFP and Spd-2^{Pmutant}-GFP at interphase centrosomes in the *spd-2* mutant background (arbitrary fluorescence units, WT normalised to 1). Data was collected from 5 embryos, 10 centrosomes per embryo were analysed. Error bars represent standard error. All scale bars are 5μm.

and could be kept as homozygous stocks, indicating that the phospho-mutations do not cause any major impairment in PCM assembly. The *spd-2* mutant is normally female sterile due to a failure to recruit PCM to the fertilising sperm centriole, which leads to a failure in pronuclear fusion and so to an arrest in embryonic development (Dix and Raff, 2007).

I filmed early embryos from both of these lines and could detect no difference in progression through the cell cycle (Figure 3.7B). I noticed, however, that in the *Spd-2^{Pmutant}-GFP, spd-2* embryos more Spd-2^{Pmutant}-GFP "flares" appeared to be ejected from centrosomes (Figure 3.7C). Flaring occurs when pieces of the PCM break away from the centrosome and move outwards (and occasionally inwards as well) on the centrosomal MTs (Lee et al., 2001; Megraw et al., 2002). The level of flaring is thought to increase if the integrity of the PCM is in some way weakened, as occurs, for example, in Cnn mutant embryos (Lucas and Raff, 2007). This increased flaring therefore suggests that the *Spd-2^{Pmutant}-GFP* protein is not as strongly maintained in the PCM as the WT protein. In support of this possibility, I measured the amount of Spd-2-GFP incorporated into the centrosome, and could see that in *Spd-2^{Pmutant}-GFP, spd-2* embryos Spd-2-GFP levels were ~20% lower than in *Spd-2^{WT}-GFP, spd-2* embryos (Figure 3.7D). These data suggest that the Spd-2^{Pmutant}-GFP may be recruited to the centrosome normally, but that it is not properly maintained in the PCM. A possible caveat to this interpretation is that the expression levels of Spd-2^{Pmutant}-GFP in brain cells appear to be lower than in the corresponding Spd-2^{WT}-GFP strain (Figure 3.7A). If this was the case in embryos, then lower levels of cytoplasmic Spd-2 could lead to lower levels in the centrosome. I think this unlikely, however, as it has been found that halving the amount of cytoplasmic Spd-2 (in heterozygous *spd-2* mutant embryos) does

not lead to lower levels of Spd-2 at the centrosome (Paul Conduit, personal communication).

3.12 Discussion

I have described the identification of phosphorylation sites in the centrosomal proteins Asl and Spd-2 using immuno-isolation of centrosomal and cytoplasmic proteins coupled with a phosphoproteomic approach. In Asl, one site (T373) was identified as being phosphorylated when Asl was at the centrosome, but not when it was in the cytoplasm. Excitingly, this site is a consensus polo-box binding site (see below) (Elia et al., 2003a). I obtained peptide antibodies that were specific for the T373 phosphorylated form of the protein and found that although Asl is associated with the centrioles throughout the cell cycle, it only becomes phosphorylated during mitosis. This coincides with the timing of mitotic PCM recruitment, raising the possibility that phosphorylation of Asl might be the crucial event that allows Asl to recruit Spd-2 and Cnn, so triggering centrosome maturation. Disappointingly, however, my analysis of Asl phospho-mutant flies in the *asl* mutant backgroundshow that phosphorylation of Asl on T373 is not essential for localising Asl to centrioles or for mitotic PCM recruitment.

Nevertheless, it cannot be ruled out that the phosphorylation of Asl at T373 may play a part in mitotic PCM recruitment. It is intriguing that the T373 site resembles a Cdk1 phosphorylation motif, and furthermore a polo box binding motif. The idea that Cdk1 might phosphorylate T373 in mitosis to recruit Polo/Plk1 to the centrosome is very attractive, as Polo is known to have a major role in recruiting the PCM during mitosis in flies (Dobbelaere et al., 2008). My analysis has shown that the centrosomal fractions of DSpd-2 and Cnn are phosophorylated, and it seems very likely that Polo will be

responsible for at least some of these phosphorylations; indeed, the phosphorylation of Cnn at centrosomes in S2 cells is known to be Polo-dependent (Dobbelaere, 2008). Although my experiments reveal that Asl T373 phosphorylation is neither necessary nor sufficient to trigger mitotic PCM recruitment, perhaps this is not surprising. In cultured cells the Plk1 dependent phosphorylation of several sites in Pericentrin seems to be all that is required to drive the recruitment of many, but not all, PCM components to the centrosome (Lee and Rhee). It could be argued, however, that having such a complicated process depend on the phosphorylation status of only a single protein is a risky strategy, as PCM recruitment could be triggered inappropriately relatively easily.

In vivo, it seems more likely that several proteins might have to be phosphorylated to trigger robust PCM recruitment. Perhaps Asl T373 phosphorylation does play a part in triggering mitotic PCM recruitment, but, *in vivo*, this process is regulated by multiple mechanisms, so preventing the phosphorylation of only one site on one protein is not enough to significantly perturb the process. I suspect, therefore, that a more careful examination will reveal that PCM recruitment is slightly perturbed in the Asl phospho-mutant flies. A good way to test this would be with FRAP experiments: the fluorescence of GFP-fusion protein of interest at the centrosome is bleached, and then the efficiency of fluorescence recovery gives an indication of how efficiently the protein is being recruited to the centrosome. It would be interesting to test whether the recovery of Spd-2-GFP and/or GFP-Cnn is subtly perturbed when Asl cannot be phosphorylated at T373.

Moreover, it is clear that Polo/Plk1 activity is regulated at many levels—in flies, for example, Polo/Plk1 is sequestered to microtubules in interphase via the microtubule-associated protein Map205, and this inhibits its cellular activity. The phosphorylation of Map205 by Cdk1 at mitotic entry relieves binding to Polo/Plk1, allowing Polo to

fulfil its mitotic functions (Archambault et al., 2008). I am planning to assess the effects of the Asl phospho-mimetic strain in a *map205* mutant background. If it turns out that Asl T373 phosphorylation does have a subtle role in triggering mitotic PCM recruitment then *in vitro* kinase assays to identify the kinase that phosphorylates T373 and binding assays to determine whether the Polo box domain can bind to phosphorylated Asl will be required to further dissect the role of this phosphorylation event.

In contrast to Asl, I identified several different sites that were preferentially phosphorylated on the centrosomal fractions of Spd-2. It has been proposed that Spd-2 and Cnn are the key players in mitotic PCM recruitment in flies as they provide a PCM scaffold around the centrioles that other PCM proteins bind to (Conduit et al., 2010). Multi-site phosphorylation of proteins can lead to changes in surface charges of proteins and/or conformational changes, potentially explaining how Spd-2 and Cnn could be activated by phosphorylation to allow them to form scaffold structures only around the centrioles and only in mitosis. Indeed, I obtained some evidence that Spd-2 phosphorylation is important for the maintenance of Spd-2 at the centrosome, as the combined mutation of several of these phosphorylation sites had a clear, but relatively minor, effect on the ability of Spd-2 to be retained within the PCM. Future experiments will require FRAP analysis to measure the recruitment rate of Spd-2^{Pmutant}-GFP to the centrosome to find out whether only maintenance of Spd-2^{Pmutant}-GFP at the centrosome is perturbed, or if the recruitment of Spd-2^{Pmutant}-GFP to the centrosome is also impaired.

A possible caveat of our analysis is that it does not represent an exhaustive analysis of all phosphosites in Spd-2. We narrowed down the number of phosphosites that we could feasibly mutate, so that some highscoring sites were neglected in our analysis

(ANSSPAGSEASSTSGFTASGR and DFGISPNLAK Supplementary Table 1). Furthermore, the sequence coverage (the part of Spd-2 that could be detected in the LC-MS/MS experiments) of Spd-2 was ~30%, which means that many potentially important phosphorylation sites were not detected at all in our analysis.

Recent experiments by Paul Conduit suggest that, similar to Spd-2, the loss of multiple phosphorylation sites in Cnn can lead to a phenotype where the amount of PCM organised by centrosomes in embryos is drastically reduced. We plan to test in the near future whether the combined abrogation of phosphorylation in both Spd-2 and Cnn can completely abolish PCM recruitment in flies.

4 The role of Sak kinase in centrosome assembly

4.1 Introduction

Drosophila Sak kinase and its homologues in mammalian cells (Plk4) and *C. elegans* (Zyg1) are essential for centriole duplication (Bettencourt-Dias et al., 2005; Habedanck et al., 2005; Peters et al., 2010). The levels of Sak/Plk4 in the cell are very low and are tightly regulated; this is accomplished, at least in part, by trans-autophosphorylation of the downstream regulatory element (DRE) (Figure 4.1A). The SCF E3 ligase recognises autophosphorylated Sak/Plk4, mediated by binding of the F-box protein Slimb (β-TrCP in mammals) to the DRE, and targets it for degradation by the proteasome (Cunha-Ferreira et al., 2009; Guderian et al., 2010; Rogers et al., 2009; Sillibourne et al., 2010). In *Drosophila* the autophosphorylation of Sak is counteracted by the phosphatase PP2A together with its targeting unit Twins (Brownlee et al., 2011). Tight regulation of Sak/Plk4 levels is crucial as overexpression leads to centriole overduplication (Kleylein-Sohn et al., 2007; Peel et al., 2007), which has been linked to chromosome missegregation (Ganem et al., 2009; Silkworth et al., 2009), tumourigenesis in flies (Basto et al., 2008) and microcephaly in mice (Marthiens et al., 2013). Furthermore, Plk4 has been shown to be aberrantly expressed in human colorectal and liver cancer (Ko et al., 2005; Macmillan et al., 2001).

In contrast to Plk1-3, Sak/Plk4 has three Polo Boxes (PB) (Figure 4.1 A). The PB1-PB2 cassette binds to Asl and mediates dimerisation (Dzhindzhev et al., 2010a; Slevin et al., 2012), while PB3 also facilitates dimerisation and binds to an unknown centriolar target (Leung et al., 2002). Despite extensive efforts the target substrates of the Sak/Plk4 kinase that are essential for centriole duplication have not yet been convincingly

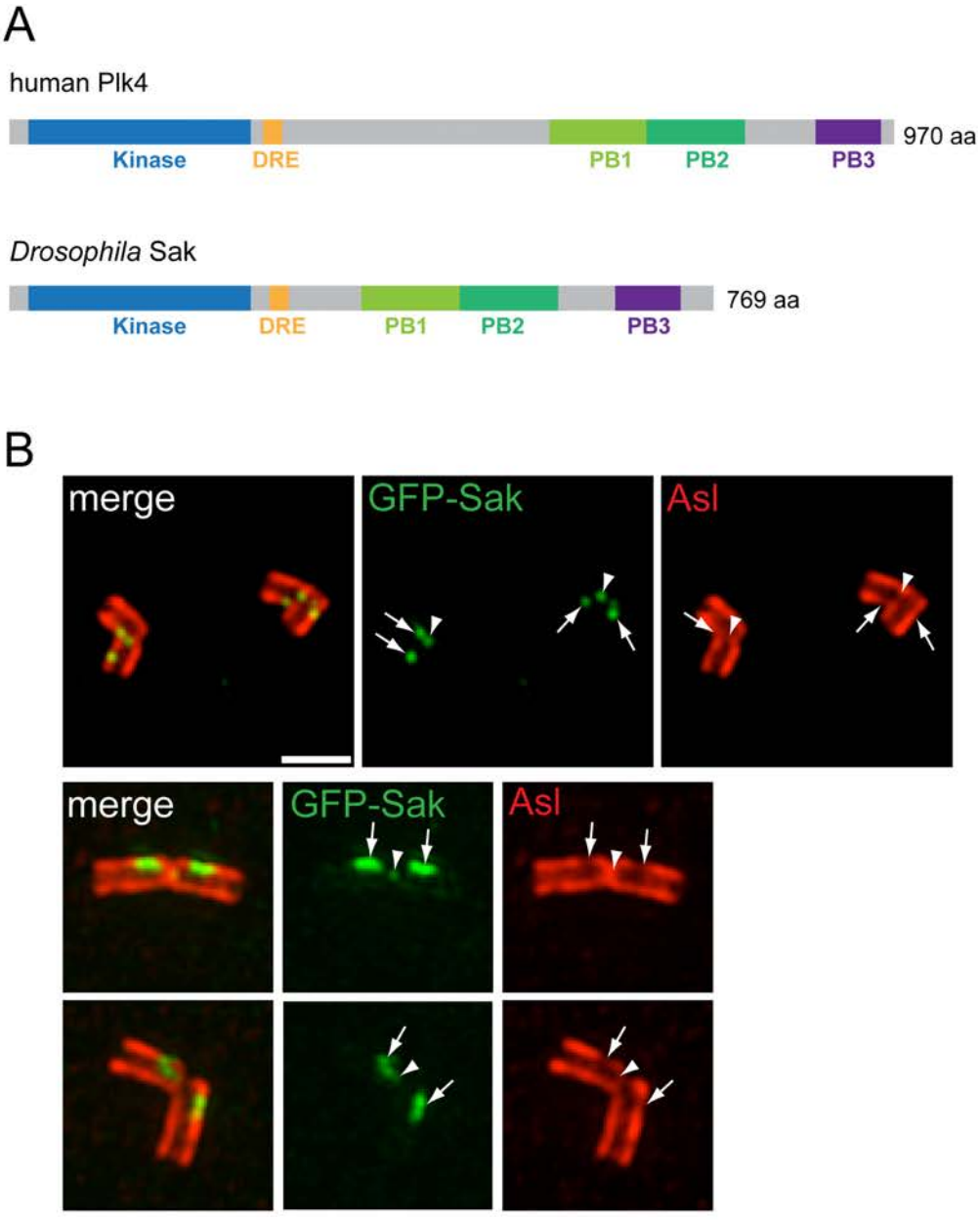

Figure 4.1: *Drosophila* Sak kinase. (A) Protein structure of human Plk4 and *Drosophila* Sak (DRE=downstream regulatory element, PB=polo box, aa=amino acids) **(B)** 3D-SIM images, GFP-Sak enhanced with GFP-booster in green and anti-Asl in red. Scale bar 1μm. Centrioles in primary spermatocytes, the first panel shows early G2 phase centrioles, and the second and third panel shows late G2 phase centrioles, which are more elongated. GFP-Sak appears to localise to the base of the cartwheel of the daughter centriole (arrowheads) and at the walls of the proximal ends of daughter and mother centriole (arrows).

identified. For example, Plk4 has been shown to phosphorylate CPAP (the mammalian homologue of DSas-4), but this is not required for procentriole assembly (Chang et al., 2010). SAS-6 proteins act early in the duplication pathway and are recruited to centrioles by Sak/Plk4 (Delattre et al., 2006; Kleylein-Sohn et al., 2007; Lettman et al., 2013; Pelletier et al., 2006a; Stevens et al., 2010b); initial data suggested that SAS-6 was indeed phosphorylated by *C. elegans* Zyg1 and this was essential for centriole duplication (Kitagawa et al., 2009). It has recently been shown very convincingly, however, that although a direct interaction between Zyg1 and SAS-6 is required to recruit SAS-6 to centrioles, ZYG-1 does not phosphorylate DSas-6 in worms (Lettman et al., 2013). Importantly, the kinase activity of ZYG-1 is subsequently needed for cartwheel assembly, but this appears to be via the phosphorylation of a different, as yet unknown, target (Lettman et al., 2013). Similarly in *Drosophila* it is known that Sak promotes the recruitment of a complex of Sas6 and Ana2 to the mother centriole (Stevens et al., 2010b), but it remains to be elucidated how Sak catalyses their incorporation into the cartwheel structure.

While Sak/Plk4 is clearly required for a very early step in centriole assembly, it is not clear whether Sak is needed for any later steps in centriole or centrosome formation. A weak hypomorphic mutation of Sak caused by a P-Element insertion into the coding region has been described in *Drosophila* (Bettencourt-Dias et al., 2005), but these flies still contain centrioles in most of their cells and these centrioles appear to organise relatively normal centrosomes. In order to better address the open questions that remain about the function of Sak I decided to generate a null mutation in the *sak* gene. Using this mutant in combination with **Sa**s-6/**A**na2 **P**article**s** (SAPs) as a proxy for centrosomes, I was able to show in collaboration with other people in our lab that Sak is

required for proper cartwheel assembly but not for any other step in the centriole or centrosome assembly pathway.

4.2 Sak localisation by super-resolution microscopy

I first wanted to assess the localisation of Sak within the centriole by using three-dimensional structured illumination microscopy (3D-SIM). In 3D-SIM the specimen is excited by an illumination pattern that varies both laterally and axially. Interference of the illumination pattern with the sample leads to a Moiré pattern visible in the emission pattern from which a high-resolution image of the specimen can be generated using image reconstruction algorithms (Gustafsson et al., 2008; Schermelleh et al., 2008; Schermelleh et al., 2010). By using 3D-SIM an eightfold increased resolution compared to the resolution of a standard confocal microscope can be facilitated.

The endogenous Sak levels are too low for detection by antibodies (Bettencourt-Dias et al., 2005), therefore I used a ubiquitin-driven Sak-GFP line (Peel et al., 2007) that leads to moderate overexpression of Sak. The GFP signal was enhanced by staining with the GFP-booster antibody, and I co-immunostained with anti-Asl antibodies to stain the outer wall of the centriole (Lawo et al., 2012; Mennella et al., 2012; Sonnen et al., 2012). Interestingly, I could detect a small amount of Sak-GFP localising to the very base of the daughter centriole (arrowheads), and to an extended "patch" on the walls of the proximal ends of both mother and daughter centrioles (Figure 4.1B). This strongly suggests that Sak-GFP is marking the position on the mother centriole where the existing daughter centriole was first formed (the staining at the very base of the daughter centriole) and also the site on the both mother and daughter centrioles at which

new daughter centrioles will assemble during the next round of centriole duplication (the patch of staining found on both centriole walls).

Previous studies have also examined the localisation of Sak/PLK4 using super-resolution microscopy. In cultured *Drosophila* cells Sak was shown to have a very similar distribution to Asl in a cylindrical structure (Fu and Glover, 2012). In contrast, in human cultured cells Plk4 was localised as a distinct dot lying on a ring structure formed by Asl (Sonnen et al., 2012). Even more interestingly, this dot colocalised with SAS6 and appeared to be present before SAS6 was recruited, suggesting that the site on the mother centriole where a nascent procentriole is formed is determined prior to detectable recruitment of SAS6, and that Plk4 is an early marker for this site (Sonnen et al., 2012). The localisation of PLK4 in human cells is therefore quite similar to the staining of Sak that I detect in *Drosophila* spermatocytes.

4.3 Making a *sak* mutant by imprecise P-element excision

The existing Sak hypomorphic mutant allele, sak^{c06612}, is caused by a P-Element insertion into the coding region of the *sak* gene (indicated by blue arrow in Figure 4.2A) (Bettencourt-Dias et al., 2005). Sak^{c06612} flies have reduced centriole numbers and hold up their wings indicating slight uncoordination, but in contrast to other mutations in core centriole duplication proteins (that die as adults because they cannot walk and feed), homozygous sak^{c06612} adults are at least sufficiently viable to live long enough to lay fertilised eggs, although these eggs then fail to develop (Rodrigues-Martins et al., 2008). To properly assess the function of Sak we thought it important to generate a stronger allele. We therefore attempted to make a *sak* null mutant by generating deletions within the *sak* gene by imprecise P-Element excision (as described in Section

2.1.4). I first chose a P-Element located towards the C-terminal end of the *sak* coding region for the excision screen (P{GawB}SAK^{NP6647}, indicated by red arrow in Figure 4.2A), as I planned to screen by PCR for deletions that extended towards the N-terminus of the coding region. I found, however, that this P-Element could not be mobilised (unpublished observations). I then decided to repeat the P-element excision screen with a different P-Element (P{GSV1}GS3043, which is inserted in the 5'UTR of the neighbouring gene *cdk12* as indicated by the green arrow in Figure 4.2A), and slightly upstream of the 5'UTR of the *sak* gene.

In collaboration with Alan Wainman, a postdoc in the laboratory, I succeeded in mobilising the P-Element. We screened ~1000 flies carrying excisions of the P-element by PCR (primers indicated in Figure 4.2B – note orientation of genes are reversed compared to Figure 4.1A) and identified a single deletion within the *sak* gene (Figure 4.2B and C). We named the allele caused by the deletion *sak*^{Aa74}. Sequencing of *sak*^{Aa74} revealed that the whole *sak* promoter region and the first third of the coding sequence, comprising nearly the entire kinase domain, were deleted (Figure 4.2B). Furthermore, a small part of the *cdk12* 5'UTR was deleted as well. We do not think, however, that the function of this gene is disrupted in *sak*^{Aa74} as all phenotypes observed in *sak*^{Aa74} are fully rescued by a GFP-Sak transgene (see below).

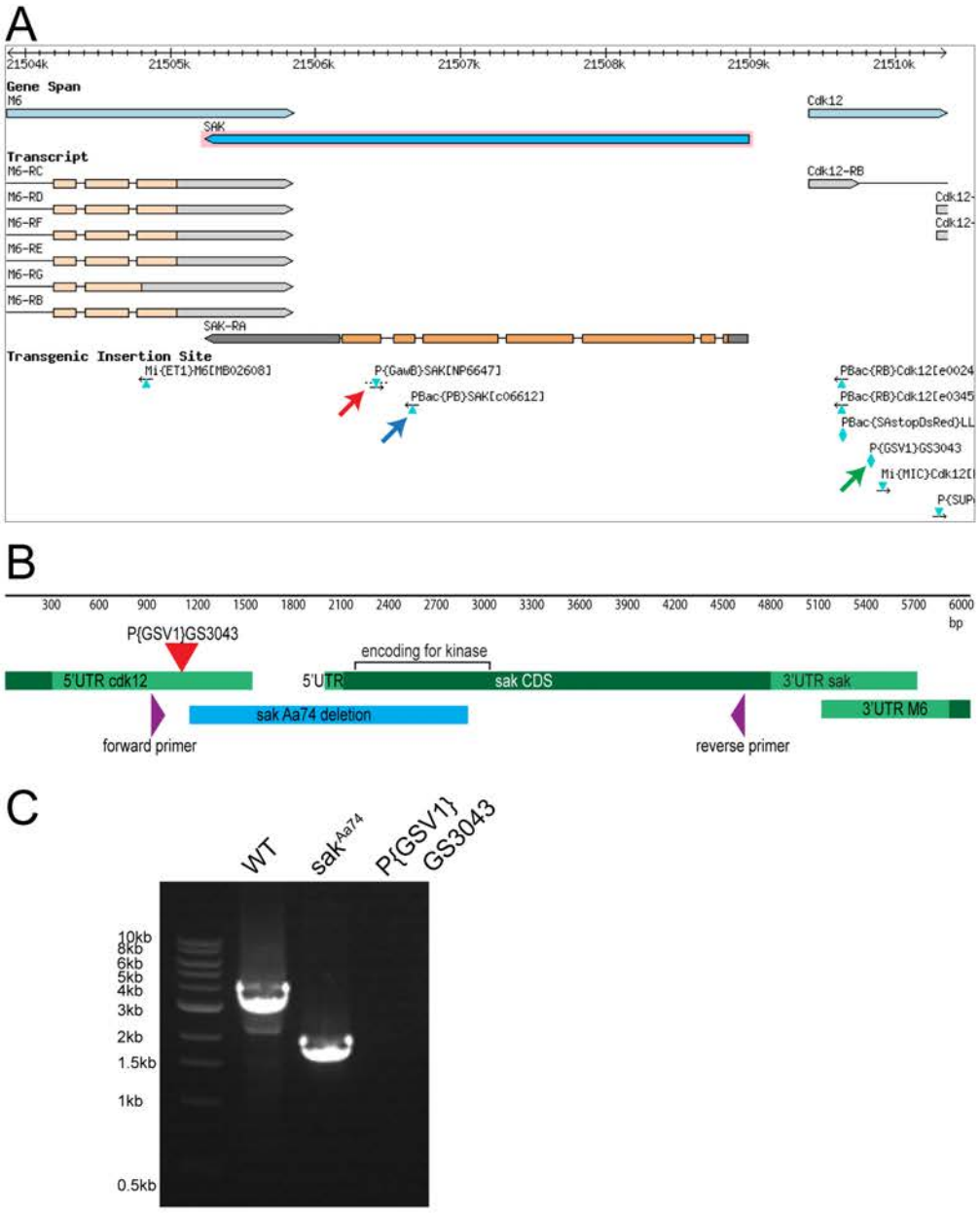

Figure 4.2: A screen for imprecise P-Element excision uncovers a deletion of the *sak* promoter and coding region. (A) Schematic of the genomic region around the *sak* gene taken from FlyBase showing the *sak* gene (light blue), its transcript (orange) and the P-element insertion sites causing the sak^{c06612} hypomorphic mutation (blue arrow), P{GawB}SAK^{NP6647} which could not be excised (red arrow), and P{GSV1GS3043} that could be used to induce a deletion (green arrow). Note that the *sak* sequence is reverse in this schematic, as compared to 4.2B. **(B)** Schematic diagram of the *sak* genome region with CDS in dark green, UTRs in light green, 1751bp deletion in sak^{Aa74} in light blue. Primers used to screen for deletions in purple, P-element that was excised in red. **(C)** PCR products observed in P-Element excision screen. Using the forward and reverse primers indicated in (B) by the purple arrows on wild type leads to a 3691bp amplicon. The resulting amplicon in sak^{Aa74} is 1940bp long. If the P{GSV1}GS3023 P-Element is not excised, the resulting sequence is too long to be amplified by PCR.

4.4 *sak*^{Aa74} mutants completely lacks centrioles and cilia in larval stages

I went on to analyse the phenotype of *sak*^{Aa74} flies. Similarly to other fly strains with mutations in core centriole duplication proteins (Basto et al., 2006; Blachon et al., 2008; Peel et al., 2007), *sak*^{Aa74} flies developed and eclosed as morphologically normal but completely uncoordinated adults, that could neither walk nor feed (Figure 4.3A). In contrast, the hypomorphic *sak*^{co6612} mutant flies were hardly uncoordinated and could feed and walk around. Expression of ubiquitin-driven GFP-Sak (Peel et al., 2007) rescued the lack of coordination of *sak*^{Aa74} flies. As discussed in section 1.2.5 uncoordinated behaviour of flies with mutations in core centriole duplication proteins originates from the lack of basal bodies and concomitant lack of cilia in their mechanosensory neurons, and I confirmed that this was the case in *sak*^{Aa74} flies (Figure 4.3B). Flies without centrioles go through larval development with near normal timing (Basto et al., 2006), so I wanted to test whether *sak*^{Aa74} flies would develop at comparable rates. I assessed the percentage of larvae pupating per day for *sak*^{Aa74} and *DSas-4* mutants and for *GFP-Sak, sak*^{Aa74} and *DSas-4-GFP, DSas-4* (Figure 4.3C). *DSas-4* mutants (as previously reported in Basto et al., 2006) and *sak*^{Aa74} mutants were both slightly delayed in pupation, and this delay was rescued by expressing *GFP-Sak* or *DSas-4GFP*, respectively, in the mutant backgrounds (Figure 4.3C).

The hypomorphic *sak*^{co6612} mutant has reduced centriole numbers, but there are still many larval brain cells with two or one centrosomes present (Bettencourt-Dias et al., 2005). In order to analyse whether *sak*^{Aa74} larval brain cells still contained centrioles I crossed the centriolar marker GFP-PACT (Martinez-Campos et al., 2004) into the *sak*^{Aa74} background to visualise centrioles. While in WT brain cells expressing GFP-

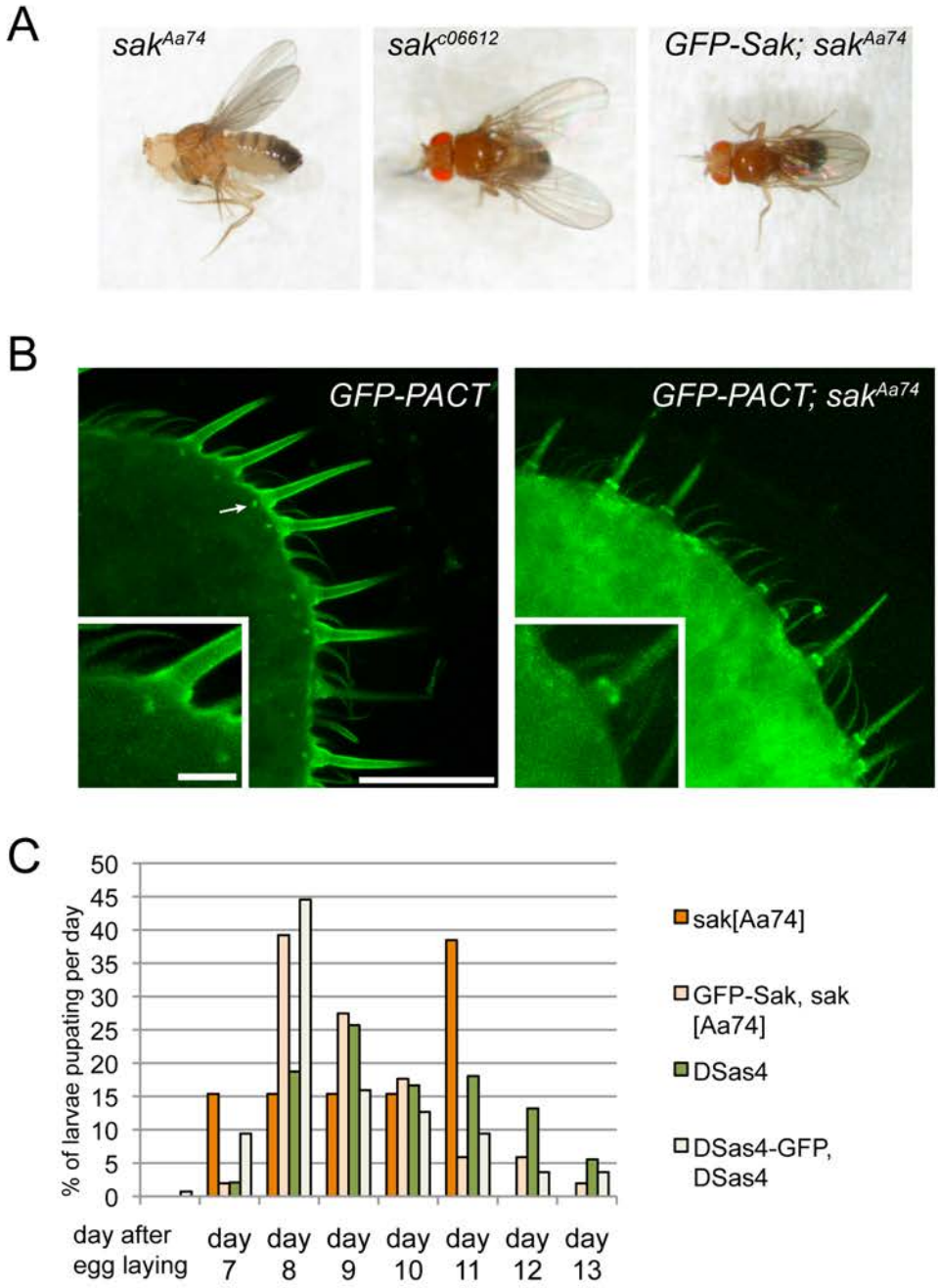

Figure 4.3: *sak*^{Aa74} homozygous flies are viable but uncoordinated as adults due to the lack of basal bodies in mechanosensory neurons. (A) Pictures of adult flies taken without anesthetising them. *Sak*^{Aa74} flies are completely uncoordinated, while the hypomorphic mutant *sak*^{c06612} can walk around. GFP-Sak expression rescues uncoordination in *sak*^{Aa74}. **(B)** WT and *sak*^{Aa74} mutant third antennal segments expressing GFP-PACT. In WT GFP-PACT signal marks the basal bodies at the base of each sensory bristle (see arrow, magnified in inset). Basal bodies are undetectable in the mutant. Scale bar is 25µm and 5µm for insets. **(C)** Development rates of *sak*^{Aa74} and *DSas-4* mutants and of *GFP-Sak, sak*^{Aa74} and *DSas-4-GFP, DSas-4* flies were analysed by counting the percentage of larvae pupating per day for each genotype (n=276 for *DSas-4-GFP, DSas-4,* 144 for *DSas-4, GFP-Sak,* 51 for *sak*^{Aa74}, 13 for *sak*^{Aa74}).

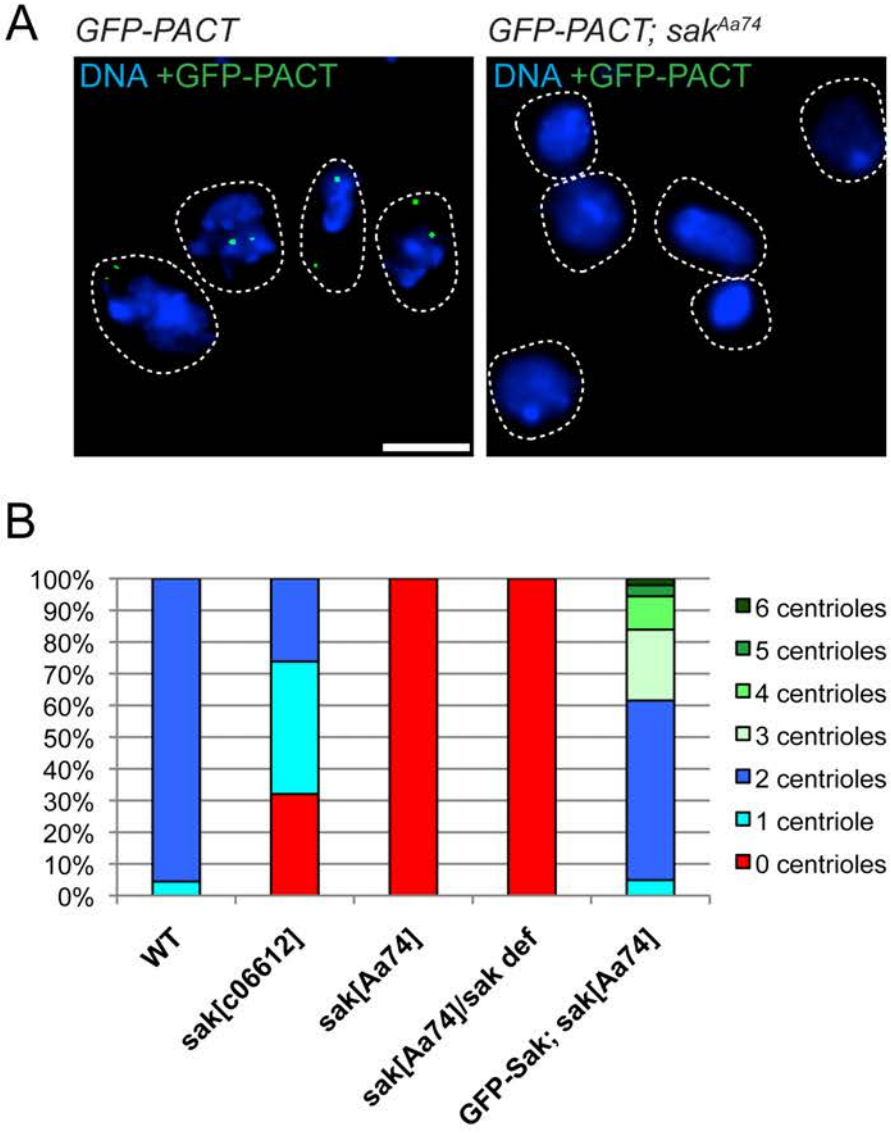

Figure 4.4: *sak*^{Aa74} mutants completely lack centrioles in third instar larval stages. **(A)** WT and *sak*^{Aa74} 3rd instar larval brains expressing GFP-PACT (green) visualising centrioles. DNA in blue. Cell outlines are indicated by the dotted line, note that *sak*^{Aa74} mutant cells lack GFP-PACT staining, indicating the lack of centrioles. **(B)** Larval brains were stained with anti-Asl and anti-Cnn and centrosomes in mitotic cells were quantified (n= 264 cells in 12 brains for WT; 237 cells in 5 brains for *sak*^{c06612}; 355 cells in 7 brains for *sak*^{Aa74}; 82 cells in 4 brains for *sak*^{Aa74}/*sak*^{deficiency}; 143 cells in 4 brains for *GFP-Sak, sak*^{Aa74}). Scale bars are 5μm.

PACT many centrioles were visible, no centrioles could be detected in sak^{Aa74} cells (Figure 4.4A). I next quantified centriole numbers in larval brains stained with anti-Asl and anti-Cnn, and could see that while 30% of sak^{co6612} cells lacked centrioles, 100% of sak^{Aa74} cells did not have any centrioles (Figure 4.4B). The sak^{Aa74} mutant crossed over the *sak* deficiency also completely lacked centrioles, indicating that sak^{Aa74} most likely is an amorph. Crossing a GFP-Sak transgene into the sak^{Aa74} mutant background lead to reappearance of centrioles, and in fact to centriole overduplication because the ubiquitin promoter leads to *Sak-GFP* overexpression. Finally, I assessed the mitotic index of sak^{Aa74} mutant brains: it was slightly elevated (1.5%) compared to WT (1%) (n=16200 cells per genotype from 8 brains), presumably due to the slightly longer time it takes to assemble acentrosomal mitotic spindles (Basto et al., 2006).

Having now established a *sak* mutant that completely lacks centrioles, we next attempted to use this as a tool to elucidate the exact step(s) Sak is responsible for in the centrosome assembly pathway.

4.5 Sak kinase plays a role in formation of the central cartwheel structure

Studying the centrosome assembly pathway in *Drosophila* is impeded by one major obstacle: in the absence of any one of the core centriole duplication proteins there are no centrioles formed at all, and hence it is not possible to analyse the molecular pathway of centriole assembly. Overexpressing the centriole duplication proteins GFP-Ana2 and GFP-Sas6 can lead to the formation of structures called SAPs (Figure 4.5A,B), that

consist of extended tubules that resemble the inner cartwheel of the centriole (Figure 4.5C) in *Drosophila* testis (Stevens et al., 2010b). These structures also form in embryos and unfertilised eggs that overexpress GFP-Ana2 and GFP-Sas6, but here they appear to be less ordered than the structures observed in testes. Unlike in testes, where the SAPs recruit several other centriole proteins (such as DSas-4 and Cep135) but do not recruit any PCM proteins, the SAPs in eggs and embryos recruit most, if not all, centriole and centrosome proteins and they organise PCM and MTs in a manner that is virtually indistinguishable from centrosomes (Catarina Vicente and Hélio Roque, unpublished data). Most importantly for my studies, SAPs can form in testes and eggs/embryos even in the absence of some of the core centriole duplication proteins, making them a powerful model to study the molecular role of centriole duplication proteins (and this has been extensively analysed by Catarina Vicente, a DPhil student in our lab).

I first wanted to assess whether the highly ordered structure of SAPs in testes was maintained in sak^{Aa74} mutants. In collaboration with Hélio Roque (who performed the Electron Tomography (ET) on testes sections) we observed that sak^{Aa74} SAPs were much more disorganised than WT SAPs (Figure 4.5D). There were many more "holes" in the internal regions of the SAPs, and there were very few well-defined cartwheel-like structures within the body of the SAPs (Figure 4.5D,E) compared to WT (Figure 4.5A,B). Thus, although GFP-DSas-6 and GFP-Ana2 appear to be able to still come together to form SAPs, they fail to assemble and/or maintain a stable cartwheel structure, indicating that Sak activity is required for cartwheel assembly – the first known step in the centriole assembly pathway.

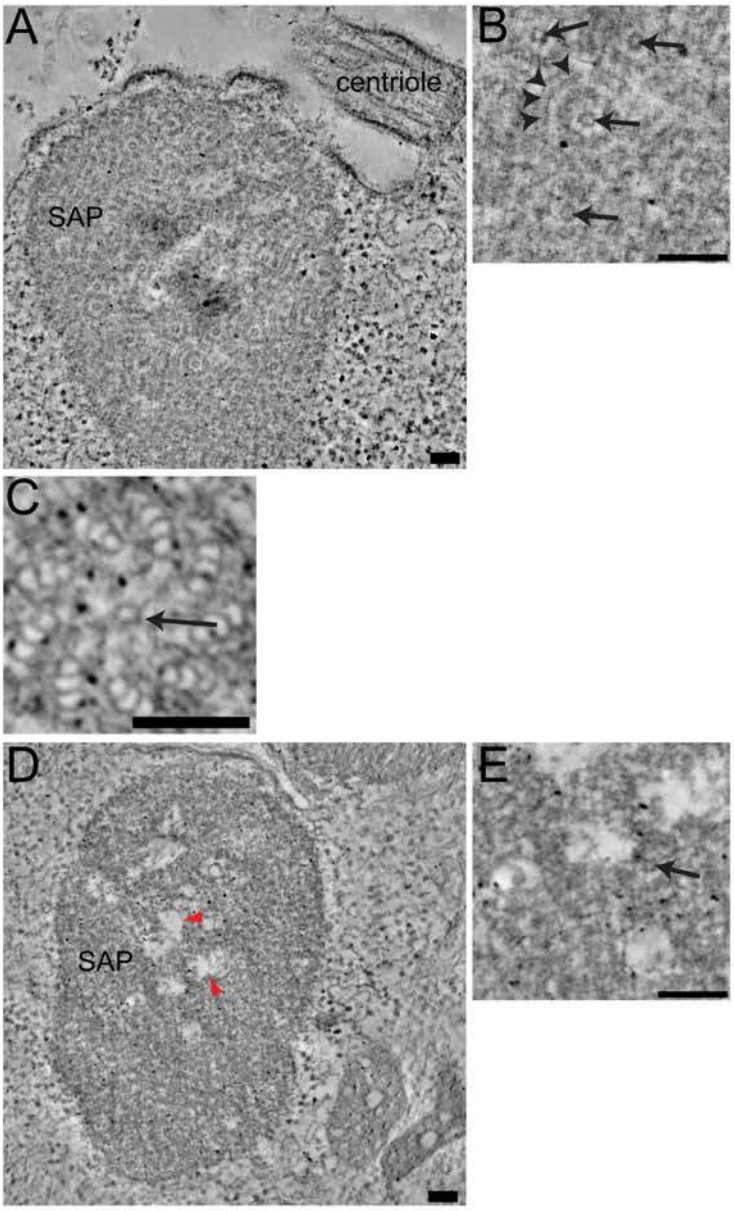

Figure 4.5: Formation of cartwheel-like structures in *sak*^{Aa74} SAPs is severely impaired. A) Low magnification and **(B)** high magnification images of a WT SAP taken from an electron tomogram (ET). Note that WT SAPs are highly structured and consist of tubes seen in cross section (arrows in B) and transverse section (arrowheads in B). **(C)** These tubes are highly reminiscent of the central cartwheel structure seen in centrioles (arrow) (image taken from Stevens et al., 2010). Low resolution **(D)** and high resolution **(E)** Images of *sak*^{Aa74}/*sak*^{deficiency} SAPs. Note that these are less structured and appear to have large holes (red arrowheads in D). There are only very few residual cartwheel-like tube structures (arrow in E) which look less well-defined than in WT SAPs. n = 6 *sak*^{Aa74}/*sak*^{deficiency} SAPs. All scale bars are 100nm. ET images have been provided by Hélio Roque.

4.6 Sak kinase is not needed for PCM recruitment

Next, I wanted to assess whether Sak is required for any later steps in the centrosome formation pathway and, in particular, whether Sak is required for efficient PCM recruitment. I therefore decided to look at the composition of SAPs in *Drosophila* eggs in the absence of Sak. SAPs in eggs are more suitable for this analysis, as they do not appear to normally form the intricate cartwheel-like structures seen in testis SAPs, and, in the WT situation, they robustly recruit PCM in a manner very similar to the way centrioles recruit PCM (Catarina Vicente, personal communication).

S*ak*^{Aa74} flies are uncoordinated, however, so they cannot mate and they cannot lay any eggs. Together with Alan Wainman, therefore I collected newly eclosed *sak*^{Aa74} mutant females and manually fed them for several days with sugar solution to keep them alive and give enough time for some of the oocytes in the females to mature to stage 14. Furthermore, the mature oocytes then needed to be chemically activated, which would normally happen during the egg laying process (Horner and Wolfner, 2008). The protocol for this *in vitro* activation of eggs (Horner and Wolfner, 2008) and subsequent fixation, antibody staining, microscopy and data analysis were performed by Catarina Vicente. The results showed that, most surprisingly, all three proteins tested (DSas-4, Asl and α-tubulin) localised to SAPs in the absence of Sak, indicating that Sak is not needed for their recruitment (Figure 4.6A). Furthermore, quantification of fluorescence levels showed that these proteins were recruited to the same levels as they were recruited in WT SAPs (Figure 4.6B). These data show that DSas-4 and Asl do not depend on Sak for their recruitment to SAPs and the presence of WT levels of α-tubulin associated with *sak*^{Aa74} SAPs suggests that PCM recruitment is not perturbed in the absence of Sak. These data strongly suggest that Sak is only essential for the very first

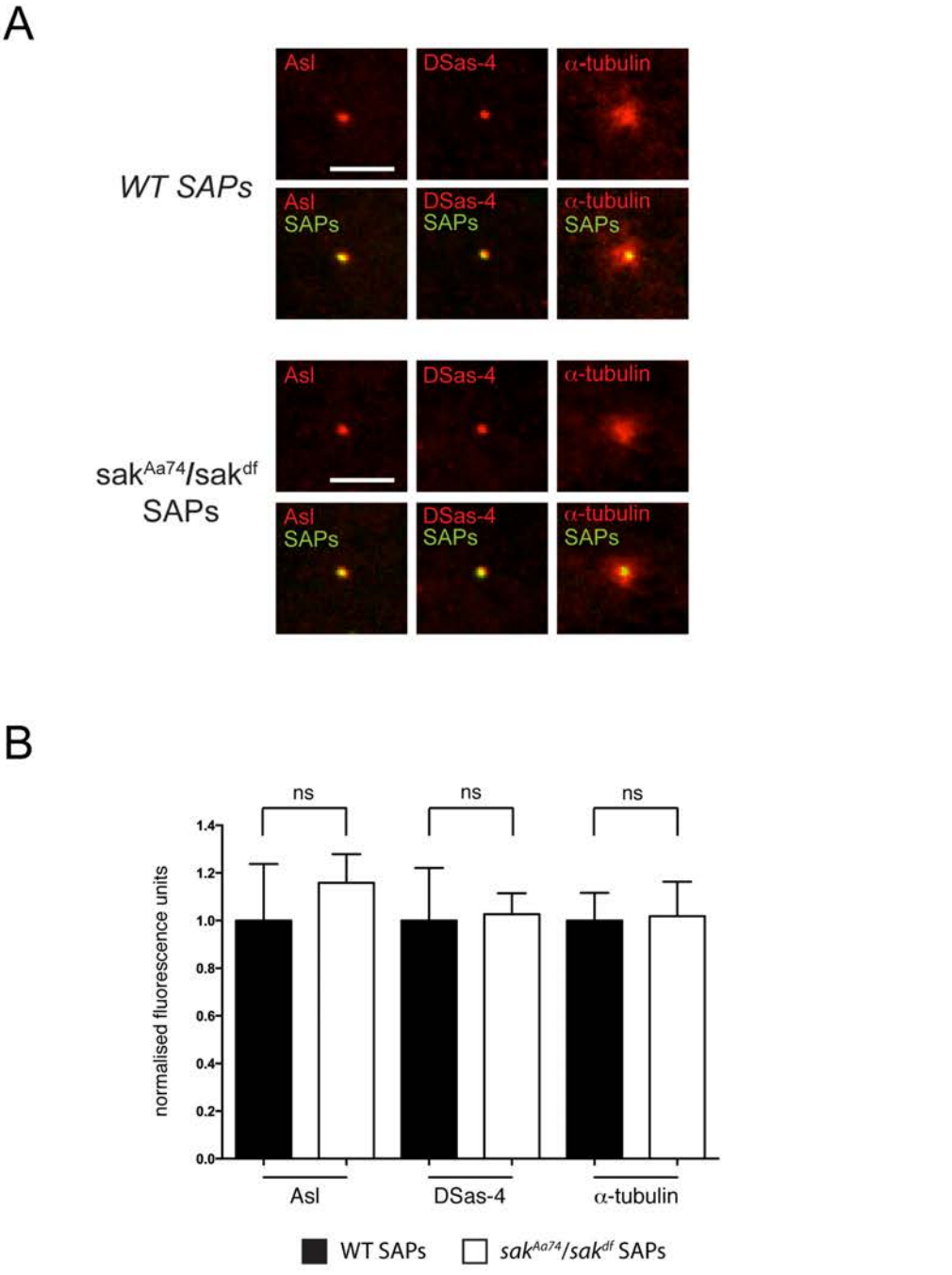

Figure 4.6: SAPs in *sak^{Aa74}* eggs can organise PCM. (A) SAPs in in vitro activated eggs expressing GFP-DSas-6 and GFP-Ana2 in the WT and *sak^{Aa74}/sak^{deficiency}* background were stained with anti-Asl, anti-DSas-4 and anti-α-tubulin. All three proteins can be recruited in the absence of Sak. Scale bar is 5μm. **(B)** The protein levels on SAPs were quantified in WT and sak^{Aa74}/sak^{deficiency} SAPs (bars represent the average of all SAPs of at least 8 different eggs, error bars showing standard error). The levels of Asl, DSas-4 and α-tubulin in *sak^{Aa74}/sak^{deficiency}* SAPs do not significantly differ from the WT levels. This figure was provided by Catarina Vicente.

step of centriole assembly - the formation of the cartwheel structure composed of Ana2 and DSas-6, and probably some additional proteins. All subsequent steps of centriole and centrosome assembly probably do not require any further Sak protein or Sak kinase activity.

4.7 Kinase dead Sak leads to centriole amplification in the presence of endogenous Sak

In mammalian cells it has been shown that overexpression of kinase dead Plk4 (Plk4-KD) can lead to amplification of centrioles in the presence of endogenous Plk4. This is caused by the ability of Plk4-KD to dimerise with endogenous Plk4, and so prevent the efficient trans-phosphorylation of the endogenous Plk4, thereby inhibiting the recognition of endogenous Plk4 by the $SCF^{betaTrCP}$ complex and its subsequent degradation by the proteasome (Guderian et al., 2010). In contrast to this observation, overexpression of kinase dead Sak (Sak-KD) in *Drosophila* embryos led to embryos lacking centrosomes, suggesting that Sak-KD was acting as a dominant-negative and inhibiting centriole duplication (Rodrigues-Martins et al., 2008). As this contradicts the data in human cells I decided to re-assess the effects of overexpressing Sak-KD in *Drosophila*.

I made a GFP-tagged Sak construct in which Lysine43 in the kinase nucleotide motif was replaced by Methionine (hereafter, GFP-Sak^{KD}), which renders the kinase domain inactive (Sillibourne et al., 2010). I tried to establish stable transgenic lines expressing GFP-Sak^{KD} under control of the ubiquitin promoter, but despite three rounds of embryo injections performed by BestGene, no transgenic line expressing the construct

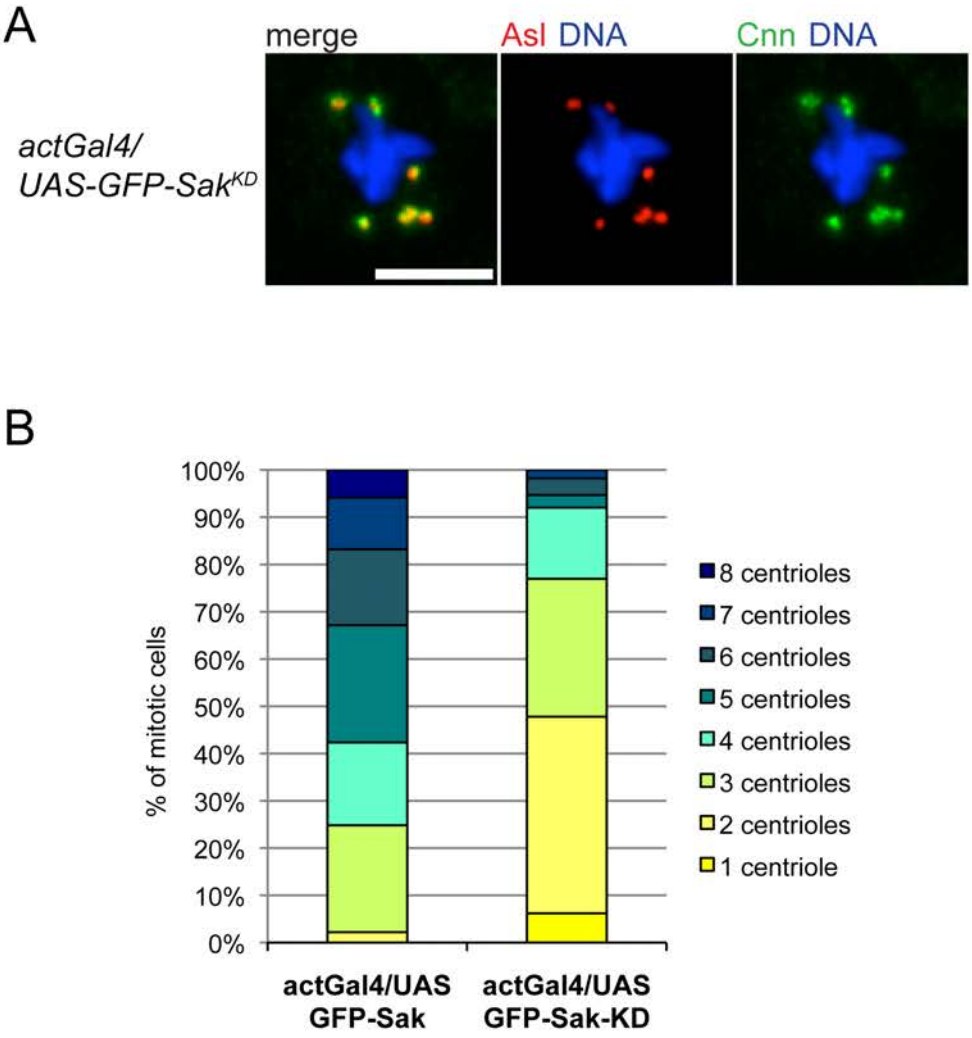

Figure 4.7: Overexpression of kinase dead GFP-Sak leads to centrosome amplification in larval brain cells. (A) Larval *Act5CGal4/UAS-GFP-Sak^{KD}* brain cell stained with anti-Asl and anti-Cnn, visualising amplified centrosomes. DNA is in blue, scale bar 5µm. **(B)** Centrioles were quantified in brains overexpressing GFP-Sak^{KD}, and GFP-Sak as control (n=141 cells from 4 brains for *actGal4/UAS-GFP-Sak*, 113 cells in 6 brains for *actGal4/UAS-GFP-Sak^{KD})*.

could be identified. Therefore I decided to use the UAS/Gal4 promoter system to try to generate stable transgenic lines that would conditionally overexpress GFP-Sak^{KD}. With this strategy I was able to generate stable transgenic lines. I then crossed these lines to Act5cGal4 lines to drive the overexpression of UAS- GFP-Sak^{KD} lines in all cells. Perhaps surprisingly, these flies were viable, and I was able to analyse centriole behaviour in larval brain cells. Interestingly, the overexpression of GFP-Sak^{KD} caused centriole amplification in many cells (Figure 4.7A).

I next quantified centriole numbers in both Sak-GFP and Sak^{KD}-GFP overexpressing cells and my data showed that while both drove centriole amplification, wild type Sak-GFP was able to drive it to a higher extent (Figure 4.7B). In order to interpret this result it will be important to assess the ability of Sak-KD to rescue the centriole duplication defect of the *sak^{Aa74}* mutant and so to see whether it can support centriole duplication and promote overduplication on its own. I suspect that Sak-KD will not be able to function in centriole duplication, and I am currently crossing UAS-Sak^{KD}-GFP into the *sak^{Aa74}* mutant background to enable me to perform this experiment.

4.8 Discussion

I here describe how I have generated a new *sak* mutant allele by imprecise P-Element excision. This new allele appears to be much stronger than the previously existing allele as, like all other strong centriole duplication mutants (Basto et al., 2006; Blachon et al., 2008; Peel et al., 2007), these *sak* mutant flies are strongly uncoordinated and they appear to completely lack centrioles in their larval brain cells and cilia in their sensory neurons. Unfortunately it is not possible to test by western blot analysis whether *sak^{Aa74}* is a true null mutation, or whether a part of the Sak protein is still being produced, as

we, and others, have been unable to detect endogenous Sak protein by western blotting. I think this is unlikely, however, as both the promoter and first third of the *sak* gene are deleted. Thus, sak^{Aa74} is at least a strong hypomorph, and probably a null mutant. Sak^{Aa74} and $sak^{Aa74}/sak^{deficiency}$ both completely lack centrioles in third instar larval brains, further indicating that sak^{Aa74} presumably is an amorph.

Working together with others in the laboratory, I used the sak^{Aa74} mutation in combination with SAPs (as a proxy for centrosomes) to try to pinpoint the exact step(s) in the centrosome assembly pathway where Sak is required. Our data reveal, that in the absence of Sak, overexpression of GFP-Ana2 and GFP-DSas-6 still leads to formation of large complexes, but these are much less well-organised and contain many fewer of the extended tubules that resemble the central cartwheel structure in WT SAPs. This indicates that Sak is likely required to lock Ana2 and DSas-6 into a stable cartwheel structure. Furthermore, my localisation of Sak by super-resolution microscopy supports its involvement in cartwheel formation, as I found GFP-Sak was localised to the base of the cartwheel and also to the sides of mother and daughter centrioles, the sites where a new procentriole would presumably assemble.

Most interestingly, analysis of the composition of SAPs in sak^{Aa74} embryos showed that recruitment of downstream centrosomal proteins and MT nucleation ability were not affected, strongly suggesting that Sak is only required for cartwheel assembly but not for PCM recruitment. As described above, these experiments are technically challenging, as one has to keep the Sak mutant females alive by manual feeding long enough for them to develop mature stage 14 oocytes, and then one has to activate these oocytes *in vitro* to drive the formation of SAPs, a process that is not very efficient (Catarina Vicente, personal communication). For this reason, only a relatively small

number of markers were tested, and the experiment has only been performed one time (although the result was very clear cut). Thus, it will be necessary to repeat this experiment and to look at the behaviour of more centriole and PCM proteins to better understand what is happening to the SAPs in the absence of Sak. Nevertheless, it is striking that morphologically normal SAPs that recruit normal amounts of centriole (Asl) and PCM (Cnn) proteins and organise normal amounts of MTs can be formed in the absence of Sak.

I have shown that in close accordance with experiments in human cells overexpression of kinase dead Sak can lead to centrosome amplification. This might be caused by the ability of Sak^{KD}-GFP to dimerise with endogenous Sak, which leads to its stabilisation through its inability to transphosphorylate the WT-Sak in the phosphodegron motif (Guderian et al., 2010). It has recently been shown in *C. elegans* that the Sak homologue Zyg1 recruits Sas-6 to the centriole by directly binding to it, and subsequently catalyses the assembly of a cartwheel structure by phosphorylating a target other than Sas-6 (Lettman et al., 2013). Similarly, in *Drosophila*, it has been shown that Sak recruits Ana2 and DSas-6 to the centriole (Stevens et al., 2010b). It would be interesting to address whether this process is also independent of the kinase function of Sak by using the GFP-Sak^{KD} construct I have described here.

The next step in the analysis of the molecular function of Sak in centriole duplication would be the identification of its target protein. Importantly, this experiment can now be addressed in *Drosophila* using the sak^{Aa74} mutant I have made. For example, it might be possible to immunoprecipitate SAPs from sak^{Aa74} mutants to yield samples enriched for centrosomal proteins, and then use a phosphoproteomic approach with specific candidate proteins, as I described for my analysis of Asl and DSpd-2 in Chapter 3.

5 A global transcriptional analysis of cells without centrosomes and with too many centrosomes

5.1 Introduction

As discussed in Section 1.1.2, centrosomes have important functions in many cell processes such as mitotic spindle assembly, cell polarity, and the positioning of organelles within the cell (Bettencourt-Dias and Glover, 2007; Doxsey et al., 2005; Nigg and Raff, 2009). In addition, centrosomes are thought to act as "coordination centres" within the cell where many proteins come together at high concentrations. Many cell cycle regulators and checkpoint proteins, for example, are concentrated at centrosomes, and Cdk1/Cyclin B is first activated at centrosomes during the entry into mitosis (Jackman et al., 2003) while Cyclin B is first destroyed at centrosomes during the exit from mitosis in fly embryos (Wakefield et al., 2000). There is also evidence that the localisation of Cdk2/Cyclin E to centrosomes is required for the proper initiation of S-Phase (Ferguson and Maller, 2010).

Several studies have addressed how centrosome loss affects cells. Early studies showed that microsurgical removal of centrosomes from monkey kidney cells could lead to cell cycle arrest prior to S-Phase entry (Hinchcliffe, 2001; Maniotis and Schliwa, 1991). This result could be repeated in human cells, where depletion of several centrosomal proteins lead to a p38-, p53- and p21-dependent cell cycle arrest in G1 (Mikule et al., 2007; Srsen, 2006). It was later shown, however, that microsurgical removal of centrosomes does not affect cell cycle progression by itself (Uetake et al., 2007). Interestingly, the authors showed that acentrosomal cells were more sensitive to exposure to blue light (which is used to excite GFP when imaging these cells). They

suggested, that centrosome loss was perceived as a stress which induces some p38 activation, but only when in combination with other stresses (such as blue light exposure) are the levels of the stress-sensor kinase p38 sufficiently high to cause a cell cycle arrest (Uetake et al., 2007). Given that these studies have shown that the loss of centrosomes or loss of their structural integrity can lead to a cellular stress response, it was very surprising when it was shown that flies that lose their centrioles after embryonic stages can proceed to develop to adulthood at near-normal rates (Basto et al., 2006) These flies, which are mutant for the centriole core duplication factor *DSas-4*, divide their cells by forming acentrosomal mitotic spindles. They eclose as morphologically normal adults, but after eclosion they are uncoordinated (unc) due to the lack of cilia in their sensory neurons, and die because the lack of mechano- and chemo-sensation means they cannot walk or feed.

Similarly, two years later, our lab showed that flies that have amplified centrosomes in most of their cells can also divide their cells in a bipolar fashion and develop to adulthood without major impairments, and can even be kept as viable and fertile stocks (Basto et al., 2008). These flies express a GFP-Sak fusion protein under the control of the Ubiquitin promoter, leading to overexpression of the centriole duplication factor Sak in all cells (these flies will be called *SakOE* in the following). The only defects that were found in these fly lines lacking centrosomes or having too many centrosomes, were a slowing down of somatic cell divisions (as it took cells longer to assemble a bipolar spindle), a small increase in chromosome segregation errors, and perturbations in the asymmetric divisions of larval neural stem/progenitor cells (neuroblasts). Interestingly, the failures in neuroblast asymmetric divisions (9% of *SakOE* neuroblasts and 15% of *DSas-4* neuroblasts ultimately divided symmetrically) are linked to a malignant overgrowth of brain tissue in abdominal transplantation assays (Basto et al.,

2008; Castellanos et al., 2008). This predisposition to tumourigenesis in cells lacking centrosomes or having too many centrosomes is thought to be explained by the inability of the mitotic spindle to correctly align to the neuroblast polarity axis, leading to the misdistribution of cell fate determinants. This results in production of two stem cells rather than a stem cell and a ganglion mother cell, and therefore could lead to overgrowth of the respective brain tissue (Castellanos et al., 2008; Gonzalez, 2007). It is, however, still not completely understood how the overgrowing stem cells can develop malignant traits. It is possible that the small increase in chromosome missegregation and the resulting aneuploidy could also be factors that promote formation of malignant tumours in these tissues, but this remains to be further investigated.

Following the demonstration that flies can proceed through the majority of their development without centrioles, the point was raised that although these flies appear to progress through development relatively normally, this alone would not suffice to prove "the dispensability of a cell function" (Gonzalez, 2008). Although these flies survive, perhaps they only do so because they up-regulate compensatory pathways and/or stress responses. The observation that brain cells without centrosomes are predisposed to form tumours (at least in abdominal transplantation assays) (Castellanos et al., 2008) would indeed argue that these cells are not completely normal. Similarly, it is also surprising that having too many centrosomes in cells appears to be relatively well tolerated by flies, given that such centrosome amplification is strongly associated with human cancer, and also leads to tissue overgrowth and tumour formation (at least in an abdominal transplantation assay) in flies (Basto et al., 2008).

When I started my D.Phil., I decided to investigate how the loss of centrosomes or centrosome amplification affects *Drosophila* cell physiology *in vivo*, in particular asking whether these two cellular states induce either a stress response or an up-regulation of some compensatory pathway(s). There are several possible readouts to assess cell physiology. For example, it would be possible to assess differences in protein abundance by using two-dimensional fluorescence difference gel electrophoresis, by using a mass spectrometric approach, or by using protein microarrays. Although these techniques can be sensitive, they can be difficult and expensive to perform and it can be difficult to detect changes in the levels of proteins with low abundance. Therefore I decided to do a genome-wide transcriptional profiling screen. I reasoned that any cell defects induced by centrosome loss or amplification would likely induce physiological changes, and at least some of these would be detectable as transcriptional changes.

Here, I describe my global transcriptional analysis of flies developing without centrosomes or with too many centrosomes in the majority of their cells. Surprisingly, I have found that these centrosome defects lead to very few changes in the global transcriptome, strongly suggesting that centrosome loss or amplification *per se* does not dramatically perturb *Drosophila* cell physiology *in vivo.*

5.2 Strategy for comparing the global transcriptome of cells that lack centrosomes or have amplified centrosomes

To assess the transcriptome of cells lacking centrosomes I used two different *Drosophila* mutant strains, *DSas-4* and *DSas-6*, which lack centrosomes in >95% of their cells during 3rd instar larval stages (Basto et al., 2006; Peel et al., 2007; Rodrigues-

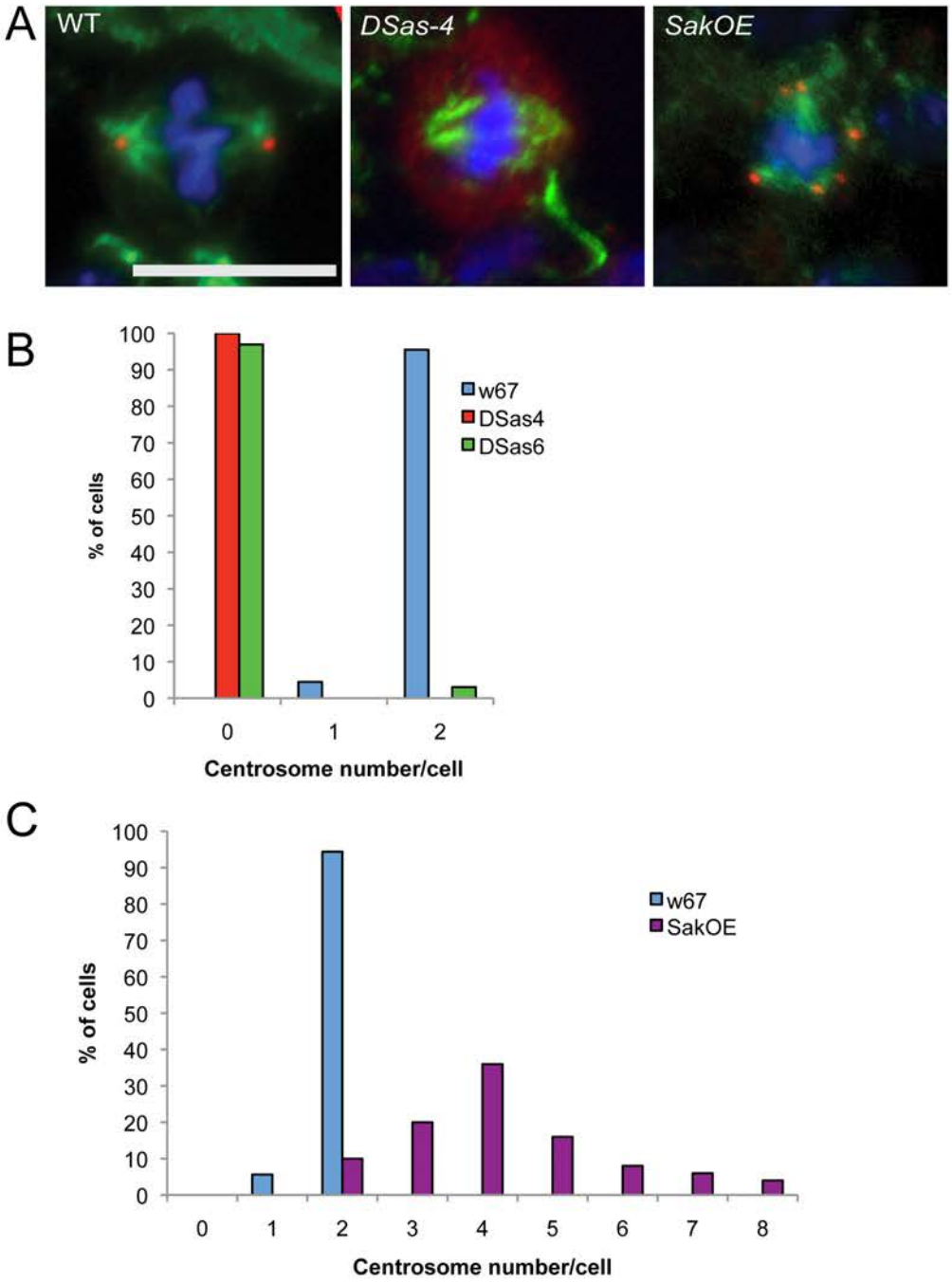

Figure 5.1: *DSas-4* and *DSas-6* mutants lack centrosomes in nearly all cells and *SakOE* cells have amplified centrosomes. (A) 3rd instar larval brains are stained with anti-Asl (red) and anti-α-tubulin (green). DNA is in blue. Wild type cells have two centrosomes at the spindle poles in metaphase, *DSas-4* mutant cells do not have centrosomes. *SakOE* cells have amplified centrosomes, which can lead to multipolar spindle formation in prometaphase. Scale bar is 5μm. **(B)** Larval brains were stained with antibodies against Asl and Cnn, and centrosomes were quantified in cells (n=295 cells in 12 brains for *DSas-6*; n=381 cells in 10 brains for *DSas-4*; n=246 cells in 12 brains for w67). **(C)** Centrosomes were quantified in *SakOE* brains as described in (B) (n=50 cells in 4 brains; n=89 cells in 6 brains for *w67*).

Martins et al., 2007b) (Figure 5.1A,B). A strain over-expressing GFP-Sak (*SakOE)* has amplified centrosomes in ~70% of its cells (Basto et al., 2008) (Figure 5.1A,C). I compared these strains to two different wild type control strains – *white*^{67} *(w67,* a wild type line carrying a point mutation in the *white* gene*)* and the commonly used Wild Type (WT) strain *OregonR (OrR)*.

In initial pilot experiments I realised quickly that different *Drosophila* strains have a lot of inherent differences in gene expression, presumably due to their being inbred and kept apart in the lab for years or even decades. Therefore I needed to make the strains genetically as similarly as possible to the control strain in order to minimise variations between strains that are not due to the differences in centrosome numbers. I decided to backcross all test strains to my control strain w^{67} for several generations. After each backcrossing step I selected flies carrying the *Pw+* marker associated with the P-element insertions causing the *DSas-4* and *DSas-6* mutations or the *SakOE* transgenic insertion (Figure 5.2A). The w^{67} control stock was initially isogenised prior to the backcrossing, so that all flies in this stock contained a nearly identical set of chromosomes. I also backcrossed the *OrR* wild type strain and a strain with a TM6 balancer chromosome to w^{67}. In these crosses I selected flies with the endogenous *w+* allele or the *tubby* marker of the TM6 chromosome after each generation, respectively. All strains were backcrossed to w^{67} for at least 5 generations, before they were crossed to the isogenised TM6 balancer chromosome, and the established stock was then directly used for microarray sample preparation. This enabled us to compare tissues from different genetic backgrounds, which were largely isogenic with the w^{67} control strain, apart from a small region around the insertion causing the mutations or *sak* overexpression (Figure 5.2B).

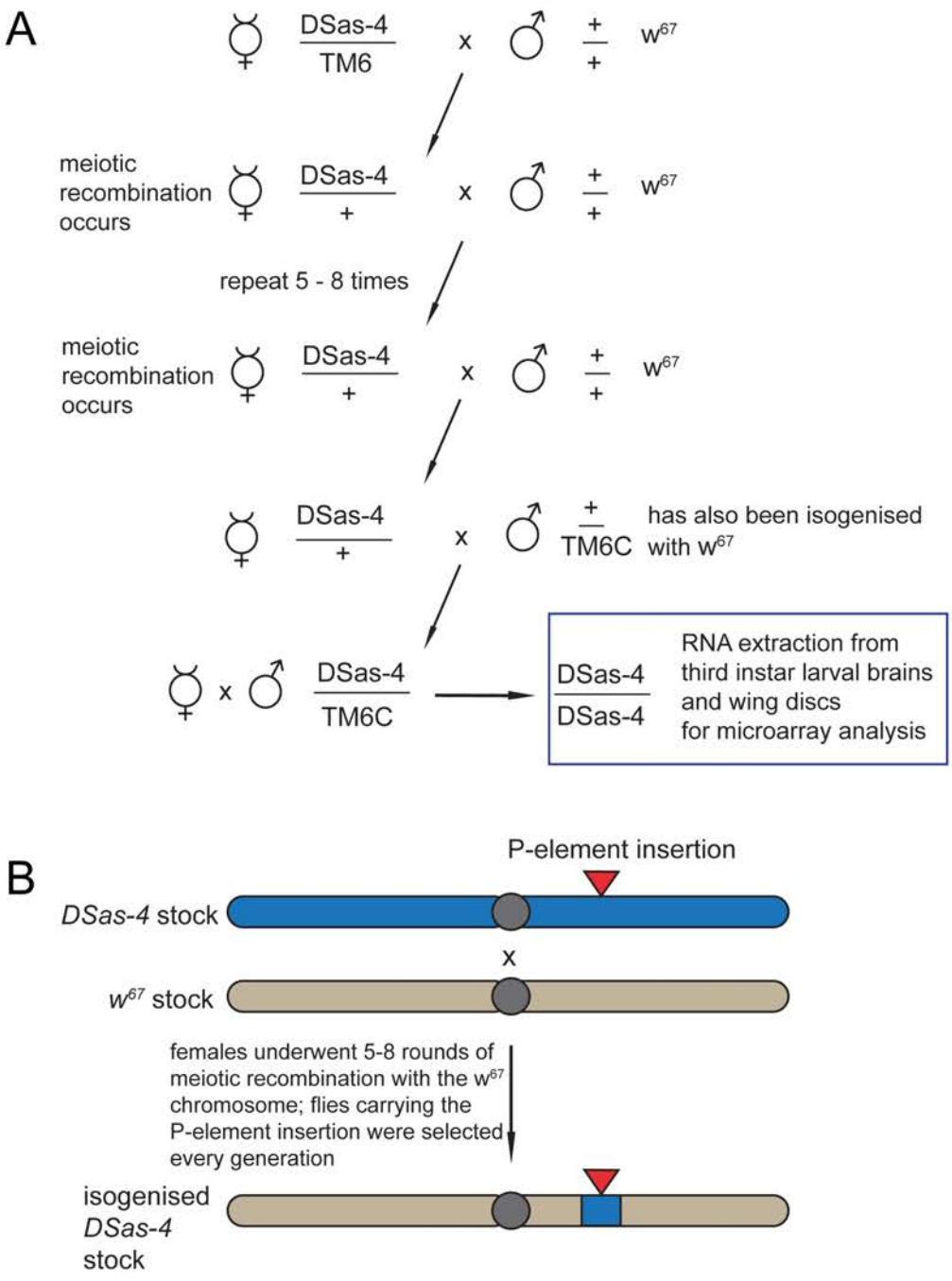

Figure 5.2: Backcrossing scheme to isogenise strains with the wild type control strains. (A) All strains were crossed to w^{67} for 5-8 generations to allow for meiotic recombination, and the stock subsequently set up by crossing to a TM6 balancer chromosome was immediately used for microarray sample preparation. **(B)** The chromosome carrying the mutation in the form of a P-Element insertion into the gene when crossed to wild type underwent recombination with the wild type chromosome during each backcrossing step. After each cross the chromosome carrying the P-Element was selected by scoring for the P*w*+ marker of the P-element. After several generations, we expect to obtain a chromosome largely isogenised with the wild type chromosome, apart from maybe a small region just around the P-element insertion.

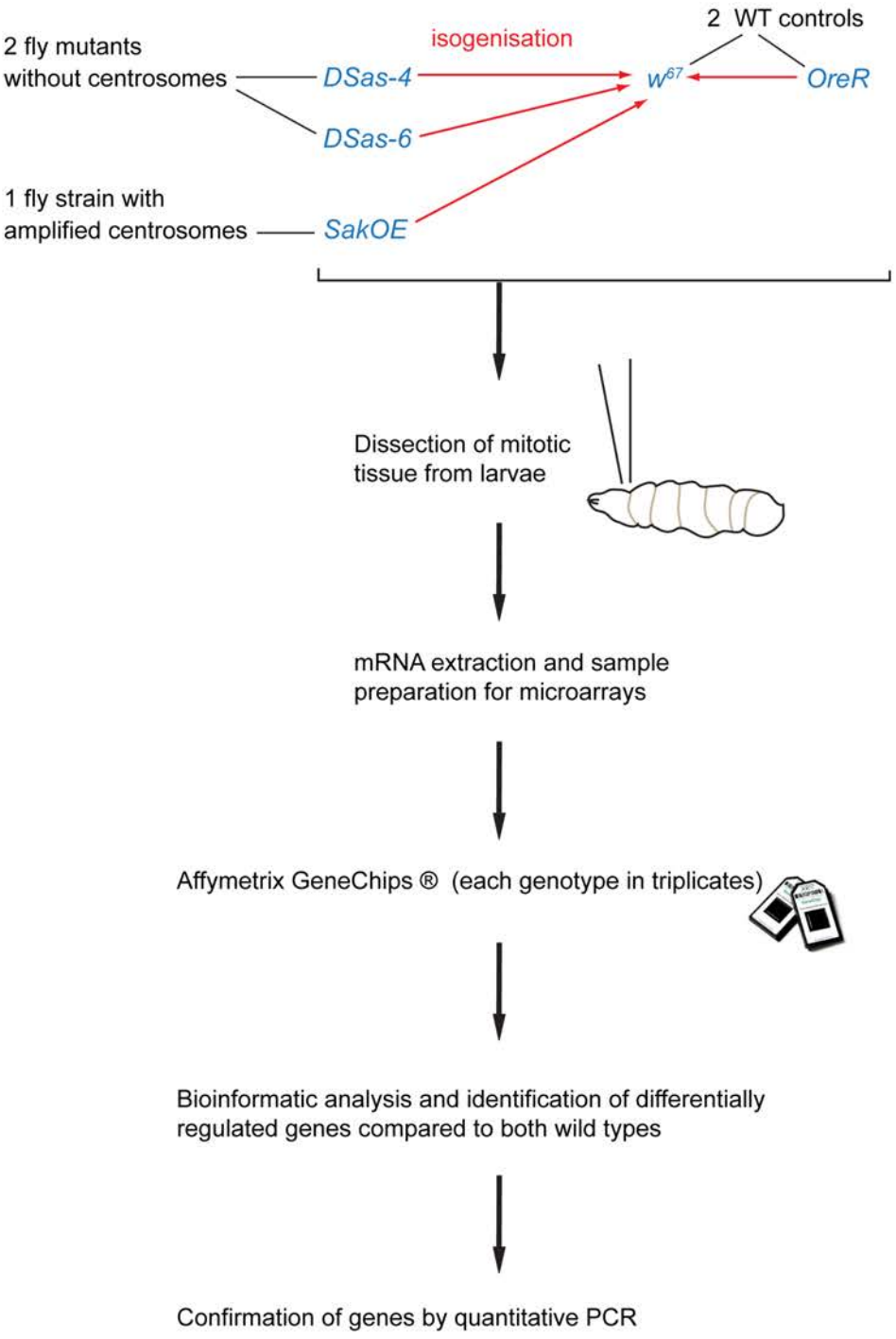

Figure 5.3: Workflow - Transcriptional profiling of cells without centrosomes and cells with too many centrosomes. For a detailed description of the workflow see text (Section 5.2).

I decided to use 3rd instar larval imaginal discs and brains for the transcriptional profiling for two reasons: first, these tissues can be easily isolated from tightly staged wandering 3rd instar larvae; second, brains and imaginal discs are morphologically complex tissues that are highly polarised and mitotically active, so these tissues would be expected to be sensitive to centrosome defects. For each genotype I dissected brains and discs from 3 independent batches of ten 3rd instar larvae. I prepared total RNA from each batch, and performed genome-wide expression profiling using *Drosophila* 2.0 GeneChips (Affymetrix). I did the sample preparation and microarry analysis under supervision of my collaborator Dr. Mitchell Levesque in his lab at the Max Planck Institute for Developmental Biology in Tübingen. With his advice I also performed the bioinformatical data analysis. I obtained lists of differentially expressed genes between the mutants and the wild type strains that were at least 1.5 fold differentially expressed and had adjusted P-values corrected for multiple hypothesis testing of ≤ 0.05.

As an internal control I first compared the w^{67} strain to the WT *OregonR* strain. The w^{67} mutation was isolated by Lefevre (Lefevre et al., 1966) in a WT Canton-S background which was collected in Canton, Ohio by C. Bridges in the 1920s, while the *OregonR* stock was collected by D.E. Lancefield in about 1925 near Roseburg, Oregon. The two wild type strains are therefore from different geographical origins and have been inbred in laboratories around the world for many decades. If my isogenisation protocol has worked and eliminated any variation in gene expression due to inherent strain differences, we would not expect any differences between the two wild type strains. Encouragingly, I did not find any significant changes in gene expression levels between these two strains. I then went on and compared the mutant strains to both wild type controls, and attempted to confirm the most highly up- and down- regulated genes by quantitative PCR (qPCR). Figure 5.3 shows a summary of the workflow.

5.3 The global transcriptome appears unaltered in *DSas-6* mutant tissue

I first compared the gene expression of *DSas-6* mutants to w^{67}. Only two genes were significantly changed in *DSas-6* mutants: *DSas-6* itself, which was down-regulated by ~16x (FDR-adjusted P-Value 0.005), and *CG8245,* which was ~10x up-regulated (FDR-adjusted P-Value 0.004). When comparing gene expression of *DSas-6* mutants to *OrR* wild type, I found *DSas-6* consistently down-regulated by ~16x (FDR-adjusted P-Value 0.001), while *CG32795* was up-regulated by ~2x (FDR-adjusted P-Value 0.05) (Figure 5.4A). I performed qPCR to test these results. Down-regulation of *DSas-6* could be confirmed (Figure 5.4B). Interestingly, the qPCR confirmed that *CG8245* expression levels were higher in *DSas-6* mutants when compared to w^{67} (~40x), but not when compared to *OrR* - where levels approximately equalled the levels in *DSas-6* mutants, thus explaining why this gene was not identified in the comparison between these two strains (Figure 5.4C). The qPCR also confirmed that *CG32795* was slightly up-regulated in *DSas-6* mutants compared to *OrR*, but not when compared to w^{67} (Figure 5.4D). The qPCR data therefore strongly support the microarray data, but reveal that the differential expression of these two genes is unlikely due to the differences in centrosome numbers, as the levels of *CG8245* and *CG32795* are also different between the two control strains.

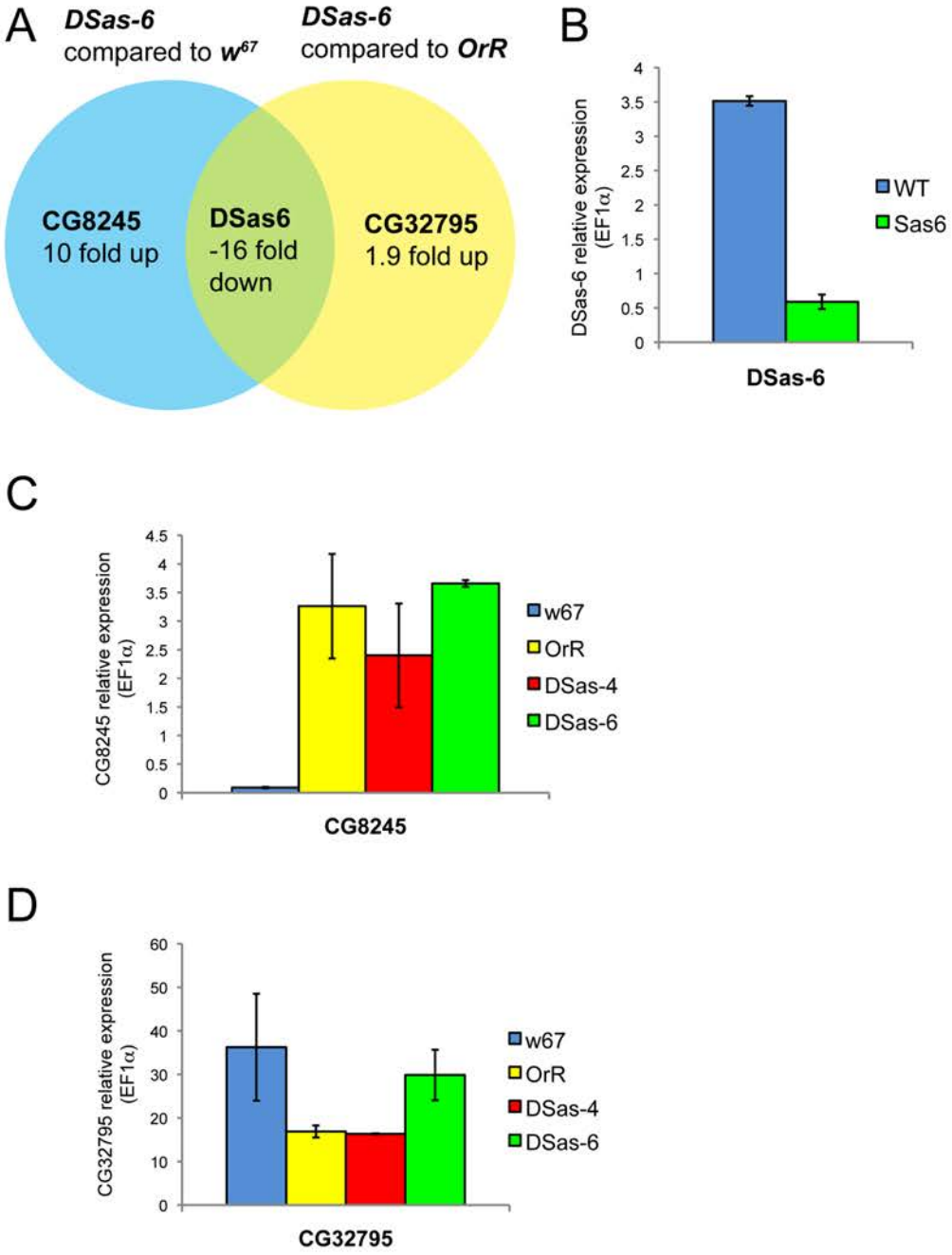

Figure 5.4: Gene expression in *DSas-6* cells. (A) Venn diagram showing significantly changed genes in *DSas-6* cells (third instar larval brains and wing discs) compared to w^{67} and *OregonR* wild type controls found in microarray analysis (≥1.5-fold, FDR-adj.P-value ≤0.05). **(B–D)** Confirmation of up- or down-regulation of these genes by qPCR was performed using mRNA isolated from third instar larval brains and wing discs (n=2 independent samples). **(B)** Confirmation of *DSas-6* downregulation. **(C)** mRNA levels of *CG8245* in w^{67}, *OregonR, DSas-4* and *DSas-6* cells. **(D)** mRNA levels of *CG32795* in w^{67}, *OregonR, DSas-4 and DSas- 6* cells.

I went back to my microarray data and saw that the differential expression of these two genes between the two control strains was picked up in the microarray comparison as well – but it did not score as statistically significant (data not shown). The qPCR data suggest that the microarray analysis provides a reliable comparison of the transcriptomes of the different strains. Remarkably, therefore, I conclude that there are few, if any, significant changes in the transcriptome of *DSas-6* mutant brains and imaginal disc cells when compared to controls.

5.4 A small number of genomic regions are aberrantly expressed in *DSas-4* mutant tissues

Next, I compared the transcriptome of the other mutant lacking centrosomes, *DSas-4,* to w^{67}. 19 genes were up-regulated and 8 genes down-regulated (Supplementary Table 3). I also compared *DSas-4* to the other wild type control, and found 15 genes to be up-regulated and 7 genes down-regulated compared to *OrR* (Supplementary Table 4). When assessing the overlap between these two comparisons, I identified 14 genes that showed altered transcript levels when compared to both WT controls, one of which is the gene *DSas-4* itself (Table 5.1, Figure 5.5A). The 14 genes did not cluster into any obvious functionally related groups, and it appeared unlikely that they were differentially regulated due to the lack of centrosomes – as these genes were not identified in my *DSas-6* analysis. Moreover, I noticed that some of the genes were located quite close to each other in the genome. The two most highly upregulated genes, *Hsc70-2* and *CG31157*, for example, are located directly adjacent to each other (Figure 5.5B). I performed qPCR on the 4 most up-regulated (*Hsc70-2, CG31157, CG31287* and *CG9279)* and the 2 most down-regulated genes (*DSas-4* and *wallenda*) to confirm

Table 5.1. *Genes significantly up or down-regulated in DSas4 mutant cells compared to both WT controls (≥1.5-fold, adj.P-value ≤ 0.05).*

Gene	Map	Fold Change[1]	Function[2]
Hsc70-2	87D10-87D10	141.10	protein folding, response to heat
CG31157	87D10-87D10	23.52	unknown
CG31287	89B7-89B7	16.92	protein folding
CG9279	76B6-76B6	8.81	microtubule-based movement
miple	61B3-61B3	4.56	unknown
Ugt86Di	86D5-86D5	3.45	metabolic process
GstD3	87B8-87B8	2.25	unknown
lig3	87B9-87B9	2.08	DNA ligation, DNA replication, DNA recombination
Rbp4	86C6-86C6	1.88	mRNA processing
CG3634	77E8-77E8	1.61	unknown
TFIIFbeta	86C6-86C6	-2.07	transcription from RNA polymerase II promoter
MED7	86C5-86C5	-2.13	transcription from RNA polymerase II promoter
wnd	76B9-76B9	-2.34	protein phosphorylation
DSas-4	84C6-84C7	-6.82	centriole duplication

[1]Fold change compared to *w67* is given
[2]GO Term for Biological Function

Table 5.2. *Genes that are differentially regulated in both DSas-4 and DSas-6 among the 100 most significant genes in each genotype.*

Gene	***CG11357***	***pathetic***	***CG32541***	***CG13822***
Fold Change *DSas-4*	8.71 ↑ (0.02[a])	6.99 ↑ (0.024[a])	-1.26 (0.055[a])	9.58 (0.065[a])
Fold Change *DSas-6*	5.31 ↑ (0.45[a])	5.31 ↑ (0.55[a])	-1.40 (1[a])	-1.18 (0.51[a])
***DSas-4* 3' qPCR**	8.5 fold ↑	no change	n.d.	n.d.
***DSas-4* 5' qPCR**	no change	no change	n.d.	n.d.
***DSas-6* 3' qPCR**	4 fold ↑	2.6 fold ↑	n.d.	n.d.
***DSas-6* 5' qPCR**	no change	no change	n.d.	n.d.

[a] (adjusted p-value)

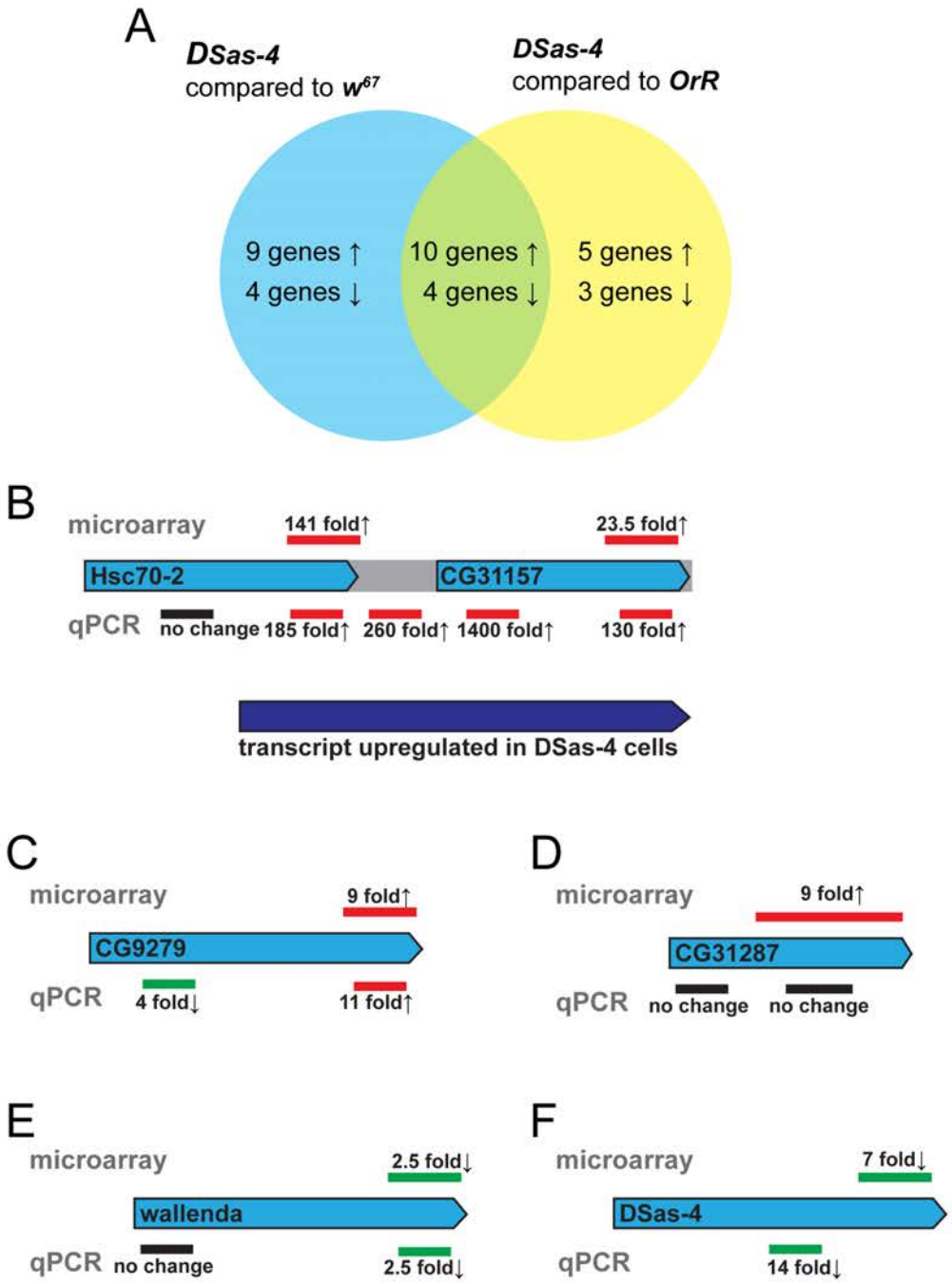

Figure 5.5: Gene expression in *DSas-4* cells. (A) Venn diagram showing significant genes in *DSas-4* cells (third instar larval brains and wing discs) compared to w^{67} and *OregonR* WT controls found in microarray analysis (≥1.5-fold, FDR-adj.P-value ≤ 0.05). **(B–F)** Validation of up- and down-regulation by qPCR. Fold change found in microarray analysis is shown above, and fold change found by qPCR analysis is given below the blue bar indicating the transcript. Red (up- regulation), green (down-regulation) and black (no change) bars indicate the position where microarray probes and qPCR primers bind to the transcript. **(B)** An unannotated transcript (dark blue), spanning the 3' end of *Hsc70-2*, the gene *CG31157* and the genomic region between the two genes, appears to be up-regulated in *DSas-4* cells.

the microarray results. For the qPCR experiments I designed two sets of primers for each gene – one that would amplify the region, in which the microarray probes bind (which are usually designed to bind to the 3' region of genes) and one that would amplify a different region of the gene. As mentioned above, the two most up-regulated genes are lying adjacent to each other and are transcribed in the same direction. The qPCR analysis showed, that the 5' region of *Hsc70-2* was not up-regulated (Figure 5.5B). The 3' region, which is the region to which the microarray probes bind, was however, up-regulated by ~185x. Both the 3' and the 5' end of *CG31157* were over-expressed by 1400x and by 130x, respectively. I designed primers that would amplify the intergenic region between the two genes, and found that this region was also over-expressed in *DSas-4* mutants by ~260x. These results indicate that an unannotated transcript which spans at least the 3' end of *Hsc70-2*, the 5' and 3' region of *CG31157* as well as the small intergenic region between the two genes is overexpressed in *DSas-4* mutants (Figure 5.5B).

Similarly, for the genes *CG9279* (Figure 5.5C) and *wallenda* (Figure 5.5E), my qPCR analysis confirmed that the 3' regions of the genes were mis-regulated as the microarray suggested, but that the 5' regions of each gene were not. For *CG31287* I could not detect any alteration in transcription levels by qPCR for either the 3' or 5' regions, suggesting that this was a false positive in the microarray analysis (Figure 5.5D). Downregulation of *DSas-4* mRNA in the *DSas-4* mutant could be confirmed by qPCR (Figure 5.5F).

Taken together, my results show that a small number of genomic regions are mis-expressed in *DSas-4* mutants. Interestingly, some of this mis-expression is due to the production of unusual transcripts that are not normally detected in WT cells. Although

the reason for this is unclear, these transcripts are unlikely to be mis-regulated due to the lack of centrosomes, as they were not mis-regulated in *DSas-6* mutant cells.

5.5 No genes appear to be consistently mis-expressed in *DSas-6* and *DSas-4* mutant tissues

As I did not identify any genes that were consistently up- or down-regulated in both mutants without centrosomes, I considered the possibility that this might be due to a high rate of false negatives. I therefore tested whether I could identify genes mis-regulated in both *DSas-6* and *DSas-4* mutant tissues if I used a less stringent statistical cut-off value. I compared the overlap between the 100 most significantly differentially regulated genes in *DSas-4* and *DSas-6* mutants. Only 4 genes could be identified, which were differentially regulated in both mutants (Table 5.2). *CG13822* was up-regulated in *DSas-4* mutants but down-regulated in *DSas-6* mutants, and *CG32541* was only 1.26x down-regulated in *DSas-4* and 1.4x down-regulated in *DSas-6* and therewith below the cut-off of ≥1.5 fold differential regulation. These two genes therefore appear to be unlikely candidates for genes that might be differentially regulated in cells without centrosomes. The genes *CG11357* and *pathetic* were up-regulated in both *DSas-4* and *DSas-6* mutants (Table 5.2), hence I decided to test their expression levels by qPCR. This showed that only the 3' region of the two genes (the region the microarray probes bind to) was up-regulated, while the 5' region was not (Table 5.2). Therefore these genes do not appear to be genuinely mis-expressed in cells lacking centrosomes (although the 3' end of both genes may be up-regulated, again for unknown reasons). This analysis confirms that the lack of centrosomes in cells appears to lead to the consistent mis-expression of only a very few, if any, genes.

5.6 A small number of genes are differentially expressed in *SakOE* cells

Next, I assessed the effects that having too many centrosomes has on cells by analysing gene expression in *SakOE* flies. When comparing *SakOE* to w^{67} and *OrR* wild types, I found 55 and 57 genes, respectively, to be differentially regulated (Supplementary Tables 5 and 6). 32 of these genes were found in both comparisons (Table 5.3 and Figure 5.6A). I did a Gene Ontology term (GO term) analysis to test whether any functionally related groups of genes were enriched in my dataset, but I could not identify any (Supplementary Tables 7A and 7B). I performed qPCR analysis on several of the most up- and down-regulated genes *(CG32055, B52, CG14687, CG9279, GNBP2, Brf, CG11999 and CG7900)*, to test whether they were genuinely misexpressed. Five of these 8 genes could be confirmed to be genuinely mis-expressed (Figure 5.6B-F). Of the remaining 3, *CG9279* was upregulated in the 3'region where the microarray probes bind, but was down-regulated in the 5' region (perhaps indicating that an aberrant transcript was being produced as was the case with some of the mis-regulated regions in the *DSas-4* mutants) (Figure 5.6G). *CG14687* and *B52* appeared to be false positives, as either no or only a small change in expression levels was detected by the qPCR (Figure 5.6H,I).

These data confirm that at least some of the 32 genes are genuinely up- or down-regulated in *SakOE* cells. It is currently unclear whether this mis-expression is due to the centrosome amplification in these cells, and the GO term analysis of these genes did not show enrichment for any particular pathway or process. As I only find a relatively small number of genes that are consistently mis-regulated in *SakOE* cells, I conclude

Table 5.3. *Differentially regulated genes in SakOE cells compared to both WT controls. (≥1.5-fold, adj.P-value ≤ 0.05).*

Gene	Map	Fold Change[1]	Function[2]
w	3B6-3B6	74.81	eye pigment biosynthetic process
CG32055	67D11-67D11	43.82	unknown
B52	87F7-87F7	14.38	nuclear mRNA splicing via spliceosome, mRNA splice site selection
CG14687	86C6-86C6	8	unknown
CG9279	76B6-76B6	7.57	microtubule-based movement
CG13032	73B6-73B6	7.3	unknown
CG5618	77B5-77B5	4.48	carboxylic acid metabolic process, proteolysis
CG31495	87F15-87F15	3.63	unknown
miple	61B3-61B3	3.47	unknown
CG7433	76D8-76E1	3.09	cellular amino acid metabolic process, gamma-aminobutyric acid metabolic process
Past1	87C6-87C6	3.07	endocytosis, germline development, imaginal disc-derived wing margin development
GNBP2	75D6-75D6	3.02	carbohydrate metabolic process, defense response
CG32939	85E4-85E4	2.32	unknown
Rbp1	86C6-86C6	2.3	nuclear mRNA splicing via spliceosome, mRNA splice site selection
CG2004	8A2-8A2	2.27	unknown
P58IPK	85D27-85D27	2.24	protein folding
SrpRbeta	66D11-66D11	2.17	neurogenesis, larval chitin based cuticle development
CG18542	85E4-85E4	1.99	unknown
p24-1	10F1-10F1	1.86	neurogenesis, post-Golgi vesicle-mediated transport
CaBP1	35F12-35F12	1.75	cell redox homeostasis, glycerol ether metabolic process
CG6951	77A3-77A4	1.71	unknown
Manf	89B13-89B13	1.67	neuron homeostasis, neuron projection development
KDELR	31E1-31E1	1.6	protein retention ER lumen
MED 7	86C5-86C5	-2.07	transcription from RNA polymerase II promoter
CG5830	72C1-72C2	-2.12	unknown

TFIIFbeta	86C6-86C6	-2.15	transcription from RNA polymerase II promoter
scaf6	73E5-73E5	-2.23	nuclear mRNA splicing via spliceosome
CG32158	73A3-73A3	-2.74	unknown
CG32027	75E2-75E2	-4.91	unknown
Brf	90A3-90A5	-7.59	Regulation of transcription from RNA polymerase III promoter
CG11999	82F10-82F10	-15.43	unknown
CG7900	84E11-84E12	-44.92	unknown

[1]Fold change compared to w^{67} is given
[2]GO Term for Biological Function

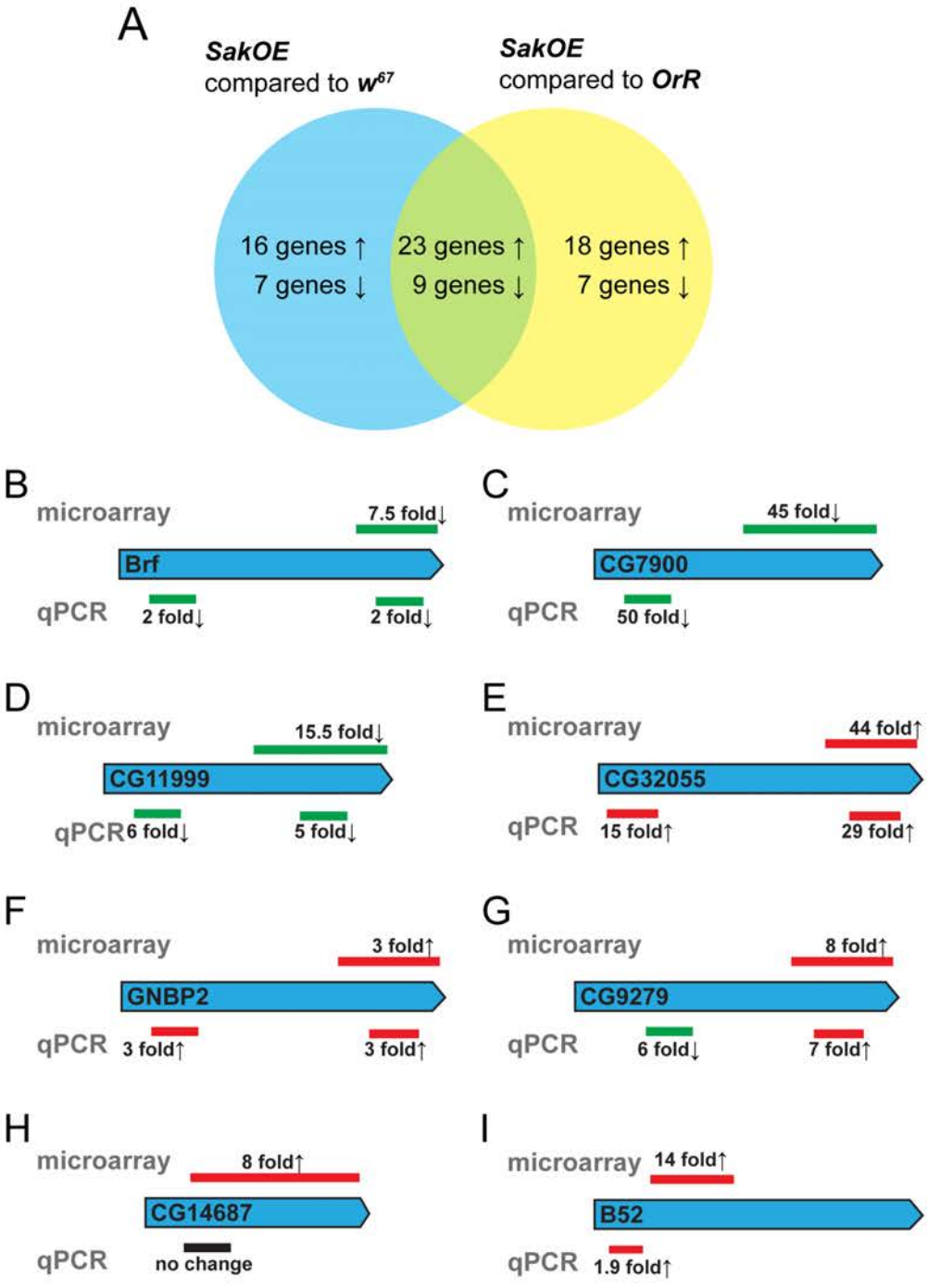

Figure 5.6: Gene expression in *SakOE* cells. (A) Venn diagram of significant genes in *SakOE* cells (third instar larval brains and wing discs) compared to w^{67} and *OregonR* WT controls found in microarray analysis (≥1.5-fold, adj.P-value ≤ 0.05). **(B–I)** Validation of up- and down-regulation by qPCR. Fold change found in microarray analysis is shown above, and fold change found by qPCR analysis is given below the blue bar indicating the transcript. Red (up-regulation), green (down-regulation) and black (no change) bars indicate the position where microarray probes and qPCR primers bind to the transcript.

that centrosome amplification does not lead to a large-scale perturbation of the transcriptome.

5.7 Discussion

I have shown that the global transcriptomes of *Drosophila* 3rd instar larval brain and imaginal disc cells that either lack centrosomes or have too many centrosomes are not dramatically altered. I could identify a small number of transcripts (~10-15) that appear to be genuinely mis-expressed in *DSas-4* cells lacking centrosomes. Some of these were clearly aberrant transcripts that do not encode for any known protein, and these sometimes appear to span two adjacent genes. It is unclear what function, if any, these transcripts have, but it seems very unlikely that they belong to a common pathway that is up-regulated in cells without centrosomes, as none of these genes were found to be differentially regulated in *DSas-6* cells, which also lack centrosomes.

In *SakOE* cells that have amplified centrosomes I could identify a slightly larger set of differentially regulated transcripts (~30). Unfortunately there is no other fly strain that efficiently drives centrosome amplification in brains and imaginal discs that we could use to compare the *SakOE* dataset to. This would be the best way to identify genes that are genuinely over- or underexpressed as a consequence of centrosome amplification. My data comparing the *DSas-4* and *DSas-6* mutants lacking centrosomes highlight the importance of being able to make such a comparison. Morover, as the misregulated transcripts I found in *SakOE* cells did not cluster into any common pathway or cell process, I remain cautious in interpreting this result, and think it perhaps unlikely that many of these genes are genuinely misregulated as a direct consequence of centrosome amplification. It has been shown that the human homologue of Sak, Plk4, can

phosphorylate the transcription factor Hand1 (Martindill et al., 2007), perhaps explaining why more genes are differentially expressed in *SakOE* cells than in cells that do not have centrosomes.

It is important to note that my data do not rule out the possibility that centrosome defects lead to significant post-transcriptional changes in proteins without affecting the transcription of many genes. Nevertheless, my findings strongly suggest that centrosome defects do not induce a major stress response in cells, and that flies without centrosomes or with amplified centrosomes do not survive only because they have extensively up-regulated compensatory pathways. This is an important finding, as in mammalian cells centrosome defects have been shown to activate a stress response via the p38 and p53 pathways (Mikule et al., 2007; Srsen, 2006; Uetake et al., 2007). It has not been tested which effects the activation of these pathways might have on gene expression in *Drosophila*, but genome wide expression studies in mammalian cells have shown that p38 stress-activated protein kinase activation leads to changes in expression of many genes, some of which are transcription factors (Ferreiro et al., 2010). My GO term enrichment analysis does not show enrichment of any known stress response genes in response to centrosome defects.

My aim with this study was to look at the global picture of how mitotically active tissues are affected by abnormal centrosome numbers *in vivo*. It was not designed to analyse the effects that centrosome defects might have in specific cell types. Neuroblasts appear to be particularly sensitive to centrosome defects, as their asymmetric divisions can be perturbed which can eventually even lead to tumourigenesis in transplantation assays (Basto et al., 2008; Castellanos et al., 2008). It would be interesting to purify neuroblasts with abnormal centrosome numbers by FACS

sorting (Harzer et al., 2013) to see whether they would show a more severe transcriptional response.

My finding that flies without centrosomes can divide their cells and develop without any detectable transcriptional alterations that are due to the loss of centrosomes is quite striking. How can this result be explained? As I have discussed in the Introduction (Section 1.4), there are several other pathways for spindle assembly that can function in the absence of centrosomes. Although centrosomes often contribute to the speed and accuracy of spindle assembly, in the case of the loss of centrosome-mediated MT nucleation, spindle MTs are nucleated in the vicinity of chromosomes, and clustered into a bipolar spindle (Basto et al., 2006; Khodjakov et al., 2000; Mahoney et al., 2006; Maiato et al., 2004) (Section 1.4.2). The augmin complex further aids in spindle assembly by nucleating MTs from within the spindle (Goshima et al., 2008a; Lawo et al., 2009; Mahoney et al., 2006; Petry et al., 2013b; Wainman et al., 2009) (Section 1.4.3).

Nevertheless I was wondering if there might be any other pathway that could explain why *DSas-4* and *DSas-6* tissues lacking centrosomes appear to be so normal, and whether there could be something else that compensates in these cells without centrosomes. Recently there has been data emerging about an additional pathway of spindle assembly mediated by acentrosomal microtubule organising centers (aMTOCs), thus, I was contemplating the possibility that aMTOCs could play a role in *DSas-4* and *DSas-6* mutants and partly compensate for the loss of centrosomes. In the next chapter I will describe my analysis of the function of aMTOCs in cells without centrosomes.

6 The contribution of acentrosomal microtubule organising centres (aMTOCs) to spindle formation

6.1 Introduction

Several pathways contribute to mitotic spindle assembly in wild type cells, amongst which are the centrosomal pathway, the chromosome-mediated pathway and the augmin pathway (Section 1.4). Recently data has emerged about an additional pathway, which is mediated by acentrosomal microtubule organising centres (aMTOCs). Depending on the cell type this pathway can have a major role in spindle formation. For example, in mouse oocytes the acentrosomal female meiotic spindle is assembled by over 80 aMTOCs that form de novo in prophase and functionally replace centrosomes (Schuh and Ellenberg, 2007; Łuksza et al., 2013). Interestingly, spindle assembly is mediated by aMTOCs until the early blastocyst stage when a centrosomal mitotic spindle assembly is established (Courtois et al., 2012). In acentrosomal *Drosophila* S2 cell lines it has been shown that PCM proteins like γ−tubulin can localise to mitotic spindle poles (Debec et al., 1995). More recently, a more detailed study of this acentrosomal cell line showed that cells appeared to have aMTOCs on the spindle poles in about 2/3 of all cells, and these stained for the centrosomal proteins γ-tubulin, Cnn, DSas-4 and D-PLP (Moutinho-Pereira et al., 2009). Moreover, these aMTOCs could also be detected in acentriolar cells generated by *DSas-4* RNAi knockdown. These aMTOCs had the ability to nucleate MTs in repolymerisation assays and required Cnn for their formation. The centriolar protein Asl has a dual role in centrosome formation, as it recruits Sak kinase by direct interaction to the mother centriole (Dzhindzhev et al., 2010a) and is required for PCM recruitment to mitotic centrosomes (Bonaccorsi et al., 1998; Conduit et al., 2010; Varmark et al., 2007). Interestingly, overexpression of an Asl mutant protein

incapable of binding to Sak leads to formation of aMTOCs in *Drosophila* embryos that consisted of DSas-4 and PCM components and were able to organise MTs. It has recently been shown that MTs emerging from centrosomes provide pushing forces needed for nuclear migration in *Drosophila* stage 9 oocytes. Interestingly, in *DSas-4* mutants that lack centrosomes, acentrosomal MTOCs marked by GFP-Cnn are formed, and can provide the pushing forces needed for nuclear migration (Zhao et al., 2012). The role of aMTOCs in *Drosophila* spindle assembly in somatic cells, however, remains unclear.

MT nucleation mediated by aMTOCs is also of great interest in human cells, as a recent study by Kleylein-Sohn et al. suggested that the aMTOC MT nucleation pathway is over-active in certain cancer cell lines. This is potentially of great interest, as this pathway could contribute to multi-polar spindle formation and so to chromosomal instability. Many cancer cells have extra centrosomes, and the kinesin HSET is required to "cluster" these extra centrosomes to ensure that these cells divide in a bipolar fashion (Kwon et al., 2008).These new studies reveal that several cancer cell lines also generate high numbers of aMTOCs (even in cells that do not have extra centrosomes), and these aMTOCs also require HSET to cluster, so preventing multipolar mitoses (Kleylein-Sohn et al., 2013). Thus, it is important to understand the potential role of aMTOCs in both normal cell division and in the potentially abnormal division of cancer cells.

These studies show that aMTOCs can potentially contribute to MT nucleation in many different cell types, and they appear to be a major driving force for MT nucleation in some cases, for example in mouse oocytes and *DSas4* mutant *Drosophila* ovaries. Therefore I was intrigued by the possibility that aMTOCs could play an enhanced role in *DSas-4* and *DSas-6* mutant cells, perhaps explaining why these cells appear to be so

normal in my microarray analysis. In this Chapter I analyse *Drosophila* mutants lacking centrosomes, and show that aMTOCs are often present in mutant somatic cells lacking centrosomes *in vivo*. I show that the formation of aMTOCs in *Drosophila* is dependent on the core centriole duplication protein Asl, and that *asl* mutants therefore lack both centrosomes and aMTOCs. This finding allowed me to probe the impact of aMTOCs in cells without centrosomes and analyse their contribution to spindle assembly in relation to the other MT nucleation pathways by simply comparing differences in spindle assembly in *DSas-4* and *asl* mutants.

6.2 *Drosophila* somatic cells without centrosomes have PCM proteins on mitotic spindle poles

Encouraged by the finding that aMTOCs can be observed in *DSas-4* RNAi-treated tissue culture cells (Moutinho-Pereira et al., 2009) I decided to test whether I could observe aMTOCs *in vivo* in *Drosophila DSas-4* mutants. I decided to use *Drosophila* brain cells for my analysis, as they provide a good model system for the analysis of mitotic phenotypes (Gatti and Baker, 1989). I stained *DSas-4* brains with antibodies against the centriolar protein Asl (to confirm the absence of centrioles), α-tubulin (to visualise the mitotic spindle), and Cnn, as this is a highly abundant PCM protein and was found by Moutinho-Pereira and colleagues to localise to aMTOCs. *DSas-4* flies completely lack centrioles in the 3rd instar larval stage (Basto et al., 2006), and this was confirmed by the complete absence of Asl staining in *DSas-4* cells, while WT cells had 2 Asl dots marking the two centrioles in all cells (Figure 6.1A). As expected, two Cnn dots were seen in all mitotic WT cells, colocalising with Asl but spreading out further into the PCM surrounding the centrioles. When analysing Cnn staining in *DSas-4*

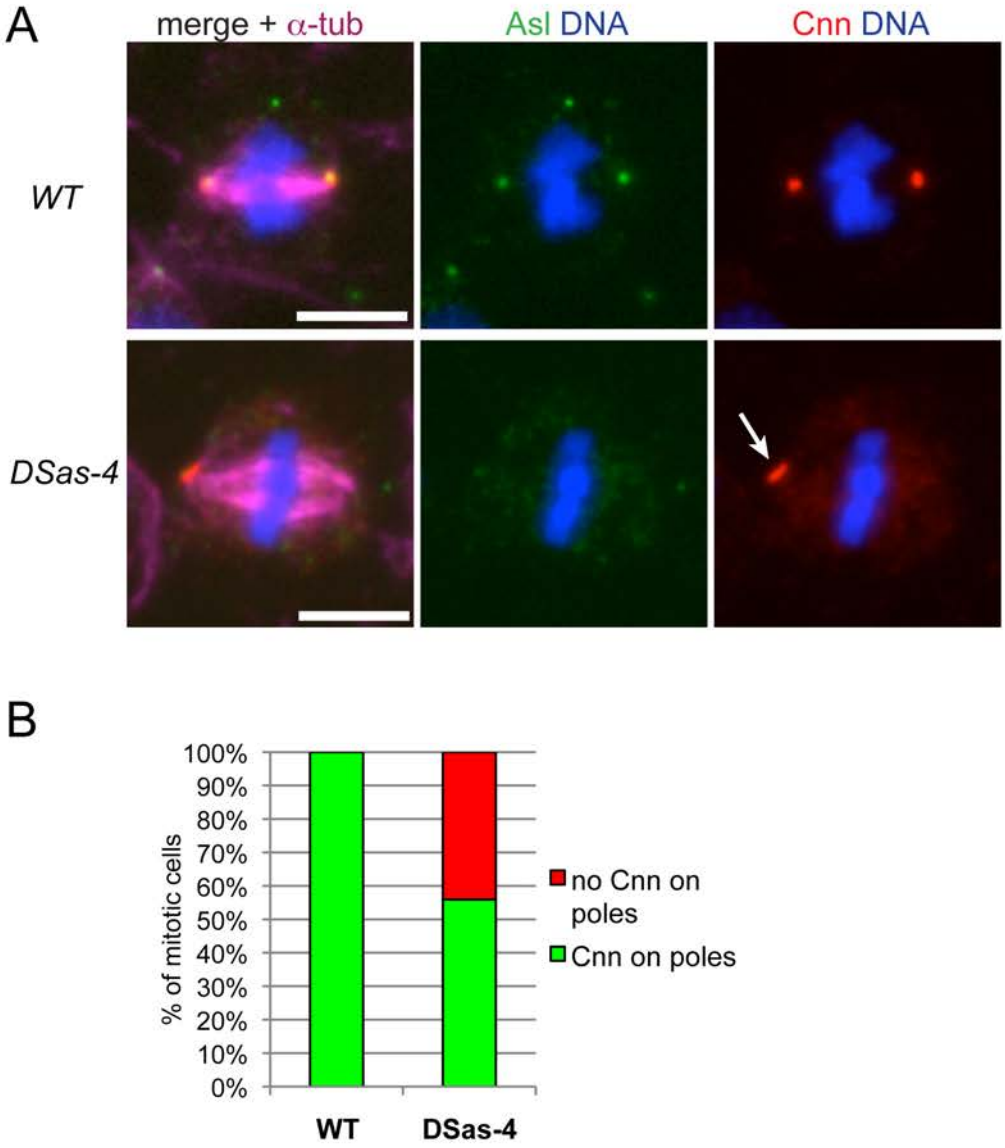

Figure 6.1: *Drosophila* somatic cells without centrioles have PCM proteins on mitotic spindle poles. (A) *Drosophila* brain cells were stained with anti Asl (green) to mark centrioles, anti α-tubulin (pink) and an antibody against the PCM protein Cnn (red). DNA is in blue. The scale bar is 5μm. *DSas-4* mutants do not have centrioles but can have Cnn mitotic spindle poles, marked by the arrow. **(B)** Brain cells were stained with antibodies against Cnn and α-tubulin, and cells with Cnn localising to spindle poles were quantified (n=246 cells in 12 brains for WT and n= 192 cells in 6 brains for *DSas-4*).

mutants, no such strong PCM staining could be observed. I could, however, find some Cnn staining on one or both mitotic spindle poles, which was often more dispersed and weaker in intensity than centrosomal PCM staining (Figure 6.1A). I quantified the number of cells with Cnn staining on spindle poles in brain cells stained with Cnn and α-tubulin, and found that while 100% of all mitotic WT cells had Cnn staining on spindle poles, 56% of all *DSas-4* mutant cells had Cnn staining on at least one of the two spindle poles (Figure 6.1B).

6.3 Many known PCM proteins localise to acentrosomal mitotic spindle poles in *Drosophila* brain cells

Moutinho-Pereira and colleagues showed colocalisation of Cnn, γ-tubulin, DPLP and DSas-4 on acentrosomal spindle poles in S2 cell lines (Moutinho-Pereira et al., 2009). Therefore, I checked whether any of these proteins were present on spindle poles in *DSas-4* mutants (apart from DSas-4 itself, which is absent in the mutant). Additionally, I decided to test whether any other known PCM components were present on spindle poles and checked colocalisation of Spd-2, Aurora A, Dgp71WD, Msps and DTACC with Cnn. By analysing fixed cells stained with antibodies directed against these proteins, I could confirm that γ-tubulin and DPLP colocalised with Cnn on spindle poles, and could detect colocalisation of Aurora A, Dgp71WD, Msps and DTACC (Figure 6.2 middle panel). Some of these stainings were very faint compared to PCM staining in WT cells that contain centrosomes (Figure 6.2 left panel), possibly because these structures are much smaller than centrosomes and require very sensitive antibodies for detection.

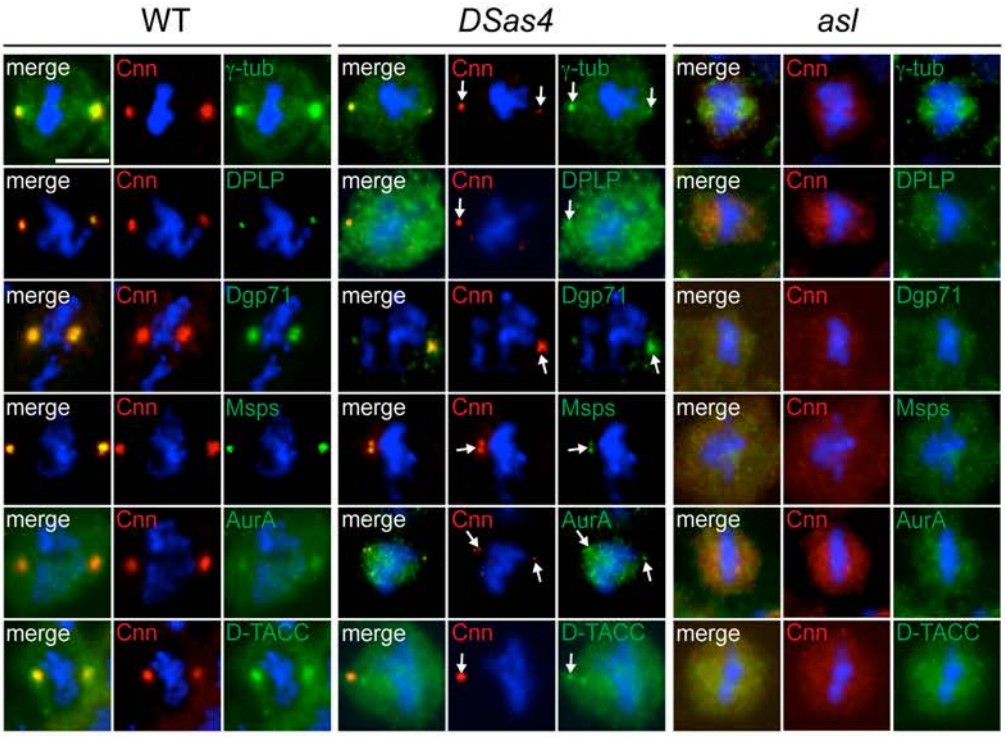

Figure 6.2: Several PCM proteins colocalise with Cnn in mitotic *DSas-4* mutant cells. Fixed *Drosophila* brain cells were stained with antibodies against Cnn (red) and γ-tubulin, Aurora A, Dgp71WD, Msps, DPLP or DTACC (green). DNA is in blue. All of these PCM proteins colocalise with Cnn in mitotic *DSas-4* cells (middle panel, indicated by white arrows). Note that the intensity of staining on the poles is much lower than in WT cells containing centrosomes (left panel). In *asl* mutants no PCM proteins localise on the spindle poles (right panel). Scale bar is 5μm.

I could not detect any Spd-2 staining (data not shown) and considered the possibility that the Spd-2 antibody was not sensitive enough to detect any DSpd-2 staining on acentrosomal poles, as the the stainings of other PCM proteins were also quite faint. Detection of transgenic GFP-tagged proteins in live tissues can be more sensitive than detection of proteins with antibodies in fixed cells, hence, together with Alan Wainman from the lab, we analysed Spd-2-GFP in the *DSas-4* mutant background. We also analysed GFP-Cnn and γ-tubulin-GFP as positive controls. We performed crosses to obtain stocks expressing one copy of either Spd-2-GFP, GFP-Cnn or γ-tubulin-GFP, respectively, and one copy of Jupiter-mCherry (to visualise spindles) in the *DSas-4* mutant background. We then performed time-lapse microscopy to observe spindle formation in living brain cells. This analysis revealed that cytoplasmic dots of Spd-2-GFP (Figure 6.3A), GFP-Cnn (Figure 6.3B) and γ-tubulin-GFP (Figure 6.3C) could be detected associating with MTs in the cytoplasm of mitotic cells, and these dots often eventually became clustered on the spindle, particularly around the poles.

Taken together these data show that several PCM proteins including Cnn, γ-tubulin, Spd-2, Dgp71WD, DPLP, Aurora A, Msps and DTACC can localise to mitotic spindle poles *in vivo* in flies lacking centrosomes. I conclude that these structures are similar to the aMTOCs described in S2 cells, and in accordance with Moutinho-Pereira et al., I will use the term acentriolar microtubule organising centre (aMTOC) to describe these PCM foci in the following.

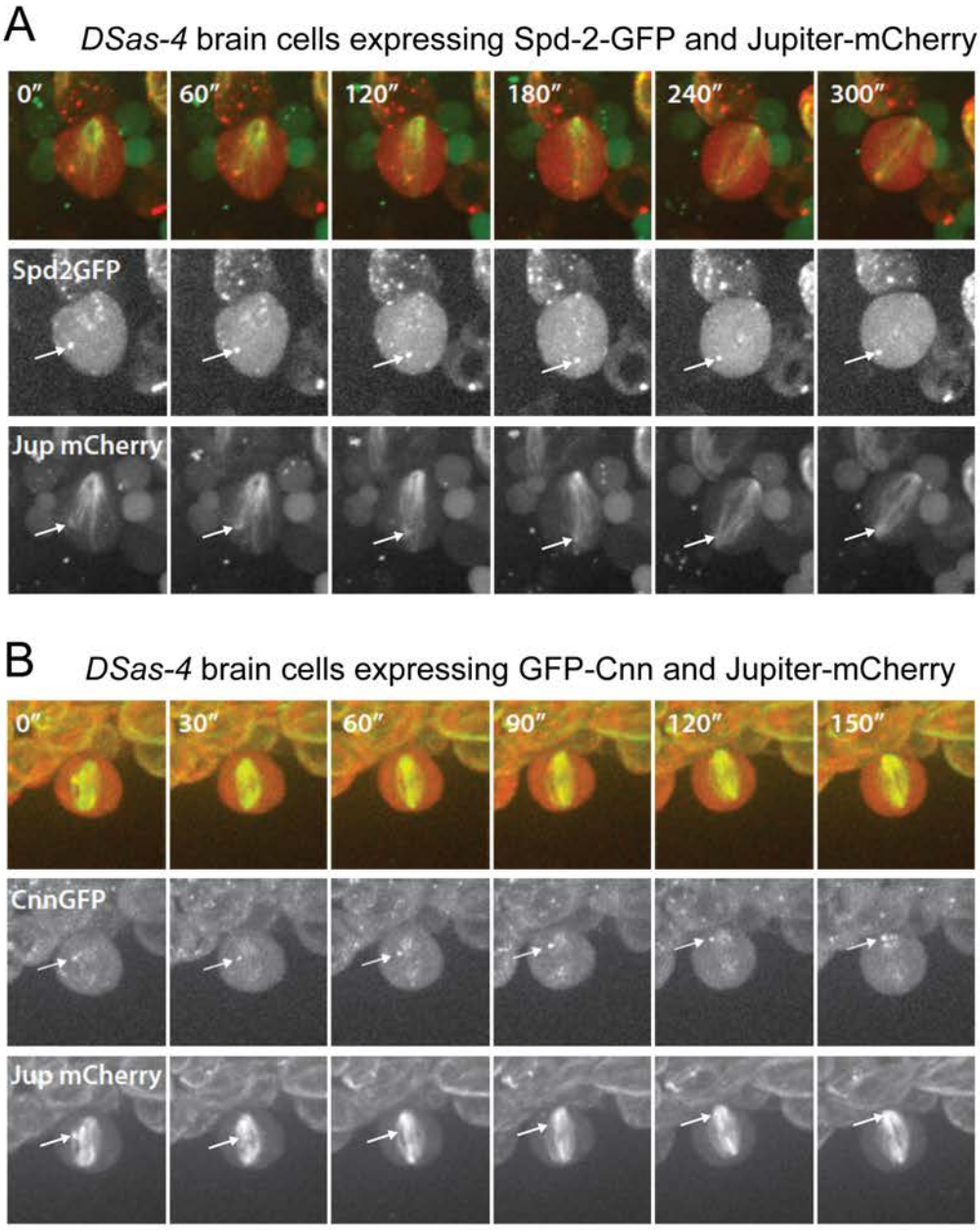

Figure 6.3: Live imaging shows that GFP-Cnn, Spd-2-GFP and γ-tubulin-GFP cluster on mitotic spindle poles in *DSas-4* neuroblasts. For Figure legend see next page.

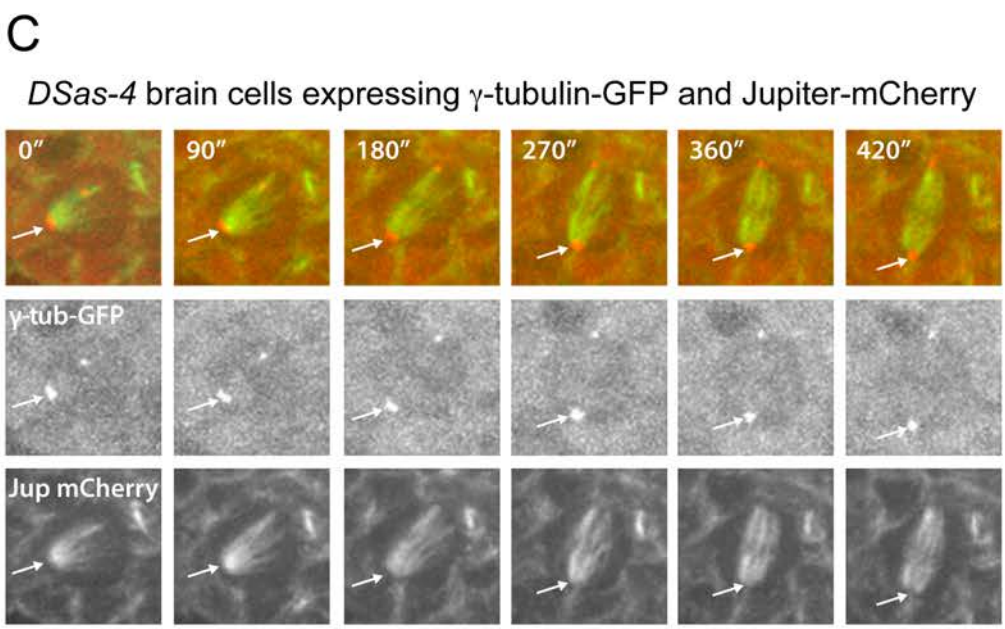

Figure 6.3: Live imaging shows that GFP-Cnn, Spd-2-GFP and γ-tubulin-GFP cluster on mitotic spindle poles in *DSas-4* neuroblasts. Spindle formation in brain cells was filmed in stocks expressing Spd2-GFP (red) and Jupiter-mCherry (green) **(A)**, GFP-Cnn (red) and Jupiter-mCherry (green) **(B)** or γ-tubulin-GFP and Jupiter-mCherry **(C)** in the *DSas-4* mutant background. Several Spd-2-GFP, GFP-Cnn and γ-tubulin-GFP foci (marked by the arrows) are in the cytoplasm in prophase which subsequently cluster and move towards the spindle poles.

6.4 Asterless mediates formation of acentrosomal MTOCs in cells lacking centrosomes

Next, I wanted to assess whether any of the core centriole duplication proteins were required for the formation and function of aMTOCs. A putative pathway of centriole and centrosome assembly in *Drosophila* has been established with data from our lab and other labs (discussed in Section 1.2.2). According to this pathway, the 5 centriolar proteins Sak, Ana2, DSas-6, DSas-4 and Asl are required for centriole duplication (Figure 6.4A), with Asl having a dual role and being required for PCM recruitment to the centriole as well. Mutations in core centriole duplication proteins lead to flies without centrioles (Basto et al., 2006; Bettencourt-Dias et al., 2005; Peel et al., 2007; Rodrigues-Martins et al., 2007b). To test if any of these core centriole duplication proteins were required for the formation of aMTOCs I stained *sak, ana2, DSas6 and asl* mutants for the presence of aMTOCs on their acentrosomal spindle poles with antibodies against Cnn and γ−tubulin (as these were the proteins I could detect most robustly by immunostaining in *DSas-4* cells).

For these studies, strong hypomorphic alleles of *ana2*, *DSas-6* and *asl* were already available (Peel et al., 2007; Rodrigues-Martins et al., 2007a; Wang et al., 2011b), but there was only a weak hypomorphic allele of *sak* (Bettencourt-Dias et al., 2005). I found that this allele had detectable centrioles in two thirds of its brain cells (Figure 4.4B), so I decided I needed to make a stronger *sak* allele for this experiment. Together with Alan Wainman, I succeeded in making a strong hypomorphic allele of *sak* that completely lacked centrioles in all of its cells; the generation of this mutant and its full analysis is described in Chapter 4.

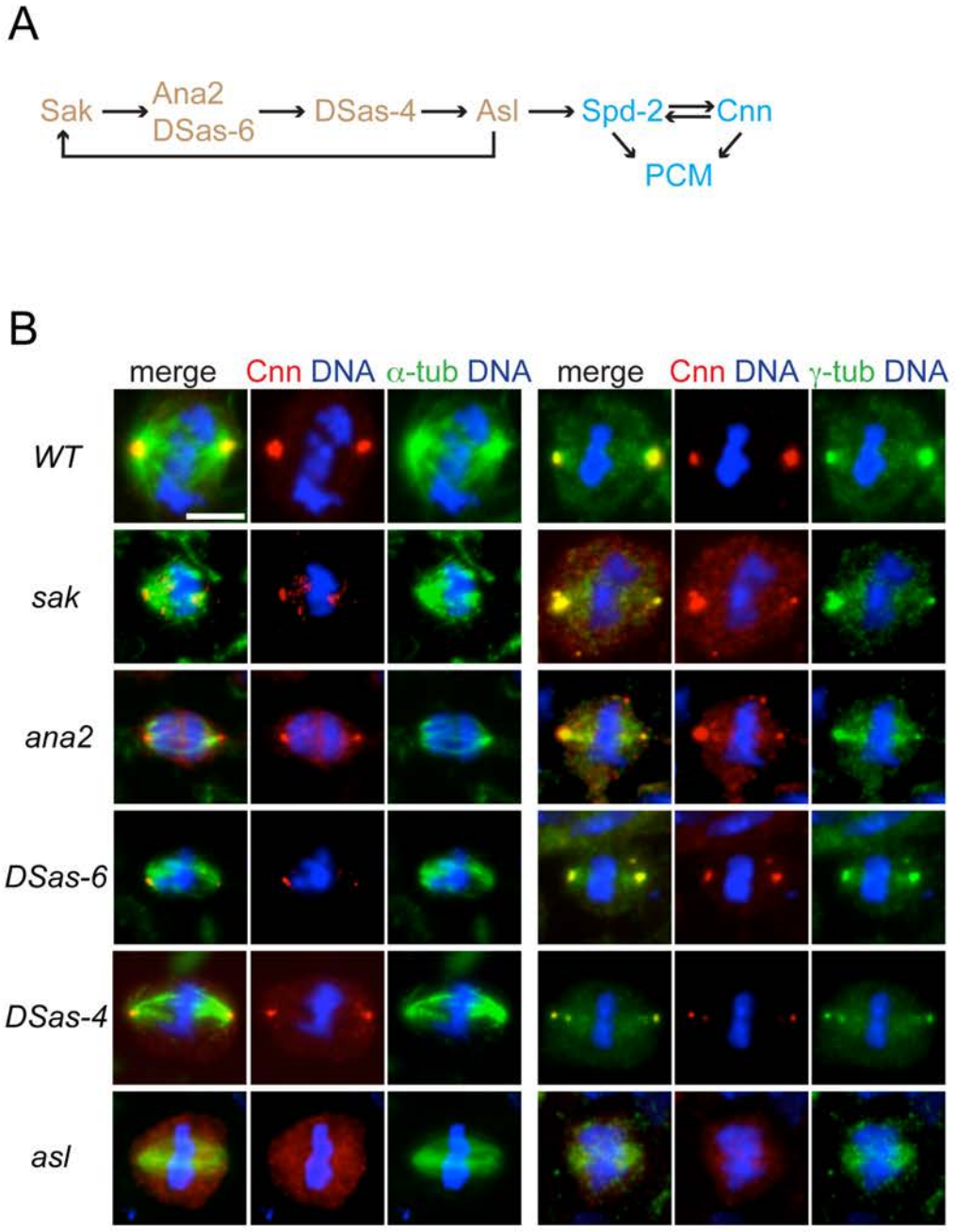

Figure 6.4: Formation of aMTOCs in cells without centrosomes is dependent on Asterless. For figure legend see next page.

C

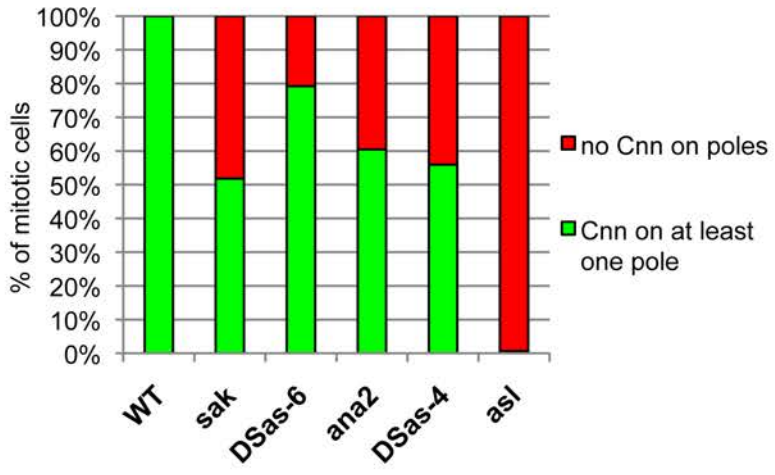

D

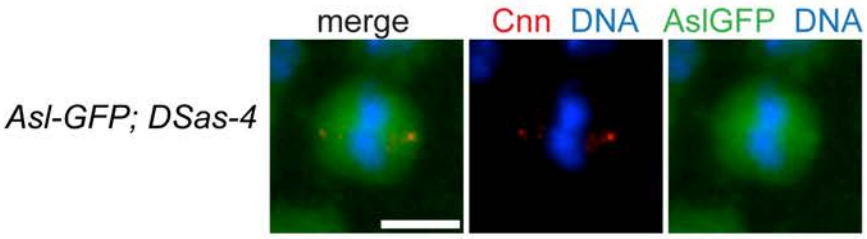

Figure 6.4: Formation of aMTOCs in cells without centrosomes is dependent on Asl. (A) Centrosome formation pathway as discussed in section 1.2, centriolar proteins are in brown and PCM proteins in blue. **(B)** Brain cells of *Drosophila* mutants that lack centrioles were stained with antibodies detecting α-tub (green) and Cnn (red) in the left panel, and Cnn (red) and γ–tub (green) in the right panel. DNA is in blue. Scale bar is 5μm. Note the absence of aMTOCs in *asl* mutants. **(C)** Quantification of Cnn staining on spindle poles in mitotic brain cells in acentriolar mutants. (n=minimum of 120 cells of at least 4 brains were quantified per genotype). **(D)** Asl-GFP, *DSas-4* cells were fixed and stained with anti-Cnn antibody (red), the GFP signal was enhanced with GFP booster (green). DNA is in blue, scale bar is 5μm. No Asl-GFP colocalising with Cnn can be detected.

I found that *sak, ana2, DSas-6 and DSas-4* mutant cells without centrioles could all form robust aMTOCs on spindle poles, indicating that the respective proteins were not required for aMTOC formation. This observation also confirmed that aMTOCs are present due to the lack of centrioles in general, rather than being specific for *DSas-4* mutants. The only mutant in which I could not detect any Cnn and γ−tubulin staining on spindle poles was *asl* (Figure 6.4B). I went on to quantify the number of mitotic cells with Cnn staining on spindle poles and found that in *sak, ana2, DSas-6 and DSas-4* mutants at least 50% of all mitotic cells had aMTOCs detectable on at least one of the spindle poles, but in *asl* no aMTOCs were detectable (Figure 6.4C). I also found that the other PCM proteins that I had found to localise on *DSas-4* spindle poles were absent from *asl* spindle poles (Figure 6.2 right panel). Thus, Asl is required to mediate the formation of aMTOCs on acentrosomal spindle poles.

Interestingly, I could not detect the presence of Asl itself on spindle poles in immunostainings of *DSas-4* mutants (Figure 4.1A). We considered that the Asl antibody might not be sensitive enough (as appears to be the case for Spd-2), and together with Alan Wainman examined living brain cells of flies expressing Asl-GFP and Jupiter-mCherry in the *DSas-4* mutant background. We could not, however, detect any localisation of Asl-GFP at aMTOCs in living cells (data not shown). I also fixed Asl-GFP-expressing *DSas-4* cells and stained them with an anti Cnn antibody, and GFP booster, which is an excellent antibody widely used in the laboratory to detect proteins present at very low abundance (Raff lab, various personal communications). I could detect Cnn staining, but no Asl-GFP on spindle poles (Figure 6.4D). Thus, while Asl appears to be required for the formation of aMTOCs in cells without centrosomes, we cannot detect co-localisation of Asl to the aMTOCs. This explains why my earlier

analysis of centrosome number in various mutant cells was not confounded by the presence of these aMTOCs (Figure 5.1A,B).

6.5 Cnn is required for aMTOC function

Asl is required for efficient PCM recruitment to the centrosome ((Bonaccorsi et al., 1998; Conduit et al., 2010; Dzhindzhev et al., 2010a; Varmark et al., 2007) and overexpression of an Asl construct that cannot bind to Sak can drive formation of multiple aMTOCs in *Drosophila* embryos in the absence of centrioles, although it was unclear in this study if Asl could directly bind to PCM components or whether this was an indirect process (Dzhindzhev et al., 2010a)). It has recently been shown in our lab, that Asl appears to be required for binding Spd-2 to the centrosome, which then in turn recruits Cnn to the centriole (Figure 6.4 A) (Conduit et al., manuscript in preparation). Some Cnn, however, can also be recruited to centrioles by a Spd-2-independent pathway in brain cells (Conduit et al, submitted). Together, Spd-2 and Cnn cooperate to ensure robust centrosome maturation, and centrosomes in brain cells lacking Cnn have severely reduced γ-tubulin levels, whereas cells lacking Spd-2 have slightly reduced γ-tubulin levels (Conduit et al., manuscript in preparation). I was wondering, whether Asl might initiate the formation of aMTOCs by forming a platform that can recruit Spd-2 and Cnn even in the absence of a centriole (as shown in embryos overexpressing a form of Asl lacking the N-terminal region (Dzhindzhev et al., 2010a). If this was the case, taking away Spd-2 or Cnn in *DSas-4* mutants that normally have aMTOCs would impair the formation and function of aMTOCs in these cells. I therefore constructed *Spd-2, DSas-4* and *cnn; DSas-4* double mutant strains and measured γ-tubulin accumulation on mitotic spindle poles as a readout for aMTOC function. I found that ~55% of all mitotic *DSas-4* mutant cells had γ-tubulin foci on spindle poles, this was the

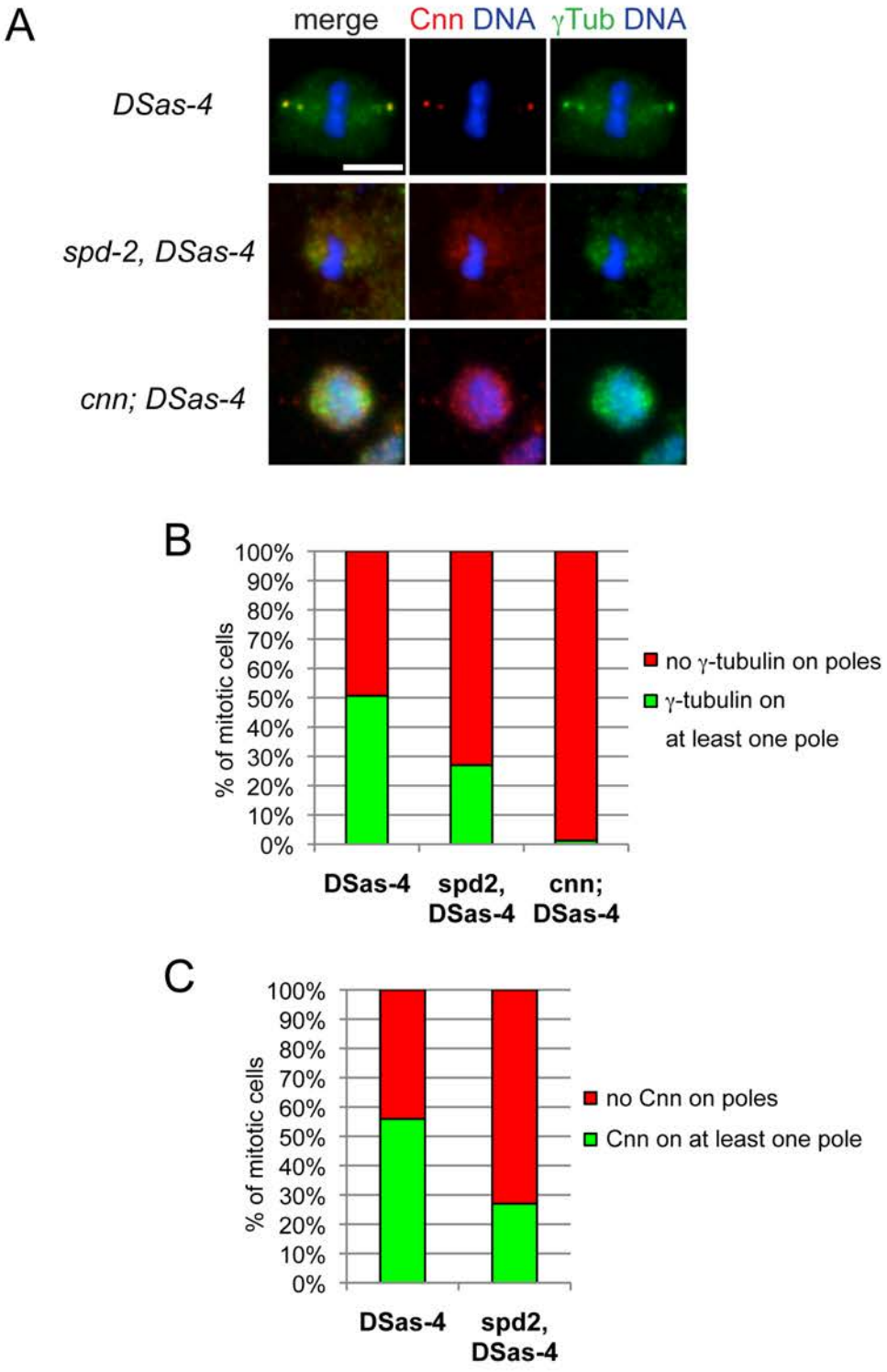

Figure 6.5: Cnn and Spd-2 are required for aMTOC function. (A) *DSas-4* mutants and *spd-2, DSas-4* and *cnn; DSas-4* double mutants were stained with antibodies against Cnn (red) and γ-tubulin (green). DNA is in blue, scale bar is 5μm. **(B)** Mitotic brain cells with γ-tubulin staining on spindle poles were quantified (n=at least 80 cells in 3-4 brains were quantified) **(C)** Mitotic brain cells with Cnn staining on spindle poles were quantified (n=at least 137 cells in 4 brains were quantified per genotype).

case for only ~27% of *Spd-2, DSas-4* (Figure 6.5A,B). In *cnn; DSas-4* cells, almost no cells had γ-tubulin on the spindle poles (~1%) suggesting that Cnn is essential for aMTOC formation (Figure 6.5A,B). The reduction in γ-tubulin on spindle poles in *Spd-2, DSas-4* cells appeared to be due to a reduction in Cnn recruitment to aMTOCs as the number of cells with Cnn on poles was also reduced by ~50% in the double mutant cells compared to *DSas-4* mutant cells (Figure 6.5A,C). These data suggest that formation of aMTOCs is completely dependent on Cnn *in vivo*, whereas depletion of Cnn in S2 cells only leads to reduced number and size of aMTOCs. Spd-2 appears to have only an indirect effect on aMTOC formation in our system by reducing Cnn recruitment to aMTOCs.

6.6 Outlining an assay to determine the impact of aMTOCs in mitotic cells

Taken together, my data so far show that aMTOCs are formed in ~50-70% of mitotic cells that lack centrioles and centrosomes and that the centriolar protein Asl and the PCM component Cnn are essential for aMTOC formation. I realised that I therefore potentially had a simple way to investigate the function of aMTOCs: *DSas-4* mutant cells lack centrioles/centrosomes, but have aMTOCs, while *asl* mutant cells lack both centrioles/centrosomes and aMTOCs. By comparing the behaviour of DSas-4 mutants to *asl* mutants I should be able to infer the contribution of the aMTOCs to any biological process.

6.7 Live analysis of spindle assembly in *DSas-4* and *asl* mutant brain cells

I first wanted to assess the contribution of aMTOCs to mitotic spindle assembly in cells lacking centrosomes. I decided to use time-lapse microscopy to measure the dynamics of spindle assembly in *DSas-4* and *asl* mutant brain cells, this experiment was performed and analysed in collaboration with Alan Wainman. We established stocks expressing Jupiter-mCherry and PACT-GFP (Martinez-Campos et al., 2004) in the *DSas-4* and *asl* mutant backgrounds to perform live-imaging of neuroblasts going through mitosis. The PACT-GFP signal was used to visualise the nuclear envelope, so that we could identify the moment of nuclear envelope break down (NEBD) (Conduit et al., 2010) (Figure 6.6A). This was important to measure the exact time between NEBD and anaphase onset. Both *asl* and *DSas-4* cells were significantly delayed in spindle assembly compared to *WT*, but there was no significant difference between spindle assembly in *asl* and *DSas-4* mutants (Figure 6.6B). Thus, aMTOCs do not measurably contribute to the efficiency of spindle assembly in cells lacking centrosomes.

MT nucleation by centrosomes is usually considered to be the dominant pathway of spindle assembly in *Drosophila* somatic cells, but, in the absence of centrosomes, other pathways can drive surprisingly efficient spindle assembly (discussed in Section 1.4). I therefore decided to probe the role of aMTOCs spindle assembly in the absence of the other spindle nucleation pathways.

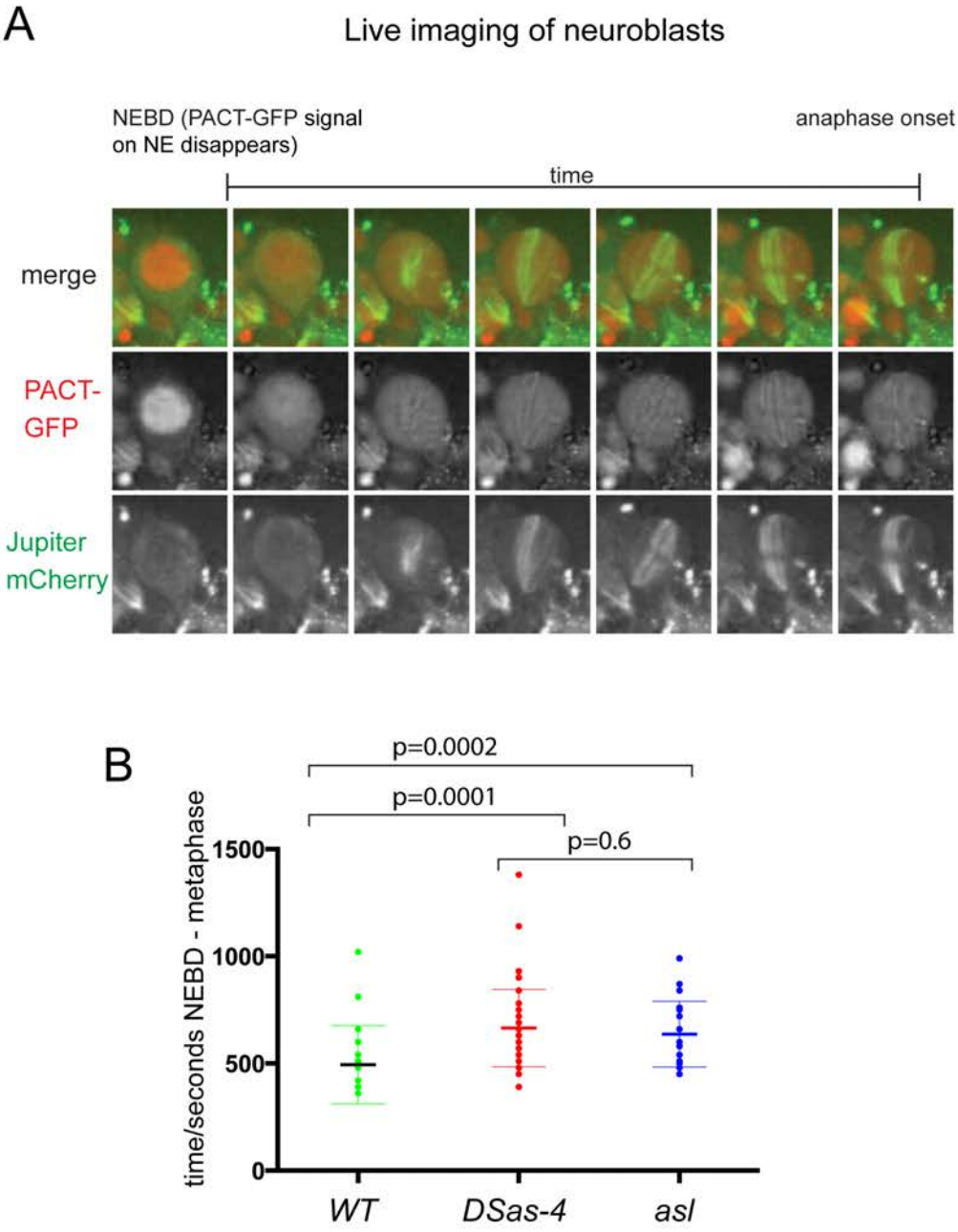

Figure 6.6: aMTOCs do not contribute to spindle assembly in the absence of centrosomes. (A) *WT, asl* and *DSas-4* neuroblasts expressing PACT-GFP and Jupiter-mCherry undergoing mitosis were filmed to compare spindle assembly dynamics. Note PACT-GFP signal during first timepoint, which gets lost as the nuclear envelope breaks down **(B)** Time between NEBD and anaphase onset was measured for *WT* (n=10 cells), *DSas-4* (n=18 cells) and *asl* (n=12 cells). A Mann-Whitney test shows that spindle assembly dynamics between *DSas-4* and *asl* do not differ significantly. *DSas-4* and *asl* cells both take significantly longer than *WT* cells.

6.8 aMTOCs do not have a major contribution to spindle assembly in the absence of the augmin/HAUS complex

The conserved augmin/HAUS complex generates MTs from the side of existing spindle MTs (Goshima et al., 2008a; Kamasaki et al., 2013; Lawo et al., 2009; Petry et al., 2013b; Wainman et al., 2009) (discussed in section 1.4.3). In the absence of functional centrosomes, the augmin complex is essential for cell division, as double mutants for centrosomal genes and genes encoding for augmin complex subunits are early pupal lethal (Reschen et al., 2012) and exhibit weak and disorganised MT arrays in mitotic cells with very few robust spindles (Wainman et al., 2009). Furthermore, it has been demonstrated that the augmin/HAUS complex is necessary for bipolar spindle assembly and to prevent multipolar mitoses in cancer cells containing aMTOCs (Kleylein-Sohn et al., 2013).

In order to test, whether aMTOCs aid in MT array assembly in cells lacking the augmin and centrosomal pathway of MT nucleation, I compared double mutants of *asl* and *DSas-4* with the augmin complex subunit *wac* (Meireles et al., 2009). In accordance with previous studies, in both *asl, wac* and *DSas-4, wac* double mutants only very few mitotic cells (identified by anti-Phospho-Histone H3 staining) showed robust spindles, and most cells had disorganised, but bipolar, spindles with very low MT density. The majority of mitotic cells did not have organised MT arrays at all (Figure 6.7A). Unlike in human cancer cells with aMTOCs, the augmin/HAUS complex was not needed to ensure spindle bipolarity as no multipolar spindles could be observed. I quantified mitotic phenotypes in both double mutants to test if aMTOCs could aid in spindle formation in the absence of centrosomes and the augmin/HAUS complex. In *DSas-4, wac* double mutants, ~26% of mitotic cells had a recognisable mitotic spindle, while

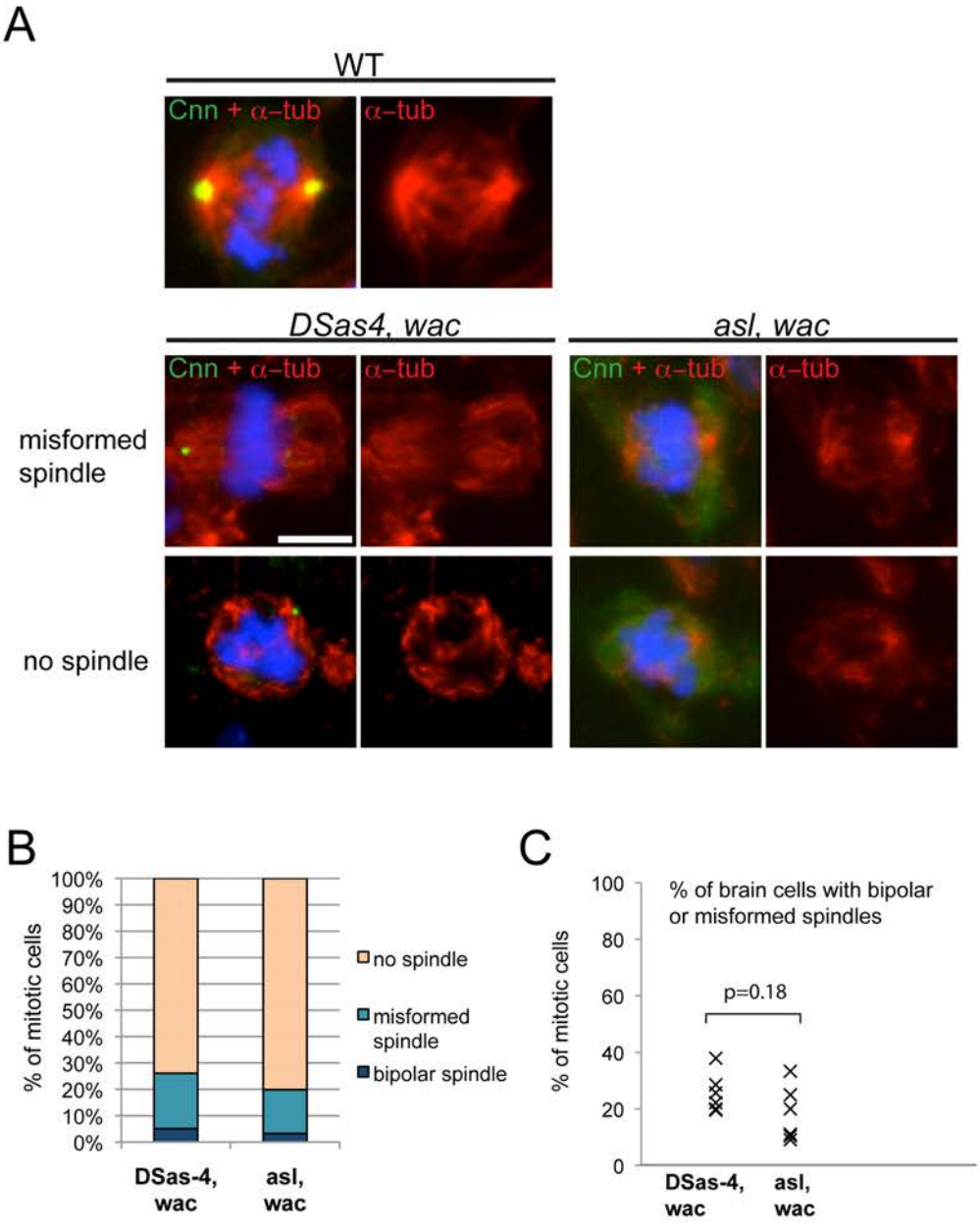

Figure 6.7: aMTOCs do not have a major contribution to spindle assembly in the absence of the augmin/HAUS complex. (A) WT; *DSas-4, wac* and *asl, wac* brain cells stained with antibodies against α-tubulin (red) and Cnn (green), DNA is in blue. Scale bar=5μm. **(B)** Quantification of spindle phenotypes in *DSas-4, wac* and *asl, wac* brain cells**. (C)** A Student's t-test shows no significant difference in spindle formation between *asl,wac* and *sas4,wac.* Every data point is the average of all cells of one brain (n= total 138 cells in 6 brains for D*Sas-4,wac* and n=total 277 cells in 7 brains for *asl,wac*).

this fell to 20% in *asl, wac* double mutant cells (Figure 6.7B). A Student's t-test suggested, however, that there was no significant difference in spindle formation ability between the two double mutants (p –value=0.18), although it may be that this is because the number of brains scored (n=6-7) is relatively low (Figure 6.7C). I conclude that in the absence of centrosomes and the augmin pathway, aMTOCs do not provide a major alternative pathway of spindle assembly; more samples will have to be analysed to see if the presence of aMTOCs subtly improves the efficiency of spindle assembly under these conditions.

6.9 aMTOCs nucleate monopolar MT arrays in the absence of centrosomal and chromosomal spindle assembly

Next, I decided to test the impact of aMTOCs in the absence of the centrosomal and chromosomal pathway of MT formation. In the chromosome-mediated spindle assembly pathway MTs are nucleated in the vicinity of the chromosomes and their plus ends are captured by the kinetochores and continue to grow from there (discussed in Section 1.4.2). Misato (Mst) is needed for kinetochore driven MT growth, and flies with mutations in *misato (mst)* are larval lethal as cells fail in mitosis due to low MT density and monopolar spindles (Mottier-Pavie et al., 2011). Interestingly, it has been shown that mitotic cells double mutant for *mst* and *DSas-4* often exhibit monopolar acentrosomal MT arrays. Furthermore, when MTs were depolymerised in these cells by cold treatment, MT arrays could regrow after release from cold from several foci in the cytoplasm; these MTs later coalesced to form a monopolar MT array (Mottier-Pavie et al., 2011). The origin of these MT-nucleating foci was unclear.

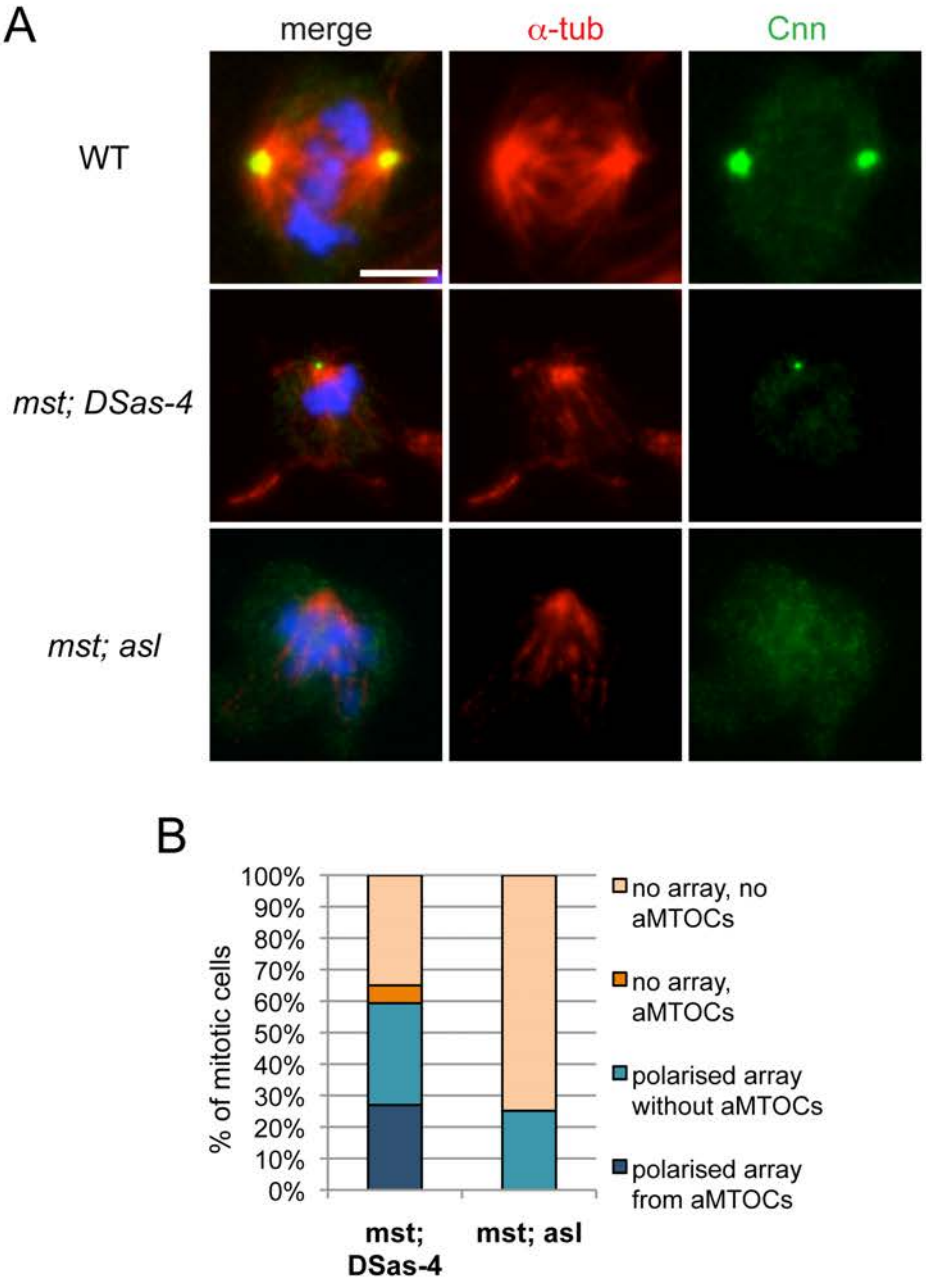

Figure 6.8: aMTOCs aid formation of microtubule arrays in the absence of centrosomal and chromosomal microtubule nucleation. (A) Mitotic brain cells of WT*; mst; DSas-4* and *mst; asl* double mutants stained with antibodies against α-tubulin (red) and Cnn (green), DNA is in blue. Note the mitotic spindle organised by the two centrosomes in WT, whereas *mst; DSas-4* cells and *mst; asl* double mutant cells only organise a monopolar array, which in the case of *mst; DSas-4* emanates from an aMTOC. Scale bar is 5μm. **(B)** Mitotic phenotypes were quantified in *mst; DSas-4* (n=263 cells in 8 brains) and *mst; asl* (n=326 cells in 9 brains) larval brains.

To test whether these foci consisted of the aMTOCs that I observed in cells without centrosomes I stained *mst; DSas-4* double mutants with antibodies against α-tubulin, Cnn and Phospho-Histone H3 (to identify mitotic cells). I found that the monopolar MT arrays formed in *mst; DSas-4* cells were emanating from Cnn foci in the cytoplasm, and therefore, presumably, from aMTOCs (Figure 6.8A). I also stained with anti-Asl antibodies to confirm the absence of centrioles (not shown). To test whether aMTOCs were essential for the formation of these monopolar arrays I generated an *mst; asl* double mutant strain. When analysing *mst; asl* brains stained with anti-α-tubulin and anti-Cnn, some cells could still be identified that were forming monopolar arrays, although these were not emanating from an aMTOC (as judged by the lack of Cnn staining at the poles) (Figure 6.8A). I proceeded to quantify MT array formation in mitotic *mst; DSas-4* and *mst; asl* cells. I confirmed that in accordance with Mottier-Pavie et al., ~ 60 % of all mitotic *mst; DSas-4* cells contained MT arrays. Furthermore, I found that 27% of these MT arrays were coming from a detectable aMTOC, defined by the presence of Cnn at the pole (Figure 6.8B). In *mst; asl* brains, however, only ~ 25 % of all mitotic cells contained MT arrays with none of these arrays coming from an aMTOC. These data suggest that aMTOCs either help to establish and/or maintain ~50% of these monopolar spindle arrays.

In order to test whether aMTOCs are required to nucleate monopolar arrays or are just stabilising them, I performed a MT-regrowth assay after cold treatment by incubating brains on ice for 40 minutes and fixing them at several time points after reintroduction to room temperature. First, I tested whether the foci from which Mottier-Pavie and colleagues observed MT nucleation in *mst; DSas-4* cells after cold treatment indeed were aMTOCs by staining brains with anti-Cnn and anti-α-tubulin. I could see that MTs grew back from one or several Cnn-marked aMTOCs in the cytoplasm after ~2 min,

elongated further after ~5 min and appeared to coalesce into one large acentrosomal monopolar array with one Cnn-marked aMTOC at its pole after ~10 min (Figure 6.9A). Next, I quantified regrowth of MT arrays in mitotic *mst; DSas-4* and *mst; asl* cells at different time points (0 min, 2 min, 5 min, 10 min, 20 min and 30 min) after return to room temperature. The number of cells with monopolar MT arrays grew steadily in *mst; DSas-4* cells, until after 30 min nearly 50% of cells contained MT arrays again. Remarkably, in *mst; asl* cells no significant regrowth of MT arrays could be observed, with less than 5% of cells exhibiting MT arrays even after 30 min (Figure 6.9B). This result suggests that in the absence of aMTOCs, MT arrays cannot efficiently be rebuilt after cold treatment in cells that lack the centrosomal and chromatin pathways of spindle assembly.

It is not clear how the MT arrays that lack aMTOCs and are found in ~25 % of mitotic *mst; asl* cells (shown in Figure 6.8B) are nucleated. The cold treatment assay shows, however, that even after a 30 min recovery period these MT arrays cannot self assemble in the absence of aMTOCs. One possibility is that these MT arrays were originally nucleated from already existing MTs (e.g. interphase MTs), and that upon their depolymerisation by cold treatment these MTs were no longer available as MT nucleation sites. My data show that although aMTOCs play a minor role when other spindle assembly pathways are active, they can actively nucleate and focus monopolar MT arrays in the absence of these pathways. Furthermore, this result is important as it shows that aMTOCs do not just passively localise to the minus ends of coalescing MTs but indeed can function as MT organising centres.

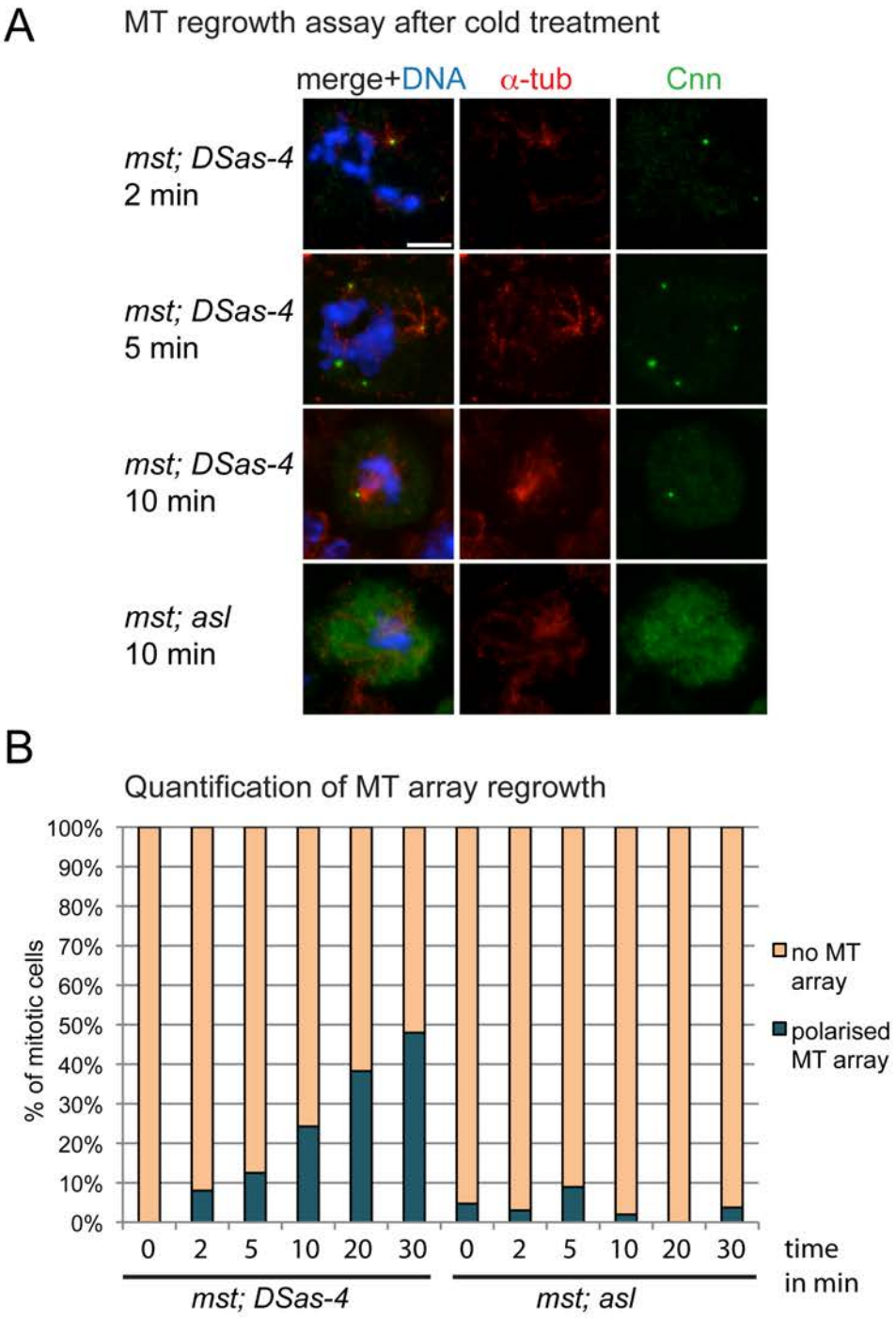

Figure 6.9: aMTOCs are required for re-assembly of MT arrays in the absence of centrosomal and chromosomal MT nucleation in cells after cold treatment. (A) *mst; DSas-4* brains were cold treated to depolymerise MTs. MT regrowth from aMTOCs was observed at several time points after return to room temperature by fixation of brains and staining α-tubulin (red) and Cnn (green). DNA is in blue. Scale bar is 5μm. **(B)** Regrowth of monopolar MT arrays was quantified at different time points after release from cold treatment in *mst; DSas-4* and *mst; asl* brains (n= at least 43 cells from 4 brains for each timepoint). No regrowth at any time could be observed in *mst; asl* cells.

6.10 aMTOCs can contribute to spindle focusing in the absence of centrosomes and the kinesin Ncd/HSET

Members of the kinesin-14 family, such as *Drosophila* Ncd or its mammalian homologue HSET, have been shown to be essential for acentrosomal spindle assembly in *Drosophila* oocytes (Hatsumi and Endow, 1992; Matthies et al., 2013), mouse oocytes (Mountain et al., 1999), *Arabidopsis* (Ambrose et al., 2005), and centrosome free *Xenopus* meiotic extracts (Walczak et al., 1998). These molecular motors can crosslink and focus MT minus-ends into two spindle poles independently of centrosomes through their MT-binding sites at their N- and C-termini and their MT-minus end directed motor activity. Accordingly, acentrosomal *Drosophila* S2 cells in which *ncd* and *DSas-4* have been knocked down have severely unfocused spindle poles (Moutinho-Pereira et al., 2009). Interestingly, Ncd is also essential to cluster supernumerary centrosomes (Basto et al., 2008; Kwon et al., 2008) and aMTOCs (Kleylein-Sohn et al., 2013; Moutinho-Pereira et al., 2009) to mitotic spindle poles. In addition to Ncd, the MT-minus end directed motor dynein also contributes to focusing aMTOCs at acentriolar poles in S2 cells, although its role was found to be less important than Ncd (Moutinho-Pereira et al., 2009). The authors suggested that these motors lead to localisation of aMTOCs to spindle poles both by keeping MT minus ends clustered, and by minus-end directed transport of aMTOCs to acentriolar poles.

To test whether MT-minus end directed motors are essential for aMTOC localisation to spindle poles in *Drosophila* cells *in vivo* I generated *DSas-4, ncd* and *DSas-4, dynein heavy chain (dhc)* double mutants. I saw that, as expected, in both double mutants many

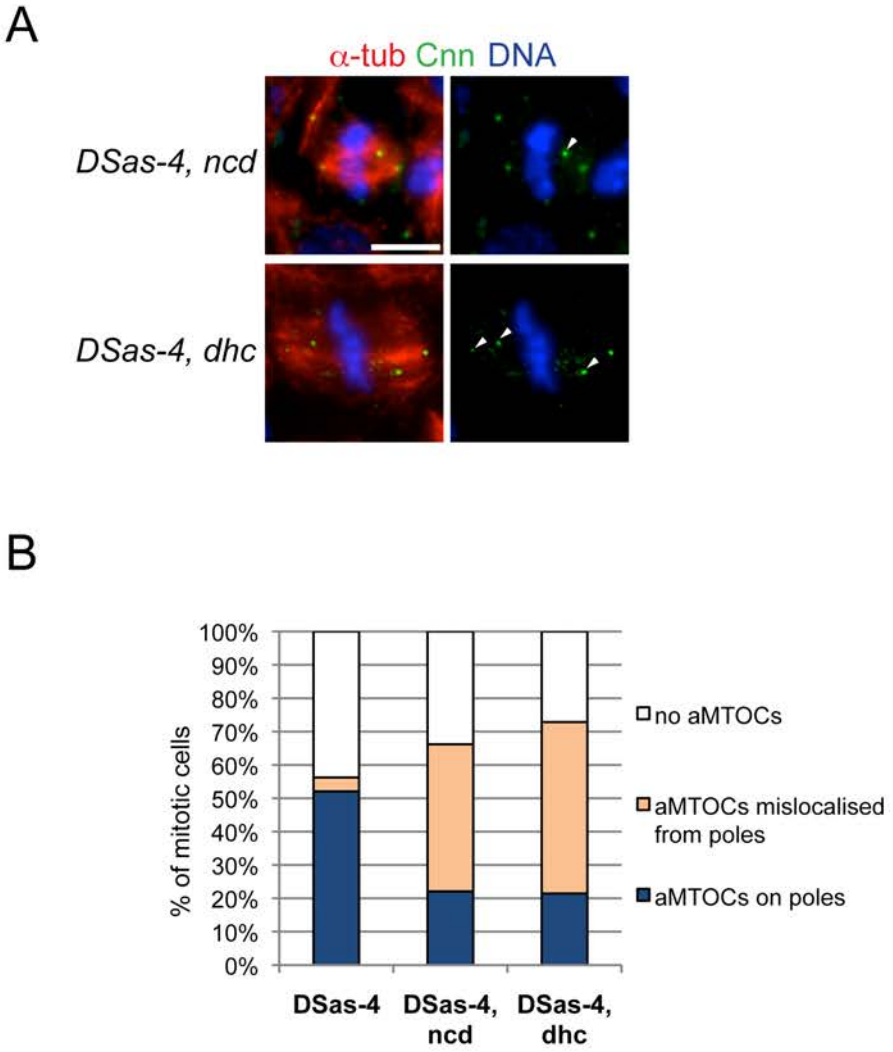

Figure 6.10: MT minus-end directed motor proteins Ncd and Dynein are required to localise aMTOCs to spindle poles. (A) Immunostaining of *DSas-4, ncd* and *DSas-4, dhc* larval brain cells (α-tubulin in red, Cnn in green, DNA in blue). Note that aMTOCs often are mislocalised from spindle poles (white arrowheads). Scale bar 5μm. **(B)** Quantification of aMTOC localisation (n=48 cells in 6 brains for *DSas-4,* n=68 cells in 6 brains for *DSas-4, ncd* and n=70 cells in 6 brains for *DSas-4, dhc)*.

cells had more than two aMTOCs, which were often mislocalised from spindle poles (Figure 6.10A, mislocalised aMTOCs marked by arrowheads). I quantified localisation of aMTOCs and saw that in both double mutants ~22% of cells had normal aMTOCs that were localised to the poles (Figure 6.10B). However, ~44% of *DSas-4, ncd* cells and ~51% of *DSas-4, dhc* cells contained aMTOCs that were mislocalised form the spindle poles, whereas in comparison only ~4% of *DSas-4* cells contained aMTOCs that were mislocalised from the poles (Figure 6.10B).

Intriguingly, I noticed that in *DSas-4, ncd* cells poles with aMTOCs often appeared to be better focused than poles lacking aMTOCs (white arrow in Figure 6.11B), suggesting that aMTOCs could play a role in helping the spindle to focus in the absence of Ncd. I decided to test this hypothesis by comparing *DSas-4, ncd* and *asl, ncd* double mutants. Given that Ncd is essential for acentrosomal spindle assembly, it was not surprising that both *DSas-4, ncd* and *asl, ncd* flies were homozygous lethal in early pupal stages. When dissecting brains of both fly strains, however, I noticed that there was a striking difference between the two double mutants: while *DSas-4, ncd* brains looked relatively normal and third instar larvae had imaginal discs, *asl, ncd* brains of the same stage were very small and these mutants had discs that were severely reduced in size, indicating a strong defect in cell proliferation (Gatti and Goldberg, 1991) (Figure 6.11A). I stained brain cells with anti-α-tubulin, anti-Cnn and anti-Phospho-Histone H3 to analyse mitotic cells. In both *DSas-4, ncd* and *asl, ncd* some cells had mitotic spindles, although many spindles were

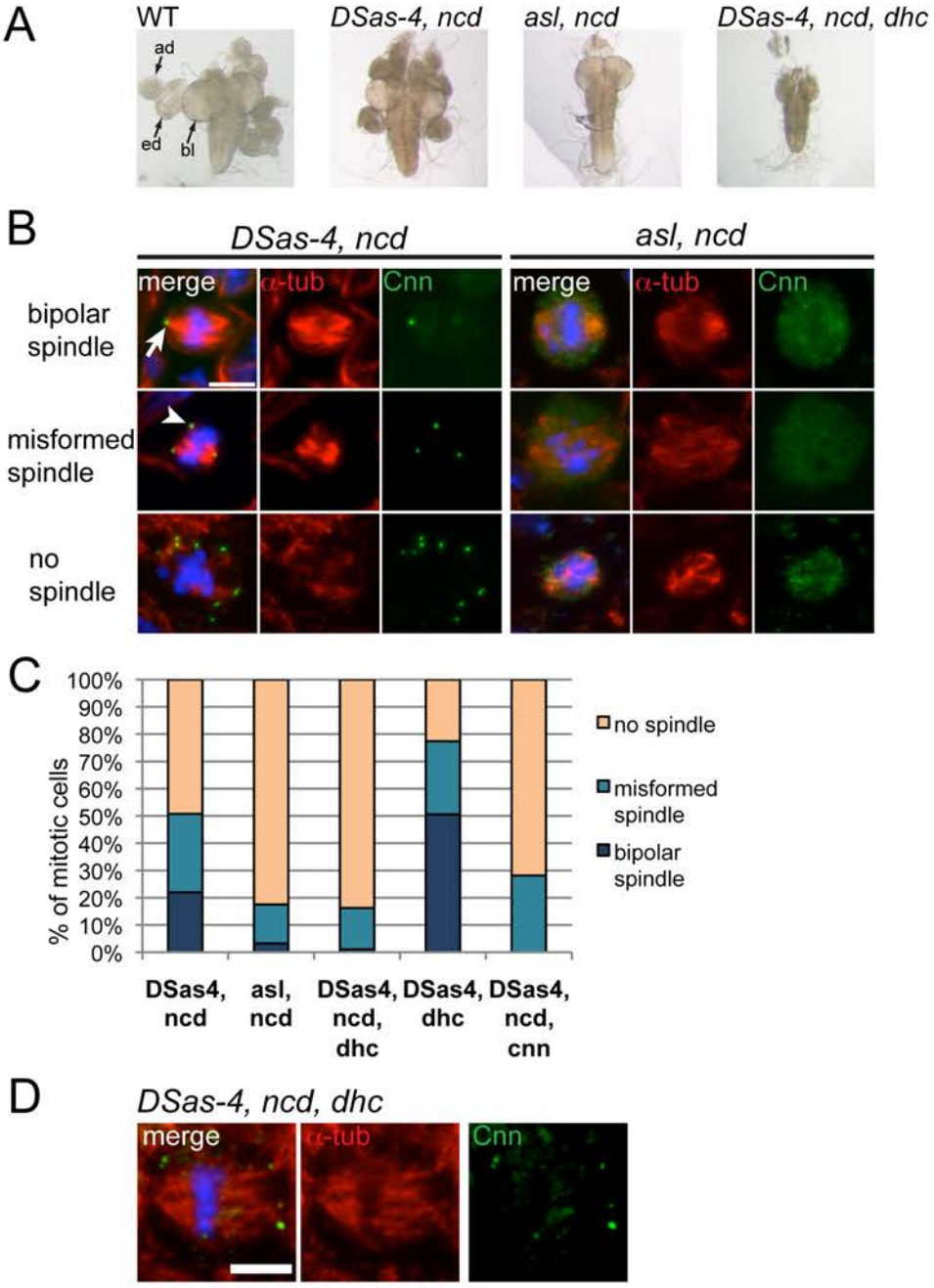

Figure 6.11: aMTOCs can contribute to spindle focusing in the absence of centrosomes and the kinesin Ncd/HSET. (A) 3rd instar larval brains from WT (bl=optic brain lobe, ed=eye disc, ad=antennal disc) and different mutants. *DSas-4, ncd* brains are relatively normal sized, whereas *asl, ncd* and *DSas-4, ncd, dhc* brains and discs are much smaller. **(B + D)** Larval brains stained with anti-Cnn (green) and anti-α-tubulin (red). DNA in blue. **(B)** Note increased focussing of spindle pole with an aMTOC in *DSas-4, ncd* (arrow) and formation of multipolar spindles (arrowhead). **(C)** Quantification of spindle phenotypes in mitotic cells (n=132 cells in 7 brains for *DSas-4, ncd* and 77 cells in 8 brains for *asl, ncd,* 197 cells in 16 brains for *DSas-4, ncd, dhc,* 71 cells in 5 brains for *DSas-4, ncd, cnn* and 93 cells in 7 brains for *DSas-4, dhc).* **(D)** *DSas-4, ncd, dhc* triple mutant cells have very few misformed spindles with broad poles. All scale bars are 5μm.

poorly focused and multipolar, and many mitotic cells did not have spindles at all (Figure 6.11B). I quantified the mitotic spindle phenotypes in *DSas-4, ncd* and *asl, ncd* brain cells. Strikingly, while 51% of all mitotic *DSas-4, ncd* had formed bipolar or misformed spindles, only 14% of *asl, ncd* cells had succeeded in doing so (6.11C). This suggests, that aMTOCs provide a mechanism to focus mitotic spindles in the absence of Ncd.

It has been shown that although the minus end directed motors Ncd and Dynein have slightly overlapping functions, Ncd is primarily required for focusing K-fibres, while Dynein transports K-fibres to the centrosomes in *Drosophila* cells (Goshima, 2005) (Figure 6.12A). This lead me to the assumption that Dynein could possibly compensate for the loss of Ncd in acentrosomal cells by transporting K-fibres towards aMTOCs and thereby focusing spindle poles in *DSas-4, ncd* cells. According to this hypothesis *asl, ncd* cells would struggle more in bipolar spindle assembly because they have no aMTOCs towards which Dynein could transport K-fibres. If this hypothesis was true, loss of Dynein in *DSas-4, ncd* cells should lead to a phenotype similar to the one in *asl, ncd* cells. I generated *DSas-4, ncd, dhc* triple mutants and saw that, similarly to *asl, ncd* double mutants, these had very small brains and imaginal discs (Figure 6.11A). Quantification of spindle phenotypes showed that only ~16% of *DSas-4, ncd, dhc* cells had recognisable mitotic spindles (Figure 6.11C), which had unclustered, broad poles (Figure 6.11D). This effect was not due to the loss of Dynein *per se*, as in *DSas-4, dhc* double mutants 77% of cells had a recognisable spindle (Figure 6.11C). Furthermore, I confirmed that the loss of aMTOCs, and not a different possible function of Asl, lead to the impairment of spindle focusing in *asl, ncd* cells by testing *DSas-4, ncd, cnn* triple mutant cells, which also cannot form aMTOCs. These mutants form spindles in only ~28% of cells (Figure 6.11C).

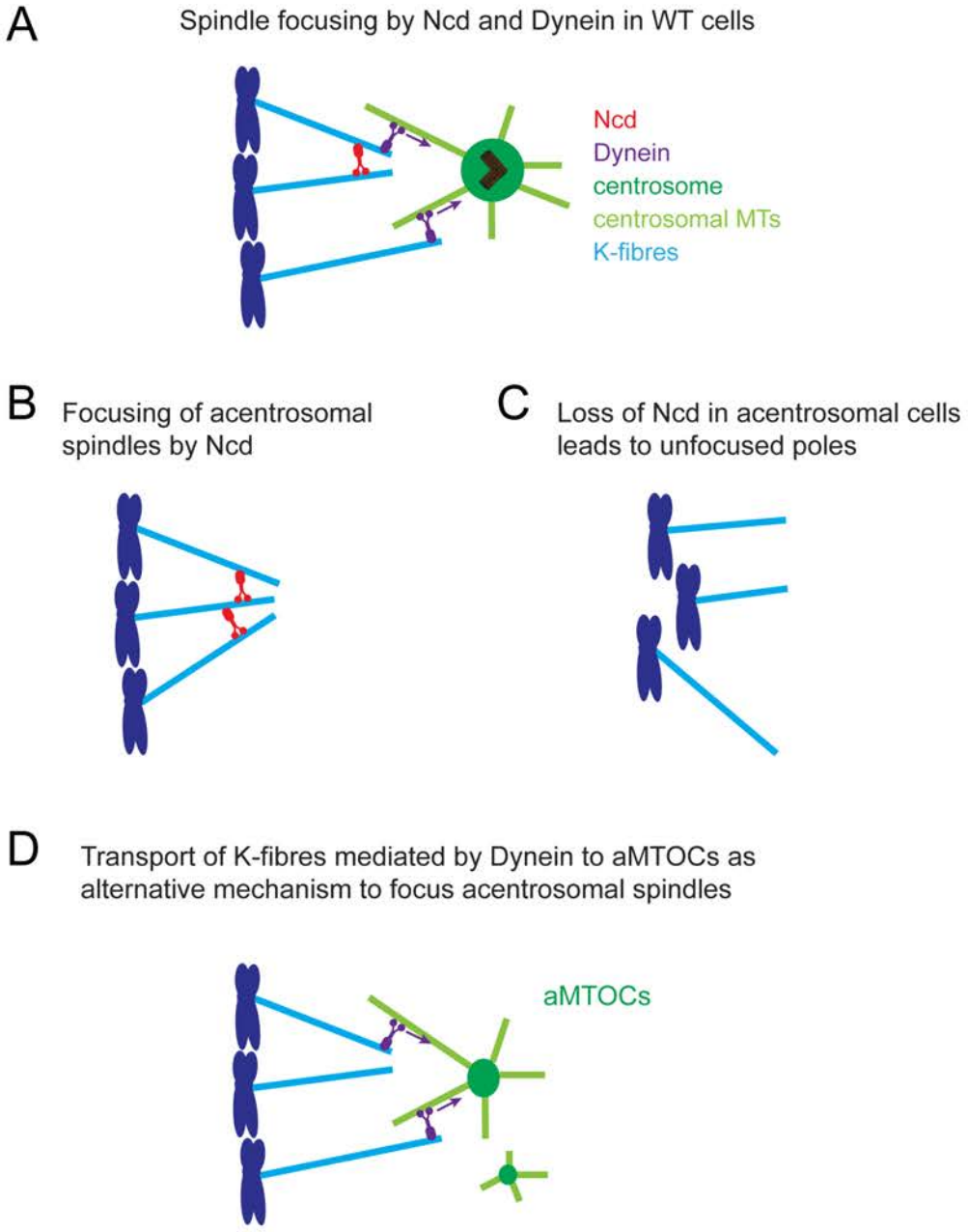

Figure 6.12: A model for alternative ways of spindle focusing in acentrosomal cells. **(A)** In cells with centrosomes, K-fibres (light blue) become crosslinked by minus end-directed motors (predominantly Ncd in *Drosophila*, in red) and other minus-end directed motors (primarily Dynein, in purple) transport the K-fibers along centrosomal MTs (light green) to the pole. Note that Ncd presumably has a second role in capturing and transporting K-fibers over a small distance along centrosomal MTs which is not shown in this schematic (Goshima et al., 2005). **(B)** In cells lacking centrosomes Ncd is required for focusing acentrosomal spindle poles by crosslinking K-fibres. **(C)** Loss of Ncd in acentrosomal cells leads to severe impairment of spindle focusing. **(D)** In acentrosomal cells with aMTOCs (for example *DSas-4, ncd* mutant cells) Dynein can transport K-fibres towards aMTOCs and thereby aid in spindle pole focusing and partly compensate for the loss of Ncd.

Thus, my data suggest the following model: In the absence of centrosomes, Ncd is required to crosslink K-fibres and lead to formation of a bipolar spindle (Figure 6.12B). In the absence of centrosomes and Ncd, cells struggle to form recognisable mitotic spindles, as spindle poles cannot be focused (Figure 6.12C) (Moutinho-Pereira et al., 2009). If aMTOCs are present in cells, Dynein motors can transport K fibers towards these, and thereby aid in spindle formation (Figure 6.12D). One caveat of this mechanism might be that there often are more than two aMTOCs in *DSas-4, ncd* cells, which can presumably lead to multipolar spindle formation (indicated by the white arrowhead in Figure 6.11B). Although spindle focusing by Dynein and aMTOCs does not fully rescue larval development, as these mutants are still pupal lethal, it does enable them to form mitotic spindles in half of their cells and develop brains and imaginal discs that are almost the size of WT brains and discs (Figure 6.11A).

6.11 Asterless-dependent aMTOCs are not required for nuclear migration in oocytes in the absence of centrosomes

One advantage of *Drosophila* as a model system is that it enables us to assess the role of aMTOCs during the development of the organism and in different cell types. Both *DSas-4* and *asl* mutants develop to adulthood and eclose as morphologically normal adults, although they are uncoordinated due to the lack of cilia in sensory neurons (Basto et al., 2006; Blachon et al., 2008). This suggests that the lack of aMTOCs in the *asl* mutant does not lead to any obvious developmental defects in addition to the defects already seen in the *DSas-4* mutant. Nevertheless I wondered whether aMTOCs might be required in certain stages of development. Dorso-ventral axis patterning in

Drosophila, for example, takes place when the oocyte nucleus migrates from the posterior to the anterior margin of the oocyte. It has recently been shown that MTs emerging from the centrosome, which is located just behind the nucleus, provide the pushing forces that lead to nuclear migration (Zhao et al., 2012). The centrosome is, however, not essential for normal oogenesis (Stevens et al., 2007). This has been postulated to be because in *DSas-4* mutant oocytes, that lack centrosomes, acentrosomal MTOCs marked by GFP-Cnn are formed, and can provide the pushing forces needed for nuclear migration (Zhao et al., 2012). I wondered whether the aMTOCs formed in *DSas-4* oocytes resemble the aMTOCs that I have described here in *Drosophila* brain cells. If aMTOCs are required for nuclear migration in *DSas-4* oocytes, and if these aMTOCs are formed in an Asl-dependent fashion similarly to the aMTOCs in brain cells, then a failure of nuclear migration would be expected in *asl* mutant oocytes. In order to test this hypothesis, I fixed and stained matured egg chambers from female *asl* flies. In all stage 8-9 oocytes that I observed, the nucleus had migrated correctly to the anterior margin of the oocyte (Figure 6.13). To test this result in a different way, I tested *cnn; spd-2* oocytes, in which any centrosomal or aMTOC-mediated MT nucleation should be abolished (Conduit et al., manuscript in preparation). The nucleus had migrated correctly in all *cnn; spd-2* oocytes as well (Figure 6.13). I tried to assess whether Cnn-marked aMTOCs could still form in *asl* mutant oocytes, but could not visualise aMTOCs by antibody staining with anti-Cnn in WT oocytes (data not shown). Presumably they can only be visualised with GFP-Cnn, but I could not assess this yet due to time constraints.

My results indicate the GFP-Cnn dots observed by Zhao et al. are unlikely to be solely responsible for providing the pushing forces needed for nuclear migration.

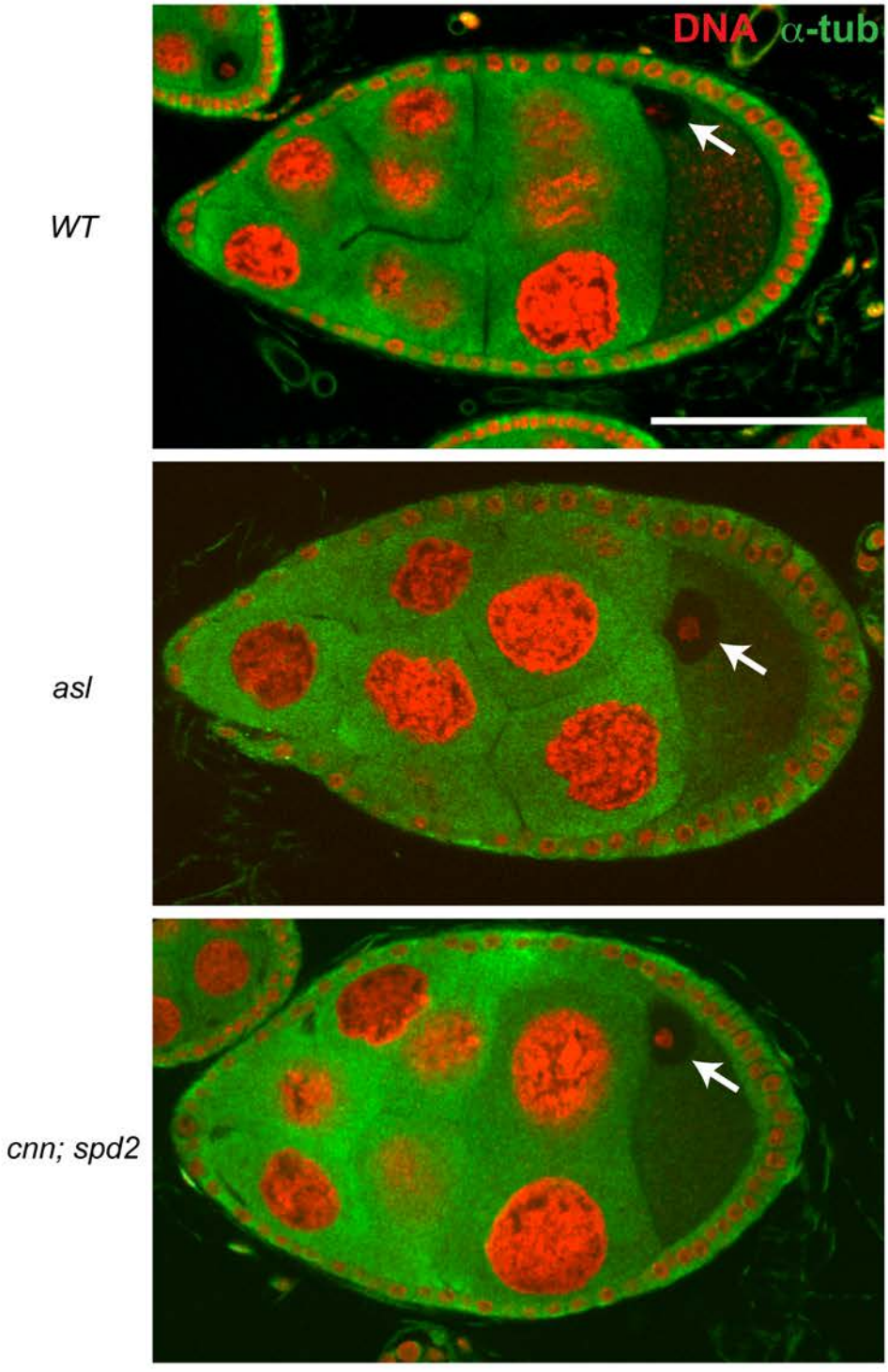

Figure 6.13: Asl-dependent aMTOCs are not required for nuclear migration in oocytes in the absence of centrioles. Egg chambers of *WT, asl and cnn; spd-2* females were fixed and stained with anti-α-tubulin (green) and Hoechst (red). Scale bar is 50μm. (n= at least 10 stage 8-9 oocytes per genotype). Nuclei are in the right position in all cells (see arrows).

Alternatively, the GFP-Cnn marked aMTOCs observed in oocytes might be different to the aMTOCs described in this chapter, and do not depend on Asl, Spd-2 and Cnn for their formation and function. In either case, my data show that *Asl*-dependent aMTOCs are not required for nuclear migration in *Drosophila* oocytes.

6.12 Discussion

I show here, that *Drosophila* cells without centrosomes often form acentrosomal MTOCs that cluster at mitotic spindle poles and consist of many known PCM proteins including Cnn, Spd-2, γ-tubulin, DPLP, Aurora A, DTACC, Dgp71WD and Msps. Formation and function of aMTOCs is dependent on the PCM protein Cnn, presumably by its ability to act as a scaffold and recruit further PCM proteins as γ-tubulin. Spd-2 is indirectly required for aMTOC function through its ability to recruit Cnn to aMTOCs. Remarkably, the centriolar protein Asl, which normally is required to recruit PCM to centrosomes (Bonaccorsi et al., 1998; Conduit et al., 2010; Varmark et al., 2007), is essential for aMTOC formation in cells without centrioles. Interestingly, it has been shown that overexpression of an Asl form lacking the N-terminus, which cannot bind to Sak anymore, leads to formation of multiple aMTOCs in *Drosophila* embryos (Dzhindzhev et al., 2010a). This truncated Asl protein could still bind to DSas-4, and furthermore, overexpression of DSas-4 could also lead to aMTOC formation. DSas-4 was, however, not essential for aMTOC formation in our system, as *DSas-4* mutants still formed aMTOCs.

My data suggest that even in the absence of centrioles endogenous levels of Asl can mediate formation of active PCM that nucleates MTs, presumably by providing a platform to which Spd-2 and Cnn can bind and become activated. This result is

surprising, because Asl cannot be detected in the aMTOCs. We could neither detect it by immunostainings nor live, and not even by boosting Asl-GFP signal with GFP booster, which is used in our lab to visualise even very scarce proteins. This suggests that cytoplasmic levels of Asl are sufficient to "catalyse" formation of active PCM, which subsequently clusters together. It has been shown, that during PCM recruitment Spd-2 and Cnn are recruited to the centre of the centrosome first (where Asl is localised) by Asl and subsequently released from their binding sites and slowly move outwards through the PCM (Conduit et al., 2010; Conduit et al., manuscript in preparation). This suggests that these PCM proteins can become "activated" by Asl but do not need to be permanently bound to Asl while still forming active PCM. This potentially provides an explanation for why we cannot detect Asl localisation in aMTOCs. In contrast, in cells containing centrioles, these presumably serve as a platform to concentrate Asl function to a certain place inside the cytoplasm and thereby suppress formation of aMTOCs in the cytoplasm.

The presence of aMTOCs has been described in *Drosophila* S2 cell lines (Moutinho-Pereira et al., 2009), and their formation was shown to be dependent on Cnn. My demonstration that *asl* mutants cannot form aMTOCs enabled us, for the first time, to perform a functional comparison between cells lacking centrosomes but forming aMTOCs, and cells that lack both. We assessed the biological significance of aMTOCs and analysed their contribution to spindle assembly by comparing *DSas-4* mutants (that lack centrosomes but can form aMTOCs) with *asl* mutants (that lack centrosomes and lack aMTOCs). In addition, the interplay of aMTOC mediated MT nucleation with other MT nucleation pathways like the chromosomal and the augmin pathway could be analysed by comparing different *asl* or *DSas-4* double mutants. Our analysis showed, that while aMTOCs only play a minor role in the absence of centrosomes, they can

partly compensate and nucleate monopolar MT arrays when both centrosomal and chromosomal MT nucleation are abolished. In contrast, in the absence of augmin-mediated MT nucleation, aMTOCs provide no, or only a very modest, advantage for spindle formation.

Interestingly, aMTOCs can provide an alternative mechanism for focusing an acentrosomal spindle when the minus-end directed motor protein Ncd is missing. The compensatory effect of aMTOCs in spindle focusing is dependent on Dynein, as cells that have aMTOCs but lack both Ncd and Dynein (*DSas-4, ncd, dhc* triple mutants), can form hardly any spindles, similar to cells that lack both aMTOCs and Ncd (*asl, ncd* double mutants) (Figure 6.11C). Failure in spindle formation in both of these strains leads to underdeveloped brains and imaginal discs in larvae (Figure 6.11A). I suggest a model in which in cells lacking centrosomes and Ncd the motor protein Dynein, which is known to transport K-fibres towards centrosomes (Goshima, 2005), can transport K-fibres towards aMTOCs and thereby aid in spindle focusing (Figure 6.12D).

Furthermore, I have shown here that Asl-dependent aMTOCs are not required for nuclear migration in oocytes, suggesting, that either aMTOCs observed in acentrosomal oocytes are formed by a different pathway, or that there is a different compensatory pathway that mediates nuclear migration in the absence of aMTOCs.

In my transcriptional analysis I have used *DSas-4* and *DSas-6* mutants to analyse how cells deal with the loss of centrosomes, and have found that they cope surprisingly well with no common genes misregulated between the two mutants (as discussed in chapter 5 of this thesis). I here show that both *DSas-4* and *DSas-6* mutants have the ability to form aMTOCs in many cells. It could be that aMTOCs can partly compensate for the

loss of centrosomes in mitotic cells, and therefore potentially help explain why these cells were so normal in my transcriptional analysis. In order to test this hypothesis it would be interesting to repeat the transcriptional analysis with *asl* mutants, which lack both centrosomes and aMTOCs. On the other hand, our data suggest that it is perhaps unlikely that aMTOCs play a major role in driving spindle assembly in the absence of centrosomes.

Many tumour cells have supernumerary centrosomes, and centrosome amplification can make cells prone to tumourigenesis (Basto et al., 2008). Cells with amplified centrosomes rely on Ncd/HSET to cluster centrosomes to two spindle poles and so avoid multipolar mitoses (Basto et al., 2008; Kwon et al., 2008). Interestingly, it has recently been shown that cancer cell lines rely on HSET for survival even when they have normal numbers of centrosomes (Kleylein-Sohn et al., 2013). This is due to increased aMTOC formation in cancer cells, which then need to be clustered into a bipolar spindle by HSET to avoid multipolar mitoses. Equivalently, in *Drosophila* Ncd contributes to focusing aMTOCs to acentriolar poles in cultured cells (Moutinho-Pereira et al., 2009) and *in vivo* (Figure 6.10A, arrowheads). It will be of great interest in the future to analyse if overactivity of aMTOCs can make cells prone to tumourigenesis. This could happen, for example, through the formation of merotelic attachments to chromosomes that takes place when cells pass through multipolar spindle intermediates in mitosis before these spindles become clustered by Ncd/HSET (be it in the presence of extra centrosomes, or in the presence of aMTOCs). These merotelic attachments lead to chromosomal instability (Ganem et al., 2009; Silkworth et al., 2009) which, at a low level, can be a driver of tumourigenesis (Weaver and Cleveland, 2009; Weaver et al., 2007). Studying aMTOCs in *Drosophila* cells could provide a useful model to study the

effects of aMTOCs in cells, which might give insight into why cancer cells have an overactivity of aMTOCs and whether this can be a driving force of tumourigenesis.

7 General Discussion

7.1 Introduction

During my DPhil I have analysed both the mechanisms that lead to a mitotically active centrosome and the consequences of centrosome loss. In this final chapter I will discuss my results in a broader context. I will first address the implications my results have on the view of how centrosome defects are linked with tumourigenesis in *Drosophila*. Then I will discuss the mechanisms of centrosome formation and the importance of the centrosome as a cell organelle in the context of the evolution of the centrosome assembly pathway.

7.2 Centrosomes and tumourigenesis in *Drosophila*

Centrosome amplification is a common feature of many cancers (Chng and Fonseca, 2009; Guo et al., 2007; Jung et al., 2007; Kawamura et al., 2003; Kayser et al., 2005; Nakajima et al., 2004; Pihan et al., 1998; Pihan et al., 2001) and centrosome defects appear in the earliest identifiable steps in human cancer (Lingle et al., 2002; Pihan et al., 2003) (Section 1.2.1). There is, however, little direct experimental evidence that addresses how centrosome defects could cause tumourigenesis (Zyss and Gergely, 2009). The first potentially causative relationship between centrosome amplification and tumourigenesis has been demonstrated in *Drosophila*, where transplantation of tissue with amplified centrosomes into the abdomen of an adult fly can lead to neoplastic overgrowth of the respective tissue (Basto et al., 2008). The centrosome amplification in this system was driven by the overexpression of a single gene (Sak/Plk4) whose only known function is in promoting centriole assembly, thus providing strong evidence that

centrosome amplification is indeed sufficient to predispose certain tissues to tumour formation. Similarly, transplantation of *Drosophila* tissues lacking centrosomes (via the mutation of *DSas-4*) also lead to tumour formation in this assay (Castellanos et al., 2008).

Why does the loss or amplification of centrosomes predispose some fly tissues to form tumours? It has been postulated that in *Drosophila* brains centrosome defects can drive tumourigenesis because of the failure in asymmetric NB divisions (Castellanos et al., 2008; Gonzalez, 2007). Nevertheless, while a failure in asymmetric division can clearly lead to an expansion of the NB pool and so to over-proliferation, it is unclear how centrosome malfunction promotes malignant transformation of these tissues (Basto et al., 2008; Castellanos et al., 2008; Caussinus and Gonzalez, 2005). It has been suggested that although flies with abnormal centrosome numbers appear to be capable of progressing through most of their development relatively normally, cell physiology could actually be significantly perturbed by these defects (Gonzalez, 2008), and there is evidence that centrosome defects increase cellular stress (Mikule et al., 2007; Srsen, 2006; Uetake et al., 2007). Furthermore, cellular stress has been implicated in tumourigenesis in other *Drosophila* tumour models (Rossi and Gonzalez, 2011; Wu et al., 2010), raising the possibility that the stress induced by centrosome defects may contribute to tumourigenesis in the abdominal transplantation models.

My microarray analysis of flies developing without centrosomes or with amplified centrosomes, however, strongly suggest that these perturbations do not result in dramatic changes in cell physiology, and I could detect no induction of any stress response in these cells (Chapter 5). If tissues with centrosome defects are relatively normal, then how do these cells ultimately acquire malignant traits, including the ability

to metastasise, chromosomal instability and immortality (Basto et al., 2008; Castellanos et al., 2008; Caussinus and Gonzalez, 2005), all of which almost certainly require large-scale changes in gene expression (Ramaswamy et al., 2002; Scott et al., 2011)? It is known that cells that have lost their centrosomes or have extra centrosomes have a small increase in chromosome segregation errors (Basto et al., 2008; Basto et al., 2006; Ganem et al., 2009; Silkworth et al., 2009). Chromosomal instability has been assumed to contribute to tumourigenesis for a long time (Boveri, 2008, Boveri 1914) and although mutations that lead to large-scale chromosomal instability do not lead to tumour formation in *Drosophila* (Castellanos et al., 2008), there is evidence that the low-level of chromosomal instability induced by centrosome defects could actually be a more effective driver of cancer (Weaver and Cleveland, 2009; Weaver et al., 2007). I suggest that overproliferation of the brain stem cells due to failures in asymmetric divisions might not be the only cause that leads to tumour formation of *Drosophila* brain tissue with centrosome defects. Rather, it is possible that in addition to the stem cell overproliferation the low level of chromosome missegregation could facilitate mutations that occasionally could lead to the generation of a malignant stem cell, which ultimately drives tumour formation. Mutations that arise in individual cells would not have been detected by my microarray analysis. It would be interesting to test whether the low level of chromosomal instability in cells without centrosomes or with too many centrosomes leads to the accumulation of mutations in neuroblasts, and transcriptional profiling experiments on single cells could answer this question in the future.

The observation that several cancer cell lines can have aMTOCs even when they have normal numbers of centrosomes is highly interesting, as these aMTOCs need to be clustered by HSET in the same fashion as supernumerary centrosomes need to be clustered (Kleylein-Sohn et al., 2013). Therefore, it is possible that clustering of

aMTOCs into two spindle poles could lead to transient merotelic attachments of the chromosomes in the same way as too many centrosomes do, thereby promoting low level chromosomal instability (Ganem et al., 2009; Silkworth et al., 2009) (Section 6.12). I propose that studying *Drosophila* cells dividing with aMTOCs could potentially give valuable insights into why cancer cells seem to upregulate the formation of aMTOCs and whether these aMTOCs can promote tumourigenesis (Chapter 6). It is for example known that *DSas-4* and *DSas-6* mutant tissues which both have aMTOCs form tumours in abdominal transplantation assays. It has, however, not been tested yet whether *asl* null mutants that lack aMTOCs form tumours as well. It will be very interesting to assess this in the future and could give insight into why *Drosophila* cells with abnormal centrosome numbers form tumours, and whether aMTOCs have the ability to promote tumourigenesis.

7.3 The evolution of the centrosome assembly pathway

During early studies the centrosome was predominantly seen as the organelle that is at the poles of the mitotic spindle, leading to the assumption that the first and foremost role of the centriole lies in facilitating mitosis (Boveri, 1914; Boveri, 2008). During the last decades, however, several studies have shown that centrosomes are often not essential for spindle assembly and cell division (Azimzadeh et al., 2012; Basto et al., 2006; Debec et al., 1995; Gueth-Hallonet et al., 1993; Khodjakov et al., 2000; Lecland et al., 2013). These observations even lead to the contrasting idea that cilia formation might be the major function of the centriole and that centrosomes function primarily to ensure that the two centriole pairs in a cell are placed on opposite poles of the mitotic spindle to ensure that each daughter cell inherits one pair of centrioles (Basto et al., 2006; Debec et al., 2010; Pickett-Heaps, 1971).

To understand these opposing arguments, one first needs to have a closer look at the evolution of centrioles and centrosomes. Centrioles presumably were present in the Last Eukaryotic Common Ancestor as they are found in all major eukaryotic groups (Carvalho-Santos et al., 2011; Cavalier-Smith, 2002). The major role of centrioles in early unicellular organisms was initially the formation of flagella, to provide cells with essential functions such as polarity, motion and sensation and to drive liquid flow enabling them to capture nutrients from the environment more efficiently (Debec et al., 2010; Marshall, 2009). Only when multi-cellular organisms arose, centrioles evolved to form centrosomes that functioned as MT cytoskeleton organisers. Centrioles were then lost again from some eukaryotic Phyla that do not form flagella, such as for example amoebas, yeast (these have modified centrosomes called spindle pole bodies, but lack a proper centriole) and higher plants (Cavalier-Smith, 2002). Importantly, all species without exception that form cilia/flagella at some point in their life cycle also have centrioles, and centrioles are essential for ciliogenesis (Dawe et al., 2006). Therefore the evolution of the centrioles is intimately linked with the evolution of cilia.

Bioinformatic approaches that assessed the conservation of proteins implicated in centriole duplication and ciliogenesis in a wide cross-section of eukaryotes have shown that the formation of centrioles to serve as basal bodies is ancestral and depends on a relatively small conserved core set of proteins (Carvalho-Santos et al., 2010; Hodges et al., 2010). The ancestral centriole was modified by addition of further gene products later in evolution, nonetheless these add-ons are not essential for centriole duplication (Marshall, 2009). Remarkably, the ability of centrioles to form a centrosome has only evolved later by adding on another set of genes, the “centrosomal” genes (for example PCM recruitment factors such as Spd-2/CEP192 and Asl/CEP152; conservation of Cnn/CDK5RAP2 was not assessed in this study), which are only present in Holozoa

(Hodges et al., 2010). Intriguingly, the set of proteins that is required for formation of mitotically active centrosomes can also get lost again in evolution when the function of centrioles to form mitotic centrosomes is lost. The planarian *S. mediterranea* uses multiciliated cells for locomotion, but does not contain centrioles in its proliferating cells or its non-ciliated differentiated cells, and remarkably it does not require centrioles at any stage of its development (Azimzadeh et al., 2012). These flat worms do not assemble centrosomes, but only assemble centrioles *de novo* during the differentiation of ciliated cells. Two protein families that are essential for PCM recruitment and therefore centrosome formation, Spd-2/CEP192 and Cnn/CDK5RAP2 were missing in the planarian *S. mediterranea* and the parasitic flat worm *S. mansoni,* and must presumably have been eliminated from the planarian genome together with the centrosome itself (Azimzadeh et al., 2012).

Hence, the evolution of centrosomal proteins, such as Asl/CEP152, Spd-2/CEP192 and Cnn/CDK5RAP2, conferred the ability to recruit PCM to centrioles. In flies Asl is special as it has a dual role: It is required for centriole duplication but it also functions in PCM recruitment (Blachon et al., 2008; Cizmecioglu et al., 2010; Conduit et al., 2010; Hatch et al., 2010; Sir et al., 2011; Varmark et al., 2007). These two separate roles appear to be mediated by separate domains of Asl. The N-terminus of Asl binds to Sak and this interaction is required for centriole duplication, while the C-terminal part of Asl binds DSas-4 and there is at least some evidence that this interaction might be required for PCM recruitment (Dzhindzhev et al., 2010a; Gopalakrishnan et al., 2011). It is very remarkable that Asl can not only confer PCM recruitment ability to centrioles when it localises there, but it can also lead to assembly of functional PCM by itself independently of centrioles. This has been shown by the overexpression of an Asl mutant construct that cannot bind to Sak anymore (Dzhindzhev et al., 2010a), and I

have demonstrated that even endogenous Asl has the ability to mediate formation of aMTOCs in the absence of centrioles (Chapter 6). This indicates that centrioles are not necessarily essential for PCM assembly, but rather they provide a platform for efficient PCM assembly and thereby restrict it to one specific place in the cytoplasm. It would be very interesting to see whether the assembly of PCM in aMTOCs in acentrosomal mutants is also regulated by phosphorylation of Spd-2 and Cnn, as appears to be the case in centrosomes (Chapter 3).

I have presented data that suggest that Sak is only needed to trigger cartwheel formation during centriole duplication, but not for PCM recruitment to the centrosome (Chapter 4). Do these data imply that Sak/PLK4 belongs to the ancestral core set of centriolar proteins? Interestingly, comparative genomics show that Sak/PLK4, although essential for centriole duplication in human cells and *Drosophila* (Bettencourt-Dias et al., 2005; Habedanck et al., 2005; Kleylein-Sohn et al., 2007), is not part of the conserved core set of centriolar components (Carvalho-Santos et al., 2010). Obviously this poses the question which protein then triggered centriole duplication in organisms that do not have Sak/PLK4. Presumably a Polo/PLK1 like protein triggered centriole biogenesis in ancestral eukaryotes, and a gene duplication of this protein then gave rise to Sak/PLK4 after the divergence of fungi and animal (Carvalho-Santos et al., 2010). Sak/PLK4 then evolved to become strictly correlated with centriole biogenesis, while Polo/PLK1 kept its other important roles in cell division (Archambault and Glover, 2009).

In the light of the evolution of centrosome formation, should centrosomes now be deemed as being essential for mitosis in animal cells or not? Do they have important functions for partitioning the chromosomal material into daughter cells, or are they dispensable for mitosis and simply localise to the poles of the mitotic spindle to “ensure

that each daughter cell inherits one pair of centrioles for ciliogenesis" (Pickett-Heaps, 1971)? As previously discussed, centrosomes are often not essential for spindle assembly and cell division (Azimzadeh et al., 2012; Basto et al., 2006; Debec et al., 1995; Gueth-Hallonet et al., 1993; Khodjakov et al., 2000; Lecland et al., 2013). Furthermore, my transcriptional analysis of cells lacking centrioles could not uncover any misregulation of gene expression due to the lack of centrioles, strongly suggesting that cell homeostasis is not dramatically perturbed (Chapter 5). This might be the case, because ancestral eukaryotic cells used centrioles solely for ciliogenesis and were using other pathways for mitotic spindle formation, and intriguingly these alternative pathways of spindle formation (Section 1.4) have been preserved during evolution even after centrioles evolved to take part in mitosis.

There is a lot of evidence, however, that once centrosomes started to participate in spindle assembly, many systems and cell types became dependent on having centrosomes for efficient mitosis. Centrosomes are very important to confer cell polarity (Bornens, 2012) and it is likely that planarians and parasitic flatworms only could afford to lose centrosomes because they undergo ways of embryonic cleavage that do not involve oriented cell divisions (Azimzadeh et al., 2012). In contrast, species closely related to flatworms, such as the basal flatworm *Macrostomum*, still have centrosomes and use a mode of embryonic development called spiral cleavage that relies on a pattern of oriented cell divisions (Azimzadeh et al., 2012). Centrosomes are important to coordinate some asymmetric stem cell divisions in *Drosophila* (Gonzalez, 2008). Even in acentrosomal *Drosophila* mutants that can go through most of their development without centrosomes, the presence of centrosomes does make mitosis more efficient and quicker (Basto et al., 2006), and centrioles are strictly needed for early embryonic development (Megraw et al., 1999; Stevens et al., 2007; Vaizel-Ohayon and Schejter,

1999). Thus, I conclude that centrosomes are often not strictly needed, but that it depends on the organism, cell type and stage whether cells have developed a dependence on centrosomes for cell division, or not. In this scenario, there are now clearly many cells, tissues and species that do depend on centrosomes for efficient cell division; understanding how these beautifully complex organelles are assembled and regulated remains an important challenge for the future.

8 Bibliography

Afzelius, B.A. (1976). A human syndrome caused by immotile cilia. *Science* **193,** 317-9

Al-Dosari, M. S., Shaheen, R., Colak, D. and Alkuraya, F. S. (2010). Novel CENPJ mutation causes Seckel syndrome. *Journal of Medical Genetics* **47**, 411–414.

Albee, A. J., Kwan, A. L., Lin, H., Granas, D., Stormo, G. D. and Dutcher, S. K. (2013). Identification of Cilia Genes That Affect Cell-Cycle Progression Using Whole-Genome Transcriptome Analysis in Chlamydomonas reinhardtti. *G3 (Bethesda)* **3**, 979–991.

Alberts et al. (2008) Molecular Biology of the Cell, 5th Edition

Alkuraya, F. S., Cai, X., Emery, C., Mochida, G. H., Al-Dosari, M. S., Felie, J. M., Hill, R. S., Barry, B. J., Partlow, J. N., Gascon, G. G., et al. (2012). Human Mutations in NDE1 Cause Extreme Microcephaly with Lissencephaly. *The American Journal of Human Genetics* **88**, 536–547.

Ambrose, J. C., Li, W., Marcus, A., Ma, H. and Cyr, R. (2005). A minus-end-directed kinesin with plus-end tracking protein activity is involved in spindle morphogenesis. *Mol Biol Cell* **16**, 1584–1592.

Andersen, J.S., Wilkinson, C.J., Mayor, T., Mortensen, P., Nigg, E.A., Mann, M. (2003). Proteomic characterization of the human centrosome by protein correlation profiling. *Nature* **426,** 570–574.

Anderson, R.G. and Brenner, R.M. (1971). The formation of basal bodies (centrioles) in the Rhesus monkey oviduct. *J Cell Biol* **50,** 10-34.

Archambault, V. and Glover, D. M. (2009). Polo-like kinases: conservation and divergence in their functions and regulation. *Nat Rev Mol Cell Biol* **10**, 265–275.

Archambault, V., D'Avino, P. P., Deery, M. J., Lilley, K. S. and Glover, D. M. (2008). Sequestration of Polo kinase to microtubules by phosphopriming-independent binding to Map205 is relieved by phosphorylation at a CDK site in mitosis. *Genes Dev* **22**, 2707–2720.

Arquint, C., Sonnen, K. F., Stierhof, Y. D. and Nigg, E. A. (2012). Cell-cycle-regulated expression of STIL controls centriole number in human cells. *J Cell Sci* **125**, 1342–1352.

Avidor-Reiss, T., Maer, A. M., Koundakjian, E., Polyanovsky, A., Keil, T., Subramaniam, S. and Zuker, C. S. (2004). Decoding cilia function: defining specialized genes required for compartmentalized cilia biogenesis. *Cell* **117**, 527–539.

Azimzadeh, J., Wong, M. L., Downhour, D. M., Alvarado, A. S. and Marshall, W. F. (2012). Centrosome Loss in the Evolution of Planarians. *Science* **335**, 461–463.

Badano, J. L., Mitsuma, N., Beales, P. L. and Katsanis, N. (2006). The ciliopathies:

an emerging class of human genetic disorders. *Annu Rev Genomics Hum Genet* **7**, 125–148.

Bahe, S. (2005). Rootletin forms centriole-associated filaments and functions in centrosome cohesion. *J Cell Biol* **171**, 27–33.

Bakircioglu, M., Carvalho, O. P., Khurshid, M., Cox, J. J., Tuysuz, B., Barak, T., Yilmaz, S., Caglayan, O., Dincer, A., Nicholas, A. K., et al. (2012). The Essential Role of Centrosomal NDE1 in Human Cerebral Cortex Neurogenesis. *The American Journal of Human Genetics* **88**, 523–535.

Barr, A. R. and Gergely, F. (2007). Aurora-A: the maker and breaker of spindle poles. *J Cell Sci* **120**, 2987–2996.

Barr, A. R., Kilmartin, J. V. and Gergely, F. (2010). CDK5RAP2 functions in centrosome to spindle pole attachment and DNA damage response. *J Cell Biol* **189**, 23–39.

Barros, T. P., Kinoshita, K., Hyman, A. A. and Raff, J. W. (2005). Aurora A activates D-TACC-Msps complexes exclusively at centrosomes to stabilize centrosomal microtubules. *J Cell Biol* **170**, 1039–1046.

Basto, R., Brunk, K., Vinadogrova, T., Peel, N., Franz, A., Khodjakov, A. and Raff, J. W. (2008). Centrosome amplification can initiate tumorigenesis in flies. *Cell* **133**, 1032–1042.

Basto, R., Lau, J., Vinogradova, T., Gardiol, A., Woods, C. G., Khodjakov, A. and Raff, J. W. (2006). Flies without centrioles. *Cell* **125**, 1375–1386.

Belmont, L. D., Hyman, A. A., Sawin, K. E. and Mitchison, T. J. (1990). Real-time visualization of cell cycle-dependent changes in microtubule dynamics in cytoplasmic extracts. *Cell* **62,** 579-589.

Benjamini, Y. and Hochberg, Y. (2005). Controlling the false discovery rate: a practical and powerful approach to multiple testing. *J. R. Stat. Soc. Ser. A Stat. Soc*. **57,** 289-300.

Berbari, N. F., Connor, A. K. O., Haycraft, C. J. and Yoder, B. K. (2009). The Primary Cilium as a Complex Signaling Center. *Curr Biol* **19**, R526–R535.

Berdnik, D. and Knoblich, J. A. (2002). *Drosophila* Aurora-A is required for centrosome maturation and actin-dependent asymmetric protein localization during mitosis. *Curr Biol* **12**, 640–647.

Betschinger, J. and Knoblich, J. A. (2004). Dare to Be Different: Asymmetric Cell Division in *Drosophila*, *C. elegans* and Vertebrates. *Current Biology* **14**, R674–R685.

Bettencourt-Dias, M. and Glover, D. M. (2007). Centrosome biogenesis and function: centrosomics brings new understanding. *Nat Rev Mol Cell Biol* **8**, 451–463.

Bettencourt-Dias, M., Hildebrandt, F., Pellman, D., Woods, G. and Godinho, S. A. (2011). Centrosomes and cilia in human disease. *Trends Genet* **27**, 307–315.

Bettencourt-Dias, M., Rodrigues-Martins, A., Carpenter, L., Riparbelli, M., Lehmann, L., Gatt, M. K., Carmo, N., Balloux, F., Callaini, G. and Glover, D. M. (2005). SAK/PLK4 Is Required for Centriole Duplication and Flagella Development. *Current Biology* **15**, 2199–2207.

Blachon, S., Cai, X., Roberts, K. A., Yang, K., Polyanovsky, A., Church, A. and Avidor-Reiss, T. (2009). A Proximal Centriole-Like Structure Is Present in *Drosophila* Spermatids and Can Serve as a Model to Study Centriole Duplication. *Genetics* **182**, 133–144.

Blachon, S., Gopalakrishnan, J., Omori, Y., Polyanovsky, A., Church, A., Nicastro, D., Malicki, J. and Avidor-Reiss, T. (2008). *Drosophila* asterless and Vertebrate Cep152 Are Orthologs Essential for Centriole Duplication. *Genetics* **180**, 2081–2094.

Blagden, S. P. and Glover, D. M. (2003). Polar expeditions--provisioning the centrosome for mitosis. *Nat Cell Biol* **5**, 505–511.

Bobinnec, Y., Khodjakov, A., Mir, L. M., Rieder, C. L., Eddé, B. and Bornens, M. (1998a). Centriole disassembly *in vivo* and its effect on centrosome structure and function in vertebrate cells. *J Cell Biol* **143**, 1575–1589.

Bobinnec, Y., Moudjou, M., Fouquet, J. P., Desbruyères, E., Eddé, B. and Bornens, M. (1998b). Glutamylation of centriole and cytoplasmic tubulin in proliferating non-neuronal cells. *Cell Motil. Cytoskeleton* **39**, 223–232.

Bodenmiller, B., Malmstrom, J., Gerrits, B., Campbell, D., Lam, H., Schmidt, A., Rinner, O., Mueller, L. N., Shannon, P. T., Pedrioli, P. G., et al. (2007). PhosphoPep—a phosphoproteome resource for systems biology research in *Drosophila* Kc167 cells. *Mol Syst Biol* **3**.

Bolstad, B. M., Irizarry, R. A., Astrand, M. and Speed, T. P. (2003). A comparison of normalization methods for high density oligonucleotide array data based on variance and bias. *Bioinformatics* **19**, 185–193.

Bolton, M. A., Lan, W., Powers, S. E., McCleland, M. L., Kuang, J. and Stukenberg, P. T. (2002). Aurora B kinase exists in a complex with survivin and INCENP and its kinase activity is stimulated by survivin binding and phosphorylation. *Mol Biol Cell* **13**, 3064–3077.

Bonaccorsi, S., Giansanti, M. G. and Gatti, M. (1998). Spindle self-organization and cytokinesis during male meiosis in asterless mutants of *Drosophila* melanogaster. *J Cell Biol* **142**, 751–761.

Bond, J., Roberts, E., Springell, K., Lizarraga, S., Scott, S., Higgins, J., Hampshire, D. J., Morrison, E. E., Leal, G. F., Silva, E. O., et al. (2005). A centrosomal mechanism involving CDK5RAP2 and CENPJ controls brain size. *Nat Genet* **37**, 353–355.

Bornens, M. (2012a). The Centrosome in Cells and Organisms. *Science* **335**, 422–426.

Bornens, M. (2001). Centrosome composition and microtubule anchoring mechanisms.

Curr Opin Cell Biol **14**, 25–34.

Boveri T. (1914). Zur Frage der Entstehung maligner Tumoren. Jena: Fischer Verlag (English translation by Boveri M (1929). The Origin of Malignant Tumors. Baltimore: Waverly Press)

Boveri, T. (2008). Concerning the origin of malignant tumours by Theodor Boveri. Translated and annotated by Henry Harris. *J Cell Sci.* **121,** Suppl 1:1-84.

Brand, A. H. and Perrimon, N. (1993). Targeted gene expression as a means of altering cell fates and generating dominant phenotypes. *Development* **118**, 401–415.

Brown, N. J., Marjanović, M., Lüders, J., Stracker, T. H. and Costanzo, V. (2013). Cep63 and Cep152 Cooperate to Ensure Centriole Duplication. *PLoS ONE* **8**, e69986.

Brownlee, C. W., Klebba, J. E., Buster, D. W. and Rogers, G. C. (2011). The Protein Phosphatase 2A regulatory subunit Twins stabilizes Plk4 to induce centriole amplification. *J Cell Biol* **195**, 231–243.

Callaini, G., Whitfield, W. G. F. and Riparbelli, M. G. (1997). Centriole and centrosome dynamics during the early embryonic cell cycles that follow the formation of the cellular blastoderm in *Drosophila*. *Exp. Cell Res.* **234**, 183- 190.

Carpenter, A. E., Jones, T. R., Lamprecht, M. R., Clarke, C., Kang, I. H., Friman, O., Guertin, D. A., Chang, J. H., Lindquist, R. A., Moffat, J., et al. (2006). CellProfiler: image analysis software for identifying and quantifying cell phenotypes. *Genome Biol* **7**, R100.

Carvalho-Santos, Z., Azimzadeh, J., Pereira-Leal, J. B. and Bettencourt-Dias, M. (2011). Evolution: Tracing the origins of centrioles, cilia, and flagella. *J Cell Biol* **194**, 165–175.

Carvalho-Santos, Z., Machado, P., Branco, P., Tavares-Cadete, F., Rodrigues-Martins, A., Pereira-Leal, J. B. and Bettencourt-Dias, M. (2010). Stepwise evolution of the centriole-assembly pathway. *J Cell Sci* **123**, 1414–1426.

Castellanos, E., Dominguez, P. and Gonzalez, C. (2008). Centrosome dysfunction in *Drosophila* neural stem cells causes tumors that are not due to genome instability. *Curr Biol* **18**, 1209–1214.

Caussinus, E. and Gonzalez, C. (2005). Induction of tumor growth by altered stem-cell asymmetric division in *Drosophila* melanogaster. *Nat Genet* **37**, 1125–1129.

Cavalier-Smith, T. (2002). The phagotrophic origin of eukaryotes and phylogenetic classification of Protozoa. *Int. J. Syst. Evol. Microbiol.* **52**, 297–354.

Cavalier-Smith, T. (1974). Basal body and flagellar development during the vegetative cell cycle and the sexual cycle of *Chlamydomonas reinhardii*. J Cell Sci 16, 529-56.

Chang, J., Cizmecioglu, O., Hoffmann, I. and Rhee, K. (2010). emboj2010118a.

EMBO J **29**, 2395–2406.

Chen, Z., Indjeian, V. B., McManus, M., Wang, L. and Dynlacht, B. D. (2002). CP110, a cell cycle-dependent CDK substrate, regulates centrosome duplication in human cells. *Dev Cell* **3**, 339–350.

Cheng, K.-Y., Lowe, E. D., Sinclair, J., Nigg, E. A. and Johnson, L. N. (2003). The crystal structure of the human polo-like kinase-1 polo box domain and its phospho-peptide complex. *EMBO J* **22**, 5757–5768.

Cheng, T.-S., Chang, L.-K., Howng, S.-L., Lu, P.-J., Lee, C.-I. and Hong, Y.-R. (2006). SUMO-1 modification of centrosomal protein hNinein promotes hNinein nuclear localization. *Life Sciences* **78**, 1114–1120.

Chng, W. J. and Fonseca, R. (2009). Centrosomes and myeloma; aneuploidy and proliferation. *Environ Mol Mutagen* **50**, 697–707.

Cho, J.-H., Chang, C.-J., Chen, C.-Y. and Tang, T. K. (2006). Depletion of CPAP by RNAi disrupts centrosome integrity and induces multipolar spindles. *Biochemical and Biophysical Research Communications* **339**, 742–747.

Choi, Y. K., Liu, P., Sze, S. K., Dai, C. and Qi, R. Z. (2010). CDK5RAP2 stimulates microtubule nucleation by the -tubulin ring complex. *J Cell Biol* **191**, 1089–1095.

Chrétien, D., Buendia, B., Fuller, S. D. and Karsenti, E. (1997). Reconstruction of the centrosome cycle from cryoelectron micrographs. *J. Struct. Biol.* **120,** 117-133.

Ciciarello, M., Mangiacasale, R. and Lavia, P. (2007). Spatial control of mitosis by the GTPase Ran. *Cell. Mol. Life Sci.* **64**, 1891–1914.

Cizmecioglu, O., Arnold, M., Bahtz, R., Settele, F., Ehret, L., Haselmann-Weiß, U., Antony, C. and Hoffmann, I. (2010). Cep152 acts as a scaffold for recruitment of Plk4 and CPAP to the centrosome. *J Cell Biol*.

Cizmecioglu, O., Krause, A., Bahtz, R., Ehret, L., Malek, N. and Hoffmann, I. (2012). Plk2 regulates centriole duplication through phosphorylation-mediated degradation of Fbxw7 (human Cdc4). *J Cell Sci* **125**, 981–992.

Cohen, P. (2000). The regulation of protein function by multisite phosphorylation--a 25 year update. *Trends Biochem. Sci.* **25**, 596–601.

Conduit, P. T. and Raff, J. W. (2010). Cnn Dynamics Drive Centrosome Size Asymmetry to Ensure Daughter Centriole Retention in *Drosophila* Neuroblasts. *Current Biology* **20**, 2187–2192.

Conduit, P. T., Brunk, K., Dobbelaere, J., Dix, C. I., Lucas, E. P. and Raff, J. W. (2010). Centrioles Regulate Centrosome Size by Controlling the Rate of Cnn Incorporation into the PCM. *Current Biology* **20**, 2178-86.

Corbit, K. C., Aanstad, P., Singla, V., Norman, A. R., Stainier, D. Y. R. and Reiter, J. F. (2005). Vertebrate Smoothened functions at the primary cilium. *Nat Cell Biol* **437**, 1018–1021.

Cottee, M. A., Muschalik, N., Wong, Y. L., Johnson, C. M., Johnson, S., Andreeva, A., Oegema, K., Lea, S. M., Raff, J. W. and Van Breugel, M. (2013). Crystal structures of the CPAP/STIL complex reveal its role in centriole assembly and human microcephaly. *eLife* **2**, e01071–e01071.

Cottee, M. A., Raff, J. W., Lea, S. M. and Roque, H. (2011). SAS-6 oligomerization: the key to the centriole? *Nature Publishing Group* **7**, 650–653.

Courtois, A., Schuh, M., Ellenberg, J. and Hiiragi, T. (2012). The transition from meiotic to mitotic spindle assembly is gradual during early mammalian development. *J Cell Biol* **198**, 357–370.

Crasta, K., Ganem, N. J., Dagher, R., Lantermann, A. B., Ivanova, E. V., Pan, Y., Nezi, L., Protopopov, A., Chowdhury, D. and Pellman, D. (2012). nature10802. *Nature* **482**, 53–58.

Culver, B. P., Meehl, J. B., Giddings, T. H. and Winey, M. (2009). The two SAS-6 homologs in Tetrahymena thermophila have distinct functions in basal body assembly. *Mol Biol Cell* **20**, 1865–1877.

Cunha-Ferreira, I., Rodrigues-Martins, A., Bento, I., Riparbelli, M., Zhang, W., Laue, E., Callaini, G., Glover, D. M. and Bettencourt-Dias, M. (2009). The SCF/Slimb ubiquitin ligase limits centrosome amplification through degradation of SAK/PLK4. *Curr Biol* **19**, 43–49.

Dauber, A., LaFranchi, S. H., Maliga, Z., Lui, J. C., Moon, J. E., McDeed, C., Henke, K., Zonana, J., Kingman, G. A., Pers, T. H., et al. (2012). Novel Microcephalic Primordial Dwarfism Disorder Associated with Variants in the Centrosomal Protein Ninein. *Journal of Clinical Endocrinology & Metabolism* **97**, E2140–E2151.

Dawe, H. R., Farr, H. and Gull, K. (2006). Centriole/basal body morphogenesis and migration during ciliogenesis in animal cells. *J Cell Sci* **120**, 7–15.

Debec, A., Détraves, C., Montmory, C., Géraud, G. and Wright, M. (1995). Polar organization of gamma-tubulin in acentriolar mitotic spindles of *Drosophila* melanogaster cells. *J Cell Sci* **108 (Pt 7)**, 2645–2653.

Debec, A., Sullivan, W. and Bettencourt-Dias, M. (2010). Centrioles: active players or passengers during mitosis? *Cell. Mol. Life Sci.*

Decker, M., Jaensch, S., Pozniakovsky, A., Zinke, A., O'connell, K. F., Zachariae, W., Myers, E. and Hyman, A. A. (2011). Limiting Amounts of Centrosome Material Set Centrosome Size in C. elegans Embryos. *Curr Biol* **21**, 1259–1267.

Delattre, M., Canard, C. and Gönczy, P. (2006). Sequential protein recruitment in *C. elegans* centriole formation. *Curr Biol* **16**, 1844–1849.

Delattre, M., Leidel, S., Wani, K., Baumer, K., Bamat, J., Schnabel, H., Feichtinger, R., Schnabel, R. and Gönczy, P. (2004). Centriolar SAS-5 is required for centrosome duplication in *C. elegans*. *Nat Cell Biol* **6**, 656–664.

Dictenberg, J. B., Zimmerman, W., Sparks, C. A., Young, A., Vidair, C., Zheng, Y., Carrington, W., Fay, F. S. and Doxsey, S. J. (1998). Pericentrin and gamma-tubulin form a protein complex and are organized into a novel lattice at the centrosome. *J Cell Biol* **141**, 163–174.

Dippell, R. V. (1968). The development of basal bodies in *Paramecium*. *Proc Natl Acad Sci USA* **61,** 461-8.

Dix, C. I. and Raff, J. W. (2007). *Drosophila* Spd-2 Recruits PCM to the Sperm Centriole, but Is Dispensable for Centriole Duplication. *Current Biology* **17**, 1759–1764.

Dobbelaere, J., Josué, F., Suijkerbuijk, S., Baum, B., Tapon, N. and Raff, J. (2008). A genome-wide RNAi screen to dissect centriole duplication and centrosome maturation in *Drosophila*. *PLoS Biol* **6**, e224.

Doe, C. Q. (2008). Neural stem cells: balancing self-renewal with differentiation. *Development* **135**, 1575–1587.

Doxsey, S., Zimmerman, W. and Mikule, K. (2005). Centrosome control of the cell cycle. *Trends Cell Biol* **15**, 303–311.

Dumont, J. and Desai, A. (2012). Acentrosomal spindle assembly and chromosome segregation during oocyte meiosis. *Trends Cell Biol* **22**, 241–249.

Dzhindzhev, N. S., Yu, Q. D., Weiskopf, K., Tzolovsky, G., Cunha-Ferreira, I., Riparbelli, M., Rodrigues-Martins, A., Bettencourt-Dias, M., Callaini, G. and Glover, D. M. (2010a). Asterless is a scaffold for the onset of centriole assembly. *Nature* **467**, 714–718.

Dzhindzhev, N. S., Yu, Q. D., Weiskopf, K., Tzolovsky, G., Cunha-Ferreira, I., Riparbelli, M., Rodrigues-Martins, A., Bettencourt-Dias, M., Callaini, G. and Glover, D. M. (2010b). Asterless is a scaffold for the onset of centriole assembly. *Nature* **467**, 714–718.

Eddé, B., Rossier, J., Le Caer, J.P., Desbruyeres, E., Gros, F. and Denoulet, P. (1990). Posttranslational glutamylation of alpha-tubulin. *Science* **247,** 83-5.

Edwards, A. S. (1999). Carboxyl-terminal Phosphorylation Regulates the Function and Subcellular Localization of Protein Kinase C beta II. *Journal of Biological Chemistry* **274**, 6461–6468.

Eggenschwiler, J. T. and Anderson, K. V. (2007). Cilia and Developmental Signaling. *Annu. Rev. Cell Dev. Biol.* **23**, 345–373.

Eley, L., Yates, L. M. and Goodship, J. A. (2005). Cilia and disease. *Curr Opin Genet Dev* **15**, 308–314.

Elia, A. E. H., Cantley, L. C. and Yaffe, M. B. (2003a). Proteomic screen finds pSer/pThr-binding domain localizing Plk1 to mitotic substrates. *Science* **299**, 1228–1231.

Elia, A. E. H., Rellos, P., Haire, L. F., Chao, J. W., Ivins, F. J., Hoepker, K., Mohammad, D., Cantley, L. C., Smerdon, S. J. and Yaffe, M. B. (2003b). The molecular basis for phosphodependent substrate targeting and regulation of Plks by the Polo-box domain. *Cell* **115**, 83–95.

Endow, S. A., Chandra, R., Komma, D. J., Yamamoto, A. H. and Salmon, E. D. (1994). Mutants of the *Drosophila* ncd microtubule motor protein cause centrosomal and spindle pole defects in mitosis. *J Cell Sci* **107 (Pt 4)**, 859–867.

Ezratty, E. J., Stokes, N., Chai, S., Shah, A. S., Williams, S. E. and Fuchs, E. (2011). A Role for the Primary Cilium in Notch Signaling and Epidermal Differentiation during Skin Development. *Cell* **145**, 1129–1141.

Fan, J., Griffiths, A. D., Lockhart, A., Cross, R. A. and Amos, L. A. (1996). Microtubule minus ends can be labelled with a phage display antibody specific to alpha-tubulin. *J Mol Biol* **259,** 325-30.

Faragher, A. J. (2003). Nek2A kinase stimulates centrosome disjunction and is required for formation of bipolar mitotic spindles. *Mol Biol Cell* **14**, 2876–2889.

Ferguson, R. L. and Maller, J. L. (2010). Centrosomal Localization of Cyclin E-Cdk2 Is Required for Initiation of DNA Synthesis. *Curr Biol* **20**, 856–860.

Ferreiro, I., Joaquin, M., Islam, A., Gomez-Lopez, G., Barragan, M., Lombardía, L., Domínguez, O., Pisano, D. G., Lopez-Bigas, N., Nebreda, A. R., et al. (2010). Whole genome analysis of p38 SAPK-mediated gene expression upon stress. *BMC Genomics* **11**, 144.

Fisk, H. A. and Winey, M. (2001). The mouse Mps1p-like kinase regulates centrosome duplication. *Cell* **106**, 95–104.

Fliegauf, M., Benzing, T. and Omran, H. (2007). When cilia go bad: cilia defects and ciliopathies. *Nat Rev Mol Cell Biol* **8**, 880–893.

Fry, A. M., Mayor, T., Meraldi, P., Stierhof, Y. D., Tanaka, K. and Nigg, E. A. (1998). C-Nap1, a novel centrosomal coiled-coil protein and candidate substrate of the cell cycle-regulated protein kinase Nek2. *J Cell Biol* **141**, 1563–1574.

Fu, J. and Glover, D. M. (2012). Structured illumination of the interface between centriole and peri-centriolar material. *Open Biology* **2**, 120104–120104.

Ganem, N. J., Godinho, S. A. and Pellman, D. (2009). A mechanism linking extra centrosomes to chromosomal instability. *Nature* **460**, 278–282.

Gatti, M. and Baker, B. S. (1989). Genes controlling essential cell-cycle functions in *Drosophila* melanogaster. *Genes Dev* **3**, 438–453.

Gatti, M. and Goldberg, M. L. (1991). Mutations affecting cell division in *Drosophila*. *Methods Cell Biol.* **35**, 543-586.

Gautier, L., Cope, L., Bolstad, B. M. and Irizarry, R. A. (2004). affy--analysis of Affymetrix GeneChip data at the probe level. *Bioinformatics* **20**, 307–315.

Gepner, J., Li, M., Ludmann, S., Kortas, C., Boylan, K., Iyadurai, S. J., McGrail, M. and Hays, T. S. (1996). Cytoplasmic dynein function is essential in *Drosophila* melanogaster. *Genetics* **142**, 865–878.

Gergely, F., Draviam, V. M. and Raff, J. W. (2003). The ch-TOG/XMAP215 protein is essential for spindle pole organization in human somatic cells. *Genes Dev* **17**, 336–341.

Gergely, F., Kidd, D., Jeffers, K., Wakefield, J. G. and Raff, J. W. (2000). D-TACC: a novel centrosomal protein required for normal spindle function in the early *Drosophila* embryo. *EMBO J* **19**, 241–252.

Giansanti, M. G., Bucciarelli, E., Bonaccorsi, S. and Gatti, M. (2008). *Drosophila* SPD-2 Is an Essential Centriole Component Required for PCM Recruitment and Astral-Microtubule Nucleation. *Current Biology* **18**, 303–309.

Giet, R., McLean, D., Descamps, S., Lee, M. J., Raff, J. W., Prigent, C. and Glover, D. M. (2002). *Drosophila* Aurora A kinase is required to localize D-TACC to centrosomes and to regulate astral microtubules. *J Cell Biol* **156**, 437–451.

Glover, D. M. (2005). Polo kinase and progression through M phase in *Drosophila*: a perspective from the spindle poles. *Oncogene* **24**, 230–237.

Godinho, S. A., Kwon, M. and Pellman, D. (2009). Centrosomes and cancer: how cancer cells divide with too many centrosomes. *Cancer Metastasis Rev* **28**, 85–98.

Gogendeau, D., Hurbain, I., Raposo, G., Cohen, J., Koll, F. and Basto, R. (2011). Sas-4 proteins are required during basal body duplication in Paramecium. *Mol Biol Cell* **22**, 1035–1044.

Gomes, E. R. and Gundersen, G. G. (2006). Real‐Time Centrosome Reorientation During Fibroblast Migration. In *Methods in Enzymology*, pp. 579–592. Elsevier.

Gomez-Ferreria, M. A., Bashkurov, M., Helbig, A. O., Larsen, B., Pawson, T., Gingras, A. C. and Pelletier, L. (2012). Novel NEDD1 phosphorylation sites regulate -tubulin binding and mitotic spindle assembly. *J Cell Sci* **125**, 3745–3751.

Gomez-Ferreria, M. A., Rath, U., Buster, D. W., Chanda, S. K., Caldwell, J. S., Rines, D. R. and Sharp, D. J. (2007). Human Cep192 Is Required for Mitotic Centrosome and Spindle Assembly. *Current Biology* **17**, 1960–1966.

Gonzalez, C. (2007). Spindle orientation, asymmetric division and tumour suppression in *Drosophila* stem cells. *Nat Rev Genet* **8**, 462–472.

Gonzalez, C. (2008). Centrosome function during stem cell division: the devil is in the details. *Curr Opin Cell Biol* **20**, 694–698.

Gonzalez, C., Tavosanis, G. and Mollinari, C. (1998). Centrosomes and microtubule organisation during *Drosophila* development. *J Cell Sci* **111 (Pt 18)**, 2697–2706.

Gopalakrishnan, J., Chim, Y.-C. F., Ha, A., Basiri, M. L., Lerit, D. A., Rusan, N. M. and Avidor-Reiss, T. (2012). ncb2527. *Nat Cell Biol* **14**, 865–873.

Gopalakrishnan, J., Mennella, V., Blachon, S., Zhai, B., Smith, A. H., Megraw, T. L., Nicastro, D., Gygi, S. P., Agard, D. A. and Avidor-Reiss, T. (2011). Sas-4 provides a scaffold for cytoplasmic complexes and tethers them in a centrosome. *Nature Communications* **2**, 359–11.

Gordon, D. J., Resio, B. and Pellman, D. (2012). nrg3123. *Nat Rev Genet* **13**, 189–203.

Goshima, G. (2005). Mechanisms for focusing mitotic spindle poles by minus end-directed motor proteins. *J Cell Biol* **171**, 229–240.

Goshima, G., Mayer, M., Zhang, N., Stuurman, N. and Vale, R. D. (2008a). Augmin: a protein complex required for centrosome-independent microtubule generation within the spindle. *J Cell Biol* **181**, 421–429.

Goshima, G., Mayer, M., Zhang, N., Stuurman, N. and Vale, R. D. (2008b). Augmin: a protein complex required for centrosome-independent microtubule generation within the spindle. *J Cell Biol* **181**, 421–429.

Goshima, G., Wollman, R., Goodwin, S. S., Zhang, N., Scholey, J. M., Vale, R. D. and Stuurman, N. (2007). Genes required for mitotic spindle assembly in *Drosophila* S2 cells. *Science* **316**, 417–421.

Gould, R.R., Borisy, G.G. (1977). The pericentriolar material in Chinese hamster ovary cells nucleates microtubule formation. *J Cell Biol* **73,** 601–615.

Gönczy, P. (2002). Mechanisms of spindle positioning: focus on flies and worms. *Trends Cell Biol* **12**, 332–339.

Gönczy, P. (2012). Towards a molecular architecture of centriole assembly *Nat. Rev. Molec. Cell Biol.* **13,** 425-435.

Griffith, E., Walker, S., Martin, C.-A., Vagnarelli, P., Stiff, T., Vernay, B., Sanna, Al, N., Saggar, A., Hamel, B., Earnshaw, W. C., et al. (2008). Mutations in pericentrin cause Seckel syndrome with defective ATR-dependent DNA damage signaling. *Nat Genet* **40**, 232–236.

Guderian, G., Westendorf, J., Uldschmid, A. and Nigg, E. A. (2010). Plk4 trans-autophosphorylation regulates centriole number by controlling TrCP-mediated degradation. *J Cell Sci* **123**, 2163–2169.

Guernsey, D. L., Jiang, H., Hussin, J., Arnold, M., Bouyakdan, K., Perry, S., Babineau-Sturk, T., Beis, J., Dumas, N., Evans, S. C., et al. (2010). Mutations in Centrosomal Protein CEP152 in Primary Microcephaly Families Linked to MCPH4. *Am J Hum Genet* **87**, 40–51.

Gueth-Hallonet, C., Antony, C., Aghion, J., Santa-Maria, A., Lajoie-Mazenc, I., Wright, M. and Maro, B. (1993). gamma-Tubulin is present in acentriolar MTOCs during early mouse development. *J Cell Sci* **105 (Pt 1)**, 157–166.

Guichard, P., Desfosses, A., Maheshwari, A., Hachet, V., Dietrich, C., Brune, A., Ishikawa, T., Sachse, C. and Gönczy, P. (2012). Cartwheel architecture of

Trichonympha basal body. *Science* **337**, 553.

Guichard, P., Hachet, V., Majubu, N., Neves, A., Demurtas, D., Olieric, N., Flückiger, I., Yamada, A., Kihara, K., Nishida, Y., et al. (2013). Native Architecture of the Centriole Proximal Region Reveals Features Underlying Its 9-Fold Radial Symmetry. *Curr Biol* 1–9.

Gul, A., Hassan, M. J., Hussain, S., Raza, S. I., Chishti, M. S. and Ahmad, W. (2006). A novel deletion mutation in CENPJ gene in a Pakistani family with autosomal recessive primary microcephaly. *J Hum Genet* **51**, 760–764.

Gunawardane, R. N., Martin, O. C., Cao, K., Zhang, L., Dej, K., Iwamatsu, A. and Zheng, Y. (2000). Characterization and reconstitution of *Drosophila* gamma-tubulin ring complex subunits. *J Cell Biol* **151**, 1513–1524.

Gundersen, G.G. and Bulinski, J.C. (1986). Microtubule arrays in differentiated cells contain elevated levels of a post-translationally modified form of tubulin. *Eur J Cell Biol* **42,** 288-94.

Guo, H.-Q., Gao, M., Ma, J., Xiao, T., Zhao, L.-L., Gao, Y. and Pan, Q.-J. (2007). Analysis of the cellular centrosome in fine-needle aspirations of the breast. *Breast Cancer Res* **9**, R48.

Gustafsson, M. G. L., Shao, L., Carlton, P. M., Wang, C. J. R., Golubovskaya, I. N., Cande, W. Z., Agard, D. A. and Sedat, J. W. (2008). Three-Dimensional Resolution Doubling in Wide-Field Fluorescence Microscopy by Structured Illumination. *Biophys J* **94**, 4957–4970.

Habedanck, R., Stierhof, Y.-D., Wilkinson, C. J. and Nigg, E. A. (2005). The Polo kinase Plk4 functions in centriole duplication. *Nat Cell Biol* **7**, 1140–1146.

Habermann, K. and Lange, B. M. (2012). 1747-1028-7-17. *Cell division* **7**, 1–1.

Habermann, K., Mirgorodskaya, E., Gobom, J., Lehmann, V., Muller, H., Blumlein, K., Deery, M. J., Czogiel, I., Erdmann, C., Ralser, M., et al. (2012). Functional Analysis of Centrosomal Kinase Substrates in *Drosophila* melanogaster Reveals a New Function of the Nuclear Envelope Component Otefin in Cell Cycle Progression. *Molecular and Cellular Biology* **32**, 3554–3569.

Hallen, M. A., Ho, J., Yankel, C. D. and Endow, S. A. (2008). Fluorescence Recovery Kinetic Analysis of γ-Tubulin Binding to the Mitotic Spindle. *Biophys J* **95**, 3048–3058.

Hammond, D., Zeng, K., Espert, A., Bastos, R. N., Baron, R. D., Gruneberg, U. and Barr, F. A. (2013). Melanoma-associated mutations in protein phosphatase 6 cause chromosome instability and DNA damage due to dysregulated Aurora-A. *J Cell Sci*.

Hannak, E. (2001). Aurora-A kinase is required for centrosome maturation in Caenorhabditis elegans. *J Cell Biol* **155**, 1109–1116.

Hannak, E. (2002). The kinetically dominant assembly pathway for centrosomal asters in Caenorhabditis elegans is gamma-tubulin dependent. *J Cell Biol* **157**, 591–602.

Haren, L. (2006). NEDD1-dependent recruitment of the -tubulin ring complex to the centrosome is necessary for centriole duplication and spindle assembly. *J Cell Biol* **172**, 505–515.

Haren, L., Stearns, T. and Lüders, J. (2009a). Plk1-Dependent Recruitment of γ-Tubulin Complexes to Mitotic Centrosomes Involves Multiple PCM Components. *PLoS ONE* **4**, e5976.

Haren, L., Stearns, T. and Lüders, J. (2009b). Plk1-Dependent Recruitment of γ-Tubulin Complexes to Mitotic Centrosomes Involves Multiple PCM Components. *PLoS ONE* **4**, e5976.

Harzer, H., Berger, C., Conder, R., Schmauss, G. and Knoblich, J. A. (2013). FACS purification of *Drosophila* larval neuroblasts for next-generation sequencing. *Nat Protoc* **8**, 1088–1099.

Hatch, E. M., Kulukian, A., Holland, A. J., Cleveland, D. W. and Stearns, T. (2010). Cep152 interacts with Plk4 and is required for centriole duplication. *J Cell Biol*.

Hatsumi, M. and Endow, S. A. (1992). Mutants of the microtubule motor protein, nonclaret disjunctional, affect spindle structure and chromosome movement in meiosis and mitosis. *J Cell Sci* **101 (Pt 3)**, 547–559.

Heald, R., Tournebize, R., Blank, T., Sandaltzopoulos, R., Becker, P., Hyman, A. and Karsenti, E. (1996). Self-organization of microtubules into bipolar spindles around artificial chromosomes in *Xenopus* egg extracts. *Nature* **382,** 420-425.

Hilbert, M., Erat, M. C., Hachet, V., Guichard, P., Blank, I. D., Flückiger, I., Slater, L., Lowe, E. D., Hatzopoulos, G. N., Steinmetz, M. O., et al. (2013). Caenorhabditis elegans centriolar protein SAS-6forms a spiral that is consistent with impartinga ninefold symmetry. 1–6.

Hinchcliffe, E. H. (1999). Requirement of Cdk2-Cyclin E Activity for Repeated Centrosome Reproduction in *Xenopus* Egg Extracts. *Science* **283**, 851–854.

Hinchcliffe, E. H. (2001). Requirement of a Centrosomal Activity for Cell Cycle Progression Through G1 into S Phase. *Science* **291**, 1547–1550.

Hiraki, M., Nakazawa, Y., Kamiya, R. and Hirono, M. (2007). Bld10p Constitutes the Cartwheel-Spoke Tip and Stabilizes the 9-Fold Symmetry of the Centriole. *Current Biology* **17**, 1778–1783.

Hirota, T., Kunitoku, N., Sasayama, T., Marumoto, T., Zhang, D., Nitta, M., Hatakeyama, K. and Saya, H. (2003). Aurora-A and an Interacting Activator, the LIM Protein Ajuba, Are Required for Mitotic Commitment in Human Cells. *Cell* **114**, 585–598.

Hodges, M. E., Scheumann, N., Wickstead, B., Langdale, J. A. and Gull, K. (2010). Reconstructing the evolutionary history of the centriole from protein components. *J Cell Sci* **123**, 1407–1413.

Hoh, R. A., Stowe, T. R., Turk, E. and Stearns, T. (2012). Transcriptional Program of Ciliated Epithelial Cells Reveals New Cilium and Centrosome Components and Links to Human Disease. *PLoS ONE* **7**, e52166.

Holland, A. J. and Cleveland, D. W. (2012a). Losing balance: the origin and impact of aneuploidy in cancer. *EMBO reports* **13**, 501–514.

Holland, A. J. and Cleveland, D. W. (2012b). Chromoanagenesis and cancer: mechanisms and consequences of localized, complex chromosomal rearrangements. *Nature Medicine* **18**, 1630–1638.

Horner, V. L. and Wolfner, M. F. (2008). Mechanical stimulation by osmotic and hydrostatic pressure activates *Drosophila* oocytes *in vitro* in a calcium-dependent manner. *Dev Biol* **316**, 100–109.

Hsu, L. C. and White, R. L. (1998). BRCA1 is associated with the centrosome during mitosis. *Proc Natl Acad Sci USA* **95**, 12983–12988.

Huang, D. W., Sherman, B. T. and Lempicki, R. A. (2009). Bioinformatics enrichment tools: paths toward the comprehensive functional analysis of large gene lists. *Nucleic Acids Res* **37**, 1–13.

Huang, D. W., Sherman, B. T. and Lempicki, R. A. (2008). Systematic and integrative analysis of large gene lists using DAVID bioinformatics resources. *Nat Protoc* **4**, 44–57.

Huang, J. and Raff, J. W. (1999). The disappearance of cyclin B at the end of mitosis is regulated spatially in *Drosophila* cells. *EMBO J* **18**, 2184–2195.

Huangfu, D., Liu, A., Rakeman, A. S., Murcia, N. S., Niswander, L. and Anderson, K. V. (2003). Hedgehog signalling in the mouse requires intraflagellar transport proteins. *Nature* **426**, 83–87.

Hussain, M. S., Baig, S. M., Neumann, S., Nürnberg, G., Farooq, M., Ahmad, I., Alef, T., Hennies, H. C., Technau, M., Altmüller, J., et al. (2012). A Truncating Mutation of CEP135 Causes Primary Microcephaly and Disturbed Centrosomal Function. *Am J Hum Genet* **90**, 871–878.

Hussain, M. S., Baig, S. M., Neumann, S., Peche, V. S., Szczepanski, S., Nurnberg, G., Tariq, M., Jameel, M., Khan, T. N., Fatima, A., et al. (2013). CDK6 associates with the centrosome during mitosis and is mutated in a large Pakistani family with primary microcephaly. *Human Molecular Genetics*.

Hutterer, A., Berdnik, D., Wirtz-Peitz, F., Žigman, M., Schleiffer, A. and Knoblich, J. A. (2006). Mitotic Activation of the Kinase Aurora-A Requires Its Binding Partner Bora. *Dev Cell* **11**, 147–157.

Ibrahim, R., Messaoudi, C., Chichon, F. J., Celati, C. and Marco, S. (2009). Electron tomography study of isolated human centrioles. *Microsc. Res. Tech.* **72,** 42-48.

Ishikawa, H. and Marshall, W. F. (2011). nrm3085. *Nat Rev Mol Cell Biol* **12**, 222–

234.

Ishikawa, H., Kubo, A., Tsukita, S. and Tsukita, S. (2005). Odf2-deficient mother centrioles lack distal/subdistal appendages and the ability to generate primary cilia. *Nat Cell Biol* **7**, 517–524.

Jackman, M., Lindon, C., Nigg, E. A. and Pines, J. (2003). Active cyclin B1–Cdk1 first appears on centrosomes in prophase. *Nat Cell Biol* **5**, 143–148.

Jackson, A. P., Eastwood, H., Bell, S. M., Adu, J., Toomes, C., Carr, I. M., Roberts, E., Hampshire, D. J., Crow, Y. J., Mighell, A. J., et al. (2002). Identification of Microcephalin, a Protein Implicated in Determining the Size of the Human Brain. *The American Journal of Human Genetics* **71**, 136–142.

Jakobsen, L., Vanselow, K., Skogs, M., Toyoda, Y., Lundberg, E., Poser, I., Falkenby, L. G., Bennetzen, M., Westendorf, J., Nigg, E. A., et al. (2011). emboj201163a. *EMBO J* **30**, 1520–1535.

Januschke, J. and Gonzalez, C. (2010). The interphase microtubule aster is a determinant of asymmetric division orientation in *Drosophila* neuroblasts. *J Cell Biol* 1–14.

Januschke, J., Llamazares, S., Reina, J. and Gonzalez, C. (2011). *Drosophila* neuroblasts retain the daughter centrosome. *Nature Communications* **2**, 243–246.

Januschke, J., Reina, J., Llamazares, S., Bertran, T., Rossi, F., Roig, J. and Gonzalez, C. (2013). ncb2671 (1). *Nat Cell Biol* **15**, 241–248.

Joo, K., Kim, C. G., Lee, M.-S., Moon, H.-Y., Lee, S.-H., Kim, M. J., Kweon, H.-S., Park, W.-Y., Kim, C.-H., Gleeson, J. G., et al. (2013). CCDC41 is required for ciliary vesicle docking to the mother centriole. *Proc Natl Acad Sci USA* **110**, 5987–5992.

Joukov, V., De Nicolo, A., Rodriguez, A., Walter, J. C. and Livingston, D. M. (2010). Centrosomal protein of 192 kDa (Cep192) promotes centrosome-driven spindle assembly by engaging in organelle-specific Aurora A activation. *Proc Natl Acad Sci USA* **107**, 21022–21027.

Jung, C. K., Jung, J. H., Lee, K. Y., Kang, C. S., Kim, M., Ko, Y. H. and Oh, C. S. (2007). Centrosome abnormalities in non-small cell lung cancer: Correlations with DNA aneuploidy and expression of cell cycle regulatory proteins. *Pathology - Research and Practice* **203**, 839–847.

Kalab, P. (2002). Visualization of a Ran-GTP Gradient in Interphase and Mitotic *Xenopus* Egg Extracts. *Science* **295**, 2452–2456.

Kalab, P. and Heald, R. (2008). The RanGTP gradient - a GPS for the mitotic spindle. *J Cell Sci* **121**, 1577–1586.

Kalay, E., Yigit, G., Aslan, Y., Brown, K. E., Pohl, E., Bicknell, L. S., Kayserili, H., Li, Y., Tuysuz, B., Nürnberg, G., et al. (2010). ng.725. *Nat Genet* **43**, 23–26.

Kamasaki, T., O'Toole, E., Kita, S., Osumi, M., Usukura, J., McIntosh, J. R. and

Goshima, G. (2013). Augmin-dependent microtubule nucleation at microtubule walls in the spindle. *J Cell Biol* **202**, 25–33.

Karsenti, E., Newport, J. and Kirschner, M. (1984). Respective roles of centrosomes and chromatin in the conversion of microtubule arrays from interphase to metaphase. *J. Cell Biol.* **99 Suppl,** 47-54.

Kawamura, K., Moriyama, M., Shiba, N., Ozaki, M., Tanaka, T., Nojima, T., Fujikawa-Yamamoto, K., Ikeda, R. and Suzuki, K. (2003). Centrosome hyperamplification and chromosomal instability in bladder cancer. *Eur Urol* **43**, 505–515.

Kayser, G., Gerlach, U., Walch, A., Nitschke, R., Haxelmans, S., Kayser, K., Hopt, U., Werner, M. and Lassmann, S. (2005). Numerical and structural centrosome aberrations are an early and stable event in the adenoma–carcinoma sequence of colorectal carcinomas. *Virchows Arch* **447**, 61–65.

Keller, L. C., Romijn, E. P., Zamora, I., Yates, J. R., III and Marshall, W. F. (2005). Proteomic Analysis of Isolated Chlamydomonas Centrioles Reveals Orthologs of Ciliary-Disease Genes. *Current Biology* **15**, 1090–1098.

Kelly, A. E., Sampath, S. C., Maniar, T. A., Woo, E. M., Chait, B. T. and Funabiki, H. (2007). Chromosomal Enrichment and Activation of the Aurora B Pathway Are Coupled to Spatially Regulate Spindle Assembly. *Dev Cell* **12**, 31–43.

Kemp, C. A., Kopish, K. R., Zipperlen, P., Ahringer, J. and O'connell, K. F. (2004). Centrosome maturation and duplication in *C. elegans* require the coiled-coil protein SPD-2. *Dev Cell* **6**, 511–523.

Khodjakov, A. (2002). De novo formation of centrosomes in vertebrate cells arrested during S phase. *J Cell Biol* **158**, 1171–1181.

Khodjakov, A. (2003). Minus-end capture of preformed kinetochore fibers contributes to spindle morphogenesis. *J Cell Biol* **160**, 671–683.

Khodjakov, A. and Rieder, C. L. (1999). The Sudden Recruitment of -Tubulin to the Centrosome at the Onset of Mitosis and its Dynamic Exchange Throughout the Cell Cycle, Do Not Require Microtubules. 1–12.

Khodjakov, A., Cole, R. W., Oakley, B. R. and Rieder, C. L. (2000). Centrosome-independent mitotic spindle formation in vertebrates. *Curr Biol* **10**, 59–67.

Kilburn, C. L., Pearson, C. G., Romijn, E. P., Meehl, J. B., Giddings, T. H., Culver, B. P., Yates, J. R. and Winey, M. (2007). New Tetrahymena basal body protein components identify basal body domain structure. *J Cell Biol* **178**, 905–912.

Kinoshita, K., Habermann, B. and Hyman, A. A. (2002). XMAP215: a key component of the dynamic microtubule cytoskeleton. *Trends Cell Biol* **12**, 267–273.

Kirkham, M., Müller-Reichert, T., Oegema, K., Grill, S. and Hyman, A. A. (2003). SAS-4 is a *C. elegans* centriolar protein that controls centrosome size. *Cell* **112**, 575–587.

Kirschner, M. and Mitchison, T. (1986). Beyond self-assembly: from microtubules to morphogenesis. *Cell* **45,** 329-342.

Kishi, K., van Vugt, M. A. T. M., Okamoto, K. I., Hayashi, Y. and Yaffe, M. B. (2009). Functional Dynamics of Polo-Like Kinase 1 at the Centrosome. *Molecular and Cellular Biology* **29**, 3134–3150.

Kitagawa, D., Busso, C., Flückiger, I. and Gönczy, P. (2009). Phosphorylation of SAS-6 by ZYG-1 Is Critical for Centriole Formation in *C. elegans* Embryos. *Dev Cell* **17**, 900–907.

Kitagawa, D., Vakonakis, I., Olieric, N., Hilbert, M., Keller, D., Olieric, V., Bortfeld, M., Erat, M. C., Flückiger, I., Gönczy, P., et al. (2011). Structural Basis of the 9-Fold Symmetry of Centrioles. *Cell* **144**, 364–375.

Klein, U. R. and Nigg, E. A. (2009). SUMO-dependent regulation of centrin-2. *J Cell Sci* **122**, 3312–3321.

Kleylein-Sohn, J., Pollinger, B., Ohmer, M., Hofmann, F., Nigg, E. A., Hemmings, B. A. and Wartmann, M. (2012). Acentrosomal spindle organization renders cancer cells dependent on the kinesin HSET. *J Cell Sci* **125**, 5391–5402.

Kleylein-Sohn, J., Westendorf, J., Le Clech, M., Habedanck, R., Stierhof, Y.-D. and Nigg, E. A. (2007). Plk4-Induced Centriole Biogenesis in Human Cells. *Dev Cell* **13**, 190–202.

Klotz, C., Dabauvalle, M.C., Paintrand, M., Weber, T., Bornens, M. and Karsenti, E. (1990). Pathenogenesis in *Xenopus* eggs requires centrosomal integrity. *J Cell Biol* **110,** 405-15.

Knoblich, J. A. (2010). Asymmetric cell division: recent developments and their implications for tumour biology. *Nature Publishing Group* **11**, 849–860.

Ko, M. A., Rosario, C. O., Hudson, J. W., Kulkarni, S., Pollett, A., Dennis, J. W. and Swallow, C. J. (2005). Plk4 haploinsufficiency causes mitotic infidelity and carcinogenesis. *Nat Genet* **37**, 883–888.

Kohlmaier, G., Loncarek, J., Meng, X., McEwen, B. F., Mogensen, M. M., Spektor, A., Dynlacht, B. D., Khodjakov, A. and Gönczy, P. (2009). Overly Long Centrioles and Defective Cell Division upon Excess of the SAS-4-Related Protein CPAP. *Curr Biol* **19**, 1012–1018.

Kollman, J. M., Merdes, A., Mourey, L. and Agard, D. A. (2011). nrm3209. *Nat Rev Mol Cell Biol* **12**, 709–721.

Kollman, J. M., Polka, J. K., Zelter, A., Davis, T. N. and Agard, D. A. (2010). nature09207. *Nature* **466**, 879–882.

Krämer, A., Mailand, N., Lukas, C., Syljuåsen, R. G., Wilkinson, C. J., Nigg, E. A., Bartek, J. and Lukas, J. (2004). Centrosome-associated Chk1 prevents premature activation of cyclin-B–Cdk1 kinase. *Nat Cell Biol* **6**, 884–891.

Kumar, A., Girimaji, S. C., Duvvari, M. R. and Blanton, S. H. (2009). Mutations in STIL, Encoding a Pericentriolar and Centrosomal Protein, Cause Primary Microcephaly. *Am J Hum Genet* **84**, 286–290.

Kwon, M., Godinho, S. A., Chandhok, N. S., Ganem, N. J., Azioune, A., Thery, M. and Pellman, D. (2008). Mechanisms to suppress multipolar divisions in cancer cells with extra centrosomes. *Genes Dev* **22**, 2189–2203.

La Terra, S. (2005). The de novo centriole assembly pathway in HeLa cells: cell cycle progression and centriole assembly/maturation. *J Cell Biol* **168**, 713–722.

Lane, H. A. and Nigg, E. A. (1996). Antibody Microinjection Reveals an EssentialRole for Human Polo-like Kinase 1 (Plkl) inthe Functional Maturation of Mitotic Centrosomes. 1–13.

Larkin, M. A., Blackshields, G., Brown, N. P., Chenna, R., McGettigan, P. A., McWilliam, H., Valentin, F., Wallace, I. M., Wilm, A., Lopez, R., et al. (2007). Clustal W and Clustal X version 2.0. *Bioinformatics* **23**, 2947–2948.

Lawo, S., Bashkurov, M., Mullin, M., Ferreria, M. G., Kittler, R., Habermann, B., Tagliaferro, A., Poser, I., Hutchins, J. R. A., Hegemann, B., et al. (2009). HAUS, the 8-Subunit Human Augmin Complex, Regulates Centrosome and Spindle Integrity. *Curr Biol* **19**, 816–826.

Lawo, S., Hasegan, M., Gupta, G. D. and Pelletier, L. (2012). ncb2591. *Nat Cell Biol* **14**, 1148–1158.

Lecland, N., Debec, A., Delmas, A., Moutinho-Pereira, S., Malmanche, N., Bouissou, A., Dupre, C., Jourdan, A., Raynaud-Messina, B., Maiato, H., et al. (2013). Establishment and mitotic characterization of new *Drosophila* acentriolar cell lines from DSas-4 mutant. *Biology Open* **2**, 314–323.

Lee, C.-Y., Robinson, K. J. and Doe, C. Q. (2006). Lgl, Pins and aPKC regulate neuroblast self-renewal versus differentiation. *Nature* **439**, 594–598.

Lee, H. S., Simon, J. A. and Lis, J. T. (1988). Structure and expression of ubiquitin genes of *Drosophila* melanogaster. *Molecular and Cellular Biology* **8**, 4727–4735.

Lee, K. and Rhee, K. (2011). PLK1 phosphorylation of pericentrin initiates centrosome maturation at the onset of mitosis. *J Cell Biol* **195**, 1093–1101.

Lee, M. J., Gergely, F., Jeffers, K., Peak-Chew, S. Y. and Raff, J. W. (2001). Msps/XMAP215 interacts with thecentrosomal protein D-TACC toregulate microtubule behaviour. 1–8.

Lefevre, G., JR and Wilkins, M. D. (1966). Cytogenetic studies on the white locus in *Drosophila Melanogaster*. *Genetics* 175–183.

Leidel, S. and Gönczy, P. (2003). SAS-4 is essential for centrosome duplication in C elegans and is recruited to daughter centrioles once per cell cycle. *Dev Cell* **4**, 431–439.

Leidel, S., Delattre, M., Cerutti, L., Baumer, K. and Gönczy, P. (2005). SAS-6

defines a protein family required for centrosome duplication in *C. elegans* and in human cells. *Nat Cell Biol* **7**, 115–125.

Lettman, M. M., Wong, Y. L., Viscardi, V., Niessen, S., Chen, S.-H., Shiau, A. K., Zhou, H., Desai, A. and Oegema, K. (2013). Direct Binding of SAS-6 to ZYG-1 Recruits SAS-6 to the Mother Centriole for Cartwheel Assembly. *Dev Cell* **25**, 284–298.

Leung, G. C., Hudson, J. W., Kozarova, A., Davidson, A., Dennis, J. W. and Sicheri, F. (2002). The Sak polo-box comprises a structural domain sufficient for mitotic subcellular localization. *Nat Struct Biol* **9**, 719–724.

Li, J. B., Gerdes, J. M., Haycraft, C. J., Fan, Y., Teslovich, T. M., May-Simera, H., Li, H., Blacque, O. E., Li, L., Leitch, C. C., et al. (2004). Comparative genomics identifies a flagellar and basal body proteome that includes the BBS5 human disease gene. *Cell* **117**, 541–552.

Li, J., D'Angiolella, V., Seeley, E. S., Kim, S., Kobayashi, T., Fu, W., Campos, E. I., Pagano, M. and Dynlacht, B. D. (2013). nature11941. *Nature* **495**, 255–259.

Lin, Y.-C., Chang, C.-W., Hsu, W.-B., Tang, C.-J. C., Lin, Y.-N., Chou, E.-J., Wu, C.-T. and Tang, T. K. (2013). emboj201356a. *EMBO J* **32**, 1141–1154.

Linck, R. W. and Stephens, R. E. (2007). Functional protofilament numbering of ciliary, flagellar, and centriolar microtubules. *Cell Motil. Cytoskeleton* **64**, 489–495.

Lindsley, D. and Zimm, G. (1992). The genome of *Drosophila* melanogaster. Academic Press.

Lingle, W. L., Barrett, S. L., Negron, V. C., D'Assoro, A. B., Boeneman, K., Liu, W., Whitehead, C. M., Reynolds, C. and Salisbury, J. L. (2002). Centrosome amplification drives chromosomal instability in breast tumor development. *Proc Natl Acad Sci USA* **99**, 1978–1983.

Livak, K. J. and Schmittgen, T. D. (2001). Analysis of Relative Gene Expression Data Using Real-Time Quantitative PCR and the 2−ΔΔCT Method. *Methods* **25**, 402–408.

Lucas, E. P. and Raff, J. W. (2007). Maintaining the proper connection between the centrioles and the pericentriolar matrix requires *Drosophila* centrosomin. *J Cell Biol* **178**, 725–732.

Lüders, J., Patel, U. K. and Stearns, T. (2005). GCP-WD is a γ-tubulin targeting factor required for centrosomal and chromatin-mediated microtubule nucleation. *Nat Cell Biol* **8**, 137–147.

Łuksza, M., Queguigner, I., Verlhac, M.-H. and Brunet, S. (2013). Rebuilding MTOCs upon centriole loss during mouse oogenesis. *Dev Biol* 1–9.

Macmillan, J. C., Hudson, J. W., Bull, S., Dennis, J. W. and Swallow, C. J. (2001). Comparative expression of the mitotic regulators SAK and PLK in colorectal cancer. *Ann. Surg. Oncol.* **8**, 729–740.

Magidson, V., O'connell, C. B., Loncarek, J., Paul, R., Mogilner, A. and Khodjakov, A. (2011). The Spatial Arrangement of Chromosomes during Prometaphase Facilitates Spindle Assembly. *Cell* **146**, 555–567.

Mahen, R., Jeyasekharan, A.D., Barry, N.P., Venkitaraman, A.R. (2011). Continuous polo-like kinase 1 activity regulates diffusion to maintain centrosome self-organization during mitosis. *Proc Natl Acad Sci USA* **108,** 9310-9315.

Mahen, R. and Venkitaraman, A. R. (2012). Pattern formation in centrosome assembly. *Curr Opin Cell Biol* **24**, 14–23.

Mahoney, N. M., Goshima, G., Douglass, A. D. and Vale, R. D. (2006). Making microtubules and mitotic spindles in cells without functional centrosomes. *Curr Biol* **16**, 564–569.

Maiato, H., Rieder, C. L. and Khodjakov, A. (2004). Kinetochore-driven formation of kinetochore fibers contributes to spindle assembly during animal mitosis. *J Cell Biol* **167**, 831–840.

Maniotis, A. and Schliwa, M. (1991). Microsurgical removal of centrosomes blocks cell reproduction and centriole generation in BSC-1 cells. *Cell* **67**, 495–504.

Manning, J. A., Shalini, S., Risk, J. M., Day, C. L. and Kumar, S. (2010). A Direct Interaction with NEDD1 Regulates γ-Tubulin Recruitment to the Centrosome. *PLoS ONE* **5**, e9618.

Maresca, T. J., Groen, A. C., Gatlin, J. C., Ohi, R., Mitchison, T. J. and Salmon, E. D. (2009). Spindle Assembly in the Absence of a RanGTP Gradient Requires Localized CPC Activity. *Curr Biol* **19**, 1210–1215.

Marshall, O. J. (2004). PerlPrimer: cross-platform, graphical primer design for standard, bisulphite and real-time PCR. *Bioinformatics* **20**, 2471–2472.

Marshall, W. F. (2009). Centriole evolution. *Curr Opin Cell Biol* **21**, 14–19.

Marshall, W. F., Vucica, Y. and Rosenbaum, J. L. (2001). Kinetics and regulation of de novo centriole assembly. Implications for the mechanism of centriole duplication. *Curr Biol* **11**, 308–317.

Marthiens, V., Rujano, M. A., Pennetier, C., Tessier, S., Paul-Gilloteaux, P. and Basto, R. (2013). Centrosome amplification causes microcephaly. *Nat Cell Biol* **15**, 1–12.

Martindill, D. M. J., Risebro, C. A., Smart, N., Franco-Viseras, M. D. M., Rosario, C. O., Swallow, C. J., Dennis, J. W. and Riley, P. R. (2007). Nucleolar release of Hand1 acts as a molecular switch to determine cell fate. *Nat Cell Biol* **9**, 1131–1141.

Martinez-Campos, M., Basto, R., Baker, J., Kernan, M. and Raff, J. W. (2004). The *Drosophila* pericentrin-like protein is essential for cilia/flagella function, but appears to be dispensable for mitosis. *J Cell Biol* **165**, 673–683.

Matsumoto, Y., Hayashi, K. and Nishida, E. (1999). Cyclin-dependent kinase 2

(Cdk2) is required for centrosome duplication in mammalian cells. *Current Biology* **9**, 429–432.

Matthies, H. J., McDonald, H. B., Goldstein, L. S. and Theurkauf, W. E. (2013). Anastral meiotic spindle morphogenesis: role of the non-claret disjunctional kinesin-like protein. *J Cell Biol* **134**, 455–464.

McIntyre, R. E., Lakshminarasimhan Chavali, P., Ismail, O., Carragher, D. M., Sanchez-Andrade, G., Forment, J. V., Fu, B., Del Castillo Velasco-Herrera, M., Edwards, A., van der Weyden, L., et al. (2012). Disruption of Mouse Cenpj, a Regulator of Centriole Biogenesis, Phenocopies Seckel Syndrome. *PLoS Genet* **8**, e1003022.

Megraw, T. L., Kilaru, S., Turner, F. R. and Kaufman, T. C. (2002). The centrosome is a dynamic structure that ejects PCM flares. *J Cell Sci* **115**, 4707–4718.

Megraw, T. L., Li, K., Kao, L. R. and Kaufman, T. C. (1999). The centrosomin protein is required for centrosome assembly and function during cleavage in *Drosophila*. *Development* **126**, 2829–2839.

Meireles, A. M., Fisher, K. H., Colombie, N., Wakefield, J. G. and Ohkura, H. (2009). Wac: a new Augmin subunit required for chromosome alignment but not for acentrosomal microtubule assembly in female meiosis. *J Cell Biol* **184**, 777–784.

Mennella, V., Keszthelyi, B., McDonald, K. L., Chhun, B., Kan, F., Rogers, G. C., Huang, B. and Agard, D. A. (2012). ncb2597. *Nat Cell Biol* **14**, 1159–1168.

Meunier, S. and Vernos, I. (2012). Microtubule assembly during mitosis - from distinct origins to distinct functions? *J Cell Sci* **125**, 2805–2814.

Meunier, S. and Vernos, I. (2011). K-fibre minus ends are stabilized by a RanGTP-dependent mechanism essential for functional spindle assembly. *Nat Cell Biol* **13**, 1406–1414.

Mikule, K., Delaval, B., Kaldis, P., Jurcyzk, A., Hergert, P. and Doxsey, S. (2007). Loss of centrosome integrity induces p38—p53—p21-dependent G1—S arrest. *Nat Cell Biol* **9**, 160–170.

Mitchison, T.J. (1993). Localization of an exchangeable GTP binding site at the plus end of microtubules. *Science* **261,** 1044-7.

Mitchison, T. and Kirschner, M. (1984). Dynamic instability of microtubule growth. *Nature* **312**, 237-42.

Moritz, M., Braunfeld, M. B., C, F. J., Sedat, J. W., Alberts, B. M. and Agard, D. A. (1995). Three-Dimensional Structural Characterization of Centrosomes from Early *Drosophila*Embryos. *J Cell Biol* 1–11.

Moritz, M. and Alberts. B.M. (1999). Isolation of centrosomes from *Drosophila* embryos. *Methods Cell Biol.* **61,** 1-12.

Mottier-Pavie, V., Cenci, G., Verni, F., Gatti, M. and Bonaccorsi, S. (2011). Phenotypic analysis of misato function reveals roles of noncentrosomal microtubules in *Drosophila* spindle formation. *J Cell Sci* **124**, 706–717.

Mountain, V., Simerly, C., Howard, L., Ando, A., Schatten, G. and Compton, D. A. (1999). The kinesin-related protein, HSET, opposes the activity of Eg5 and cross-links microtubules in the mammalian mitotic spindle. *J Cell Biol* **147**, 351–366.

Moutinho-Pereira, S., Debec, A. and Maiato, H. (2009). Microtubule cytoskeleton remodeling by acentriolar microtubule-organizing centers at the entry and exit from mitosis in *Drosophila* somatic cells. *Mol Biol Cell* **20**, 2796–2808.

Musacchio, A. and Salmon, E. D. (2007). The spindle-assembly checkpoint in space and time. *Nat Rev Mol Cell Biol* **8**, 379–393.

Müller, H., Schmidt, D., Steinbrink, S., Mirgorodskaya, E., Lehmann, V., Habermann, K., Dreher, F., Gustavsson, N., Kessler, T., Lehrach, H., et al. (2010). emboj2010210a. *EMBO J* **29**, 3344–3357.

Nakajima, T., Moriguchi, M., Mitsumoto, Y., Sekoguchi, S., Nishikawa, T., Takashima, H., Watanabe, T., Katagishi, T., Kimura, H., Okanoue, T., et al. (2004). Centrosome aberration accompanied with p53 mutation can induce genetic instability in hepatocellular carcinoma. *Mod Pathol* **17**, 722–727.

Nakazawa, Y., Hiraki, M., Kamiya, R. and Hirono, M. (2007). SAS-6 is a Cartwheel Protein that Establishes the 9-Fold Symmetry of the Centriole. *Current Biology* **17**, 2169–2174.

Nauli, S. M., Alenghat, F. J., Luo, Y., Williams, E., Vassilev, P., Li, X., Elia, A. E. H., Lu, W., Brown, E. M., Quinn, S. J., et al. (2003). Polycystins 1 and 2 mediate mechanosensation in the primary cilium of kidney cells. *Nat Genet* **33**, 129–137.

Nigg, E. A. and Raff, J. W. (2009). Centrioles, centrosomes, and cilia in health and disease. *Cell* **139**, 663–678.

Nonaka, S., Tanaka, Y., Okada, Y., Takeda, S., Harada, A., Kanai, Y., Kido, M. and Hirokawa, N. (1998). Randomization of left-right asymmetry due to loss of nodal cilia generating leftward flow of extraembryonic fluid in mice lacking KIF3B motor protein. *Cell* **95**, 829–837.

O'Connell, C. B. and Khodjakov, A. L. (2007). Cooperative mechanisms of mitotic spindle formation. *J Cell Sci* **120**, 1717–1722.

O'Connell, K. F., Caron, C., Kopish, K. R., Hurd, D. D., Kemphues, K. J., Li, Y. and White, J. G. (2001). The *C. elegans* zyg-1 gene encodes a regulator of centrosome duplication with distinct maternal and paternal roles in the embryo. *Cell* **105**, 547–558.

O'Connell, K. F., Maxwell, K. N. and White, J. O. (2000). The spd-2 gene is required for polarization of the anteroposterior axis and formation of the sperm asters in the Caenorhabditis elegans zygote. *Dev Biol* **222**, 55–70.

Oegema, K., Wiese, C., Martin, O. C., Milligan, R. A., Iwamatsu, A., Mitchison, T. J. and Zheng, Y. (1999). Characterization of two related *Drosophila* gamma-tubulin complexes that differ in their ability to nucleate microtubules. *J Cell Biol* **144**, 721–733.

Ohta, K., Shiina, N., Okumura, E., Hisanaga, S., Kishimoto, T., Endo, S., Gotoh, Y., Nishida, E. and Sakai, H. (1993). Microtubule nucleating activity of centrosomes in cell-free extracts from *Xenopus* eggs: involvement of phosphorylation and accumulation of pericentriolar material. *J Cell Sci* **104 (Pt 1)**, 125–137.

Okuda, M., Horn, H. F., Tarapore, P., Tokuyama, Y., Smulian, A. G., Chan, P. K., Knudsen, E. S., Hofmann, I. A., Snyder, J. D., Bove, K. E., et al. (2000). Nucleophosmin/B23 is a target of CDK2/cyclin E in centrosome duplication. *Cell* **103**, 127–140.

Oliveira, R. A. and Nasmyth, K. (2013). Cohesin cleavage is insufficient for centriole disengagement in *Drosophila*. *Curr Biol* **23**, R601–R603.

Paintrand, M., Moudjou, M., Delacroix, H. and Bornens, M. (1992). Centrosome organization and centriole architecture: their sensitivity to divalent cations. *J. Struct. Biol.* **108,** 107-128.

Palacios, M.J., Joshi, H.C., Simerly, C., and Schatten, G. (1993). Gamma-tubulin reorganization during mouse fertilization and early de- velopment. *J. Cell Sci.* **104,** 383–389.

Palazzo, R. E., Vogel, J. M., Schnackenberg, B. J., Hull, D. R. & Wu, X. (2000). Centrosome Maturation. *Curr. Top. Dev. Biol.* **49,** 449–470.

Peel, N., Stevens, N. R., Basto, R. and Raff, J. W. (2007). Overexpressing centriole-replication proteins *in vivo* induces centriole overduplication and de novo formation. *Curr Biol* **17**, 834–843.

Pelletier, L., O'Toole, E., Schwager, A., Hyman, A. A. and Müller-Reichert, T. (2006a). Centriole assembly in Caenorhabditis elegans. *Nature* **444**, 619–623.

Pelletier, L., O'Toole, E., Schwager, A., Hyman, A. A. and Müller-Reichert, T. (2006b). Centriole assembly in Caenorhabditis elegans. *Nature* **444**, 619–623.

Pelletier, L., Özlü, N., Hannak, E., Cowan, C., Habermann, B., Ruer, M., Müller-Reichert, T. and Hyman, A. A. (2004). The Caenorhabditis elegans Centrosomal Protein SPD-2 Is Required for both Pericentriolar Material Recruitment and Centriole Duplication. *Current Biology* **14**, 863–873.

Peters, N., Perez, D. E., Song, M. H., Liu, Y., Muller-Reichert, T., Caron, C., Kemphues, K. J. and O'Connell, K. F. (2010). Control of mitotic and meiotic centriole duplication by the Plk4-related kinase ZYG-1. *J Cell Sci* **123**, 795–805.

Petry, S., Groen, A. C., Ishihara, K., Mitchison, T. J. and Vale, R. D. (2013a). Branching Microtubule Nucleation in *Xenopus* Egg Extracts Mediated by Augmin and TPX2. *Cell* **152**, 768–777.

Petry, S., Groen, A. C., Ishihara, K., Mitchison, T. J. and Vale, R. D. (2013b). Branching Microtubule Nucleation in *Xenopus* Egg Extracts Mediated by Augmin and TPX2. *Cell* **152**, 768–777.

Pickett-Heaps, J. (1971). Autonomy of the centriole-fact or fallacy? *Cytobios* **3**, 205.

Pihan, G. A., Purohit, A., Wallace, J., Knecht, H., Woda, B., Quesenberry, P. and Doxsey, S. J. (1998). Centrosome defects and genetic instability in malignant tumors. *Cancer Res* **58**, 3974–3985.

Pihan, G. A., Purohit, A., Wallace, J., Malhotra, R., Liotta, L. and Doxsey, S. J. (2001). Centrosome defects can account for cellular and genetic changes that characterize prostate cancer progression. *Cancer Res* **61**, 2212–2219.

Pihan, G. A., Wallace, J., Zhou, Y. and Doxsey, S. J. (2003). Centrosome abnormalities and chromosome instability occur together in pre-invasive carcinomas. *Cancer Res* **63**, 1398–1404.

Piperno, G. and Fuller, M.T. (1985). Monoclonal antibodies specific for an acetylated form of alpha-tubulin recognize the antigen in cilia and flagella from a variety of organisms. *J Cell Biol* **101,** 2085-94.

Puklowski, A., Homsi, Y., Keller, D., May, M., Chauhan, S., Kossatz, U., Grünwald, V., Kubicka, S., Pich, A., Manns, M. P., et al. (2011). ncb2282. *Nat Cell Biol* **13**, 1004–1009.

Quintyne, N. J., Reing, J. E., Hoffelder, D. R., Gollin, S. M. and Saunders, W. S. (2005). Spindle multipolarity is prevented by centrosomal clustering. *Science* **307**, 127–129.

Ramaswamy, S., Ross, K. N., Lander, E. S. and Golub, T. R. (2002). A molecular signature of metastasis in primary solid tumors. *Nat Genet* **33**, 49–54.

Rauch, A., Thiel, C. T., Schindler, D., Wick, U., Crow, Y. J., Ekici, A. B., van Essen, A. J., Goecke, T. O., Al-Gazali, L., Chrzanowska, K. H., et al. (2008). Mutations in the Pericentrin (PERICENTRIN) Gene Cause Primordial Dwarfism. *Science* **319**, 816–819.

Rebollo, E., Llamazares, S., Reina, J. and Gonzalez, C. (2004). Contribution of Noncentrosomal Microtubules to Spindle Assembly in *Drosophila* Spermatocytes. *PLoS Biol* **2**, e8.

Reinders, Y., Schulz, I., Gräf, R. and Sickmann, A. (2006). Identification of Novel Centrosomal Proteins in Dictyosteliumdiscoideumby Comparative Proteomic Approaches. *J. Proteome Res.* **5**, 589–598.

Reschen, R. F., Colombie, N., Wheatley, L., Dobbelaere, J., St Johnston, D., Ohkura, H. and Raff, J. W. (2012). Dgp71WD is required for the assembly of the acentrosomal Meiosis I spindle, and is not a general targeting factor for the -TuRC. *Biology Open* **1**, 422–429.

Rhodes, D. R., Yu, J., Shanker, K., Deshpande, N., Varambally, R., Ghosh, D.,

Barrette, T., Pandey, A. and Chinnaiyan, A. M. (2004). Large-scale meta-analysis of cancer microarray data identifies common transcriptional profiles of neoplastic transformation and progression. *Proc Natl Acad Sci U S A* **101**, 9309-14**.**

Rieder, C. L. (1981). The structure of the cold-stable kinetochore fiber in metaphase PtK1 cells. *Chromosoma* **84,** 145-158

Rieder, C.L., Faruki, S. and Khodjakov, A. (2001). The centrosome in vertebrates: more than a microtubule-organizing center. *Trends Cell Biol* **11,** 413-9.

Riparbelli, M. G., Stouthamer, R., Dallai, R. and Callaini, G. (1998). Microtubule organization during the early development of the parthenogenetic egg of the hymenopteran Muscidifurax uniraptor. *Dev Biol* **195**, 89–99.

Riparbelli, M. G., Tagu, D., Bonhomme, J. and Callaini, G. (2005). Aster self-organization at meiosis: a conserved mechanism in insect parthenogenesis? *Dev Biol* **278**, 220–230.

Roberts, D. (1986). *Drosophila*, a practical approach. IRL Press, Oxford.

Robertson, H. M., C. R. Preston, R. W. Phillis, D. Johnson-Schlitz, W. K. Benz and W. R. Engels. (1988). A stable genomic source of P element transposase in *Drosophila melanogaster*. *Genetics* **118:**461-470.

Rodrigues-Martins, A., Bettencourt-Dias, M., Riparbelli, M., Ferreira, C., Ferreira, I., Callaini, G. and Glover, D. M. (2007a). DSAS-6 Organizes a Tube-like Centriole Precursor, and Its Absence Suggests Modularity in Centriole Assembly. *Current Biology* **17**, 1465–1472.

Rodrigues-Martins, A., Bettencourt-Dias, M., Riparbelli, M., Ferreira, C., Ferreira, I., Callaini, G. and Glover, D. M. (2007b). DSAS-6 Organizes a Tube-like Centriole Precursor, and Its Absence Suggests Modularity in Centriole Assembly. *Current Biology* **17**, 1465–1472.

Rodrigues-Martins, A., Riparbelli, M., Callaini, G., Glover, D. M. and Bettencourt-Dias, M. (2007c). Revisiting the role of the mother centriole in centriole biogenesis. *Science* **316**, 1046–1050.

Rodrigues-Martins, A., Riparbelli, M., Callaini, G., Glover, D. M. and Bettencourt-Dias, M. (2008). From centriole biogenesis to cellular function: centrioles are essential for cell division at critical developmental stages. *Cell Cycle* **7**, 11–16.

Rogers, G. C., Rusan, N. M., Peifer, M. and Rogers, S. L. (2008). A multicomponent assembly pathway contributes to the formation of acentrosomal microtubule arrays in interphase *Drosophila* cells. *Mol Biol Cell* **19**, 3163–3178.

Rogers, G. C., Rusan, N. M., Roberts, D. M., Peifer, M. and Rogers, S. L. (2009). The SCFSlimb ubiquitin ligase regulates Plk4/Sak levels to block centriole reduplication. *J Cell Biol* **184**, 225–239.

Roque, H., Wainman, A., Richens, J., Kozyrska, K., Franz, A. and Raff, J. W.

(2013). *Drosophila* Cep135/Bld10 maintains proper centriole structure but is dispensable for cartwheel formation. *J Cell Sci* **125**, 5881–5886.

Rossi, F. and Gonzalez, C. (2011). Synergism between altered cortical polarity and the PI3K/TOR pathway in the suppression of tumour growth. *EMBO reports* 1–6.

Roy, S. (2012). Cilia and Hedgehog When and how was their marriage solemnized? *Differentiation* **83**, S43–S48.

Sampath, S. C., Ohi, R., Leismann, O., Salic, A., Pozniakovski, A. and Funabiki, H. (2004). The Chromosomal Passenger Complex Is Required for Chromatin-Induced Microtubule Stabilization and Spindle Assembly. *Cell* **118**, 187–202.

Santos, Dos, H. G., Abia, D., Janowski, R., Mortuza, G., Bertero, M. G., Boutin, M., Guarín, N., Méndez-Giraldez, R., Nuñez, A., Pedrero, J. G., et al. (2013). Structure and Non-Structure of Centrosomal Proteins. *PLoS ONE* **8**, e62633.

Satir, P. and Christensen, S. T. (2008). Structure and function of mammalian cilia. *Histochem Cell Biol* **129**, 687–693.

Schermelleh, L., Carlton, P. M., Haase, S., Shao, L., Winoto, L., Kner, P., Burke, B., Cardoso, M. C., Agard, D. A., Gustafsson, M. G. L., et al. (2008). Subdiffraction Multicolor Imaging of the Nuclear Periphery with 3D Structured Illumination Microscopy. *Science* **320**, 1332–1336.

Schermelleh, L., Heintzmann, R. and Leonhardt, H. (2010). A guide to super-resolution fluorescence microscopy. *J Cell Biol* **190**, 165–175.

Schindelin, J., Arganda-Carreras, I., Frise, E., Kaynig, V., Longair, M., Pietzsch, T., Preibisch, S., Rueden, C., Saalfeld, S., Schmid, B., et al. (2012). Fiji: an open-source platform for biological-image analysis. *Nature Publishing Group* **9**, 676–682.

Schmidt, T. I., Kleylein-Sohn, J., Westendorf, J., Le Clech, M., Lavoie, S. B., Stierhof, Y.-D. and Nigg, E. A. (2009). Control of Centriole Length by CPAP and CP110. *Curr Biol* **19**, 1005–1011.

Schmit, A. C. (2002). Acentrosomal microtubule nucleation in higher plants. *International Review of Cytology.* **220,** 257-289.

Schöckel, L., Möckel, M., Mayer, B., Boos, D. and Stemmann, O. (2011). Cleavage of cohesin rings coordinates the separation of centrioles and chromatids. *Nat Cell Biol* **13**, 1–9.

Schuh, M. and Ellenberg, J. (2007). Self-Organization of MTOCs Replaces Centrosome Function during Acentrosomal Spindle Assembly in Live Mouse Oocytes. *Cell* **130**, 484–498.

Scott, K. L., Nogueira, C., Heffernan, T. P., van Doorn, R., Dhakal, S., Hanna, J. A., Min, C., Jaskelioff, M., Xiao, Y., Wu, C.-J., et al. (2011). Proinvasion Metastasis Drivers in Early-Stage Melanoma Are Oncogenes. *Cancer Cell* **20**, 92–103.

Shah, A. S., Ben-Shahar, Y., Moninger, T. O., Kline, J. N. and Welsh, M. J. (2009). Motile Cilia of Human Airway Epithelia Are Chemosensory. *Science* **325**, 1131–1134.

Shen, J. (2005). ASPM mutations identified in patients with primary microcephaly and seizures. *Journal of Medical Genetics* **42**, 725–729.

Silkworth, W. T., Nardi, I. K., Scholl, L. M. and Cimini, D. (2009). Multipolar spindle pole coalescence is a major source of kinetochore mis-attachment and chromosome mis-segregation in cancer cells. *PLoS ONE* **4**, e6564.

Sillibourne, J. E., Hurbain, I., Grand-Perret, T., Goud, B., Tran, P. and Bornens, M. (2013). Primary ciliogenesis requires the distal appendage component Cep123. *Biology Open* **2**, 535–545.

Sillibourne, J. E., Tack, F., Vloemans, N., Boeckx, A., Thambirajah, S., Bonnet, P., Ramaekers, F. C. S., Bornens, M. and Grand-Perret, T. (2010). Autophosphorylation of pololike kinase 4 and its role in centriole duplication..full. *Mol Biol Cell* **21**, 547–561.

Singla, V. (2006). The Primary Cilium as the Cell's Antenna: Signaling at a Sensory Organelle. *Science* **313**, 629–633.

Sir, J.-H., Barr, A. R., Nicholas, A. K., Carvalho, O. P., Khurshid, M., Sossick, A., Reichelt, S., D'Santos, C., Woods, C. G. and Gergely, F. (2011). ng.971. *Nat Genet* **43**, 1147–1153.

Slevin, L. K., Nye, J., Pinkerton, D. C., Buster, D. W., Rogers, G. C. and Slep, K. C. (2012). The Structure of the Plk4 Cryptic Polo Box Reveals Two Tandem Polo Boxes Required for Centriole Duplication. *Structure/Folding and Design* 1–13.

Smyth, G. K. (2005). Limma: linear models for microarray data. In Bioinformatics And Computational Biology Solutions Using R And Bioconductor (ed. R. Gentleman, V. Carey, S. Dudoit, R. Irizarry and W. Huber), pp. 397-420. New York: Springer.

Songyang, Z., Blechner, S., Hoagland, N., Hoekstra, M. F., Piwnica-Worms, H. and Cantley, L. C. (1994). Use of an oriented peptide library to determine the optimal substrates of protein kinases. *Curr Biol* **4**, 973–982.

Sonnen, K. F., Gabryjonczyk, A. M., Anselm, E., Stierhof, Y. D. and Nigg, E. A. (2013). Human Cep192 and Cep152 cooperate in Plk4 recruitment and centriole duplication. *J Cell Sci* **126**, 3223–3233.

Sonnen, K. F., Schermelleh, L., Leonhardt, H. and Nigg, E. A. (2012). 3D-structured illumination microscopy provides novel insight into architecture of human centrosomes. *Biology Open* **1**, 965–976.

Sorino, C., Bruno, T., Desantis, A., Di Certo, M. G., Iezzi, S., De Nicola, F., Catena, V., Floridi, A., Chessa, L., Passananti, C., et al. (2013). Centrosomal Che-1 Protein Is Involved in the Regulation of Mitosis and DNA Damage Response by Mediating Pericentrin (PERICENTRIN)-dependent Chk1 Protein Localization. *J Biol Chem* **288**, 23348–23357.

Sorokin, S. (1962). Centrioles and the formation of rudimentary cilia by fibroblasts and smooth muscle cells. *J. Cell Biol.,* **15,** 363 – 377.

Srsen, V. (2006). Inhibition of centrosome protein assembly leads to p53-dependent exit from the cell cycle. *J Cell Biol* **174**, 625–630.

Stenoien, D. L., Sen, S., Mancini, M. A. and Brinkley, B. R. (2003). Dynamic association of a tumor amplified kinase, Aurora-A, with the centrosome and mitotic spindle. *Cell Motil. Cytoskeleton* **55**, 134–146.

Stevens, N. R., Dobbelaere, J., Brunk, K., Franz, A. and Raff, J. W. (2010a). *Drosophila* Ana2 is a conserved centriole duplication factor. *J Cell Biol* **188**, 313–323.

Stevens, N. R., Raposo, A. A. S. F., Basto, R., St Johnston, D. and Raff, J. W. (2007). From stem cell to embryo without centrioles. *Curr Biol* **17**, 1498–1503.

Stevens, N. R., Roque, H. and Raff, J. W. (2010b). DSas-6 and Ana2 Coassemble into Tubules to Promote Centriole Duplication and Engagement. *Dev Cell* **19**, 913–919.

Strnad, P., Leidel, S., Vinogradova, T., Euteneuer, U., Khodjakov, A. and Gönczy, P. (2007). Regulated HsSAS-6 Levels Ensure Formation of a Single Procentriole per Centriole during the Centrosome Duplication Cycle. *Dev Cell* **13**, 203–213.

Stucke, V.M., Sillje, H.H., Arnaud, L., and Nigg, E.A. (2002). Human Mps1 kinase is required for the spindle assembly checkpoint but not for centrosome duplication. *EMBO J.* **21,** 1723–1732.

Sturtevant, A. H. (1929). The claret mutant type of *Drosophila* simulans: a study of chromosome elimination and of cell-lineage. *Z. Wiss. Zool.* **135,** 323-356.

Sumiyoshi, E., Sugimoto, A. and Yamamoto, M. (2002). Protein phosphatase 4 is required for centrosome maturation in mitosis and sperm meiosis in *C. elegans*. *J Cell Sci* **115**, 1403–1410.

Sunkel, C. E. and Glover, D. M. (1988). polo, a mitotic mutant of *Drosophila* displaying abnormal spindle poles. *J Cell Sci* **89 (Pt 1)**, 25–38.

Takada, S., Kelkar, A. and Theurkauf, W. E. (2003). *Drosophila* checkpoint kinase 2 couples centrosome function and spindle assembly to genomic integrity. *Cell* **113**, 87–99.

Tang, C.-J. C., Fu, R.-H., Wu, K.-S., Hsu, W.-B. and Tang, T. K. (2009). ncb1889. *Nat Cell Biol* **11**, 825–831.

Tang, C.-J. C., Lin, S.-Y., Hsu, W.-B., Lin, Y.-N., Wu, C.-T., Lin, Y.-C., Chang, C.-W., Wu, K.-S. and Tang, T. K. (2011). emboj2011378a. *EMBO J* **30**, 4790–4804.

Tanos, B. E., Yang, H. J., Soni, R., Wang, W. J., Macaluso, F. P., Asara, J. M. and Tsou, M. F. B. (2013). Centriole distal appendages promote membrane docking, leading to cilia initiation. *Genes Dev* **27**, 163–168.

Thompson, S. L., Bakhoum, S. F. and Compton, D. A. (2010). Mechanisms of

chromosomal instability. *Curr Biol* **20**, R285–95.

Tilney, L.G., Bryan, J., Bush, D.J., Fujiwara, K., Mooseker, M.S., Murphy, D.B. and Snyder, D.H. (1973). Microtubules: evidence for 13 protofilaments. *J Cell Biol.* **59**, 267-75.

Tram, U. and Sullivan, W. (2000). Reciprocal inheritance of centrosomes in the parthenogenetic hymenopteran Nasonia vitripennis. *Curr Biol* **10**, 1413–1419.

Tritarelli, A., Oricchio, E., Ciciarello, M., Mangiacasale, R., Palena, A., Lavia, P., Soddu, S. and Cundari, E. (2004). p53 localization at centrosomes during mitosis and postmitotic checkpoint are ATM-dependent and require serine 15 phosphorylation. *Mol Biol Cell* **15**, 3751–3757.

Tseng, B. S., Tan, L., Kapoor, T. M. and Funabiki, H. (2010). Dual Detection of Chromosomes and Microtubules by the Chromosomal Passenger Complex Drives Spindle Assembly. *Dev Cell* **18**, 903–912.

Tsou, M.-F. B. and Stearns, T. (2006). Mechanism limiting centrosome duplication to once per cell cycle. *Nature* **442**, 947–951.

Tsou, M.-F. B., Wang, W.-J., George, K. A., Uryu, K., Stearns, T. and Jallepalli, P. V. (2009a). Polo Kinase and Separase Regulate the Mitotic Licensing of Centriole Duplication in Human Cells. *Dev Cell* **17**, 344–354.

Tsou, M.-F. B., Wang, W.-J., George, K. A., Uryu, K., Stearns, T. and Jallepalli, P. V. (2009b). Polo Kinase and Separase Regulate the Mitotic Licensing of Centriole Duplication in Human Cells. *Dev Cell* **17**, 344–354.

Tulu, U. S., Fagerstrom, C., Ferenz, N. P. and Wadsworth, P. (2006). Molecular Requirements for Kinetochore-Associated Microtubule Formation in Mammalian Cells. *Current Biology* **16**, 536–541.

Ueharaa, R., Nozawab, R.-S., Tomiokaa, A., Petryc, S., Ronald D Valec, Obuseb, C.Gohta Goshimaa (2009). The augmin complex plays a critical role in spindlemicrotubule generation for mitotic progressionand cytokinesis in human cells. 1–6.

Uetake, Y., Loncarek, J., Nordberg, J. J., English, C. N., La Terra, S., Khodjakov, A. and Sluder, G. (2007). Cell cycle progression and de novo centriole assembly after centrosomal removal in untransformed human cells. *J Cell Biol* **176**, 173–182.

Uhlmann, F., Lottspeich, F. and Nasmyth, K. (1999). Sister-chromatid separation at anaphase onset is promoted by cleavage of the cohesin subunit Scc1. *Nature* **400**, 37–42.

Vaizel-Ohayon, D. and Schejter, E. D. (1999). Mutations in centrosomin reveal requirements for centrosomal function during early *Drosophila* embryogenesis. *Curr Biol* **9**, 889–898.

Van Breugel, M., Hirono, M., Andreeva, A., Yanagisawa, H.-A., Yamaguchi, S., Nakazawa, Y., Morgner, N., Petrovich, M., Ebong, I.-O., Robinson, C. V., et al.

(2011). Structures of SAS-6 Suggest Its Organization in Centrioles. *Science* **331**, 1196–1199.

Varmark, H., Llamazares, S., Rebollo, E., Lange, B., Reina, J., Schwarz, H. and Gonzalez, C. (2007). Asterless is a centriolar protein required for centrosome function and embryo development in *Drosophila*. *Curr Biol* **17**, 1735–1745.

Verde, F., Labbé, J.C., Dorée, M., Karsenti, E. (1990). Regulation of microtubule dynamics by cdc2 protein kinase in cell-free extracts of *Xenopus* eggs. *Nature* **18,** 233–238.

Vérollet, C., Colombié, N., Daubon, T., Bourbon, H.-M., Wright, M. and Raynaud-Messina, B. (2006). *Drosophila* melanogaster gamma-TuRC is dispensable for targeting gamma-tubulin to the centrosome and microtubule nucleation. *J Cell Biol* **172**, 517–528.

Vorobjev, I.A. and Chentsov Yu, S. (1982) Centrioles in the cell cycle. I. Epithelial cells. *J Cell Biol* **93,** 938-49.

Vulprecht, J., David, A., Tibelius, A., Castiel, A., Konotop, G., Liu, F., Bestvater, F., Raab, M. S., Zentgraf, H., Izraeli, S., et al. (2012). STIL is required for centriole duplication in human cells. *J Cell Sci* **125**, 1353–1362.

Wainman, A., Buster, D. W., Duncan, T., Metz, J., Ma, A., Sharp, D. and Wakefield, J. G. (2009). A new Augmin subunit, Msd1, demonstrates the importance of mitotic spindle-templated microtubule nucleation in the absence of functioning centrosomes. *Genes Dev* **23**, 1876–1881.

Wakefield, J. G., Huang, J. Y. and Raff, J. W. (2000). Centrosomes have a role in regulating the destruction of cyclin B in early *Drosophila* embryos. *Curr Biol* **10**, 1367–1370.

Walczak, C. E., Vernos, I., Mitchison, T. J., Karsenti, E. and Heald, R. (1998). A model for the proposed roles of different microtubule-based motor proteins in establishing spindle bipolarity. *Curr Biol* **8**, 903–913.

Wang, C., Li, S., Januschke, J., Rossi, F., Izumi, Y., Garcia-Alvarez, G., Gwee, S. S. L., Soon, S. B., Sidhu, H. K., Yu, F., et al. (2011a). An Ana2/Ctp/Mud Complex Regulates Spindle Orientation in *Drosophila* Neuroblasts. *Dev Cell* **21**, 520–533.

Wang, C., Li, S., Januschke, J., Rossi, F., Izumi, Y., Garcia-Alvarez, G., Gwee, S. S. L., Soon, S. B., Sidhu, H. K., Yu, F., et al. (2011b). An Ana2/Ctp/Mud Complex Regulates Spindle Orientation in *Drosophila* Neuroblasts. *Dev Cell* **21**, 520–533.

Wang, H., Somers, G. W., Bashirullah, A., Heberlein, U., Yu, F. and Chia, W. (2006). Aurora-A acts as a tumor suppressor and regulates self-renewal of *Drosophila* neuroblasts. *Genes Dev* **20**, 3453–3463.

Warnke, S., Kemmler, S., Hames, R. S., Tsai, H.-L., Hoffmann-Rohrer, U., Fry, A. M. and Hoffmann, I. (2004). Polo-like Kinase-2 Is Required for Centriole

Duplication in Mammalian Cells. *Current Biology* **14**, 1200–1207.

Weaver, B. A. A. and Cleveland, D. W. (2009). The role of aneuploidy in promoting and suppressing tumors. *J Cell Biol* **185**, 935–937.

Weaver, B. A. A., Silk, A. D., Montagna, C., Verdier-Pinard, P. and Cleveland, D. W. (2007). Aneuploidy acts both oncogenically and as a tumor suppressor. *Cancer Cell* **11**, 25–36.

Wollman, R., Cytrynbaum, E. N., Jones, J. T., Meyer, T., Scholey, J. M. and Mogilner, A. (2005). Efficient Chromosome Capture Requires a Bias in the "Search-and-Capture" Process during Mitotic-Spindle Assembly. *Current Biology* **15**, 828–832.

Woods, C. G., Bond, J. and Enard, W. (2005). Autosomal recessive primary microcephaly (MCPH): a review of clinical, molecular, and evolutionary findings. *Am J Hum Genet* **76**, 717–728.

Wu, M., Pastor-Pareja, J. C. and Xu, T. (2010). Interaction between Ras(V12) and scribbled clones induces tumour growth and invasion. *Nature* **463**, 545–548.

Wu, Z. and Irizarry, R. A. (2007). A statistical framework for the analysis of microarray probe-level data. *Ann. Appl. Stat.* **1**, 333–357.

Yabe, T., Ge, X. and Pelegri, F. (2007). The zebrafish maternal-effect gene cellular atoll encodes the centriolar component sas-6 and defects in its paternal function promote whole genome duplication. *Dev Biol* **312**, 44–60.

Yang, Z., Loncarek, J., Khodjakov, A. and Rieder, C. L. (2008). Extra centrosomes and/or chromosomes prolong mitosis in human cells. *Nat Cell Biol* **10**, 748–751.

Yu, T. W., Mochida, G. H., Tischfield, D. J., Sgaier, S. K., Flores-Sarnat, L., Sergi, C. M., Topçu, M., Mcdonald, M. T., Barry, B. J., Felie, J. M., et al. (2010). Mutations in WDR62, encoding a centrosome-associated protein, cause microcephaly with simplified gyri and abnormal cortical architecture. *Nat Genet* **42**, 1015–1020.

Zhai, B., Villén, J., Beausoleil, S. A., Mintseris, J. and Gygi, S. P. (2008). Phosphoproteome Analysis of *Drosophila* melanogaster embryos. *J. Proteome Res.* **7**, 1675–1682.

Zhang, J. and Megraw, T. L. (2007). Proper recruitment of gamma-tubulin and D-TACC/Msps to embryonic *Drosophila* centrosomes requires Centrosomin Motif 1. *Mol Biol Cell* **18**, 4037–4049.

Zhao, T., Graham, O. S., Raposo, A. and St Johnston, D. (2012). Growing Microtubules Push the Oocyte Nucleus to Polarize the *Drosophila* Dorsal-Ventral Axis. *Science* **336**, 999–1003.

Zheng, Y., Wong, M.L., Alberts, B. and Mitchison, T. (1995). Nucleation of microtubule assembly by a gamma-tubulin-containing ring complex. *Nature* **378,** 578-83.

Zhu, F., Lawo, S., Bird, A., Pinchev, D., Ralph, A., Richter, C., Müller-Reichert, T., Kittler, R., Hyman, A. A. and Pelletier, L. (2008a). The Mammalian SPD-2 Ortholog Cep192 Regulates Centrosome Biogenesis. *Current Biology* **18**, 136–141.

Zhu, F., Lawo, S., Bird, A., Pinchev, D., Ralph, A., Richter, C., Müller-Reichert, T., Kittler, R., Hyman, A. A. and Pelletier, L. (2008b). The mammalian SPD-2 ortholog Cep192 regulates centrosome biogenesis. *Curr Biol* **18**, 136–141.

Zhu, H., Fang, K. and Fang, G. (2009). FAM29A, a target of Plk1 regulation, controls the partitioning of NEDD1 between the mitotic spindle and the centrosomes. *J Cell Sci* **122**, 2750–2759.

Zimmerman, W. C., Sillibourne, J., Rosa, J. and Doxsey, S. J. (2004). Mitosis-specific anchoring of gamma tubulin complexes by pericentrin controls spindle organization and mitotic entry. *Mol Biol Cell* **15**, 3642–3657.

Zyss, D. and Gergely, F. (2009). Centrosome function in cancer: guilty or innocent? *Trends Cell Biol* **19**, 334–346.

Supplementary Table 1. *Phosphorylation sites in centrosomal Asl and Spd-2. Phosphorylated residues are marked in red.*

protein	peptide sequence	modification	exp mr[1]	pep calc mr[2]	pep score[3]	pep expect[4]
Asl	TRETADNLRLELER	Phospho (ST)	1794.8614	1794.8625	18.18	2.2
Asl	LVGSTPLNPLDR	Phospho (ST)	1360.6726	1360.6752	25	0.073
Spd2	GTNISFEPAEITGR	Phospho (ST)	1570.7027	1570.7028	53.03	0.0018
Spd2	TNQPLLEPESNVTLD SVGEK	Phospho (ST)	2249.0448	2249.0464	65.26	6.10E-05
Spd2	RPPSSSEILSLSAIDK	Phospho (ST)	1778.8803	1778.8815	38.85	0.015
Spd2	KPLSPLADHPQITISR	Phospho (ST)	1851.9624	1851.9608	34.55	0.034
Spd2	RVSIATMGLIPR	Oxidation (M); Phospho (ST)	1252.6244	1252.625	29.93	0.074
Spd2	GLGTSSVAVPR	Phospho (ST)	1122.5449	1122.5434	64.8	1.80E-05
Spd2	NLSPLSSPR	Phospho (ST)	1049.4886	1049.4906	42.33	0.0029
Spd2	NLSPLSSPR	2 Phospho (ST)	1129.4593	1129.457	7	0.77
Spd2	VFGDLSSFSK	Phospho (ST)	1165.5078	1165.5057	17.63	0.94
Spd2	ANSSPAGSEASSTSG FTASGR	Phospho (ST)	2007.8158	2007.8171	60	9.5E-0.6
Spd2	DFGISPNLAK	Phospho (ST)	1140.5206	1140.5216	32	0.016

[1]*experimental relative molecular mass of the matched peptide*
[2]*calculated relative molecular mass of the matched peptide*
[3]*Ion Score is −10log(P), with P being the probability that the observed match is a random event. Individual ions scores > 29 indicate identity or extensive homology (p<0.05).*
[4]*Expectation Value, indicates probability that the observed match between MS/MS spectra and peptide sequence would be found by chance. The lower the expectation value, the more significant the score.*

Supplementary Table 2. *Phosphorylation sites in cytoplasmic Asl and Spd-2. Phosphorylated residues are marked in red.*

protein	peptide sequence	modification	exp mr[1]	calc mr[2]	pep score[3]	pep expect[4]
Asl	TRETADNLR	Phospho (ST)	1154.5086	1154.5081	40.95	0.029
Asl	SNSVSPSDPSPK	Phospho (ST)	1280.5273	1280.5286	26	0.018
Spd2	NLSPLSSPR	Phospho (ST)	1049.4919	1049.4906	33.91	0.058
Spd2	LLRSPR	Phospho (ST)	820.4323	820.432	19	0.46
Spd2	SENIWNIVSNSSPNR	Phospho (ST)	1795.7852	1795.789	41	0.00076

[1]*experimental relative molecular mass of the matched peptide*
[2]*calculated relative molecular mass of the matched peptide*
[3]*Ion Score is −10log(P), with P being the probability that the observed match is a random event. Individual ions scores > 29 indicate identity or extensive homology (p<0.05).*
[4]*Expectation Value, indicates probability that the observed match between MS/MS spectra and peptide sequence would be found by chance. The lower the expectation value, the more significant the score.*

Supplementary Table 3. *Genes significantly up- or down-regulated in DSas-4 in comparison to* w^{67} *(≥1.5-fold, adj.P-value ≤ 0.05).*

Affymetrix ID	Gene	Fold Change	P.Value	adj.P-Value
1636055_at	*Hsc70-2*	141.10	1.35E-08	0.000
1637465_at	*CG31157*	23.52	2.04E-08	0.000
1640426_at	*CG31287*	16.92	6.21E-06	0.015
1631082_at	*B52*	10.68	2.34E-05	0.022
1635802_s_at	*CG9279*	8.81	7.01E-06	0.015
1632063_s_at	*CG11357*	8.71	2.38E-05	0.022
1627214_s_at	*CG7650*	7.03	2.67E-05	0.022
1640075_a_at	*path*	6.99	3.11E-05	0.024
1626667_at	*miple*	4.56	1.06E-05	0.019
1641242_at	*Ugt86Di*	3.45	2.16E-05	0.022
1637046_at	*l(2)03659*	2.75	1.14E-05	0.019
1623522_at	*CG11668*	2.40	9.68E-05	0.041
1640112_at	*Cys*	2.27	2.39E-05	0.022
1635701_at	*GstD3*	2.25	1.33E-05	0.021
1638486_at	*Rbp1*	2.12	8.40E-05	0.038
1636131_at	*lig3*	2.08	1.79E-05	0.022
1637121_at	*Rbp4*	1.88	3.43E-06	0.012
1636551_at	*CG14683*	1.71	5.94E-05	0.035
1634970_at	*CG3634*	1.61	3.56E-05	0.026
1634113_at	*geko*	-1.69	2.04E-05	0.022
1636600_a_at	*Mf*	-1.74	3.67E-05	0.026
1633349_at	*TFIIFβ*	-2.07	4.64E-06	0.012
1630318_at	*MED7*	-2.13	8.87E-07	0.004
1633727_s_at	*wnd*	-2.34	4.46E-05	0.030
1633520_at	*CG32027*	-2.88	2.59E-05	0.022
1638398_at	*ShaI*	-3.31	8.15E-05	0.038
1627558_at	*DSas-4*	-6.83	3.60E-05	0.026

Supplementary Table 4. *Genes significantly up- or down-regulated in DSas-4 in comparison to OrR (≥1.5-fold, adj.P-value ≤ 0.05).*

Affymetrix ID	Gene	Fold Change	P.Value	adj.P-Value
1636055_at	*Hsc70-2*	96.76	2.71E-05	0.032
1637465_at	*CG31157*	22.50	1.41E-07	0.003
1640426_at	*CG31287*	11.92	4.31E-05	0.039
1635802_s_at	*CG9279*	7.85	1.14E-06	0.008
1626878_at	*CG42348*	4.45	5.74E-05	0.041
1641242_at	*Ugt86Di*	3.69	1.20E-06	0.008
1625195_s_at	*shn*	3.66	2.28E-05	0.029
1632873_at	*MtnA*	3.36	1.61E-05	0.027
1626667_at	*miple*	3.31	2.90E-05	0.032
1636131_at	*lig3*	2.08	3.18E-06	0.012
1635701_at	*GstD3*	1.98	2.03E-05	0.029
1637121_at	*Rbp4*	1.85	3.32E-05	0.033
1639023_at	*Nsf2*	1.76	5.65E-05	0.041
1639552_s_at	*CG6951*	1.61	1.11E-05	0.023
1634970_at	*CG3634*	1.51	5.76E-05	0.041
1627532_at	*Rpb4*	-1.54	6.75E-05	0.044
1630318_at	*MED 7*	-2.12	1.03E-05	0.023
1633349_at	*TFIIFβ*	-2.14	2.14E-05	0.029
1633727_s_at	*wnd*	-2.18	2.94E-06	0.012
1639564_a_at	*CG7768*	-2.77	5.91E-05	0.041
1633627_at	*CG13023*	-3.81	8.43E-05	0.048
1627558_at	*DSas-4*	-7.31	1.95E-05	0.029

Supplementary Table 5. *Genes significantly up- or down-regulated in SakOE in comparison to* w^{67} *(≥1.5-fold, adj.P-value ≤ 0.05).*

Affymetrix ID	Gene	Fold Change	P-Value	adj.P-Value
1624393_at	*w*	74.81	2.74E-06	0.005
1626021_at	*CG32055*	43.82	0.0001087	0.030
1633201_at	*CG8245*	15.21	0.0002610	0.048
1631082_at	*B52*	14.38	3.22E-05	0.016
1640075_a_at	*path*	11.98	3.15E-05	0.016
1637008_at	*CG14687*	8.00	4.87E-05	0.021
1635802_s_at	*CG9279*	7.57	4.44E-08	0.001
1630684_at	*CG13032*	7.30	8.65E-06	0.007
1627352_at	*Oat*	5.35	1.00E-06	0.005
1623238_at	*CG5618*	4.48	0.000273	0.049
1624075_at	*CG31495*	3.63	4.88E-06	0.005
1626667_at	*miple*	3.47	0.000105	0.029
1626489_s_at	*CG7433*	3.09	3.84E-06	0.005
1638011_a_at	*Past1*	3.07	3.10E-06	0.005
1631633_a_at	*GNBP2*	3.02	0.000121	0.031
1640979_at	*CG1681*	2.64	7.44E-05	0.023
1625860_s_at	*CG32939*	2.32	6.89E-06	0.006
1638486_at	*Rbp1*	2.30	1.06E-05	0.007
1635725_a_at	*Unc-115b*	2.30	4.22E-06	0.005
1637125_at	*CG2004*	2.27	3.91E-05	0.018
1641563_at	*P58IPK*	2.24	5.83E-05	0.022
1630713_at	*SrpRβ*	2.17	0.000121	0.031
1636865_at	*Os-C*	2.17	0.000106	0.029
1629142_at	*DopR*	2.10	0.000225	0.044
1636456_at	*CG13053*	2.10	0.000250	0.047
1640746_at	*CG18542*	1.99	0.000231	0.044
1624054_at	*Adgf-A*	1.99	1.38E-05	0.009

1633304_at	*p24-1*	1.86	3.28E-05	0.016
1636528_at	*Gp93*	1.79	3.81E-05	0.018
1626196_at	*CaBP1*	1.75	6.95E-05	0.022
1639552_s_at	*CG6951*	1.71	6.83E-05	0.022
1639410_at	*Manf*	1.67	1.58E-05	0.010
1641295_s_at	*KDELR*	1.60	7.65E-06	0.006
1634945_at	*CG7830*	1.57	2.78E-05	0.015
1641489_at	*CG33169*	1.56	0.000139	0.032
1635423_s_at	*Hsc70-3*	1.54	0.000150	0.034
1633390_at	*tay*	1.53	7.38E-05	0.023
1631245_s_at	*CG9706*	1.52	0.000229	0.044
1635051_a_at	*Herp*	1.51	4.11E-06	0.005
1625388_at	*CG4893*	-1.58	9.89E-05	0.029
1627510_at	*CG12842*	-1.59	8.18E-05	0.024
1633566_at	*CG7694*	-1.83	0.000114	0.030
1627073_a_at	*CG10126*	-1.98	2.76E-05	0.015
1636600_a_at	*Mf*	-2.05	4.46E-06	0.005
1630318_at	*MED7*	-2.07	3.18E-06	0.005
1625794_at	*CG5830*	-2.12	2.71E-05	0.015
1633637_at	*CG17026*	-2.14	0.000202	0.042
1633349_at	*TFIIFβ*	-2.15	5.61E-06	0.005
1629438_at	*scaf6*	-2.23	6.81E-05	0.022
1641693_s_at	*CG32158*	-2.74	2.99E-05	0.016
1633520_at	*CG32027*	-4.91	5.56E-05	0.022
1626187_at	*Brf*	-7.59	5.60E-06	0.005
1623356_at	*CG11999*	-15.43	1.26E-06	0.005
1641552_at	*Cyp4g1*	-23.18	7.18E-05	0.023
1623486_at	*CG7900*	-44.92	1.84E-06	0.005

Supplementary Table 6. *Genes significantly up- or down-regulated in SakOE in comparison to OrR (≥1.5-fold, adj.P-value ≤ 0.05).*

Affymetrix ID	Gene	Fold Change	P.Value	adj.P-Value
1626021_at	*CG32055*	40.61	0.0001230	0.029
1624393_at	*w*	13.93	1.05E-07	0.001
1631082_at	*B52*	10.23	0.0001995	0.038
1637008_at	*CG14687*	9.48	3.42E-05	0.017
1630684_at	*CG13032*	7.34	1.34E-05	0.012
1635802_s_at	*CG9279*	6.12	1.33E-05	0.012
1623238_at	*CG5618*	4.38	9.72E-06	0.012
1626489_s_at	*CG7433*	3.47	7.98E-05	0.024
1624075_at	*CG31495*	2.92	0.000204	0.039
1625195_s_at	*shn*	2.83	4.69E-05	0.018
1638011_a_at	*Past1*	2.77	5.75E-05	0.021
1631633_a_at	*GNBP2*	2.74	0.0001786	0.037
1636894_s_at	*CG31188*	2.62	7.14E-06	0.012
1638486_at	*Rbp1*	2.61	9.39E-05	0.026
1632873_at	*MtnA*	2.52	7.74E-05	0.024
1626667_at	*miple*	2.44	4.07E-05	0.018
1639320_a_at	*Ddc*	2.33	0.0002934	0.047
1625860_s_at	*CG32939*	2.17	2.14E-05	0.016
1637309_a_at	*Cyp12e1*	2.16	0.0001950	0.038
1630713_at	*SrpRβ*	2.11	0.0002458	0.043
1635583_s_at	*fz2*	1.97	0.0001522	0.034
1637125_at	*CG2004*	1.95	0.0001081	0.028
1641563_at	*P58IPK*	1.91	0.0001225	0.029
1626831_at	*CG6579*	1.91	0.0002917	0.047
1636762_a_at	*scf*	1.88	0.0001888	0.038
1634922_s_at	*CG32795*	1.86	4.28E-06	0.010
1640746_at	*CG18542*	1.81	5.14E-05	0.019

1633304_at	*p24-1*	1.80	2.85E-05	0.016
1640215_at	*CG4338*	1.79	1.90E-05	0.016
1634471_at	*CG33214*	1.76	0.0001383	0.032
1639552_s_at	*CG6951*	1.68	0.0001220	0.029
1626196_at	*CaBP1*	1.65	4.19E-05	0.018
1624450_at	*Orct*	1.63	9.27E-05	0.026
1633810_at	*l(3)76BDm*	1.60	0.0003121	0.049
1639410_at	*Manf*	1.54	5.95E-05	0.021
1637571_at	*CG11577*	1.53	1.24E-05	0.012
1626358_at	*Fer1*	1.53	0.0001947	0.038
1641295_s_at	*KDELR*	1.51	0.0002070	0.039
1626749_a_at	*CG18135*	1.51	0.0003204	0.050
1625250_at	*CG5802*	1.51	0.0002705	0.046
1631100_at	*Lkr*	1.50	4.54E-05	0.018
1636864_at	*corto*	-1.58	0.0003104	0.049
1623518_s_at	*CG31305*	-1.77	4.36E-05	0.018
1633254_at	*CG7787*	-1.77	0.0003305	0.050
1625794_at	*CG5830*	-1.98	6.31E-06	0.012
1624473_at	*DNApol-α60kD*	-1.98	2.66E-05	0.016
1630318_at	*MED7*	-2.10	3.04E-05	0.016
1633349_at	*TFIIFβ*	-2.18	1.20E-05	0.012
1629953_at	*giant*	-2.19	0.0002347	0.042
1629438_at	*scaf6*	-2.24	8.53E-06	0.012
1636615_at	*elav*	-2.27	3.09E-05	0.016
1632170_a_at	*CapH2*	-2.31	0.0001044	0.027
1641693_s_at	*CG32158*	-3.05	5.88E-05	0.021
1633520_at	*CG32027*	-4.95	8.71E-05	0.025
1626187_at	*Brf*	-10.05	2.33E-05	0.016
1623356_at	*CG11999*	-18.00	2.47E-06	0.009
1623486_at	*CG7900*	-41.85	1.06E-07	0.001

Supplementary Table 7A. *GO analysis*
Enriched biological processes in SakOE up regulated genes

Biological Process	Count	%[a]	p-Value[b]	Genes
GO:0034976~response to endoplasmic reticulum stress	2	40	0.015	Herp, SrpRbeta
GO:0006984~ER-nuclear signaling pathway	2	25	0.023	Herp, SrpRbeta

[a] % of known annotated Affymetrix tags for GO term biological process BP_FAT
[b]Some biological processes have significant p-values, but clusters with small numbers of genes are likely to not have any biological meaning.

Supplementary Table 7B. *GO analysis*
Enriched biological processes in SakOE down regulated genes

GO-Term	Count	%[a]	p-Value[b]	Genes
GO:0006461~protein complex assembly	4	2.47	2.65E-04	CG31256, Med7, Mf, TFIIFbeta
GO:0070271~protein complex biogenesis	4	2.47	2.65E-04	CG31256, Med7, Mf, TFIIFbeta
GO:0065003~macromolecular complex assembly	4	1.71	7.84E-04	CG31256, Med7, Mf, TFIIFbeta
GO:0043933~macromolecular complex subunit organization	4	1.49	0.0012	CG31256, Med7, Mf, TFIIFbeta
GO:0006352~transcription initiation	3	4.17	0.0017	CG31256, Med7, TFIIFbeta
GO:0006351~transcription, DNA-dependent	3	2.27	0.0055	CG31256, Med7, TFIIFbeta
GO:0032774~RNA biosynthetic process	3	2.22	0.0058	CG31256, Med7, TFIIFbeta
GO:0006367~transcription initiation from RNA polymerase II promoter	2	3.13	0.0561	Med7, TFIIbeta
GO:0006350~transcription	3	0.66	0.0585	CG31256, Med7, TFIIFbeta

GO:0006366~transcription from RNA polymerase II promoter	2	2.04	0.0849	Med7, TFIIbeta

[a] % of known annotated Affymetrix tags for GO term biological process BP_FAT
[b] Some biological processes have significant p-values, but clusters with small numbers of genes are likely to not have any biological meaning.